UNIVERSIDAD DE MURCIA

FACULTAD DE BIOLOGÍA

Characterization of the Atmospheric Dynamics by Means of the Circulation Types and its Relation to the Climate Variability in the Iberian Peninsula

Caracterización de la Dinámica Atmosférica mediante Tipos de Circulación y su Relación con la Variabilidad Climática en la Península Ibérica

D. Juan Andrés García Valero

2015

Agradecimientos

¡Por fin!, es la palabra que más he deseado escribir desde que me propuse acabar y entregar esta tesis. Han pasado ya unos cuantos años desde que comencé en este periplo de mi vida cuando decidí hacer una tesis que tuviera algo que ver con mi profesión. El análisis de mapas sinópticos definidos en los Tipos de Circulación y de su variabilidad climática asociada es un entrenamiento muy gratificante para cualquier persona dedicada y apasionada por la meteorología.
Quiero empezar agradeciendo y de manera muy destacada a mi director de tesis, Juan Pedro, por el apoyo que siempre me ha ofrecido, así como la libertad que me ha otorgado para que pudiera ir eligiendo el camino de esta tesis, siempre con su buena guía y sus acertados consejos. Quiero agradecerle su tiempo dedicado, del que me consta en muchas ocasiones ha tenido que robarlo del suyo, y eso siempre es digno de agradecer. Me siento también agradecido por sus charlas sobre ciencia a las que le debo prácticamente todo lo que he aprendido sobre clima, casi diría a un nivel de significación del 95% por hablar en términos estadísticos. Su capacidad de liderazgo, su gestión sobre el grupo de personas que dirije, su calidad humana y me atrevo a decir su amistad, es sin duda algunas de las cosas más gratificantes que me llevo de todos estos años con más luces que sombras.
También quiero agradecer a Pedro Jiménez su apoyo prestado en muchos momentos, no sólo logísticos con el inglés y por sus buenos consejos, sino por enseñarme que la eficacia no está reñida con la eficiencia. También quiero agradecer el apoyo recibido por el resto de compañeros del grupo MAR. Con ellos sin duda me hubiera gustado compartir más tiempo. De todos modos, en el tiempo que he podido disfrutar a su lado en la universidad, en algún congreso u otro acontecimiento, siempre me he sentido como uno más del grupo. En todos ellos la expresión "cultura del esfuerzo" adquiere una especial relevancia. Desde luego, Juanjo, Sonia J, Raquel, Nuno, Rocío y Sonia F, son una generación de la que particularmente me siento orgulloso. Su espíritu de sacrificio en el trabajo, su afán por prosperar, y la inestimable ayuda que cada uno en su medida me ha ofrecido a lo largo de estos años, han propiciado en mí un mayor afán de superación que me ha dado fuerzas para ir afrontando las dificultades que han ido apareciendo a lo largo de esta tesis.
Quiero agradecer también especialmente a Parodi, mi compañero de despacho en AEMET, por aguantar mis charlas relacionadas con esta tesis y desviarlo de la

atención de sus tareas, y aún así, darme buenas ideas, consejos y excelentes datos para trabajar. También quiero agradecer al resto de mi compañeros de AEMET de la Delegación de Murcia sus palabras de ánimo, especialmente tan necesarias en estos últimos meses de tesis.

Me gustaría agradecer también a todos los desarrolladores de software libre en el que me he apoyado para la realización de esta investigación: proyecto R, openSUSE, Gridded Map Tools (GMT), GNUPLOT, Climate Data Operators (CDO) y compiladores GNU. Así como a todas las instituciones que han proporcionado los datos necesarios como AEMET, Universidad de Murcia, Universidad de Cantabria, Centro Europeo de Predicción a Medio Plazo, consorcio EC-EARTH, proyecto CCSM (NCAR y UCAR) e Instituto de Meteorología Max Planck.

También quiero agradecer a toda mi familia por haberme apoyado siempre en esta tarea: a mi suegra, cuñada, cuñados, sobrinos; y en especial a mis hermanas que siempre han depositado una gran confianza en mí por encima de lo que realmente pienso me merecía, pero que sin duda ha hecho que me plantee metas que anteriormente creía inabordables. En un lugar muy destacado quiero agradecer todo lo que soy a mis padres. De ambos he aprendido que el trabajo es la base de todo y que hay que confiar en las posibilidades de una mismo, y que sin esfuerzo no hay recompensa. ¡Gracias!, ¡gracias!, ¡gracias! y ¡mil gracias! a los dos por haberme apoyado tanto y tantas veces, pues a pesar de no haber tenido en estos años de tesis el apoyo en vida de mi padre, si lo he podido sentir desde su recuerdo.

Quiero agradecer a mis dos hijos la gran felicidad que me han dado durante estos años de tesis, y aunque su existencia haya hecho que el río de esta tesis tuviera meandros en su camino, han sido la energía potencial necesaria para que esta tesis llegara hata el mar. Por último, y por encima de todo, quiero agradecer esta tesis a mi mujer, sin su ayuda en tantos momentos, sin su comprensión en otros muchos, y sin su confianza hacia mí, esta tesis no hubiera visto su fin, por ello, esta tesis va dedicada a ti Mari Paz.

.

A mis padres,
Mis hijos,
y Mari Paz

Resumen General

El clima a lo largo de toda su historia ha sufrido modificaciones importantes con un alto impacto en las sociedades y ecosistemas. Por ello, el estudio y análisis de las causas que provocaron dichos cambios presenta un gran interés, y más hoy en día, cuando las proyecciones de cambio climático, ligadas a una gran incertidumbre pero con una tendencia compartida en todos los estudios relacionados, nos informan de la posibilidad de cambios muy profundos en el clima a lo largo del presente siglo. No obstante, en el siglo pasado ya han empezado a producirse cambios significativos. Uno de los más destacados es el aumento de la temperatura media global del planeta, sobre el que los estudios de atribución señalan como principal culpable al aumento de las concentraciones en la atmósfera de Gases de Efecto Invernadero (GEI), provocado fundamentalmente por el mayor desarrollo de las actividades humanas desde principios de la revolución industrial. No obstante, tanto los cambios observados como las proyecciones de cambio climático reflejan comportamientos regionales diferenciados a lo largo del planeta. Así pues, algunos trabajos donde se emplearon simulaciones climáticas de épocas pasadas, han demostrado que el patrón espacial de calentamiento global que reflejan las proyecciones de cambio climático es el mismo en el que se proyectaron los cambios en el pasado, aunque con algunas diferencias regionales que podrían estar relacionadas con cambios en la circulación atmosférica inducidos por el forzamiento antrópico.

Si nos centramos en un escala más regional, la Península Ibérica (PI) en nuestro caso, se aprecia que los cambios difieren de unas regiones a otras. Así, por ejemplo, el descenso de la precipitación durante el invierno y principios de la primavera es más notable en la región atlántica peninsular, y no tanto en la zona mediterránea donde apenas hay tendencia. Otro ejemplo son las temperaturas máximas estivales, cuando las mayores tendencias observadas se están produciendo en las regiones del centro peninsular. Muchas de estas diferencias, principalmente a escalas regionales sólo pueden ser totalmente entendidas si se tienen en cuenta los cambios en la circulación atmosférica.

La circulación atmosférica junto con la oceánica es uno de los medios trans-

misores del exceso de calor desde las regiones excedentarias como las tropicales, hacia otras deficitarias como son las polares. En latitudes medias, la dinámica atmosférica está regida por la corriente en chorro de niveles altos que actúa en la génesis, desarrollo y decaimiento de la borrascas extratropicales, así como en el mantenimiento, intensificación y localización de las regiones de altas presiones. A grandes rasgos, el chorro de niveles altos controla la posición de los principales centros de presión a escala sinóptica. La distribución del campo de presiones en superficie y en altura, define la dinámica atmosférica. Permite inferir los flujos reinantes sobre las diferentes regiones del planeta, y por tanto el carácter cálido/frío y húmedo/seco de las masas de aire advectadas por la circulación sobre una determinada región. La interacción de estos flujos con la orografía, y su variabilidad a lo largo de las estaciones y los años, condiciona en gran medida la caracterización climática de la región. Caracterizar qué cambios han tenido lugar en la dinámica atmosférica ayuda a entender en parte los cambios pasados, presentes y proyectados para el futuro. Por tanto, la caracterización de la circulación atmosférica sobre una región es un aspecto clave para entender sus variaciones climáticas.

Las leyes físicas que gobiernan la dinámica atmosférica hacen que ésta presente en esencia un comportamiento caótico, existiendo a priori un conjunto infinito de estados atmosféricos. Por ello, se requiere de técnicas estadísticas para abordar cualquier ejercicio de clasificación de la circulación atmosférica. Una de las técnicas habitualmente empleadas hace uso del análisis de componentes principales para determinar los modos que dominan la variabilidad atmosférica de baja frecuencia. Algunos ejemplos muy conocidos de estos modos son la Oscilación del Atlántico Norte (NAO por sus siglas en inglés), Oscilación del Ártico (AO), Oscilación del Sur (SO), etc. Otros métodos de clasificación se basan en la creación de índices de circulación que caracterizan las situaciones en función de la dirección del flujo y de su tipo de rotación. Otro de los métodos de caracterización son los Tipos de Circulación (TCs). Estos constituyen un conjunto reducido y manejable de situaciones en los que se puede resumir la gran variabilidad atmosférica a escala diaria. Desde el punto de vista de un meteorólogo podrían definirse como aquellas situaciones atmosféricas tipo que se suelen recordar, y a las que se les suele asociar unos patrones de precipitación y temperatura característicos, denominados sus Tipos de Tiempo (TTs). La obtención de estos TCs requiere del uso de técnicas de agrupación. Para ésto, se han implementado diferentes algoritmos estadísticos que por lo general tienden a buscar, especificado un número de grupos, una agrupación óptima que tienda hacia grupos lo más homogéneos posibles y diferentes entre ellos. Esto se puede medir y definir mediante un índice de calidad de la agrupación.

Uno de los objetivos primordiales de esta tesis es profundizar en las relaciones entre la Circulación Atmosférica y la gran variabilidad climática existente sobre la Península Ibérica, utilizando para ello la óptica de los TCs y de sus TTs asociados.

A pesar de que hay disponibles una serie de clasificaciones de TCs desarrolladas para la región Euroatlántica, así como algunas otras específicas para la PI, se ha desarrollado una nueva clasificación de TCs centrada en la PI. Para ello se han empleado datos diarios de reanálisis (ERA40) y análisis operativos del Centro Europeo de Predicción a Plazo Medio (CEPPM), que se extienden a un mayor número de años (1958-2008) y que presentan una mayor resolución espacial (1.125º) que aquellos usados en anteriores clasificaciones desarrolladas para la PI. El hecho de poder extender la longitud temporal que abarcan estas clasificaciones permite su cruce con bases de datos observacionales también de mayor duración. Esto permite que se pueda llevar a cabo un análisis más completo de las relaciones entre la circulación atmosférica y la variabilidad climática. La nueva clasificación se hizo para cada una de las estaciones del año con el fin de mejorar el grado de calidad de los grupos obtenidos, empleándose como campos atmosféricos la presión a nivel del mar (SLP por sus siglas en inglés) y la altitud geopotencial en el nivel de 500 hPa (Z500). Ambas consideraciones también son novedosas respecto a las anteriores clasificaciones, normalmente desarrolladas anualmente y para una sóla variable atmosférica. El uso de dos variables permite entender mejor las relaciones entre los TCs con variables como la precipitación en aquellas regiones de la PI como las mediterráneas, dónde las precipitaciones no sólo están gobernadas por los flujos en superficie, más propio de las regiones de clima atlántico, sino también por la circulación en altura. Otras consideraciones adoptadas, como son el algoritmo de agrupación y la ventana de agrupación, también representan un elemento diferenciador de anteriores clasificaciones.

Un condición muy importante de este tipo de clasificaciones es que los grupos formados sean estables. Esto significa que la clasificación deber ser lo más independiente posible del período de tiempo utilizado. Este hecho es fundamental a la hora de usar las frecuencias de los TCs para analizar tendencias en los TCs y su relación con posibles tendencias en la variable climática. Por ello, la clasificación se hizo con el algoritmo que dio mejores resultados de estabilidad tras testar dos algoritmos distintos de agrupación, uno de uso más tradicional en este tipo de aplicaciones como K-medias, y otro de uso más reciente como SANDRA.

La clasificación de TCs obtenida se ha evaluado con el fin de ver si responde bien a las características conocidas de la circulación en las diferentes épocas del año. Se ha profundizado en el análisis de tendencias en la frecuencia de ocurrencia de los distintos TCs, así como en el de su persistencia y de las transiciones entre ellos.

En general, muy pocos TCs presentan tendencias significativas, fundamentalmente en primavera e invierno. Se observa una tendencia al aumento en la frecuencia de las situaciones anticiclónicas y disminución de las ciclónicas en ambas estaciones. Hecho que podría estar conectado con las tendencias negativas en precipitación reportadas en numerosos estudios. Por otro lado, el análisis de persistencia de las situaciones y de las transiciones revela que los TCs pueden presentar una mayor persistencia en primavera y otoño, o una mayor probabil-

idad en otoño y primavera, en el descuelgue de bajas presiones extratropicales desde el Noroeste de la PI hacia el Suroeste, que en las estación de invierno.

Una vez clasificada la circulación atmosférica sobre la PI, otro punto de esta investigación ha consistido en la obtención de los regímenes asociados de tiempo en precipitación y temperaturas máximas (Tx) y mínimas (Tm) diarias. Para ello se ha hecho uso de las nuevas bases de datos observaciones de tipo reticular surgidas en los últimos años y que abarcan un largo período de tiempo. En este caso se ha utilizado la Base de Datos de Spain02, de gran resolución espacial (0.2º) y largo período temporal que se extiende desde 1951 hasta 2008. La relación entre los TCs y sus TTs permite ahondar en el análisis de la variabilidad espacial sobre la PI a escala diaria provocada por la interacción de los distintos TCs con su compleja orografía. Además, a partir de la series de frecuencia de los distintos TTs se ha analizado el grado en que los TTs son capaces de explicar la varianza y la variabilidad temporal observada tanto a escala diaria como estacional de las diferentes variables climáticas. En general, la clasificación explica razonablemente bien la variabilidad a escala estacional aunque con ciertas diferencias entre las variables consideradas. La variabilidad de las temperaturas se explica mejor en las estaciones equinocciales y en verano que en invierno. Por contra, la precipitación se explica mejor en invierno. La precipitación se reproduce mejor en las regiones de clima atlántico que en las mediterráneas, mientras que con las temperaturas máximas sucede lo contrario, especialmente en invierno. La secuencia de los TTs nos explica en parte, las tendencias observadas en precipitación y temperatura, concretamente la tendencia negativa de la precipitación en invierno en la fachada atlántica peninsular a lo largo de la segunda mitad del siglo XX, y las tendencias positivas en temperatura en primavera y otoño, observadas fundamentalmente en el último cuarto de siglo. No obstante, aunque la secuencia de los TTs es una herramienta útil para entender la variabilidad temporal media a escala estacional, las limitaciones de ésta técnica, debidas en gran parte al elevado nivel de ruido presente en las clasificaciones, impiden que la variabilidad a escala diaria pueda ser reproducida adecuadamente. La aplicación de este tipo de clasificaciones para el análisis de eventos extremos a escala diaria, de gran impacto e interés para la sociedad, puede tener limitaciones importantes.

Sin duda, el interés por los cambios en la frecuencia de eventos extremos adquiere una especial relevancia por su gran impacto en la sociedad. En la Península Ibérica las proyecciones de Cambio Climático apuntan, con un nivel de incertidumbre menor que en otro tipo de variables, a que la frecuencia de eventos extremos en verano relacionados con las temperaturas máximas se va a incrementar de manera muy significativa, hasta el punto de considerarse a la PI como uno de los puntos calientes a nivel global. Por ello, el estudio y análisis del papel de la dinámica atmosférica en dichas proyecciones presenta un gran interés.

Para dar respuesta a esta inquietud, otro de los objetivos de esta tesis ha con-

sistido en desarrollar una nueva clasificación de TCs desarrollada para el verano con el fin de sortear las limitaciones que las clasificaciones de TCs como la anterior, de tipo más generalista, presentan para responder a la variabilidad de este tipo de eventos extremos. La nueva clasificación se ha basado en una regionalización de las temperaturas máximas (Tx) de Spain02. Las 8 regiones obtenidas aportan una nueva visión de la variabilidad de las temperaturas máximas en escalas espaciales relativamente menores a las 3 grandes regiones tradicionales: Atlántica, Cantábrica y Mediterránea.
Para la clasificación de TCs se ha trabajado con información derivada de las series regionales, a priori más homogéneas que las series de tipo puntual, y cuya variabilidad está también más controlada por la circulación atmosférica que en el caso de las series puntuales. Se ha analizado las ocurrencia de eventos extremadamente cálidos (EHD por sus siglas en inglés) en las distintas regiones, definiéndose estos eventos como aquellos episodios en los que se supera el percentil 95 de la serie regional para el período 1958-2008. Se ha observado la existencia de tendencias positivas muy significativas en prácticamente todas las regiones, notablemente mayores en las regiones del centro y noreste peninsular. El objetivo principal de desarrollar la nueva clasificación consiste en investigar la posible atribución de estas tendencias a cambios en la circulación atmosférica.

Con el fin de evitar que las situaciones atmosféricas ligadas a este tipo de eventos, a priori poco frecuentes, puedan quedar muy repartidas entre los diferentes grupos que constituyen los TCs, y por tanto sus posibles tendencias enmascaradas, la nueva clasificación parte precisamente de una primera agrupación obtenida exclusivamente para los días identificados como extremos en todas las regiones. La clasificación definitiva se consigue tras una asignación a estos primeros grupos del resto de días no considerados en la primera agrupación, permitiendo que días con situaciones muy distintas, desde un punto de vista sinóptico, queden fuera de esta asignación. De esta manera, se puede evaluar la eficiencia de los diferentes TCs en la ocurrencia de días EHD en las distintas regiones, así como evaluar su tendencia en la ocurrencia de dichos patrones sinópticos representados en los centroides de los TCs. Ambos resultados se utilizan en un ejercicio sencillo de atribución a la circulación atmosférica de las tendencias regionales observadas. Además, con el fin de evaluar el impacto de las variables atmosféricas usadas en la definición de los TCs, se han obtenido diferentes clasificaciones mediante el uso individual y pareado de tres variables atmosféricas, SLP, Temperatura al nivel de 850 hPa (T850), y Z500. Los resultados de atribución, siguiendo nuestra metodología, evidencian que en general una fracción relativamente alta de las tendencias observadas no puede explicarse por cambios en la circulación atmosférica, siendo mucho menor la atribución en las regiones del interior peninsular. Esto apunta a que otras causas, posiblemente atribuidas a cambios en la humedad del suelo, así como al calentamiento global podrían estar detrás de una gran parte de la tendencia observada. Además, se observa una importante sensibilidad de los resultados de atribución a los campos atmosféricos utilizados en la definición de

los TCs. En general se observa un mejor comportamiento en la mayoría de las regiones para la clasificación formada por la combinación SLP-T850.

Una vez definida la nueva clasificación de TCs, otro de los objetivos de esta tesis es la proyección de estos TCs hacia el futuro con el fin de obtener a su vez proyecciones de la frecuencia de EHDs en las distintas regiones. Para ello se han empleado las salidas de los campos atmosféricos de tres modelos del Sistema Tierra (ESM) usados en el proyecto de evaluación CMIP5: MPIM-MR, EC-EARTH y CCSM4; y ejecutados bajo dos escenarios distintos de emisiones de GEI, RCP4.5 y RCP8.5. Independientemente del modelo empleado y del escenario escogido, uno de los resultados más destacables es el significativo incremento de la frecuencia de algunos TCs relacionados con una alta probabilidad de ocurrencia (eficiencia) de evento extremo en muchas regiones de forma simultánea, y en especial en las regiones del interior y noreste peninsular, manteniéndose así el mismo patrón espacial observado en el período de reanálisis. Estas proyecciones están afectadas por tres fuentes de incertidumbre: modelos, escenarios y clasificaciones de TCs. Así, se ha analizado la evolución de la importancia relativa de cada una de estas fuentes en la incertidumbre de las proyecciones en cada una de las regiones a lo largo del período 1950-2100. En general, se observa que la incertidumbre asociada a los modelos climáticos controla durante todo el período más del 50% de la incertidumbre, mientras que la incertidumbre relativa a los escenarios es importante a partir del 2020, siendo la segunda fuente en importancia (30%) hasta los últimos 30 años de siglo, momento en que la incertidumbre asociada a las clasificaciones de TCs aumenta considerablemente. Así, en términos generales, se proyecta que la frecuencia media estacional de EHDs en el período 2071-2100 sea en la mayoría de las regiones del orden de el doble e incluso el triple en algunas otras, que la frecuencia correspondiente al período 1950-2005, con un intervalo de incertidumbre centrado en estos valores no superior al 30% en la mayoría de las regiones.

La evolución del clima sobre la Tierra ha ido marcada a lo largo del tiempo por la propia variabilidad natural o variabilidad interna, y por una serie de forzamientos externos. En el último milenio hay disponibles un conjunto de reconstrucciones y simulaciones climáticas para Europa que nos informan de la existencia de una importante variabilidad climática en el continente, relacionada en gran medida con cambios en los forzamientos externos. Así, en la segunda mitad del milenio se observa un período frío conocido como Pequeña Edad de Hielo, e incluidos en este período otros subperíodos más fríos asociados con mínimos en la actividad solar (mínimo de Maunder), o con una mayor actividad volcánica (mínimo de Dalton).
Un objetivo principal de esta tesis es el análisis de la influencia de los forzamientos externos, como la actividad solar, volcánica y las emisiones antropogénicas de GEI en la evolución de los TCs en invierno y verano. Este ejercicio es la primera vez que se aplica bajo la óptica de los TCs. Para ello, se han obtenido una serie

de clasificaciones de TCs en una ventana euroatlántica a partir de la variable SLP, obtenida en el período 1500-1990, a partir de 4 simulaciones paleoclimáticas, dos de ellas desarrolladas con el modelo global ECHO-G, y las otras dos con la versión climática del modelo regional MM5 alimentado en su frontera por las dos simulaciones globales anteriores. Cada pareja de simulaciones están ejecutadas con el mismo modelo y los mismos forzamientos externos (éstos iguales para las cuatro simulaciones), cambiando tan sólo sus condiciones iniciales de partida. Así partiendo de estas premisas, y de las series de frecuencia de los TCs que son similares entre las simulaciones pareadas, es posible evaluar el papel de los forzamientos en conjunto, y por separado, en la evolución de los distintos TCs.

Los resultados evidencian que existe una relación significativa, aunque débil, entre los forzamientos y 2(6) TCs de invierno(verano). Sin embargo, no hay resultados estadísticamente significativos de la influencia por separado de los forzamientos solar y antrópico. En relación al forzamiento volcánico, sí hay una influencia clara en invierno. Los resultados obtenidos indican la aparición de anomalías positivas de temperatura y precipitación en el Norte de Europa los inviernos posteriores a una gran erupción, el cuál es coherente con los resultados obtenidos en otros estudios basados en reconstrucciones y simulaciones.

Abstract

Climate has suffered important changes along its history causing large impacts on society and ecosystems. Therefore, the analysis of the causes provoking such changes has a great interest, and much more nowadays, when climate change projections inform about the possibility of deep changes on climate along this century.
Important climate changes have been occurred during the past century. One of the most significant is the global warming. Many studies point out to the human activities as the main responsible of such warming due to the huge anthropogenic Green House Gases (GHGs) emissions since the beginning of the industrial period.
As the changes observed in the last decades as those projected for future, show regional behaviors overall the planet. Some works employing paleosimulations have demonstrated that the spatial warming pattern projected by the climate change simulations, is the same than that obtained for paleosimulations in the past, but with some regional differences maybe related to changes in the atmosphere circulation caused by anthropogenic forcing.

At more regional scales like the Iberian Peninsula, the changes observed differ from some places to another. For example, the decrease of precipitation in winter and early spring is more significant in the peninsular atlantic half, but not as important in the mediterranean regions. Another example is the positive trend of summer temperature affecting more to the inner regions. More of these regional differences ca be completely understood if changes in atmospheric circulation are taken into account.

At midlatitudes, the atmospheric circulation is governed by the jet stream located at the highest troposphere levels. It acts in the cyclogenesis, development and declining of extratropical lows. In a great extent, the jet controls the position of the large synoptical pressure centers. The distribution of the pressure fields, both at surface and higher levels, define the atmospheric dynamics. This allows to infer the prevalent fluxes over the different regions under its control, and as consequence, in the warm/cold and dry/wet character of the air masses advected

towards these regions. The interactions of these fluxes with orography and their variability along the seasons and years, lead the climate of the different regions. The characterization of the changes occurred in the atmospheric dynamics helps to understand not only the climate changes occurred in the past, rather also those projected for future. Therefore, this is a key factor for understanding the climatic variations of a given region.

Laws governing the air movement within the atmosphere describe non-linear processes, making that the atmospheric circulation had in essence a chaotic nature. A priori, there exists an infinite number of atmospheric states needing of statistical techniques to aboard any attempt of characterization of the atmospheric dynamics.
One of the techniques frequently used is based on Principal Component Analysis (PCAs) to determine the main modes of low frequency variability. Some examples are the North Atlantic Oscillation (NAO), Artic Oscillation (AO), East Atlantic (EA), Southern Oscillation (SO), Scandinavian (SCAN), etc. Another classification method is based on the obtainment of circulation indices. These classify the circulation attending to the direction and vorticity of the air fluxes. Circulation Types (CTs) are another method of classification. CTs are a handy ensemble of atmospheric situations summarizing the great atmospheric daily variability. From the point of view of a meteorologist, CTs are as those atmospheric patterns that he used to remember and which he is able to associate with some weather regimes of precipitation and temperature, called as their Weather Types (WTs). To obtain the CTs statistical clustering techniques are required. For this, different clustering algorithms have been implemented. In general, they try to look for an optimal clustering deriving clusters the more homogenous as possible and different among them. This is measurable by means of the definition of a quality index.

One of the primordial tasks of this Thesis is to deep in the relationships between the atmospheric circulation and the great climate variability existing over the Iberian Peninsula (IP), using for this the CTs perspective and of their associated WTs.

Despite different CT classifications have been developed for the Euroatlantic region, as well as some others for the IP, a new CT classification over the IP have been obtained. To perform this, daily reanalysis (ERA40) and operational analysis from the European Center Model Weather Forecast (ECMWF) have been employed. These data cover a longer temporal period (1958-2008) and have a larger spatial resolution (1.125º) than those used in previous classifications. The longer period facilitates crossing the classification with observational datasets also with a longer temporal period than those used before. In this way, a more complete analysis of the relationships between the dynamics and climate variability can be to carried out.
The new CT classification was performed using a seasonal division for improving

the quality of the clusters, and considering the Sea Level Pressure (SLP) and Geopotential Height at 500 hPa Level (Z500) fields as variables for defining the CTs. Both considerations are novel respect to the previous classifications which were obtained without seasonal division and considering only one variable. The use of two variables permits to understand better the links between CTs and variables like precipitation, especially in the mediterranean regions of the IP. Another adopted considerations like the clustering algorithm and the window used for clustering, are also two differentiating elements of previous CT classifications.

An important condition of this kind of classifications is that the obtained clusters were stable. This means that classifications should be the most independent of the time period considered for its construction. This fact is fundamental for using the frequencies of CTs for the analysis of trends in the different CTs and of their possible connections with trends in the climatic variable. The stability results of two algorithms were compared in order to chose that with better performing. The compared algorithms were one of traditional use as K-means and other of more recent use as SANDRA.

The obtained CT classification have been evaluated to check if it describes well the annual cycle of the atmospheric circulation over the IP. It has been deepened on the analysis of trends in the occurrence of the different CTs, as well as on their persistence and the transitions among them.
In general, few CTs present significant trends, mainly in spring and winter. It is observed a positive(negative) trend in the frequency of anticyclonic(cyclonic) situations. On the other hand, the study of the persistence and transitions reveals that CTs can have a larger persistence during spring and autumn, as well as a higher probability in spring and autumn than in winter of the transition of the extratropical lows at NW of the IP towards the SW of the IP.

Another point of this Thesis has consisted of the obtainment of the precipitation, maximum (T_X) and minimum (T_m) temperature WTs associated with the different CTs of the above classification. New observational grided datasets available for the IP have been used for that. In this case the Spain02 dataset of high spatial resolution (0.2°) and covering the period 1950-2008 is used. Links between CTs and WTs allow the analysis of the spatial climate variability over the IP at daily scale caused by the interaction of the different CTs with its complex orography. Furthermore, the time sequence of WTs is a tool for exploring the observed variance and time variability, as at daily as seasonal scales of the different climate variables.
In general, the atmospheric classification explains reasonable well the variability observed at seasonal scale but with some differences among the variables considered. Variability of temperatures is better explained in the equinoctial seasons and summer than in winter, whereas precipitation is better explained in winter. Precipitation is better reproduced in the atlantic regions than the mediterranean

ones, whereas the contrary situation occurs for temperature, especially in winter. Sequence of WTs justifies the observed trends in precipitation and temperature, especially the negative precipitation trend in winter occurred in the atlantic regions during the period 1958-2008, and the positive temperature trends during spring and summer, mainly observed in the last quarter of the past century.
However, this technique has important drawbacks for reproducing daily variability, probably due to the important level of noise existing in the CT classifications. Therefore, the application of this method for the analysis of extremes at daily scale could have serious limitations.

The interest for analyzing changes in the frequency of extreme events acquires large importance by their great impacts on society. Climate change projections for the IP point to a significant increase of the frequency of extreme events related to maximum temperature in summer. Indeed, under such changes, the IP is considered as one of the hot-spots of the Globe. Therefore, the analysis of the role of the dynamics on these projections is of great importance.
To give a response to this concern. another of the goals of this Thesis has consisted of developing a new CT classification for summer specific for the analysis of extremes. The new classification is based on a regionalization of the T_X variable derived from Spain02. The eight regions obtained give new insights about the spatial variability existing over the IP beyond of the three traditional regions (Cantabrian, Atlantic and Mediterranean). A priori, regional series are more homogeneous and are larger controlled by dynamics than local ones. Information of these regions have been used for the new classification. The occurrence of extremely hot days (EHDs) in the different regions has been analyzed, defined these events as those when regional T_X overcomes the 95th percentile of the regional series derived from the period 1958-2008. The existence of significant positive trends have been observed practically in all regions, being higher in the central and northeastern regions. The main goal of developing the new CT classification is to investigate the possible attribution of trends to changes in the atmosphere circulation.

The new classification starts from a first clustering obtained exclusively by using those days defined as extremes in all regions. This avoid that atmospheric situations linked to extreme events, a priori of few frequency, can be very shared by the different clusters composing the classifications, and therefore their possible trends can be masked by the noise. The definitive classification is obtained through the assignation of the rest of days, initially not considered, to the groups obtained from the first clustering. In this way, the efficiency of different clusters on leading to EHD occurrences in the different regions can be evaluated, as well as the trends in the occurrence of such synoptical patterns represented by the centroids of the different CTs. Both results are used for an exercise of attribution of the observed regional trends to the dynamics. In addition, in order to determine the impact of atmospheric variables used for the definition of the CTs,

different CT classifications have been obtained by means of the individual and paired use of three atmospheric variables, SLP, Z500 and temperature at 850 hPa level (T850).
The attribution results show that a relatively high percentage of the observed trends can not be attributed to changes in the CTs, being this attribution lower in the inner regions. This points to other factors, maybe related to changes on soil moisture and global warming, could be behind of such trends. Furthermore, an important sensitivity of the results to the atmospheric fields chosen for defining the CTs is observed. In general a better behaviour of the SLP-T850 classification for most regions is obtained.

Once defined the specific CT classifications for the analysis of extremes, another task of this Thesis is the future projection of these CTs in order to obtain EHD projections for the different regions. To perform this, numerical outputs of the atmospheric fields (SLP, Z500 and T850) derived from three Earth System Models (ESMs): MPIM-MR, EC-EARTH and CCSM4 are used. Models were run under two representative concentration pathways (RCPs), RCP4.5/8.5. Independently of the ESM and RCP used, one of the outstanding results is the significant increase of the frequency of some CTs related to a high efficiency in the occurrence of EHDs at most regions simultaneously. This leads to a significant increase in the occurrence of EHD in the different regions, especially at those located in the inner and northeastern regions. Projections are linked to several uncertainty sources: models, scenarios and CT classifications. Hence, the evolution of the relative importance of each source in the EHD projections has been analyzed for the different regions along the period 1950-2100. In general, the uncertainty linked to the models control more than 50% of the total uncertainty along the overall period, whereas scenarios uncertainty is important from 2020, being the second source of uncertainty (30%) untill the last 31 years period of the century (2071-2100) when CT classifications increase in a prominent way. In general terms, the mean EHD frequency projected for the majority of regions in the period 2071-2100 will be double or even triple for some regions, in relation to the mean frequencies observed in the 1950-2005 period. The uncertainty linked to this projection for most region does not overcome the 30% of the mean EHD projected values in most regions.

Along the time, the Earth climate evolution has been driven by external forcings and internal variability. The existence of climate reconstructions and paleosimulations for Europe manifest that climate evolution over Europe in the last millennium has been linked to changes in the external forcing. Hence, it is observed colder periods during the little Ice Age associated with low solar activity as the Maunder Minimum occurred around 1700, or to a higher volcanic activity as the Dalton Minimum about 1800. In addition, the large increase of the anthropogenic forcing since the second half of the ninetieth century leads to the significant warming recorded during the last century.

A main task of this Thesis is the analysis of the influence of the external forcings, such as changes in the solar and volcanic activity, and changes in the GHGs concentrations on the evolution of the CTs in winter and summer. This exercise is the first time that is applied under the CTs perspective. To perform this, different CT classifications for an Euroatlantic region have been obtained in the period 1500-1990. For this, four paleosimulations, two of them performed with the same global model, ECHO-G, and the others obtained by using the regional climate model MM5 fed on its borders by the global simulations. Both global paleosimulations were obtained considering the same external forcings, but started from different initial conditions. Under these circumstances, it is possible the evaluation of the role of the forcing using the temporal correlation obtained between the frequency series of those CTs which are identical in the different CT classifications obtained for each paleosimulation.

Results indicate the existence of some weak statistical significant correlation between the forcings and two(six) CTs in winter(summer). However, there are not some response, at least with the followed methodology, between the solar and GHGs forcings and CTs when the influence of both forcings are analysed individually. Regarding the volcanic forcing, there is a significant influence in winter. Hence, results show the appearing of positive precipitation and temperature anomalies in the northern of Europe during the winters following to a big eruption. This result agrees with those informed by other studies based on reconstructions and paleosimulations.

Contents

Chapter 1

Introduction

1.1 Climate variability

Many definitions have been used for climate. One of them consider the climate as the mean state of meteorological variables (temperature, precipitation, humidity, wind, pressure, etc), obtained for a given spatial scale (normally the local scale) and for an specific period of time (normally of 30 years). However, this definition is incomplete because it can not respond to the important changes observed along the past century, associated not only with the mean state if not with other statistical parameters of the statistical population like the variance or percentiles, as well as to another temporal characteristics of the series such as trends, persistence, etc. In addition, a more complete definition should also consider the relationships between different variables, as it could be the covariance, necessary to understand some changes in variables like droughts. Hence, climate change refers to a change in the state of the climate that can be identified (e.g., by using statistical tests) by changes in the mean and/or the variability of its properties, and that persists for an extended period, typically decades or longer (IPCC, 2014).

Despite climate is normally referred to atmospheric variables, the fact is that climate is the result of complex interactions of the Earth's climate system, formed by five components: Atmosphere, Hydrosphere, Criosphere, Biosphere and Lithosphere. These are exchanging energy, mass and moment among them looking for a global equilibrium which is governed by the energy existing in the Earth's climate system. This energy is the result of a budget in the top of the atmosphere (TOA) between the short wave radiation (SWR) incoming to the system and the low wave radiation (LWR) outcoming. Changes in some of the subsystems could causing changes in this budget and therefore changes in climate. Figure 1.1 shows the most updated annual mean energy budget published in the fifth assessment report (AR5) of the intergovernmental panel on climate change (IPCC). Despite notable uncertainties remain in this budget in relation to the non-radiative fluxes at surface (latent and sensible heats) (IPCC, 2014), the net result of this is an imbalance of $+0.6$ W/m^2 adding more energy to the system. The significant rise

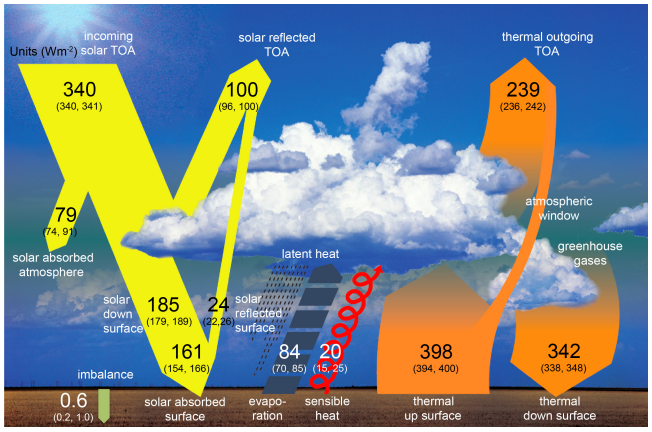

Figure 1.1: Mean annual radiative energy budget in the Earth's climate system (IPCC, 2014).

of 0.86 °C of the global mean surface temperature (combining land and ocean surface temperature) observed from 1880 to 2012 is probably one of the footprints of this imbalance. As it has mentioned above, whatever change in some of the components of the climate system will affect the energy budget, causing a chain of changes in the rest of subsystems. The initial changes are normally called as radiative forcing.

The complex interrelationships among the components cause feedbacks processes which in some cases tend to diminish the initial change (negative feddback) or to amplify it (positive feedback). Figure 1.2 shows some of the key feedbacks occurring in the Earth's climate system, as well as the different time scales of the lasting of each one. Negative feedbacks have to be prevalent to maintain the dynamical equilibrium of the climate system, being one of the dominant ones that related to the higher emission of LWR to space when an increase in the Earth's temperature occurs. Some example of positive feedbacks is that favoring the increase of greenhouse gases (GHGs) concentrations in the atmosphere (water vapor, dioxide carbon, methane, etc), explaining these a significant part of the observed global, especially due to the anthropogenic GHGs emissions.

Apart from the changes observed in the last centuries, the history of the Earth's climate reconstructed from historical documents and proxy data (ice scores, boreholes, ring trees, sediments, etc), teaches that global surface temperature has suffered important variations along millennia and millions of years. Two equilibrium states, glacial and interglacial, of one hundred thousand years and ten thousand years of mean duration, respectively, have been reproduced by paleoclimatological information. The main reason of these variations at these longer temporal scales obeys mainly to changes in the total solar irradiance (TSI) arriving the TOA which suffers variations because of periodical changes in the Earth's orbital parameters Berger (1988). In addition, unpredictable changes in

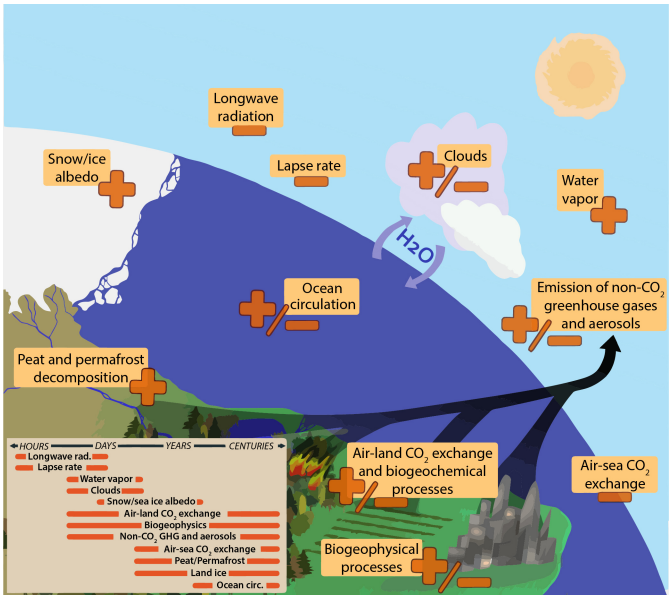

Figure 1.2: Key feedbaks processes in the Earth's climate system (IPCC, 2014).

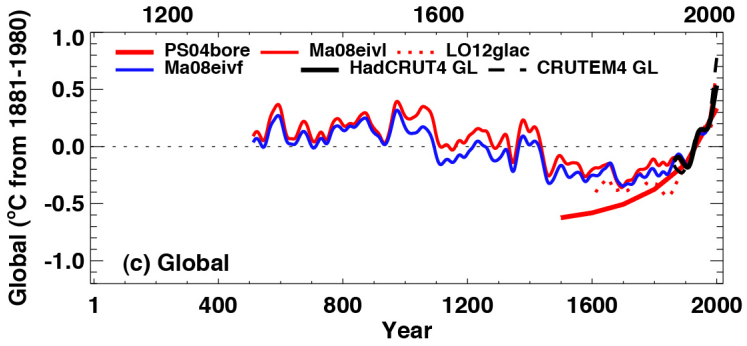

Figure 1.3: Reconstructed global annual temperature anomalies during the last 2000 years (IPCC, 2014).

the solar activity provokes also variations at shorter time scales as well as the eruptions of big volcanoes. The most significant effect of volcanoes is the modification of the Earth's albedo caused by the release of substantial amounts of aerosols into the stratosphere, causing a cooling in the next years after eruptions. The combination of TSI variations and big volcanic eruptions seem to be some of the causes leaders to the most relevant variations occurred along the past millennium. Figure 1.3 shows some reconstructions of the global surface temperature anomalies during the last two millennia. It can be seen the existence of a colder period between 1450-1850 defined as the Little Ice Age (LIA) and whose existence seems to obey to changes in TSI and big volcanic events. In addition, it can be observed such as the global temperature suffers variations at different time scales from decennial to multi-centennial years.

Variations in temperature respond to the forcings and the complex feedback processes making that the equilibrium of the system was a continuum dynamical process. In addition, if the forcings are kept constant in time, the climate fluctuates at interdecadal or even larger time scales. This random fluctuations, deriving from the chaotic nature of the climate system, is defined as internal variability (Huybers and Curry, 2006). Therefore, internal variability affect the climate evolution at different temporal scales, amplifying or hampering the climate modifications guided by the forcings.

In the current context of economical crisis, one of the most important challenges for recovering the global economy goes trough a sustainable environment. To this way, the knowledge about future variations of climate along the current century is necessary for a better planning of energy resources, agricultural activities, infrastructures (hydrological, construction, etc), etc. Therefore, climate simulations are needed to this target. Global Circulation Models (GCMs) are the most suitable tools for simulating the climate system. They consist of a three-dimensional representation of the different climate subsystems, and they try to solve many of the known complex processes of exchange of energy, matter and momentum among the different subsystems. Furthermore, to simulate more realistically the Earth's climate system external radiative forcings according to changes in TSI, volcanoes and anthropogenic GHGs emissions have to be included for simulations.

The improvement of CMs have been spectacular in recent decades. It has been linked to the increase in the computing power of computers, following the inclusion of more climate subsystems as well as of more complex processes to the extent that the spatial resolution of models have increased. Figure 1.3 shows a summary of the CMs's evolution. In the first models (middle 70s), only some processes occurring in the atmosphere, land surface, ocean and sea ice were simulated, whereas the models used in the last IPCC report (IPCC, 2014) are capable of simulating a larger number of processes affecting to aerosols, carbon cycle, dynamic vegetation, atmospheric chemistry and land ice.

GCMs are used for climate change experiments as well as to determine to what extent the current climate change obeys to anthropogenic causes. However, the climate projections present a number of problems to consider before models are run. The first one is the important uncertainties existing in the future evolution of external forcings, being some of them unpredictable such as the evolution of TSI and volcanoes. There are another natural forcings which can be considered constant at the time scale the projection is designed for (typically 100 years), such as modification in the lithosphere (this is, the distribution of continents and oceans) or the Earth's orbital parameters. The evolution of the Biosphere is another important factor which is affected by climate variations (indeed there are important feedbacks between both subsystems) and which normally is taken as constant in climate simulations because of the important uncertainties existing

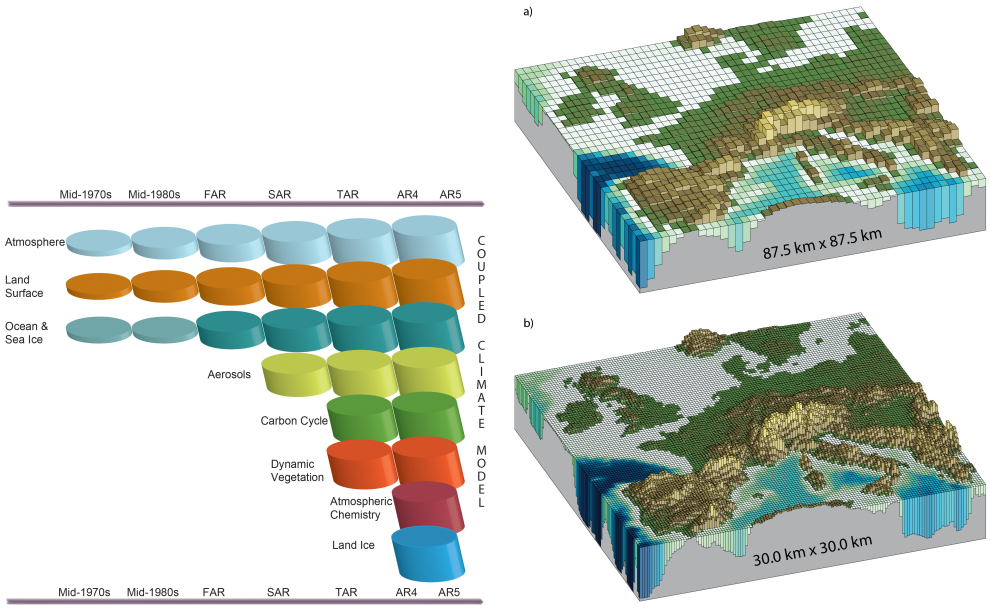

Figure 1.4: Evolution of the global circulation models in recent decades (IPCC, 2014).

in the complex mechanisms between climate and life. Finally, the anthropogenic forcing may determine critically the evolution of the climate. They include, but are not limited to, evolution in the concentration of GHGs, aerosols and modifications in land use (IPCC,2013). These factors are however affected by a huge uncertainty, since they depend on the future unpredictable socio-economical evolution of the current civilizations around the Globe. The only way to deal with such uncertainties is an statistical approach. A number of possible evolutions of the socio-economical factors, with their respective implications in the available technology, and thus in the future GHGs and aerosols emissions, are hypothesized. These hypothetic futures are denominated representative concentration path ways (RCP), also called traditionally as scenarios. This input information is used to conduct simulations with several state-of-the-art GCMs, and the results of this ensemble of simulations are considered in an statistical way (IPCC, 2014). Figure 1.5 illustrates the result of this process showing the mean of the ensemble series of global temperature projected under several RCPs.

Depending on the application of the climate change projections (CCP) the spatial coarse resolution of GCMs (see Figure 1.4) can be insufficient and CCP of larger spatial resolution could be necessaries. The analysis of the impacts of future changes for adopting strategies of adaptation and mitigation are a clear example of activities demanding CCPs with higher spatial resolution. Downscaling techniques are employed to procure CCPs of high resolution, existing two generic downscaling approaches, dynamical and statistical. The former consist of using regional climate models (RCMs) of higher resolution than GCMs. These

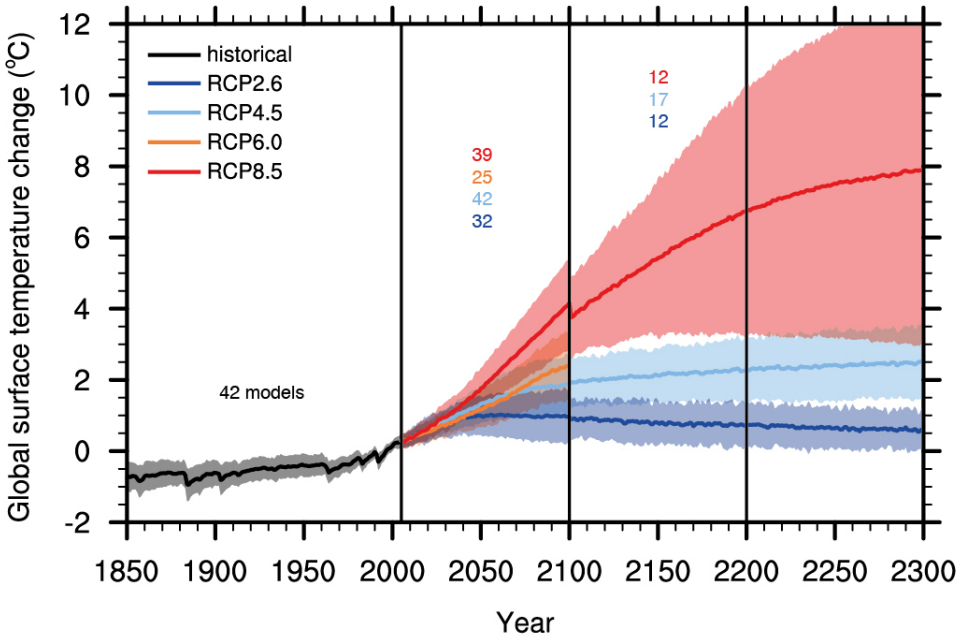

Figure 1.5: Ensemble projections of changes in the global surface temperature under different climate change scenarios (IPCC, 2014).

models simulate only a limited area domain, with well defined borders. The information in the borders have to be provided somehow externally, so a model with these features need to be coupled to a GCM providing this information. The advantage of this type of model is its lower computational cost, allowing its implementation to greater spatial resolution (the order of tens of kilometers). The latter downscaling approach consists of using some outputs of GCMs (defined as predictors), normally large scale atmospheric fields well resolved by the global model, for developing statistical-empirical relationships between these predictors and local climate data (predictands) derived from meteorological stations (Wilby et al., 2004). Both downscaling approaches have drawbacks and strengths. In the case of RCMs its outputs are dynamical consistent because they simulate real processes but they require an important computational cost. Furthermore, they are strong dependent on the GCM in which they are embedded. By contrast, statistical downscaling requires low computational cost, but it assumes that empirical-statistical relationships keep constant along the time and this would be problematic in a context of climate change.

1.2 Atmospheric dynamics

The movement of the air within the atmosphere is denominated as atmospheric circulation (AC). Considering a global scale, the main mission of the AC is to carry the excess of heat at low latitudes towards the most deficient polar regions. This allows to maintain constant the Earth's temperature in the annual scale.

At shorter-scales, whatever imbalance (of pressure, temperature, humidity, etc) within the atmosphere will be restored to its equilibrium state by appearing some kind of air circulation.

AC differs largely between tropical and extratropical latitudes. In the tropical regions the AC is driven by the Hadley cell, whereas in midlatitudes the circulation is guided by the jet stream. The Hadley cell is a closed circulation located between the equator and tropics. Air at surface equatorial regions is unstable and rises, leading to a region of low pressures at surface. Over the tropics high pressures domain at surface, mainly due to the existence of air subsidence over this region. Therefore, a circulation from tropics to the equatorial region (trade winds) is produced at surface level governed by the gradient pressure force. At higher levels the cell is closed by a southern circulation towards the tropics.
At midlatitudes, AC obeys mainly to the unstability of the jet stream. The jet stream is an intense circulation occurring at high atmospheric levels whose formation is due to the existence of intense temperature gradients between tropical and polar regions. On average, the jet stream is a zonal and circumpolar circulation from western but it suffers some deviations of its trajectory. These deviations are governed by physical laws related to the conservation of the potential vorticiy. In the northern hemisphere, polarward (southward) undulations of the jet are called as ridges (troughs). In the ridges patterns the air vorticity is negative (clockwise air movement) and positive temperature anomalies take place in the medium troposphere. By contrast, positive vorticity and negative temperature anomalies appear under the trough configuration. Ridges and troughs of large amplitude and wavelength are regions with persistence weather conditions, prevailing the stabilitly and instability of the atmosphere, respectively. Quasi-geostrophic theory teaches that the pressure field at surface levels is in a great extent driven by the jet stream undulations, leading to areas of high(low) pressures under ridge(trough) configurations (Holton and Hakim, 2012). This is of very importance because of the location of the areas of high and low pressures control the prevalent wind regime affecting directely to the regimes of precipitation and temperature of the regions under the influence of the jet stream. In addition, the cyclogenesis, lifetime and dissipation of the low extratropical systems, of great importance in the climate at midlatitudes, is also controlled by the jet stream. Finally, the interactions of the AC with other factors such as the orography determine the climate of the different regions.

Laws governing the air movement within the atmosphere describe non-linnear processes, making that the AC had in essence a chaotic nature (Lorenz, 1969). Atmospheric circulation models (ACM) used for the weather forecast simulate the evolution of the atmosphere states. Unlike of climate models, ACMs simulate only the atmosphere and they need to be initialized from an initial state. This state, also known as analysis is derived from a huge number of weather observations collected from several observational platforms: weather stations, air soundings,

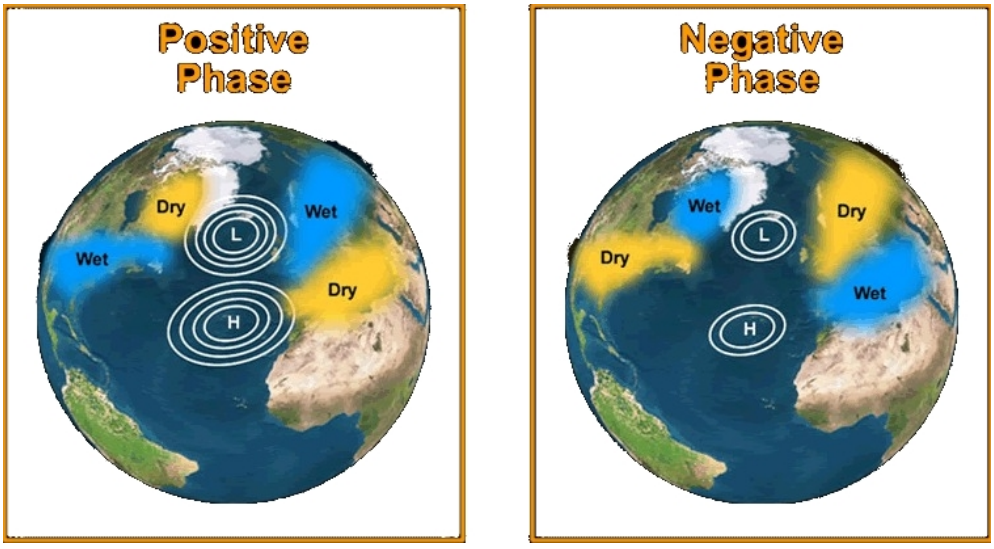

Figure 1.6: Phases of the Nort Atlantic Oscillation.

satellites, meteorological radars, ocean buoys, ships, etc. Assimilation processes are necessaries to join all this information and to procure a gridded initial state for running the ACMs. For the construction of the grid, interpolation techniques applied over the observations are used, and then, a process to analyze the physical consistency of the initial state is performed. Once consistent initial state is obtained, not exempt of errors, the ACM forecasts its evolution. The sensitivity of the atmospheric simulations to the initial state is a fundamental characteristic of the chaotic systems. Initial errors are amplifying along the forecast time steps, invalidating, in general terms, the forecast beyond 10 days. Therefore, ACs have to be initialized frequently.

One of the steps of the weather forecast has important application for climatological studies. The obtained initial states are very useful for climate applications constituting the nearest approximation to the real observations. In addition, the observations recorded before the ACMs began to be used, can also be used for models for reconstructing the past atmospheric states. These data are called as reanalysis.

An interesting exercise with important implications in climatology is the characterization of the atmospheric dynamics. Low frequency modes of variability, based on Principal Component Analysis (PCA) (Barnston and Livezey, 1987) applied to Sea Level Pressures (SLP) or to a given geopotential height field, is one of the ways for its characterization. These modes, also called as teleconnection-patterns, are, in a great extent, responsible of the climate variability observed in large areas at interannual and decadal time scales (Rodriguez-Puebla et al., 1998). The main mode controlling the climate variability over Europe is the North Atlantic Oscillation (NAO) (Barnston and Livezey, 1987). The two phases

of this mode are represented in the Figure 1.6.Its positive phase reflects a dipole of Sea Level Pressures (SLP) anomalies over the north Atlantic Ocean, observing negative(positive) anomalies at northern(southern). This configuration favors over the northern Atlantic coasts of Europe warm and wet air advection, causing positive anomalies of precipitation and temperature over these areas, but negative precipitation anomalies in the southern of Europe. By contrast, during the negative phase, anomaly patterns are reversed. Apart from the NAO, there are some other modes of variability affecting also to the different European regions such as the Artic Oscillation (AO), the East Atlantic (EA), the Scandinavian (SCAND), etc (Barnston and Livezey, 1987). An example of other variability modes affecting even to the interannual global temperature variability is the Southern Oscillation (SO) (Zhang et al, 1997).

The obtainment of circulation indices (Jones et al, 1993) and Circulation Types (CTs) (Beck and Philipp, 2010; García-Valero et al., 2012) are two ways of characterizing the prevalent atmospheric circulation over a region at daily time scale. Circulation indices characterizes the atmospheric situations in order to the direction of fluxes and their vorticity. CTs are a handy ensemble of atmospheric patterns on which the huge number of daily atmospheric situations can be simplified. Hence, from the point of view of a meteorologist, the CTs are those atmospheric situations that he could remember and which are associated with some precipitation and temperature spatial patterns, normally called as their weather regimens or Weather Types (WTs). Links between CTs and WTs are traditionally used to explore the climate variability (Romero et al (1999); Yiou and Nogaj (2004); Fernández-Montes et al (2012), among others) and also for downscaling purposes (Wilby and Wigley, 1997).

1.3 Climate variability in the Iberian Peninsula

The IP is a region with a large climate variability (Font-Tullot, 2000; Lorente-Plazas et al, 2015). Its location at midlatitudes determines the presence of a large variety of atmospheric situations over this territory (García-Valero et al., 2012). In addition, its position between the Mediterranean Sea and the Atlantic Ocean, of very different temperatures especially at the end of summer, autumn and winter, favors that the air masses advected towards the IP acquire very distinct properties on humidity and temperature depending on their provenance regions. This leads to the occurrence of different meteorological phenomena of large spatial-time variability. All these factors joined to its complex orography justify its large climate diversity.

In the last decades, significant changes in precipitation and temperature have been observed in the IP. On the one hand, a decreasing of precipitation in winter and early spring in large areas of the central, western and northern (Corte-Real et al, 1998; MJ. et al, 1998; Serrano et al, 1999; Paredes et al, 2006; López-Bustins

et al, 2008; Martin-Vide and de Luisa, 2009; de Luis et al, 2010; González-Hidalgo et al, 2011; Gallego et al, 2011; Hidalgo-Muñoz et al, 2011; Luna et al, 2012) have been reported. On the other hand, significant positive trends in maximum temperatures (Tx) in spring and summer, practically generalized over the entire territory, as well as similar trends in minimum temperatures (Tm) in the same seasons and autumn have been informed (Brunet et al, 2007; Bermejo and Ancell, 2009; García-Valero et al, 2015). Finally, climate change projections inform about the continuity of such changes in the future, defining this region as one of the hot-spots of the Globe (Giorgi, 2006), especially by the large increase projected for temperatures in summer.

1.4 Objectives and structure of this Thesis

In the former sections, the high degree of the relationships between the prevalent atmospheric dynamics over a region and its climate variability has been manifested. The appearing in the recent years of new observational climate datasets developed for the IP, with a higher temporal-spatial resolution and covering a longer period of years than those available previously, allows a more complete analysis of its climate variability. In the same way, the availability of reanalysis and analysis atmospheric data, of great spatial and time resolution, since the middle of the past century favors to cross them with the observational climate datasets. This facilitates to deep in the relationships existing between the atmospheric and climatic variability. The objective of this Thesis are various.

The first objective consist of characterizing the prevailing atmospheric situations over the IP. To perform this, a seasonal CT classifications is obtained for an historical-recent period (1958-2008). Despite different CT classifications are available for the IP, the longer period covered by this new classification and the methodology followed for its construction are two improvements respect to the previous classifications. Although here, CT classification is obtained for analyzing the variability of temperature and precipitation, this classification can be potentially used for several kind of researchers, from the analysis of other climate variables to environmental applications. Indeed, it has been employed for the characterization of wind and of the air extreme pollution events over the IP.

Another objective is to investigate the influence of the CTs obtained above on the precipitation and temperature variability over the IP along the historical period. To deep on these links, the WTs associated with the CTs are obtained. The WTs are an usefulness tool for carrying out this kind of analysis. They allow to analyze the attribution degree of possible trends in the mean variability of climate variables to the changes in the atmospheric circulation. In addition, they allow to deep about the spatial variability caused under different atmospheric conditions in a territory of great orographical complexity like the IP is.

A third objective is the analysis of the occurrence of summer extremely hot situations under the influence of the atmospheric circulation. The study of these situations through CT classifications as the obtained above could have important difficulties due to the low statistical load that these kind of situations have. Therefore, a new methodology for obtaining specific CT classifications for the analysis of extreme events is proposed. The application of these specific classifications to attribute significant positive trends in the extreme occurrence found in several Spanish regions to changes in the frequency of the CTs is another task of this analysis.

The next objective is the projection of the specific CT classifications to the future (untill 2100), using for that different climate change scenarios. This permits to obtain projections of extreme hot occurrences at several Spanish regions. Different atmospheric field outputs derived from three Earth System Models (ESMs), recently used for the Fifth Assessment Report of the IPCC (2013), are used. Projections allows to investigate the role that dynamics could have on the projections that point to significant temperature increase in the IP.

The final task of this Thesis is to deep on the role of the external forcings on the atmospheric dynamics, and therefore on the climate variability. Three external forcings are analyzed: changes in the total solar irradiance, changes in the atmosphere concentrations of GEI and volcanic activity. To perform this, an ensemble of generalist CT classifications for the Euroatlantic region are stablished from the data of four paleosimulations. The period 1500-1990 is investigated. This exercise is the first attempt of this kind analysis under the CTs perspective.

The structure of this Thesis is as follows. Chapter 1 introduces the Thesis exposing some basic concepts in relation to the climate system, the atmospheric dynamics and the main characteristics of the PI as well as the latest changes occurred in its climate variability. Chapter 2 describes the methodology used for the construction of the CT classification during the period 1958-2008. The synoptical description of the obtained CTs, the analysis of trends in the frequency of CTs as well as of their persistence and of the main transitions among them are also included in this part. In the Chapter 3 the WTs associated with the different CTs are obtained and used for analyzing the role of the CTs on the mean variability of temperature and precipitation over the IP. Chapter 4 presents the methodology for obtaining the specific CTs for the analysis of extremely hot days occurrences over the IP. The method of attribution of trends in this kind events to the atmospheric circulation is also included on this chapter. Chapter 5 includes the results of the climate change projections of the extremely hot events at several Spanish regions. Chapter 6 illustrates the methodology followed to analyze the influence of the forcings on the dynamics under the optics of the CTs. Finally, Chapter 7 outlines the main conclusions obtained in this Thesis. All chapters include an introduction and a methodology part which further describes their

contents.

Bibliography

Barnston, A. G. and Livezey, R. E.: Classification, seasonality and persistence of low-frequency atmospheric circulation patterns, Monthly weather review, 115, 1083–1126, 1987.

Beck, C. and Philipp, A.: Evaluation and comparison of circulation type classifications for the European domain, Phisics and Chemistry of the Earht, 35, 374–387, 2010.

Berger, A.: Milankovitch Theory and climate, Reviews of Geophysics, 26, 624–657, doi:10.1029/RG026i004p00624, URL `http://dx.doi.org/10.1029/RG026i004p00624`, 1988.

Bermejo, M. and Ancell, R.: Observed changes in extreme temperatures over Spain during 1957-2002, using Weather Types, Revista de Climatología, 9, 45–61, 2009.

Brunet, M., Jones, P., Sigró, J., Saladié, O., Aguilar, E., Moberg, A., Della-Marta, P., Lister, D., Walther, A., and López, D.: Temporal and spatial temperature variability and change over Spain during 1850-2005, Journal of Geophysical Research, 112, 2007.

Corte-Real, J., Qian, B., and Xu, H.: Regional climate change in Portugal: precipitation variability associated with large-scale atmospheric circulation, International Journal of Climatology, 18, 619–635, 1998.

de Luis, M., Brunetti, M., Gonzalez-Hidalgo, J. C., Longares, L. A., and Martin-Vide, J.: Changes in seasonal precipitation in the Iberian Peninsula during 1946–2005, Global and Planetary Change, 74, 27–33, 2010.

Fernández-Montes, S., Rodrigo, F., Seubert, S., and Sousa, P.: Spring and summer extreme temperatures in Iberia during last century in relation to circulation types, Atmospheric Research, 2012.

Font-Tullot, I.: Climatología de España y Portugal, University of Salamanca (Spain), 2000.

Gallego, M., Trigo, R., Vaquero, J., Brunet, M., García, J., Sigró, J., and Valente, M.: Trends in frequency indices of daily precipitation over the Iberian Peninsula during the last century, Journal of Geophysical Research: Atmospheres (1984–2012), 116, 2011.

García-Valero, J. A., Montávez, J. P., Gómez-Navarro, J. J., and Jiménez-Guerrero, P.: Attributing trends in extremely hot days to changes in atmospheric dynamics, Natural Hazards and Earth System Science, 15, 2143–2159, doi:10.5194/nhess-15-2143-2015, URL `http://www.nat-hazards-earth-syst-sci.net/15/2143/2015/`, 2015.

García-Valero, J., Montavez, J., Jerez, S., Gómez-Navarro, J., Lorente-Plazas, R., and Jiménez-Guerrero, P.: A seasonal study of the atmospheric dynamics over the Iberian Peninsula based on circulation types, Theoretical and Applied Climatology, 110, 291–310, doi:10.1007/s00704-012-0623-0, URL `http://dx.doi.org/10.1007/s00704-012-0623-0`, 2012.

Giorgi, F.: Climate change hot-spots, Geophysical Research Letters, 33, 2006.

González-Hidalgo, J. C., Brunetti, M., and de Luis, M.: A new tool for monthly precipitation analysis in Spain: MOPREDAS database (monthly precipitation trends December 1945–November 2005), International Journal of Climatology, 31, 715–731, 2011.

Hidalgo-Muñoz, J., Argüeso, D., Gámiz-Fortis, S., Esteban-Parra, M., and Castro-Díez, Y.: Trends of extreme precipitation and associated synoptic patterns over the southern Iberian Peninsula, Journal of Hydrology, 409, 497–511, 2011.

Holton, J. R. and Hakim, G. J.: An introduction to dynamic meteorology, vol. 88, Academic press, 2012.

Huybers, P. and Curry, W.: Links between annual, Milankovitch and continuum temperature variability, Nature, 441, 329–332, 2006.

IPCC: Climate Change 2013: The physical science basis: Working group I contribution to the fifth assessment report of the Intergovernmental Panel on Climate Change, Cambridge University Press, 2014.

Jones, P., Hulme, M., and Briffa, K.: A comparison of Lamb circulation types with an objective classification scheme, International Journal of Climatology, 13, 655–663, 1993.

López-Bustins, J., Martín-Vide, J., and Sánchez-Lorenzo, A.: Iberia winter rainfall trends based upon changes in teleconnection and circulation patterns, Global and planetary change, 63, 171–176, 2008.

Lorente-Plazas, R., Montávez, J., Jimenez, P., Jerez, S., Gómez-Navarro, J., García-Valero, J., and Jimenez-Guerrero, P.: Characterization of surface winds over the Iberian Peninsula, International Journal of Climatology, 35, 1007–1026, 2015.

Lorenz, E. N.: Atmospheric predictability as revealed by naturally occurring analogues, Journal of the Atmospheric sciences, 26, 636–646, 1969.

Luna, M., Guijarro, J., and López, J.: A monthly precipitation database for Spain (1851–2008): reconstruction, homogeneity and trends, Adv. Sci. Res, 8, 1–4, 2012.

Martin-Vide, J. and de Luisa, M.: Monthly precipitation trends on the Mediterranean fringe of the Iberian Peninsula during the second-half of the twentieth century (1951–2000), Int. J. Climatol, 29, 1415–1429, 2009.

MJ., E.-P., Rodrigo, F., and Castro-Diez, Y.: Spatial and temporal patterns of precipitation in Spain for the period 1880-1992, International Journal of Climatology, 18, 1557–1574, 1998.

Paredes, D., Trigo, R. M., Garcia-Herrera, R., and Trigo, I. F.: Understanding precipitation changes in Iberia in early spring: weather typing and storm-tracking approaches, Journal of Hydrometeorology, 7, 101–113, 2006.

Rodriguez-Puebla, C., Encinas, A., Nieto, S., and Garmendia, J.: Spatial and temporal patterns of annual precipitation variability over the Iberian Peninsula, International Journal of Climatology, 18, 299–316, 1998.

Romero, R., Sumner, G., Ramis, C., and Genovés, A.: A classification of the atmospheric circulation patterns producing significant daily rainfall in the spanish mediterranean area, International Journal of Climatology, 19, 765–785, 1999.

Serrano, A., Mateos, V., and Garcia, J.: Trend analysis of monthly precipitation over the Iberian Peninsula for the period 1921-1995, Physics and Chemistry of the Earth, Part B: Hydrology, Oceans and Atmosphere, 24, 85–90, 1999.

Wilby, R. and Wigley, T.: Downscaling general circulation model output: a review of methods and limitations, Progress in Physical Geography, 21, 530, doi:10.1177/030913339702100403, 1997.

Wilby, R., Charles, S., Zorita, E., Timbal, B., Whetton, P., and Mearns, L.: Guidelines for use of climate scenarios developed from statistical downscaling methods, 2004.

Yiou, P. and Nogaj, M.: Extreme climatic events and weather regimes over the North Atlantic: When and where?, Geophysical Research Letters, 31, 1–4, 2004.

Zhang, Y., Wallace, J. M., and Battisti, D. S.: ENSO-like interdecadal variability: 1900-93, Journal of Climate, 10, 1004–1020, URL <GotoISI>://A1997XB77300010, 1997.

Chapter 2

A seasonal study of the Atmospheric Dynamics over the Iberian Peninsula based on Circulation Types

2.1 Introduction

The classification of the atmospheric circulation over a region in a discrete set of atmospheric patterns may result an unrealistic task if we take into account the chaotic nature of the atmospheric dynamics (Lorenz, 1956). Nevertheless, from a synoptic point of view, the atmospheric patterns defined by large-scale variables (generally sea level pressure or geopotential at a given level) present recurrent spatial configurations that could be considered as the attractors of the system. They are usually named Circulation Types (CTs). Traditionally, the CTs have been used for the analysis of the regional climatic variability of elements such as precipitation (Gallego, 1995; Romero et al, 1999), temperature (Bermejo and Ancell, 2009; Philipp et al., 2006; Cassou et al, 2005; Yiou et al, 2008) and wind (Jiménez et al, 2008) so that their influence in these variables has been used to develop conceptual models or empirical-statistical relations useful for prediction. Nowadays its use has been extended to other interesting climatological applications like the validation of climate models (Crane and Barry, 1988; Hulme et al, 1993; Huth, 2000) or the possible changes in the circulation under different climate change scenarios (Kyselý and Huth, 2006; Huth, 1997).

The first classifications started to be developed in the second half of the twentieth century (Hess and Brezowsky, 1952; Lamb, 1950). The synoptic patterns were grouped according to a number of subjective rules adopted by experts. The limitation of these classifications lied on the assignation of the states in the different groups when the databases were very large; so, they were usually developed for relatively short periods (10-15 years). The availability of gridded atmospheric databases (e.g. NCAR, ERA40) carried out the development of objective techniques on assignation. The most frequently used among them are: (1) correlation method (Lund, 1963); (2) sums of squares (Kirchhofer, 1974); (3) cluster analysis

(Key and Crane, 1986); and (4) principal component analysis (PCA) (Richman, 1981). Huth (1996) shows a comparative study of the aforementioned methods, concluding that those using PCA get the best results. Specifically, the T-mode rotated PCA is the method reproducing more realistically the underlying physic structure of the data, providing the most stable clusters in time and space. Furthermore, the non-hierarchical grouping method K-means obtains a larger separation among clusters, albeit requires a set of seeds for its initialization. With the aim of joining the quality of two methods, Huth (2000) and Kyselý and Huth (2006) proposed a clustering methodology in two stages. The first stage provides a set of seeds as a result of applying the T-mode rotated PCA, whereas the second stage consists on a K-means grouping initialized from the seeds obtained in the previous stage. In the last years new classifications have added considering other non-hierarchical clustering methods like SANDRA (Simulated Annealing and Diversified Randomization, Philipp et al. (2006)) and SOM (Self Organizing Maps, Bermejo and Ancell (2009); Hewitson and Crane (2002)). The main attribute of SANDRA is its capability to obtain clusters with an high quality and stability (Philipp et al., 2006). The quality of a clustering is defined as the proportion of the original variance explained by the groups (Ec. 2.1), while the stability is defined as the probability to obtain the same clusters when they are achieved using shorter or different temporal periods. Clusters with high quality and stability allow making more realistic studies of the frequencies, persistences and transitions of the different CTs (Beck and Philipp, 2010; Huth, 1996). The trend analysis of the annual or seasonal frequency series of the CTs is an interesting exercise that helps understanding, under a climate change context, some of the regional changes observed (Bárdossy and Caspary, 1990; Philipp et al., 2006) or projected in precipitation, temperature or other variables if we previously know the influence on them of the CTs. Despite the number of methods existing, none of them present a clearly superior behavior (Philipp et al, 2010, COST733) so that its selection depends on the criteria of the researchers based on their experience and the objectives of the classification (Casado et al, 2008).

The results of the clustering process are sensitive not only to the method considered, but also to other parameters such as the large-scale variable or variables considered for the definition of the CTs, the size and the resolution of the clustering window (Jiménez et al, 2008; Demezure et al, 2008; García-Bustamante et al, 2012), the seasonalization (or not) of the classification, the number of principal components (PCs) to be retained (when adopting a classification scheme based on the PCA) and the number of clusters to consider (Michelangeli et al, 1995; Philipp et al., 2006; Fereday et al, 2008). These variables largely affect the results of the classification. The election of the synoptic variables for characterizing the CTs obeys to practical criteria (e.g. their availability and mainly the objective of the classification). Frequently most of those obtained for Europe and other regions were developed using the sea level pressure (SLP) in order to relate the classifications to regional variables influenced directly by the state of the low levels of the atmosphere, like surface temperature (Philipp et al., 2006; Cassou

et al, 2005; Yiou et al, 2008), the sea surface temperature (Fereday et al, 2008) or the wind (Jiménez et al, 2008). Other classifications used the geopotential at 500 hPa (Z500) (Kirchhofer, 1974; Casado et al, 2008; Yiou and Nogaj, 2004), which provides a global vision of the average state of the atmosphere. In a lesser extent, several authors used together the SLP and Z500 for characterizing the atmospheric dynamics with the aim of analyzing precipitation (Gallego, 1995; Romero et al, 1999; Petisco, 2003). Precipitation is specially sensitive to the moisture fluxes at low levels, governed by the distribution of the pressure field at those levels. Nonetheless, in regions where the rain regime is very irregular and most of precipitation is convective, as occurring during the warm half of the year in the mediterranean area of the Iberian Peninsula (Font-Tullot, 2000), the advective component of the low levels defined by the SLP is not enough to explain its variability, and hence it should be to consider in addition the degree of average atmospheric instability represented by Z500.

The size and resolution of the clustering window are two parameters which should be adequated to the objectives of the classification. An indirect relation should exist between them to improve the quality of the clusters; that is, high resolutions should be avoided when using large windows, and low resolutions when the windows are small. Generally, most of the authors that have characterized the circulation in big regions as Europe used windows that covered this entire region and a large portion of the northern Atlantic, with resolutions between 2.5^o and 5^o. Here we intend to characterize the circulation over a smaller area, and hence it seems logical to use higher resolutions and smaller windows, covering at least the target area. Working with small windows helps improving the quality of the clustering, specially when the clustering method uses the results of a PCA, because the variability modes whose origin responds to remote areas with small influence in the target area will not appear in the clusters. The idea of developing (or not) seasonal classifications is another aspect to consider, and depends in a great extent on the level of detail persued by the classification. Furthermore, the reduction of the database in more homogeneous samples may lead to an improvement in the quality of the clusters obtained. On the other hand, if the regional variable analyzed with the CTs presents an important seasonal variability, the separation by seasons will be more justified.

Probably one of the most determining factors is the number of groups to consider in the classification. Choosing a reduced number could be not enough to characterize the atmospheric variability; albeit the election of a too large number deviates from the sense of this kind of classifications, which is having a handy number of situations. For its election, different methods have been used (Milligan, 1980) based upon quality (pseudo-F indicator (Calinski and Harabasz, 1974), variance fraction explained by the groups,...) and stability criteria (Michelangeli et al, 1995). More sophisticated indices have been developed like Silhouette (Kaufman and Rousseeuw, 1990), which indicates that the centroids of the clusters are located in regions of high object density, or Overlap (Gesterngarbe and Werner, 1997), which assesses the overlaping ratio of object between two clus-

ters. However, in all these indices the researcher must take a subjective decision, because generally there is always more than a possible option that highlights the nonexistence of a genuine number of groups (Philipp et al., 2006; Fereday et al, 2008).

The Iberian Peninsula (IP) is considered as a climate change hot-spot (Giorgi, 2006). The trends for temperature and precipitation along the 20th century highlight a rising temperature specially during summer and spring (Brunet et al, 2007); and a decrease of precipitation at the end and beginning of winter and spring, respectively, mainly in the last three decades (Serrano et al, 1999). The decrease of precipitation has been related with a northern shift of the storm tracks (Paredes et al, 2006), which is compatible with the increase and/or decrease in frequency or persistence of some CTs. The trends observed together with the projections of climate change forecasting drier and warmer conditions in summer and spring make of this region a place of special interest for the study of the atmospheric circulation.

Hence, this work aims to characterize the daily circulation over the IP. For that, several clusters of CTs have been obtained for each season of the year; thus improving the up-to-date classifications for the Iberian Peninsula (Petisco, 2003; Rasilla, 2003; Romero et al, 1999; Goodess and Palutikof, 1998; Jiménez et al, 2008), who did not take into account the seasonal separation. The characterization of the CTs has been made considering SLP and Z500. Both have been included together in the PCA previous to the clustering method considered, which involves a differentiating element from the rest of the classifications using two variables (that used the PCA separately for each of them, Romero et al 1999). The classification period covered was 1958-2008 extending the periods considered in the previous works aforementioned. This period presents an important relevance for the analysis of frequencies, persistence and transitions of the CTs because of the great variability depicted over the IP. So, in the first half of the period there was a predominance of cold and wet years, meanwhile in the last years there are some of the warmest and driest years during the instrumental period (Brunet et al, 2007). This contribution is organized as follows: Sec. 2 describes the database and the clustering window considered; Sec. 3 shows a previous comparative study of the algorithms K-means and SANDRA over the target clustering window and describes the method followed for the classifications. Sec. 4 indicates the CTs obtained and the analysis of their frequency and persistence together with the most significant transitions. Conclusions are summarized in Sec. 5.

2.2 Data

Daily operational analysis (2003-2008) and reanalysis (1958-2002) at 12:00 UTC data from the European Center for Medium-Range Weather Forecast (ECMWF) (Uppala et al., 2005) have been used for the characterization of the CTs. The variables employed were sea level pressure (SLP) and 500 hPa geopotential height (Z500).

The maximum common resolution (1.125 degrees) was used, covering the period 1958-2008 (18973 days). The use of analysis and reanalysis data togheter could be a potential problem, obtaining some inconsistencies. In order to guarantee the homogeneity of the Analysis plus Reanalysis data we have analyze the mean and variance of the time series of both variables (spatial averaged over the small window) SLP and Z500. We have detected some small changes, but anyway they pass the Penalized Maximal F test (Wang, 2008)

The spatial window considered for the characterization of the CTs consist of 150 grid points, with coordinates ranging from 34.875^{o}N-45^{o}N and 10.125^{o}W-5.625^{o}E. Nevertheless, in order to have a view of the synoptic situation defined by each CT a larger window has been used for their representation, formed by 1364 grid points and centered over the IP (Fig 2.1).

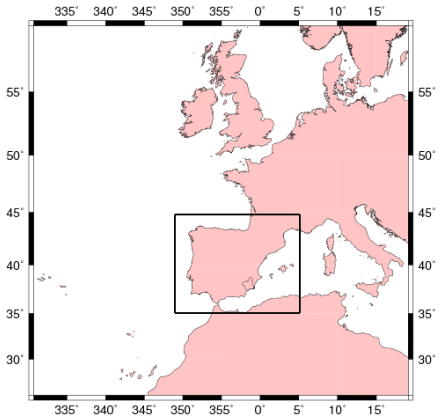

Figure 2.1: Windows employed for representation (larger) and clustering (inner).

2.3 Clustering methodology

As commented in Section 2.1 there are many clustering algorithms that are frequently used for getting CTs. Depending on the region where they are obtained a same algorithm might perform very differently, so it might be a good algorithm for certain regions and not as good for others (Beck and Philipp, 2010; Philipp et al, 2010). Therefore, in order to select a good algorithm for the study region, in this section it is performed a comparison study of the results obtained over the Iberian Peninsula, using two methods: K-means one of the most widely methods employed, and SANDRA more recently used for this purpose (Philipp et al., 2006). Both methods were initialized using the results from a previous Principal Components Analysis (PCAs) applied to the data, the details about the PCA analysis are also explained in this section. To evaluate the results of both clustering methods we have taken into account the quality and stability of the clusters. First, a summary discussion of these statistics is presented in this section. The

definitive clustering method followed to obtain the CTs for this study is presented at the end of this section.

Principal Component Analysis (PCA)

The Principal Component Analysis (PCA) is a tool extensively used in climatological research. A more detailed description can be found in Storch and Zwiers (1999); Hannachi et al (2007); Preisendorfer (1988). Its objective is the representation of the original data in a new orthogonal space of functions representing the main variation modes of the system. Hence, the correlation degree existing in the initial data is removed, and therefore eliminating a significant source of noise for other types of analysis like clustering. The variation modes are named Empirical Orthogonal Functions (EOFs) and correspond to the eigenvectors of the correlation matrix or covariance of the anomalies of the original data. The projections of the original data in these new functions are called Principal Components (PCs). Their main characteristic is the non-existence of correlation among them. For the projections, only the EOFs with a significant weight in the global variance are used, and that corresponds to those whose eigenvalues associated have the highest values. The election of the number of representative EOFs involves a high degree of subjectivity, and therefore different methodologies have been developed (Cattell, 1966; Wilks, 1995).

In this study, the PCA has been carried out in the S-Mode of operation, considering the grid points as variables and the temporal stages as events. This configuration is adopted because of the lower number of dimensions in the correlation matrix, 300 (150 for SLP and 150 for Z500) versus over 4500 (number of episodes of each of the seasonal matrices) in the case of choosing a T-Mode configuration (temporal stages as variables). The joint use of SLP and Z500 in the PCA requires of a previous step of complete standardization by grid point for both variables, in order to avoid the dominance of the variable with the largest variability in the PCA (in this case, Z500). For the standardization long term mean and variance were considered for each grid point. The utilized method for retaining the number of EOFs uses the graphic log(eigenvalue) vs. number of PCs. (Wilks, 1995). Its shape determines the number of PCs retained, which comes conditioned by the number of components to the right of a line extrapolated to the left from a significant discontinuity of the value of log(eigenvalue) (Fig.2.2).

Testing methods

Any process whose objective is the clustering of elements in series of ensembles should take into account that each cluster must be as homogeneous as possible and different from the rest. The ratio of the global Explained Cluster Variance (ECV) is a quality index that allows assessing the goodness of the cluster (Ec 2.1). This index is defined as the ratio between the sum of the internal variance of all the groups (with cluster Sum of Squares, WSS) and the total variance of all the

elements without clustering (Total Sum of Squares, TSS). It ranges between 0 and 1. The zero value indicates that the cluster obtained is worthless, meanwhile the unit value refers to a perfect clustering, generally obtained when considering as many groups as elements. Hence, the higher the number of clusters considered, the better the quality of the clustering.

$$ECV = 1 - (WSS/TSS) \tag{2.1}$$

The aim of studies like this is to obtain a reduced number of clusters with an important representation of the variability observed. The election of a reduced but manageable number provokes that a fraction of the variance cannot be explained with the clustering, especially in those cases when the number of elements is high.

In addition to the ECV, there are more indices informing about other interesting aspects of the clustering obtained. One among them is that index measuring the degree of stability of the clustering, determining the robustness of the different clusters. Clustering is meaningless if we obtain different clusters every time we apply the clustering methodology to the same period or comparable temporal periods, whereas robust clustering methods can reproduce the same or very similar clusters in different temporal periods. This index can be obtained through the cross-validation technique, that compares the clusters obtained for a long period with groups obtained for shorter times and contained in the former period, and that can be selected specifically or randomly.

If we choose a number of clusters (for the short periods) identical to the clustering we are testing, we will be able to cross the common elements in each cluster of the short period with the long period. Hence, each short-period cluster will present a higher percentage of its days in common with any of the long-period cluster. The stability of the long-period clusters is defined as the percentage of common days with its most-related short cluster, getting the percentage with respect to the total number of days of the short cluster. If the cross-validation test is made considering more than a short period, the stability of each group is defined as the average of their stability. The stability of the whole clustering is defined as the average of the stability of all the clusters of the long period. Differently from the quality, the stability of a clustering increases when the number of considered clusters is lower, since the possibilities of assigning elements in different clusters is lower (Fereday et al, 2008; Michelangeli et al, 1995).

The skill of both algorithms, K-means and SANDRA, was tested over the study region for wintertime (DJF). It can be found a more detailed information of these algorithms in Hartigan and Wong (1979) for K-means and in Philipp et al. (2006); Fereday et al (2008) for SANDRA. Both were applied to the Principal Components of the data. For the initialization of both algorithms, we used the same seeds achieved trough a K-means multistart clustering, initialized 1000 times with seeds randomly chosen in each run. SANDRA algorithm was specifically developed to allow relocation of 15% of the furthest elements from each cluster. The consideration of these elements to form the neighborhood reduces

the computational cost required by SANDRA, and even more if we chose a cooling coefficient of 0.9 (as used in this study), which forces to run the algorithm an important number of times for a higher approach of the cluster to the global optimum (Fereday et al, 2008). Therefore, 1000 runs were performed considering the highest quality run as the definitive clustering.

For the stability tests, two periods of 50 and 25 years were used, the latter included in the former. For both periods, the seeds were those obtained through K-means multistart in the shorter period. The quality results obtained by SANDRA were slightly better, but the stability of the clusters found for K-means was notably higher (stabilities over 75% in 75% of the clusters; with SANDRA just 40% of the clusters achieved that stability). The stability results, essential for analyzing other characteristics of the CTs (frequency, persistence and transitions), together with the higher computational time required by SANDRA, led us to consider K-means as clustering algorithm.

2.3.1 Final clustering method

Albeit the comparison tests described before used the seeds from the K-means multistart, for the final clustering we decided to use seeds coming from a PC-ModeT clustering whose ability to form groups with physical sense has been demonstrated elsewhere (Huth, 1996). The PC-ModeT method uses the T-Mode EOFs, obtained from the PCs of the S-Mode used here (Section 2.3) normalizing the components by the squared root of their associated eigenvalue. To provide a higher physical sense, the T-Mode EOFs were rotated using the varimax method (Richman, 1981). The T-Mode EOFs represent temporal variability patterns, so that the days with a weight contribution similar to those modes also present similar spatial patterns. PC-ModeT utilizes this property to assign the elements to different clusters. So, the days whose highest weight presents the same sign in the same EOF are grouped together. The positive or negative sign of the weights defines the number of clusters to consider, twice as many as the number of the PCs retained, allowing a simple and objective election of the number of clusters. Starting from the PC-ModeT clusters, the seeds needed for the initialization of K-means run over the PCs of the S-mode were obtained.

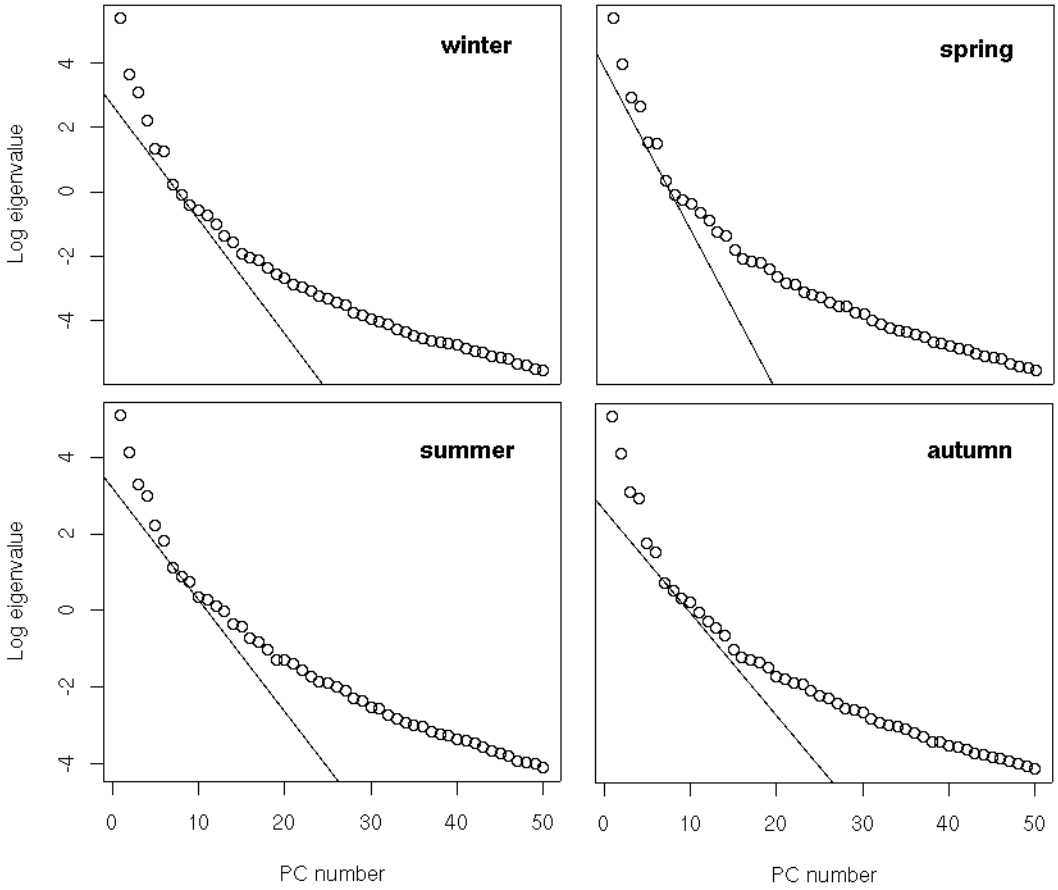

Figure 2.2: log(eigenvalue) vs PC number used for the retention of the proper number of principal components. For all seasons, the value of log(eigenvalue) stabilizes from the sixth component.

2.4 Results

2.4.1 Seasonal Circulation Types

Figure 2.2 depicts the PCA results when applied to the reanalysis data for each season. According to the retention method of PCs (Section 2.3), in all them six components are enough for an accurate representation of the variance, retaining with them the 97% of the variance for spring, autumn and summer, and 94% for summertime. Taking into account the clustering method explained in the Subsection 2.3.1, six PCAs define twelve CTs or clusters. In Figures 2.3, 2.4, 2.5 y 2.6 the centroids of each cluster obtained for each season are represented. The numbering corresponds to the number (frequency) of situations clustered, so that CT1 is the most crowded. Their relative seasonal frequencies are shown in Table 2.1.

If we analyze the centroids obtained from a synoptic point of view, some of them belonging to different seasons have a very similar pattern. Hence, the spring

Table 2.1: Relative Seasonal frequencies of CTs. Units are percentage.

	CT1	CT2	CT3	CT4	CT5	CT6	CT7	CT8	CT9	CT10	CT11	CT12
Winter	13.9	12.3	9.5	9.0	8.0	7.5	7.3	7.0	6.8	6.4	6.3	5.8
Spring	13.7	9.7	9.2	9.2	8.9	8.5	7.8	7.4	6.8	6.6	6.2	5.9
Summer	12.5	12.4	10.9	9.9	9.7	8.6	8.1	6.6	6.3	6.0	4.9	4.0
Autumn	15.2	13.6	12.4	8.9	7.7	7.3	6.5	6.3	6.1	5.8	5.8	4.4

Table 2.2: Patterns described by the CTs. Five general situations were used for the classification: Cyclonic (C), Anticyclonic (A), Zonal (Z), Hybrid-Mixed (M) and Summer patterns (S)

Description	CTs
A1. Anticyclone over the IP at all levels	CT1-wi,CT3-sp
A2. Anticyclone of meridian axis at the eastern Azores	CT8/12-wi,CT9-sp,CT10-au
A3. Anticyclone at the SW UK with anticyclonic circulation aloft over the IP	CT9-wi,CT4-sp,CT9-au
A4. Anticyclone at the NW IP of tilted axis (SW-NE) with northern circulation aloft	CT4-wi,CT6-sp
A5. Anticyclone over the Azores of tilted axis (SW-NE) with NW circulation aloft over the IP	CT6/7-su,CT4-au
A6. Anticyclone of zonal axis over central Europe with anticyclonic circulation aloft over the IP	CT5-wi,CT3-au
C1. Extratropical Cyclone at the NW IP	CT6-wi,CT7-sp,CT8-au
C2. Extratropical Cyclone towards the S IP	CT11-wi,CT8-sp,CT12-su,CT7-au
C3. Extratropical Cyclone at the E IP	CT10-wi,CT10-sp,CT12-au
C4. High-amplitude trough over the IP	CT11-sp
Z1. Extratropical Cyclone close to the UK with zonal circulation aloft over the IP	CT3/7-wi,CT5-sp,CT11-su,CT5/11-au
M1. Anticyclone of zonal axis over central Europe with cyclonic circulation aloft over the IP	CT2-wi,CT6-au
M2. Anticyclone at the SW UK with cyclonic circulation aloft over the IP	CT12-sp
M3. Anticyclone of tilted axis (SW-NE) over the Azores with SW circulation aloft over the IP	CT5-su
S1. Stagnant situation over the IP and anticyclonic ridge aloft	CT1-sp,CT1-au
S2. Stagnant situation with SW circulation aloft	CT2-sp,CT4/9-su,CT2-au
S3. Thermal low at the SW IP	CT1-su
S4. Thermal low at the central IP	CT2-su
S5. Thermal low at the SE IP	CT3-su
S6. Thermal low at the central-S IP and trough aloft	CT8/10-su

and autumn patterns become a mixture of winter and summer patterns. An example of this behavior is shown in the cyclonic situations at the northwestern of the IP during winter, spring and autumn (CT6-wi, CT7-sp and CT8-au), as well as in conditions of low pressure gradient over the IP, which are more frequent during the warm months (CT2-sp, CT4/9-su and CT8-au). In order to simplify the interpretation of the 48 CTs obtained, they have been regrouped subjectively (clusters with similar synoptic patterns) into 21 situations (Table 3.1) with diverse synoptic characteristics over the IP. The naming and order of each of these situations refer to a more generalist clustering in 5 groups: Anticyclonic (A), Cyclonic (C), Zonal (Z), Summertime (S) and Hybrid-Mixed (M). The groups A and C cover the CTs presenting an important degree of cyclonity (both negative and positive, respectively) in the surface (SLP) and height variables (Z500). Z group is considered when the patterns defined by Z500 show an important western circulation. S group is related to the summertime situations where mesoscale centers of low pressure appear over the IP, resulting from the strong surface heating inland the IP. Within these summer types, also similar situations appearing during spring and autumn have been included. They are those with a negligible pressure gradient over the IP. Last, M situations cover those CTs related to the existence of low pressures at the surface and high pressures aloft (or vice versa); that is, situations with a clear disconnection between the low and high levels of the atmosphere.

The CTs obtained form a cluster of synoptic patterns that can be recognized in other previous classifications over the IP. Those classifications were obtained through subjective (Font-Tullot, 2000; Gallego, 1995) and objective methods (Petisco, 2003; Rasilla, 2003; Romero et al, 1999). The comparison with all them is a complex exercise due to the diverse methodologies, atmospheric variables, time periods and geographic windows considered, and also because of the different applications they were designed for. If the comparison is done versus classifications obtained with larguer windows and lower resolution (5^o) (Petisco, 2003; Rasilla, 2003) a better representation of the extratropical disturbances is obtained in the surroundings of the IP in our classification, together with a higher level of detail in mesoscale meteorological structures. An example is observed in the CTs related to summertime situations where the usual position of the Thermal Lows formed inland the IP is clearly depicted (CT1/3-su). Another mesoscale perturbation is the Mediterranean coastal trough, which is a well-known print of the surface pressure field originated by orographic effects after the pass of frontal system through the eastern IP (CT7/8-wi). On the other hand, if comparing with the classification obtained by using similar windows and variables, such as Romero et al (1999), generally a high coincidence is observed between those patterns related to the existence of extratropical cyclones over the IP. The classification of Romero et al (1999) was developed with the aim of characterizing the CTs responsible for the precipitations over the Mediterranean slope of the IP, therefore it presents an important bias towards cyclonic situations (they only used rainfall days) which hampers the comparison of the rest of CTs obtained here. Last, if we compare versus the 23 situations obtained subjectively in Font-Tullot (2000), very similar patterns to those observed with the pseudo-subjective 21 generic situations obtained in this work (Table 3.1). Anyway, several differences are appreciated especially in those patterns related to the presence of deep low pressure sysmtems located at the northern Atlantic, far from the geographic window considered in our classification.

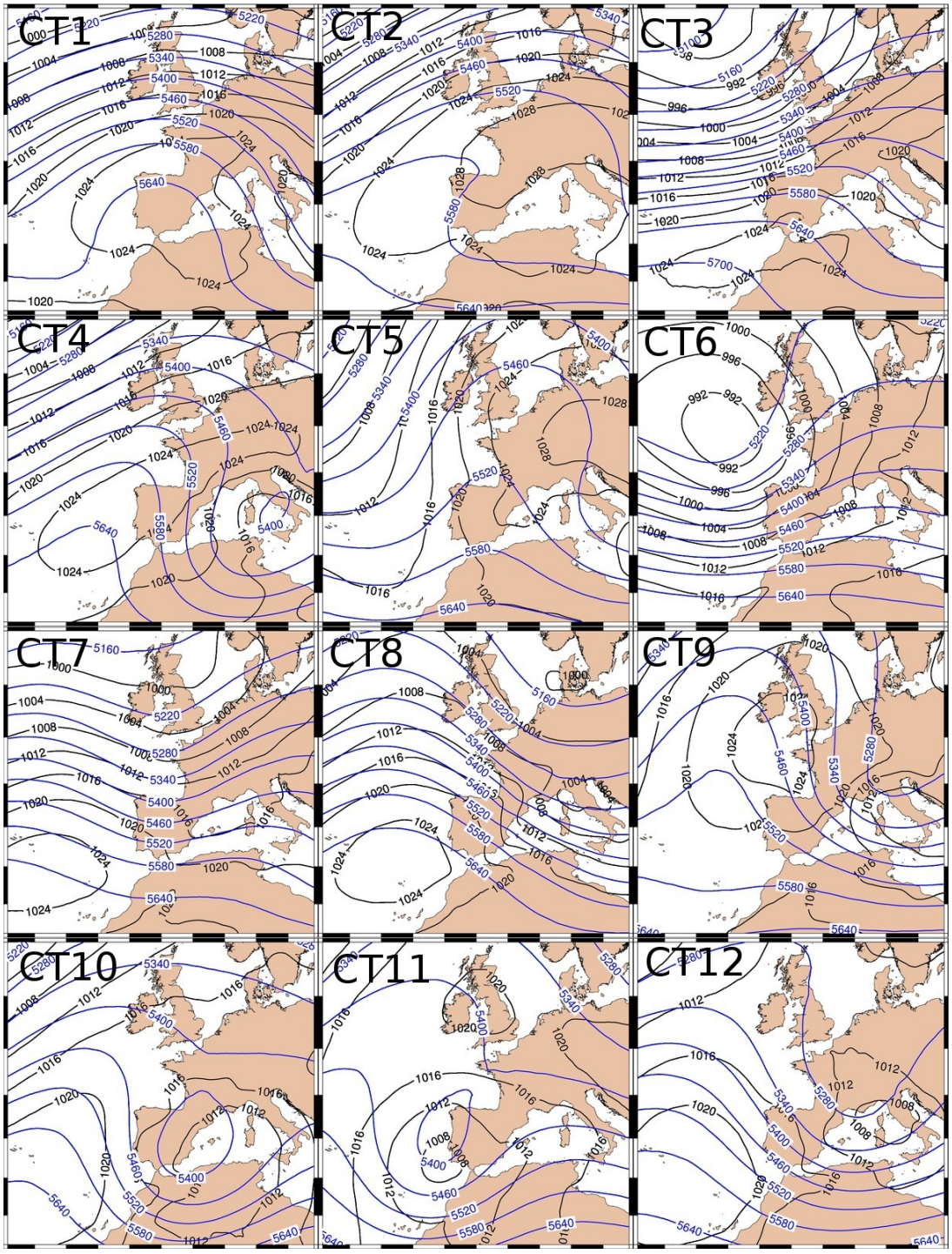

Figure 2.3: Wintertime CTs. The order corresponds to the higher or lower number of days grouped within each cluster. CT1 clusters the largest number of days. Black contours show SLP isobars and blue contours Z500.

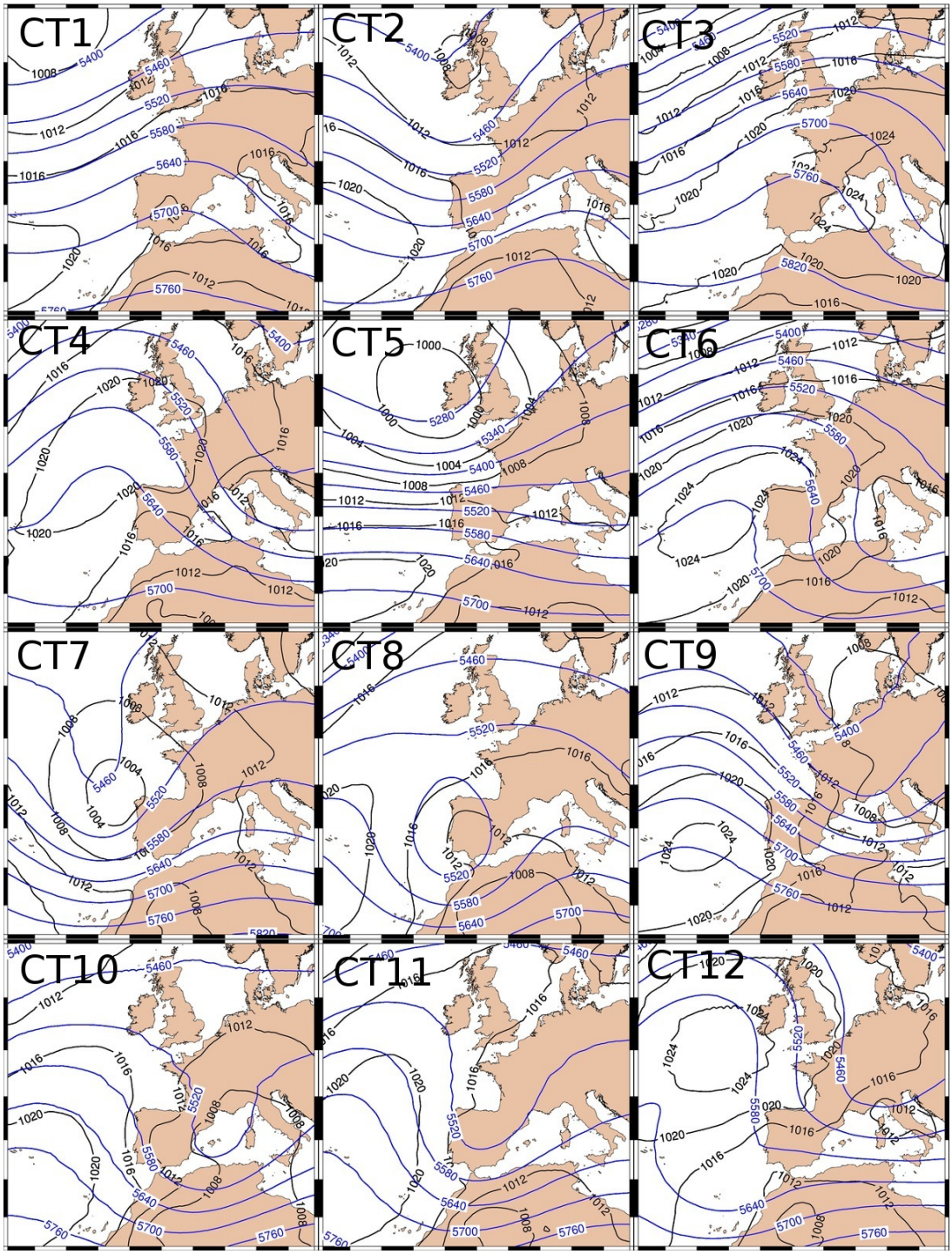

Figure 2.4: As figure 2.3 for Spring.

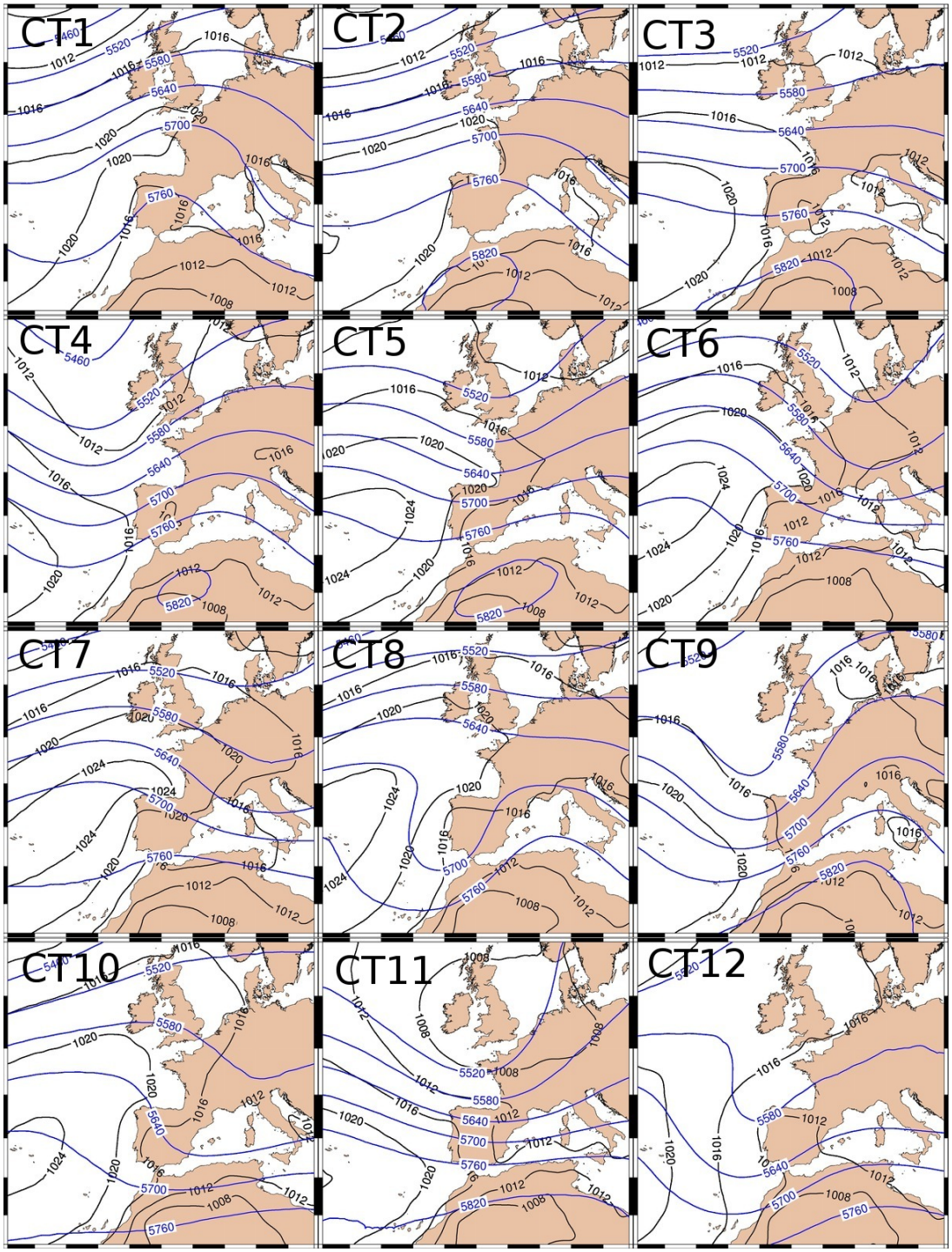

Figure 2.5: As figure 2.3 for Summer.

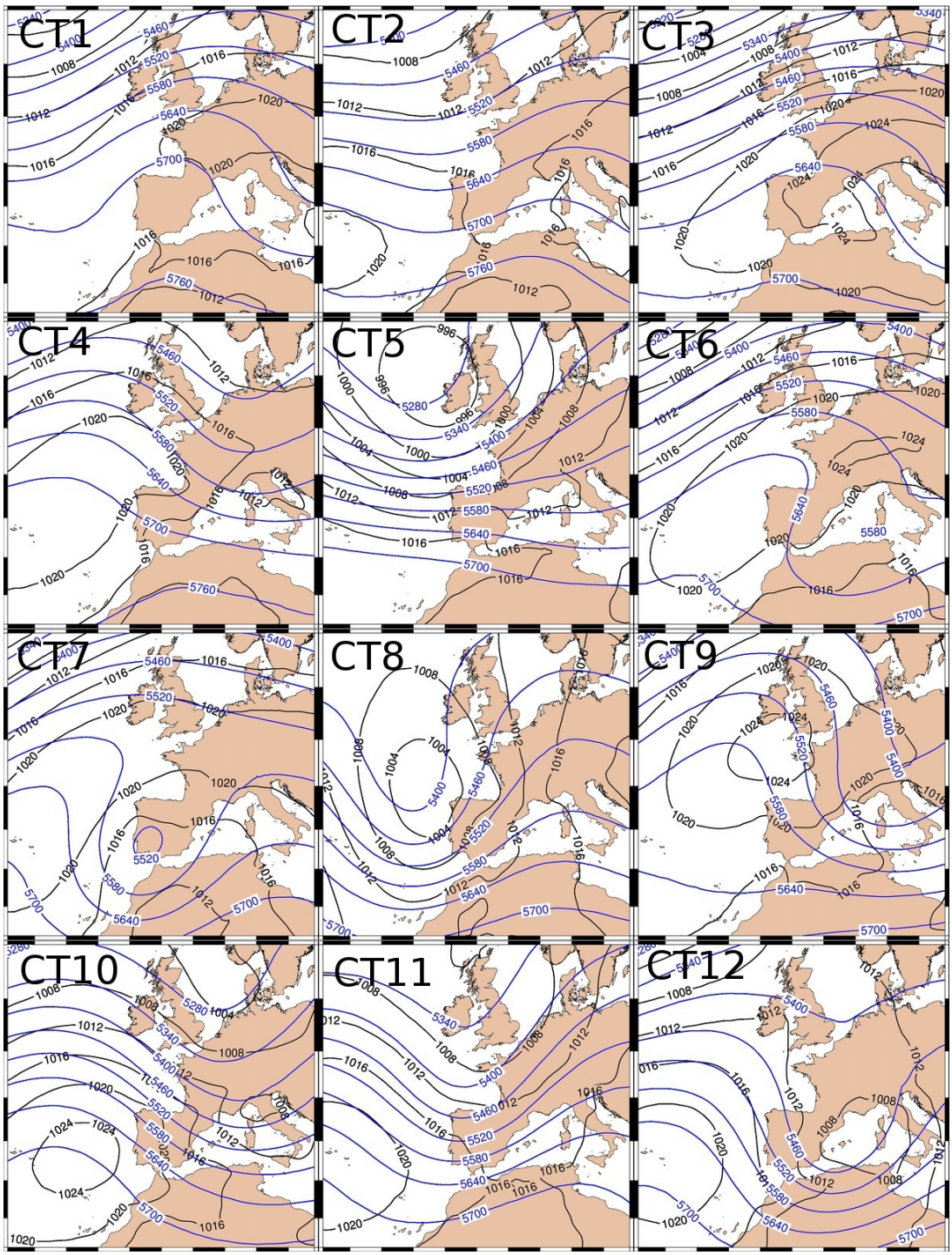

Figure 2.6: As figure 2.3 for Autumn.

2.4.2 Seasonal frequency

The seasonal frequency of the different CTs dominating over a region is associated, more or less directly, to the annual cycle of climatic elements (precipitation, temperature, etc.). Here we will try to relate in a descriptive way the seasonal frequency obtained for each of the five large situations obtained (Section 2.4.1) to the annual cycle observed over the IP of some climatic elements such as precipitation. It is important to remind that over most of the regions in the IP a Mediterranean climate dominates, whose essential characteristic is the scarce precipitation during summertime. However, in its northern border (an also in some regions in its western half) they present an Atlantic-influenced climate, and therefore a more regular precipitation regimen throughout all the year (Font-Tullot, 2000).

Table 2.1 shows the seasonal frequencies for each of the CTs obtained, whereas Table 2.3 depicts the seasonal frequencies for each of the five general situations (Table 3.1). Generally, a dominance of anticyclonic patterns is observed during most of the year (except during summertime), especially in winter, when their frequency is close to 50% of the total frequency of the rest of situations. Also in winter the zonal situations present a higher frequency (around 20%) which is the highest value of the year for this kind of situations. During wintertime the frequency of cyclonic situations is similar to zonal; however they suffer a significant increase in springtime, reaching its highest annual value, 30%. Similarly, the patterns with negligible pressure gradient over the IP (stagnant situations) acquire a higher leadership, conversely to what happens with zonal and anticyclonic situations. The increase during springtime of cyclonic and stagnant situations favors the development of atmospheric instability, which is related to the increase of the precipitation days observed in several regions of eastern part of the IP (Font-Tullot, 2000). In summer, the low pressure gradients dominate; at the same time there is a nearly complete absence of the cyclonic perturbations and a notable decrease of the zonal circulation. This enhances the atmospheric stability and weak surface winds, favoring the formation of breezes, helping to the cooling of the continental mass of the IP. This atmospheric situation, very unfavorable for the development of precipitation, only allows the development of thunderstorms at certain regions that, because of their geographic characteristics, enhance the convergence of surface land and sea winds. In autumn, an increase in the frequency of anticyclonic and stagnant situations is produced, reaching values similar to those during springtime. On the other hand, the frequency of cyclonic and zonal situations is still very low. Regarding the annual distribution of the frequency of hybrid situations, it is low in spring and autumn. In winter and summer it presents important values. In winter cold anticyclones can be generated (high continental pressures and lows aloft). Instead, in summer one warm cyclones appears (warm low pressure at surface and highs aloft). Both situations keep an stable atmosphere over IP.

Table 2.3: Seasonal frequencies of general situations.

	A	C	Z	M	S
Winter	50.5	20.2	16.9	12.3	0.0
Spring	33.9	28	8.9	5.9	23.4
Summer	16.7	4	4.9	9.7	64.7
Autumn	33.2	12.8	13.5	7.3	28.8

2.4.3 Quality and stability of CTs

This section depicts the quality and stability indices (see Subsection 2.3) of the different CTs obtained. Taking into account the quality results, the best (worst) indices are obtained in winter (summer), with values of 53.9% (47.2%). In equinoctial seasons the values are similar, 52.2% in autumn and 51.1% in spring. These results highlight an important fraction of the original variance not explained by the clusters, indicating the existence of a strong heterogeneity with respect to the type of situations within each cluster, which is normal taking into account the high number of grouped episodes. When comparing the results to other similar studies, small differences can be found. Philipp et al. (2006) obtained a value of 51.7% for a 12 CTs clustering for wintertime months (DJF) during and exercise of comparison among different clustering algorithms. This value, the best of all those obtained with each method utilized, was obtained with SANDRA algorithm. Together with the results obtained here, this fact reveals that values around 50% could be usual in this kind of clustering works. Unfortunately, there is a lack of studies which may help confirming robustly this hypothesis.

Regarding the stability analysis, a cross-validation process similar to Fereday et al (2008) has been used. We have crossed the dates of the clusters obtained in the 50-year classification with those others of the clusters obtained with the half of years. They were considered 100 short-periods whose days were randomly selected among the days of the long period.The classifications for each subsample was performed using the seeds obtained for the whole period. The stability results obtained can be found in Table 2.4. Some CTs present stabilities around 90% (CT1/2/10-wi, CT4-sp, CT8/10-su and CT1/2/3/10-au), while some other CTs do not exceed 55% (CT11-sp). If we analyze the mean seasonal stability of each of the seasonal classifications (mean of the stabilities of the clusters, last column in Table 2.4), the results indicate higher stability in autumn (82.8%) and summer (78%) meanwhile stabilities decrease in winter (77.6%) and spring (72.0%). Comparing the wintertime stability value with that of Fereday et al (2008) (73%), obtained for 10 CTs in January and February 1949-1999, in our case is slightly higher. Again, the limited available number of classification studies hampers further criticism about the obtained results.

Table 2.4: Stability (%) of the diverse CTs.

	CT1	CT2	CT3C	CT4	CT5	CT6	CT7	CT8	CT9	CT10	CT11	CT12	Mean
Winter	88.7	88.4	73.9	75.6	68.0	78.3	81.6	73.2	65.0	88.5	74.3	76.5	77.6
Spring	78.6	71.0	86.1	59.7	84.4	70.1	80.4	72.3	63.5	80.1	55.2	62.5	72.0
Summer	72.3	83.0	78.7	70.1	78.6	82.3	80.1	90.1	75.3	90.1	84.9	77.2	80.2
Autumn	87.3	87.0	92.4	73.1	85.1	76.0	84.3	90.1	77.2	80.1	82.4	79.0	82.8

2.4.4 Trends in the CTs

The analysis of the series of seasonal frequency of the CTs may help understanding some of the dynamical causes compatible with the observed changes in variables like precipitation and temperature over the IP throughout the second half of the XX century. Table 2.5 depicts the trends of the series, together with the p-values obtained by the Mann-Kendall test (Kendall, 1970). Results highlight that just a few CTs present significant trends at 95%: two winter CTs (cyclonic, CT6/10-wi) and one CT in spring, also cyclonic (CT5-sp). All of them have a negative trend but present a different intensity. In CT6-wi, the trend (-0.13 d/y) is twice as much as that obtained for the other two patterns. If taking into account a lower significance level (90%), three additional patterns appear with significant trends: two in winter (CT2/3-wi), anticyclonic and zonal respectively; and one in summer, CT3-su. In this case, all of them show a positive trend. An interesting result is that there is no significant trend at all in the autumn CTs.

When comparing these results to those of other previous studies, we can find some similarities. In particular, the decrease of the number of CT6-wi situations and the increase of CT3-wi is a result compatible with the movement towards the north of the storm-track observed in Paredes et al (2006). It could be related to the decrease of winter precipitation measured in most of the IP (Serrano et al, 1999). Another result compatible with other author (e.g. López-Bustins et al (2008)) is the positive (negative) trend (despite not significant) observed in most of the winter anticyclonic (cyclonic) patterns. The decrease of the frequency springtime of CT5-sp, as well as the non-significant increase in the blocking situations over the IP (CT3/6/9-sp) may be related to the decrease observed for precipitation during this season.

Although the trends obtained are just valid for the IP, their positive or negative sense is similar to the results of Kyselý and Huth (2006), who observed a significant increase of the frequency of anticyclonic and blocking over the Western and Central Europe, together with a decrease of the cyclonic patterns. Last, we should highlight the negative trend found for CT6-wi, identical to the trend detected for the period 1850-2000 of the CT6 winter pattern of Philipp et al. (2006), whose synoptic configuration is similar to our pattern.

Table 2.5: Trend and p-values of the seasonal frequency of CTs. The p-values shown comes from applying the Mann-Kendall test to the seasonal frequency series of the CTs. The trend is expressed in days/year.** denote the values with a 95% significance level and * 90% significance level

CTs	winter		spring		summer		autumn	
	p-value	trend	p-value	trend	p-value	trend	p-value	trend
CT1	0.2376	+0.080	0.5628	+0.003	0.8830	+0.020	0.4993	-0.028
CT2	0.1275*	+0.128	0.4682	+0.035	0.4533	-0.033	0.8961	-0.011
CT3	0.1081*	+0.045	0.2157	+0.064	0.1062*	+0.070	0.7200	+0.001
CT4	0.2193	+0.041	0.3280	-0.017	0.6652	+0.045	0.4281	+0.038
CT5	0.4778	+0.048	0.0481**	-0.059	0.7257	+0.028	0.8129	-0.004
CT6	0.0075**	-0.132	0.8831	+0.013	0.6304	-0.013	0.8703	+0.012
CT7	0.6703	-0.019	0.8829	-0.001	0.4314	-0.028	1.0000	+0.002
CT8	0.3104	-0.038	0.4988	+0.020	0.9350	+0.007	0.7313	-0.017
CT9	0.6173	-0.028	0.6526	+0.002	0.7802	+0.004	0.7616	+0.001
CT10	0.0025**	-0.057	0.6650	-0.011	0.1721	-0.040	0.3754	-0.023
CT11	0.3561	-0.025	0.9935	-0.022	0.7191	-0.030	0.7009	+0.015
CT12	0.3154	-0.042	0.5785	-0.032	0.1560	-0.033	0.6643	+0.010

2.4.5 Persistence of CTs

An interesting characteristic of the global circulation is the tendency of several situations to persist during a large number of days, provoking blocking situations. Persistence is defined as the duration (or average life) of the events within a same situation. Event is taken as the non-interrupted sequence of days belonging to a situation (CT). Nonetheless, this definition, which takes into account the mean value, can mask that some patterns can present lasting blocking events albeit they have low mean persistence values. Therefore, for a more complete description of the persistence, other parameters of its distribution function have been considered, like extreme values or some percentiles. In Table 2.6 are shown the median, mean, third quartile values and maximum duration of events obtained for the diverse CTs during the different seasons.

The analysis of Table 2.6 indicates that the anticyclonic situations CT2/1-wi are the most persistent in winter, if we consider the mean values (2.7 and 2.5 days, respectively), with CT2-wi being the pattern with the longest-lasting event (17 days). Conversely, the zonal situation CT7-wi is the least persistent (mean value 1.2 days). In spring, CT1/3/12-sp are the most persistent types, highlighting the lack of correlation between persistence and frequency for CT12-sp. During springtime there is, generally, a higher persistence of the patterns than in winter. On the other hand, the situations CT1/3/5-sp present the events with the largest duration (13 days), meanwhile CT9-sp (Atlantic blocking) is the least persistent situation (1.5 days). In summertime, the mean persistence of situations presents the lowest spread in all the year, between 1.5 and 2.1 days. In this case, we have considered not only the mean value of the persistence but also its median value in order to discriminate the persistence of the situations. With

Table 2.6: Persistence. Rows show the median, mean, third quartile (3qt) and max values of the persistence (number of days) of the CTs (columns) for each season. Last column depicts the mean value (considering all CTs) of the 3qt and max values.

Winter	CT1	CT2	CT3	CT4	CT5	CT6	CT7	CT8	CT9	CT10	CT11	CT12	Mean
median	2.0	2.0	1.0	1.0	1.0	1.0	1.0	1.0	1.0	1.0	1.0	1.0	–
mean	2.5	2.7	1.4	1.5	1.7	1.9	1.2	1.5	1.6	1.5	1.8	1.6	–
3qt	3.0	3.0	2.0	2.0	2.0	2.0	1.0	2.0	2.0	2.0	2.0	2.0	2.1
max	12	17	6	5	13	9	4	8	6	6	9	5	8
Spring	CT1	CT2	CT3	CT4	CT5	CT6	CT7	CT8	CT9	CT10	CT11	CT12	Mean
median	2.0	1.0	2.0	1.0	1.0	1.0	1.0	1.0	1.0	1.0	1.0	1.5	–
mean	2.9	1.8	2.4	2.0	1.7	1.9	1.8	2.0	1.5	1.6	1.6	2.0	–
3qt	4.0	2.0	3.0	3.0	2.0	2.0	2.0	2.8	2.0	2.0	2.0	2.0	2.4
max	13	10	13	11	13	9	8	6	11	7	8	6	9.6
Summer	CT1	CT2	CT3	CT4	CT5	CT6	CT7	CT8	CT9	CT10	CT11	CT12	Mean
median	1.0	2.0	1.0	1.0	1.0	1.0	1.0	2.0	1.0	2.0	1.0	1.0	–
mean	2.0	1.9	1.8	1.5	1.6	1.8	1.8	1.8	1.6	2.1	1.9	1.6	–
3qt	2.0	2.0	2.0	2.0	2.0	2.0	2.0	2.0	2.0	2.0	3.0	2.0	2.1
max	9	7	10	8	6	12	6	7	6	11	7	8	8.1
Autumn	CT1	CT2	CT3	CT4	CT5	CT6	CT7	CT8	CT9	CT10	CT11	CT12	Mean
median	2.0	2.0	2.0	1.0	1.0	2.0	2.0	1.0	1.0	1.0	1.0	1.0	–
mean	2.4	2.2	2.7	1.8	1.6	2.0	2.0	1.9	2.0	1.6	1.4	1.8	–
3qt	3.0	3.0	3.0	2.0	2.0	2.0	3.0	2.0	3.0	2.0	2.0	2.0	2.4
max	14	13	25	10	7	9	7	11	6	7	5	5	9.9

this criterion, CT10/2-su are the most persistent patterns. In both cases the surface pattern (SLP) is very similar, but the pattern of the former is related to a trough of SW-NE axis; the latter is related to a ridge whose axis is oriented in the same direction. In this case the longest event is CT6-su (12 days). The least persistent situations are CT4/5/9/12-su, reflecting a similar Z500 configuration (SW flow over the IP). Regarding autumn, the anticyclonic situation CT3-au has the longest persistence, and CT11-au (related to the pass of a trough over the IP) shows the shortest persistence.

Summarizing, the main conclusions of this analysis are: in autumn and winter the most persistent situations are those related to an anticyclonic situation with a large extension over Central- and South-Western Europe (CT2-wi and CT3-au), while in summer and spring they are the stagnant or thermal low situations. On the contrary, the situations with a shorter persistence in autumn and winter are zonal (CT7-wi y CT11-au), in spring related to anticyclonic types and in summer to a SW circulation in medium-high levels. Last, if we compare the mean seasonal value of the third quartile for different seasons, autumn and spring situations present a longer duration than for winter and summer.

Another interesting aspect of the persistence is the analysis of its interannual variability. For that the mean annual persistence of the diverse CTs has been obtained; that will allow analyzing the existence of trends in some CTs. Furthermore, averaging the annual values obtained for the diverse patterns belonging to a same season permits the analysis of the season in which the atmospheric circulation presents the highest (or lowest) variability of the persistence.

Results obtained for the analysis of the annual trend (not shown here) indicate

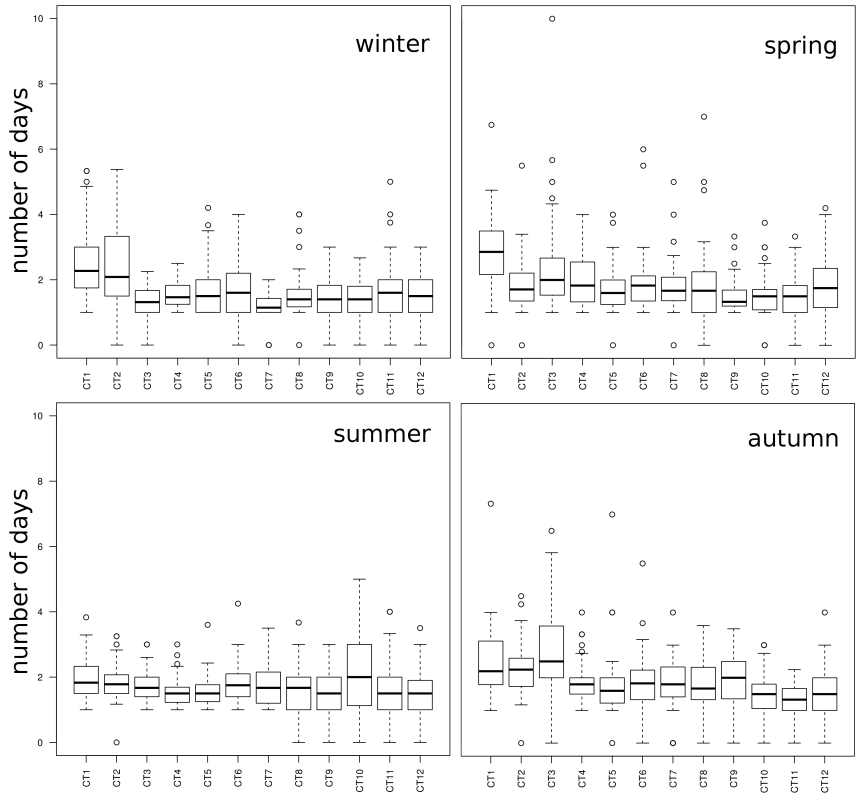

Figure 2.7: Boxplot of the interannual variability of the CTs persistence. Period: 1958-2008

the existence of a significant trend at 95% in two patterns, CT6-wi and CT9-sp. The former has a negative trend similar to that obtained for its frequency series (see Sec 2.4.4). For the latter, a pattern less persistent of springtime (CT9-sp), the trend obtained is positive. If the significance for the trend test is 90%, there are trends for three more patterns: two in spring (CT3/12-sp, with positive and negative trend respectively) and one in summer (CT2-su) showing a positive trend.

All trends obtained in spring depict, on the one hand, an increase of the persistence in situations of atmospheric stability (related to scarce precipitations); and on the other hand there is a decrease in the persistence of those patterns related to precipitation episodes. This result is compatible with the decrease of precipitation measured in the IP during the second half of the XX century (Bladé et al, 2010; Serrano et al, 1999; Paredes et al, 2006).

Finally, results regarding interannual variability averaged for all the CTs belonging to a same season highlight that spring and autumn are the periods with a higher variability (Fig. 2.7), with a standard deviation of 0.90 and 0.85 days, in that order. The values obtained for winter and summer are 0.74 ad 0.67 days, respectively.

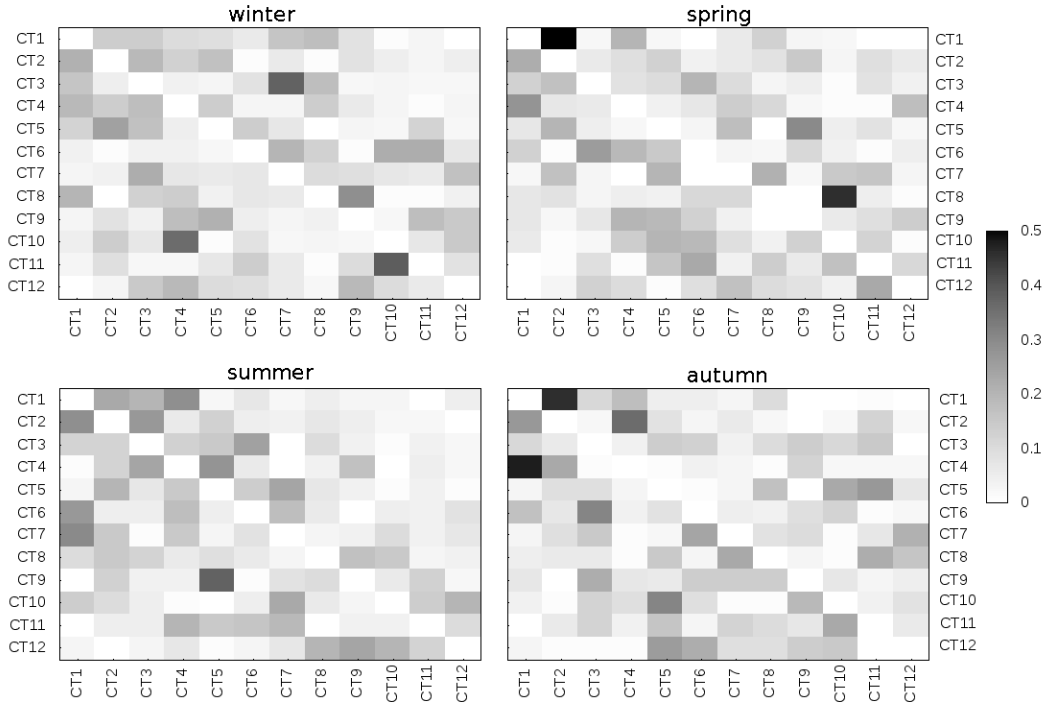

Figure 2.8: Pictures represent the transition matrices obtained for CTs in winter (top left), spring (top right), summer (bottom left) and autumn (bottom right). The darker or lighter tone is related to a greater or lesser probability respectively, of transition from a CT (row) towards another CT (column).

2.4.6 Transitions of CTs

Knowing the probability of transition from a CT to another is a useful tool for atmospheric predictability at medium term (James, 2007). The transitions resulting from very complex internal processes of the atmospheric dynamics, related to phase changes of the intraseasonal atmospheric waves (Sanchez-Gómez and Terray, 2005), can be estimated as the mean probability in which a determined CT evolves towards others.

Figure 2.8 shows the transition matrices between CTs. Each cell represents the probability that a given CT (row) evolves to another CT (column). Generally, when analyzing the transitions from any CT towards the rest for each season, we observe the existence of some transitions more probable than the rest, as well as an important number of transitions with a low probability. Here it is worth reminding that the matrices include an important noise signal due to the large heterogeneity of each cluster defining the diverse CTs. The noisy mixture of situations can provoke the appearance of fictitious residual transitions with no physical sense. Hence, the analysis of transitions included here has just considered the most probable transitions, admitting the hypothesis that in these cases the ratio signal/noise will be higher.

The analysis of the most probable transition sequences (starting from any of

the CTs) indicates that some of them respond to cyclic sequences (origin and end at the same CT), meanwhile the rest are just linear sequences finishing at some CT leading to a cyclic transition. Considering all the most probable transition sequences, a total of 7 cycles are obtained: two in winter, spring and autumn, and one in summer. One of the winter cycles represents a sequence of transitions including exclusively anticyclonic situations (Winter CT1→8→9→5→2→1) while in the other the transitions are between zonal situations (winter CT3→7→3). The anticyclonic cycle seems to describe a clockwise movement of a high pressure system (Fig. 2.9-left), which is located initially over the IP, and then moves to the Atlantic and the SW United Kingdom, and from there it moves to Central-Northern Europe, with the end of the cycle in the western part of Central Europe. The second winter cycle is related to the alternation of the zonal situation (CT3-wi) and the pass of troughs with a low amplitude over the IP (CT7-wi). The configuration of the pressure systems playing a role in this cycle is analogous to the negative phase of the variability mode of the North Atlantic, whose most notable influence over the IP is the appearance of very wet winters in the Atlantic face of the IP.

Two cycles appear in springtime. The first includes the two most frequent CTs, (spring CT1→2→1) and stands for a transition between stagnant situation at the surface with the alternation of ridges and troughs over the IP. The second incorporates just two anticyclonic situations (spring CT3→6→3). The former is a meteorological situation provoking a great atmospheric stability over the IP, but in the latter a cold air mass with a northern component is observed in the eastern part of the IP (see Z500 field for CT6-sp), and that can enhance the development of instability over this region. This result can explain, in part, the higher number of rainy days observed in this region in spring. During the summer, the cycle is mixed, and is formed by two stagnant situations and two anticyclonic situations (summer CT1→4→5→7→1). It describes the West-East evolution of trough aloft over the IP, with corresponding modifications in the SLP field (movement of a region of low relative pressures initially at the SW of the IP towards the center, and from there to SE Spain). In autumn there are, once more, two cycles. The first is very similar to the summer cycle (autumn CT1→2→4→1→), while the second (autumn CT5→11→10) describes the transitions from the zonal circulation to the deepening of troughs over the IP and the later atmospheric stabilization with the appearance at the end of the cycle of an anticyclonic region at the western IP. None of the cyclic sequences described respond to exclusively cyclonic cycles.

For longer linear sequences with a higher number of CTs, their origin is analogous for winter, spring and autumn (extratropical cyclone at the NW IP, CT6-wi, CT7-sp y CT8-au) and their end is an anticyclonic situation leading to a cyclic sequence (see Figure 2.9-right). Overall, the sequence describes the stabilization process of the atmosphere over the IP. Conversely, none of the CTs transits at the maximum probability level towards the situation originating this longer sequence. On the other hand, this particular situation evolves to two cyclonic

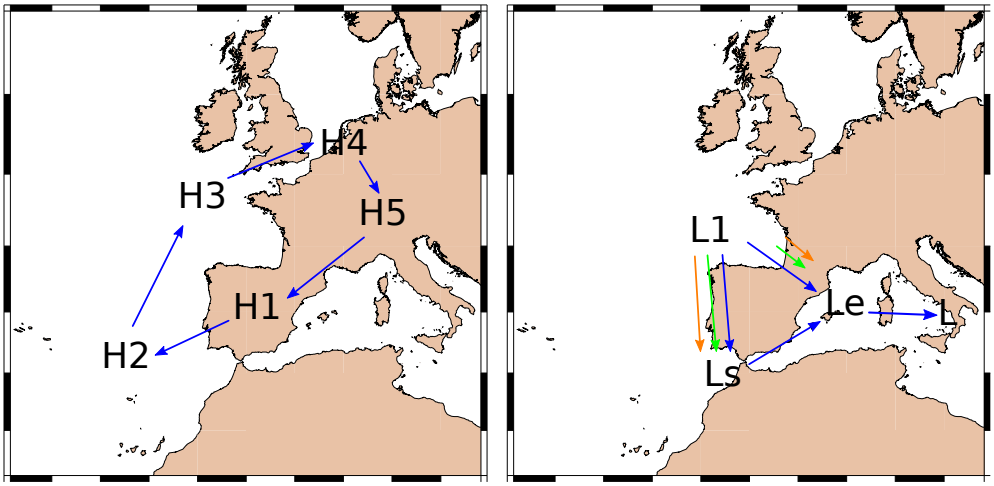

Figure 2.9: The figure on the left illustrates the winter anticyclonic cycle. We can see the clockwise movement of a high pressure system located initially over the IP (H1), and finally in the western part of Central Europe (H5). The right figure shows the transition of a low pressure system from the NW of the IP (L1) to the South (Ls) or to the East (Le). The length of the arrows indicate the greater probability of transition (long arrows) or lesser (short arrows). The colors of the arrows represent the seasons (blue: winter, green: spring, orange: autumn).

situations, Cyclone at the South IP (CT11-wi, CT8-sp and CT7-au) and extratropical disturbance at the East IP (CT10-wi, CT10-sp and CT12-au) showing both transitions a strong seasonal dependency. Therefore, in winter the transition towards both situations has the same level of probability (22%), while in summer and autumn the probability is higher towards the low located to the south (21% vs. 15% in spring; 23% vs. 15% in autumn). Hence, the equinoctial seasons the atmospheric dynamics seems to present a more meridional component, being frequent the southern movement of the extratropical cyclone. These results are in agreement with the lasting persistence of the situations obtained for these seasons, because the meridional circulation leads to a higher persistence of the situations. Finally, following the longest linear sequence, the transition from a extratropical cyclone located at the South IP towards the low located at the East presents one of the highest probabilities (40% in winter and spring) among those obtained for all the CTs. The result confirms the usual eastern movement of this type of extratropical perturbations developed at mid-latitudes. Conversely, the opposite transition is not very likely (Figure 2.8).

2.5 Conclusions

This work presents a new seasonal classification of CTs centered over the IP. The classification updates and completes others developed previously for the IP. For that, we used a clustering of the PCs obtained jointly for the daily reanalysis and analysis fields of SLP and Z500 (ERA40) covering the period 1958-2008. As a

clustering method we used K-means, initialized from seeds coming from a PC-ModeT cluster, which allows a less subjective selection of the number of clusters than other methods. K-means provides more stable clusters when starting from a specific group of seeds, as shown in a previous exercise of comparison against SANDRA clustering method. The stability of the clusters provided by K-means turns it into a reliable method for analyzing some of the characteristics of the clusters, such as frequency, persistence and transitions.

Overall 12 CTs were obtained for each season. Most of them were very similar to those obtained for other previous classifications. The main differences are caused by the classification method followed (geographical window, atmospheric variables used, spatial resolution of reanalysis data, clustering method, etc.). The CTs obtained for wintertime are different from summer, meanwhile autumn and spring show a hybrid/mixed pattern between the winter and summer. Hence, the proposed pseudo-subjective classification of the CTs in 21 situations groups those patterns whose centroids are very similar along the year. The situations of this latter classification are included within another more general classification that divides the situations in Anticyclonic, Cyclonic, Zonal, Summertime and Hybrid-Mixed.

The analysis of the frequency of the CTs describes accurately the annual cycle observed for the main synoptic structures over the IP. The high frequency of anticyclonic and zonal situations in winter, cyclonic in spring and situations with a low pressure gradient in summer are some of the results derived of the joint analysis of the frequency of the patterns belonging to each general category. On the other hand, the trend analysis of the frequency of the diverse CTs reveals the non-existence of significant trends (95%) in most of them, except for three cyclonic CTs occurring in winter and spring. The most important among them (decreasing) is produced in the winter pattern, whose centroid depicts a deep low northwestern the IP. However, some trends have been found (although not very significant) in other patterns. In this sense, an increase of the frequency of most of the anticyclonic situations in winter and spring has been observed, together with a decrease in cyclonic situations. This result is similar to other studies, justifying some of the likely causes of the decrease observed in winter and spring precipitation over the IP in the last 50 years.

With respect to the analysis of persistence, generally the most persistent CTs are the most frequent too (formed by a greater number of episodes), albeit this rule not always occurs, as in CT12-sp, a blocking situation in the North Atlantic ocean, whose persistence is high against its low frequency . Generally, the most persistent situations in winter and autumn are those related to an anticyclonic region with a noticeable extension over Central- and Southern-Western Europe; meanwhile for summer and spring these persistent situations show low pressure gradients in surface and aloft fields. Conversely, the least persistent situations in autumn and winter are zonal (CT7-wi and CT11-au), in spring they are anticyclonic, and in summer they are related to a southwestern circulation in medium-high levels. Broadly, when focusing on the averaged value of the third

quartile of the persistence for every CTs of a season, results indicate that in spring and autumn the patterns may result more persistent than in winter and summer. The interannual variability of the mean persistence has been analyzed, giving a higher value in spring and autumn. Also, the trend of the mean persistence of the CTs shows a negative trend very significant in the same winter pattern as that experiencing a similar trend in the frequency (CT6-wi). Moreover, in spring there is a very significant positive trend of the least persistent pattern (CT9-sp) , which is related with a situation depicting blocking in the North Atlantic ocean. The rest of the CTs do not show significant trends.

The analysis of the transition sequences among the different CTs has also been shown in this work. In order to avoid the noise of each cluster, we have just considered in the analysis those transitions with the highest probability. We have observed cyclic and linear sequences. Those cycles are present in all seasons. The largest cycle, involving a higher degree of CTs, is produced in winter and is formed exclusively by anticyclonic situations justifying the high frequency of this type of situations obtained for wintertime. The rest of the cycles represent the destabilization and later stabilization of the atmosphere, alternating patterns related to zonal circulation, and with troughs and ridges over the IP. It is important to highlight the non-existence of cyclonic cycles. With respect to the linear sequences, the longest (that involving a higher number of patterns) has as origin the extratropical cyclone located at the northwest of the IP. This usually moves towards other two situations: extratropical cyclone at the south of the IP (sagging of the trough to low latitudes) or extratropical disturbance at the east of the IP (trough moving eastwards). The probability of transition towards both situations is identical in winter; however moving to the south is more probable in spring and autumn. This fact suggests that in spring and autumn the atmospheric circulation presents a meridional component which is more important than in winter, supporting the previous results obtained regarding the higher mean persistence of the spring and autumn patterns.

The classification proposed accurately describes some of the known characteristics of the circulation over the IP, as its seasonal distribution, but also presents some new concepts related to the persistence and the transition among patterns. On the other hand, it is beyond the scope of the paper to quantitatively describe the degree of correlation with variables like precipitation and temperatures; however, some of the future works currently going on are related to the development of a downscaling method based on the degree of correlation between the CTs obtained and the anomaly patterns observed in precipitation and temperature at a regional scale. The analysis of those correlations will allow discussing about the trends observed in the CTs and their influence in climatic variables. It will also complement the assessment of the CTs classification obtained here.

Bibliography

Bárdossy A, Caspary H (1990) Detection of climate change in europe by analyzing european atmospheric circulation patterns from 1881 to 1989. Theoretical and Applied Climatology 42:155–167

Beck C, Philipp A (2010) Evaluation and comparison of circulation type classifications for the european domain. Physics and Chemistry of the Earth, Parts A/B/C 35(9-12):374 – 387, doi:10.1016/j.pce.2010.01.001

Bermejo M, Ancell R (2009) Observed changes in extreme temperatures over spain during 1957-2002, using weather types. Revista de Climatología 9:45–61

Bladé I, Cacho I, Castro-Díez Y, Gomis D, González-Sampériz P, Miguez-Macho G, Pérez F, Rodríguez-Fonseca B, Rodríguez-Puebla C, Sánchez E, Sotillo M, Valero-Garcés B, Vargas-Yááñez M (2010) Clima en españa: Pasado, presente y futuro. Tech. rep., CLIVAR-España

Brunet M, Jones P, Sigró J, Saladié O, Aguilar E, Moberg A, Della-Marta P, Lister D, Walther A, López D (2007) Temporal and spatial temperature variability and change over spain during 1850-2005. Journal of Geophysical Research 112:12,117

Calinski T, Harabasz J (1974) A dendrite method for cluster analysis. Communications in Statistics 3:1–27

Casado M, Pastor M, Doblas-Reyes F (2008) Euro-atlantic circulation types and modes of variability in winter. Theoretical and Applied Climatology 96:17–29

Cassou C, terray L, Phillips A (2005) Tropical atlantic influence on european heat waves. Journal of Climate 18:2805–2811

Catell R (1966) The scree test for the number of pcs. Multivariate Behavioral Research 1:245–276

Crane R, Barry R (1988) Comparison of the msl synoptic pressure patterns of the artic as observed and simulated by the giss general circulation model. Metorology and Atmospheric Physics 39:169–183

Demezure M, Werner M, van Lipzig N, Roeckner E (2008) An analysis of present and future echam5 pressure fields using a classification of circulation patterns. International Journal of Climatolology 29:1796–1810

Fereday D, Knight J, Scaife A, Folland C (2008) Cluster analysis of north atlantic-european circulation types and links with tropical pacific sea surface temperatures. Journal of Climate 21:3687–3703

Font-Tullot I (2000) Climatología de España y Portugal. University of Salamanca (Spain)

Gallego F (1995) Situaciones de flujo mediterráneo y precipitaciones asociadas. aplicación a la predicción cuantitativa en la cuenca del segura. PhD thesis, Universidad de Murcia (Spain)

García-Bustamante E, González-Rouco J, Navarro J, Xoplaki E, Jiménez P, Montávez J (2012) North atlantic atmospheric circulation and surface wind in the northeast of the iberian peninsula: uncertainty and long term downscaled variability. Climate Dynamics 38(1):141–160, URL `http://dx.doi.org/10.1007/s00382-010-0969-x`, 10.1007/s00382-010-0969-x

Gesterngarbe F, Werner P (1997) A method to estimate the statistical confidence of cluster separation. Theoretical and Applied Climatology 57:103–110

Giorgi F (2006) Climate change hot-spots. Geophysical Research Letters 33:08,707

Goodess C, Palutikof J (1998) Development of daily rainfall scenarios for southeast spain using a circulation-type approach to downscaling. International Journal of Climatology 18(10):1051–1083

Hannachi A, Jolliffe I, Stephenson D (2007) Empirical orthogonal functions and related techniques in atmospheric science: A review. International Journal of Climatology 27(9):1119–1152

Hartigan J, Wong M (1979) A k-means clustering algorithm. Applied Statistics 28:100–108

Hess P, Brezowsky H (1952) Katalog der Grosswetterlagen Europas. Deutscher Wetterdienst in d. US-Zone

Hewitson B, Crane R (2002) Self-organizing maps: applications to synoptic climatology. Climate Research 22:13–26

Hulme H, Briffal K, Jones P, Senior C (1993) Validation of gcm control simulations using indices of daily airflow types over the british isles. Climate Dynamics 9:95–105

Huth R (1996) An intercomparison of computer-assisted circulation classification methods. International Journal of Climatology 16:893–922

Huth R (1997) Continental-scale circulation in the ukhi gcm. Journal of Climate 10:1545–1561

Huth R (2000) A circulation classification scheme applicable in gcms studies. Theoretical and Applied Climatology 67:1–18

James P (2007) An objective classification method for hess and brezowsky gross-wetterlagen over europe. Theoretical and Applied Climatology 88:17–42

Jiménez P, González-Rouco J, Montávez J, García-Bustamante E, Navarro J (2008) Climatology of wind patterns in the northeast of the iberian peninsula. International Journal of Climatology 29:501–525

Kaufman L, Rousseeuw P (1990) Finding groups in data: an introduction to cluster analysis, vol 39. Wiley Online Library

Kendall M (1970) Rank Correlation Methods. Griffin

Key J, Crane R (1986) A comparison of synoptic classification schemes based on objective procedures. International Journal of Climatology 6:375–388

Kirchhofer W (1974) Classification of European 500 mb patterns. Working reports of the Swiss Meteorological Institute, Swiss Meteorological Institute

Kyselý J, Huth R (2006) Changes in atmospheric circulation over europe detected by objective and subjective methods. Theoretical and Applied Climatology 85:19–36

Lamb H (1950) Types and spells of weather around the year in the british isles: annual trends, seasonal structure of the year, singularities. Quarterly Journal of Royal Meteorological Society 76:393–429

López-Bustins J, Martín-Vide J, Sánchez-Lorenzo A (2008) Iberia winter rainfall trends based upon changes in teleconnection and circulation patterns. Global and planetary change 63:171–176

Lorenz E (1956) Technical report, Statistical Forecast Project Report 1. Dep.of Meteorology.MIT 49, vol 1, Massachusetts Institute of Technology, chap Empirical orthogonal functions and statistical weather prediction, p 52

Lund I (1963) Map-pattern classification by statistical methods. Journal of Applied Meteorology 2:56–65

Michelangeli P, Vautard R, Legras B (1995) Weather regimes: Recurrence and quasi stationary. Journal of the Atmospheric Sciences 52:1237–1256

Milligan G (1980) An examination of the effect of six types of error perturbation of fifteen clustering algorithms. Psichometrika 45:325–342

Paredes D, Trigo R, García-Herrera R, Trigo I (2006) Understanding precipitation changes in iberia in early spring: weather typing and storm-tracking approaches. Journal of Hydrometerology 7:101–113

Petisco E (2003) Metodología para una caracterización de la circulación atmosférica en el entorno de la península ibérica y baleares.nt nº 9. Tech. rep., INM

Philipp A, Della-Marta P, JJacobett, Fereday D, Jones P, Moberg A, Wanner H (2006) Long-term variability of day north atlantic-european pressure patterns since 1850 classified by simulated annealing clustering. Journal of Climate 20:4065–4095

Philipp A, Bartholy J, Beck C, Erpicum M, Esteban P, Fettweis X, Huth R, James P, Jourdain S, Kreienkamp F, Krennert T, Lykoudis S, Michalides SC, Pianko-Kluczynska K, Post P, Álvarez DR, Schiemann R, Spekat A, Tymvios FS (2010) Cost733cat – a database of weather and circulation type classifications. Physics and Chemistry of the Earth, Parts A/B/C 35(9-12):360 – 373, doi:10.1016/j.pce.2009.12.010

Preisendorfer R (1988) Principal components analysis in meteorology and oceanography. Elsevier Science Ltd

Rasilla D (2003) Aplicación de un método de clasificación sinóptica a la península ibérica. Investigaciones Geográficas 30:27–44

Richman M (1981) Obliquely rotated principal componentes: an improved meteorological map typing technique. Journal of Applied Meteorology 24:1145–1149

Romero R, Sumner G, Ramis C, Genovés A (1999) A classification of the atmospheric circulation patterns producing significant daily rainfall in the spanish mediterranean area. International Journal of Climatology 19:765–785

Sanchez-Gómez E, Terray L (2005) Largue scale atmospheric dynamics and local intense precipitation epidodes. Geophysical Research Letters 32:24,711

Serrano A, Garcia J, Mateos V, Cancillo M, Garrido J (1999) Monthly modes of variation of precipitation over the iberian peninsula. Journal of Climate 12:2894–2919

Storch V, Zwiers W (1999) Statistical analysis in climate research, Cambridge University Press, chap Empirical ortogonal functions, pp 135–192

Uppala S, Kallberg P, Simmons A, Andra U, da Costa Beechtold V, Fiorino M, Gibson J, Haseler J, Hernandez A, Kelly G, Li X, Onogi K, Saarinen S, Sokka N, Allan R, Andersson E, Arpe K, Balmaseda M, Beljaars A, van de Berg L,

Bidlot J, Bormann N, Caires S, Chevallier F, Dethof A, Dragosavac M, Fisher M, Fuentes M, Sagemann, EH E, Hoskins B, Isaksen L, Janssen P, RJenne, McNally A, Mahfouf J, Mocrette J, Rayner N, Saunders R, Simon P, Sterl A, Trenberth K, AU A, Vasiljevic D, Viterbo P, Woollen J (2005) The era-40 re-analysis. Royal Meteorological Society 131:2961–3012

Wang X (2008) Penalized maximal f test for detecting undocumented mean shift without trend change. Journal of Atmospheric and Oceanic Technology 25(3):368–384

Wilks D (1995) Statistical methods in the atmospheric sciencies: an introduction. International geophysics series, Academic Press

Yiou P, Nogaj M (2004) Extreme climatic events and weather regimes over the north atlantic: When and where? Geophysical Research Letters 31:1–4

Yiou P, Goubanova K, Nogaj M (2008) Weather regime dependence of extre value statistics for summer temperature and precipitation. Nonlinear Processes in geophysics 15:365–378

Chapter 3

Links between the Climate Variability over Spain and the Atmospheric Circulation

3.1 Introduction

In the synoptical scale, the circulation prevailing over a given region depends on the location of the main high and low pressure systems. This define the prevalent fluxes over the region conditioning the kind of the advection cold/warm and wet/dry. The interactions of these fluxes with the orography, as well as its variability along the seasons, control in a great extent the climate variability of the region. Therefore, the characterization of the atmospheric circulation over a region is a key factor to understand its climate variability.

The physical laws governing the atmospheric dynamics, make that this had, in essence, a chaotic behaviour. A priori, there exist an infinite number of atmospheric states being necessary the use of statistical techniques to face to any exercise of the atmospheric dynamics characterization. One of the methods frequently employed is based on Principal Component Analysis (PCA) (Barnston and Livezey, 1987; Storch and Zwiers, 1999), mainly used to determine the low frequency modes of variability such as the North Atlantic Oscillation (NAO) (Barnston and Livezey, 1987), Artic Oscillation (AO), Southern Oscillation (SO) (Zhang et al, 1997), etc. Some others are based on circulation indices which characterize the situations in order to the direction of fluxes and their vorticity (Jones et al, 1993). Another method of characterization are the Circulation Types (CTs) (Beck and Philipp, 2010; García-Valero et al., 2012). These are a handy ensemble of atmospheric patterns on which the huge number of daily atmospheric situations can be simplified. Hence, from the point of view of a meteorologist, the CTs are those situations that he could remember and which are associated with some precipitation and temperature spatial patterns, normally called as their weather regimens or Weather Types (WTs). Links between CTs and WTs are traditionally used to explore the climate variability (Romero et al

(1999); Yiou and Nogaj (2004); Fernández-Montes et al (2012), among others) and also for downscaling purposes (Wilby and Wigley, 1997). Therefore, they are usefulness for analyzing the role of the CTs on the changes observed in climate variability.

This study is centered over the IP where several CT classifications have been proposed in the last years (Petisco, 2003; Rasilla, 2003; Romero et al, 1999; Goodess and Palutikof, 1998; Jiménez et al, 2008; García-Valero et al., 2012). One of the most recent classifications was presented in García-Valero et al. (2012). This presents significant improvements respect to the previous CT classifications (García-Valero et al., 2012). Among the advantages are its seasonality and the use of two atmospheric variables for defining the CTs (Sea Level Pressure (SLP) and Geopotential Height at 500 hPa level). In addition, the period covered by the classification (1958-2008) extends the time of the other classifications allowing to investigate the role of the dynamics on the existence of possible long-term climate variability changes. In addition, in García-Valero et al. (2012) significant changes along the period of classification were found for some CTs of winter, spring and autumn. The implication of such changes on the climate variability have not been yet analyzed.

The IP is a region with a large climate variability (Font-Tullot, 2000; Lorente-Plazas et al, 2015). Its location at midlatitudes determines the presence of a large variety of atmospheric situations over this territory (García-Valero et al., 2012). In addition, its position between the Mediterranean Sea and the Atlantic Ocean, of very different temperatures especially at the end of summer, autumn and winter, favors that the air masses advected towards the IP acquire very distinct properties on humidity and temperature depending on their provenance regions. This leads to the occurrence of different meteorological phenomena of large spatial-time variability. All these factors joined to its complex orography justify its large climate diversity.

In the last decades, significant changes in precipitation and temperature have been observed in the IP. On the one hand, a decreasing of precipitation in winter and early spring in large areas of the central, western and northern (Corte-Real et al, 1998; MJ. et al, 1998; Serrano et al, 1999; Paredes et al, 2006; López-Bustins et al, 2008; de Luis et al, 2010; González-Hidalgo et al, 2011; Gallego et al, 2011; Hidalgo-Muñoz et al, 2011; Luna et al, 2012) have been reported. On the other hand, significant positive trends in maximum temperatures (Tx) in spring and summer, practically generalized over the entire territory, as well as similar trends in minimum temperatures (Tm) in the same seasons and autumn have been informed (Brunet et al, 2007; Bermejo and Ancell, 2009; García-Valero et al, 2015). Finally, climate change projections inform about the continuity of such changes in the future, defining this region as one of the hot-spots of the Globe especially by the large increase projected for temperatures in summer.

The aim of this study is to explore the influence of the CTs of the García-Valero et al. (2012) classification on the climate variability observed over the

peninsular Spain and the Balearic Islands in the period 1958-2008. To perform this, this contribution is organized as follows: Sec.3.2 describes the data employed as well as the methods used; Sec.3.3 shows a description of the precipitation and temperature WTs relating these to their associated CTs. Sec.3.4 presents how the WTs describe the observed variability at daily and seasonal scales, as well as its influence on the observed trends in precipitation and temperatures. Conclusions are summarized in Sec.3.5.

3.2 Data and Methodology

3.2.1 Data

A daily characterization of the atmospheric circulation over the IP is considered for this study. This characterization is based on the seasonal CT classification presented in García-Valero et al. (2012). The characterizations is formed by 12 CTs for each season and it extends to the period 1958-2008.

Daily series of precipitation, T_x and T_m of the gridded Spain02 dataset (Herrera et al., 2010; Herrera et al, 2015) are used for obtaining the WTs associated with the CTs. This data set covers the mainland Spain and the Balearic Island, having a spatial resolution of (0.2^o). Versions 2.1 and 3.0 of Spain02 are used for temperature and precipitation, respectively.

3.2.2 Procedure for WTs obtainment

WTs are the mean daily anomaly patterns calculated from the days belonging to a given CT. Equations 3.1 and 3.2 show the calculations followed to obtain temperature and precipitation WTs, respectively. At each grid point of the Spain02 (j subscript), and for a given CT (i subscript), the seasonal mean of temperature and precipitation ($\bar{X}_j^i$) is calculated from those days beloging to the CT_i, and for all days of the season without considerind the CT classification ($\bar{X}_j$). Hence, in the case of temperature, the mean anomaly (WT_j^i) is obtained by subtracting to the mean of days belonging to the CT_i ($\bar{X}_j^i$), the mean obtained from all days ($\bar{X}_j.$). Anomalies for precipitation are obtained from a similar way but they have also divided by the standard deviation calculated from all days the season (σ_j). This standardization is performed for a better spatial representation of the precipitation WTs.

$$WT_j^i = \bar{X}_j^i \bar{X}_j \tag{3.1}$$

$$WT_j^i = \frac{\bar{X}_j^i \bar{X}_j}{\sigma_j} \tag{3.2}$$

3.2.3 Analysis of the variability using WTs

To analyze the influence of the atmospheric dynamics on the climate variability, anomaly series of precipitation and temperature have been reproduced taking into account the information derived from the time sequence of the WTs. In this way, three comparisons between these reproduced series and the series of Spain02 are proposed. The first analyzes the time correlation between the reproduced and observational ones, whereas the second analyzes the ratio between the variances of two kind of series, ie, the explained variance (EV) by the CTs. In addition, long-term trends in both kind of series are obtained for investigating the possible links between them. To perform this, the period 1958-2008 is considered. Furthermore, the Sen's estimator is used for the obtainment of trends (Sen, 1968), whereas the Mann-Kendall test is employed for analyzing the statistical significance of trends. Correlation and EV analysis are carried out for two time scales, daily and seasonal, whereas for the analysis of trends only seasonal series have been considered.

3.3 Weather Types description

Figures 3.1,3.2, 3.3, 3.4, 3.5, 3.6, 3.7 and 3.8 show the seasonal CTs of the atmospheric classification obtained in García-Valero et al. (2012) (first column) as well as their associated WTs of precipitation (2nd column) and extreme temperatures (T_x/T_m in 3rd/4th columns). To facilitate the analysis and interpretation of them, they have been grouped into the 20 semi-subjective synoptic categories included in the five general atmospheric situations proposed in García-Valero et al. (2012) and presented in the Table 3.1. In this section a description of each general classes and related WTs is presented.

Following the main WTs characteristics are described:

3.3.1 Anticyclonic situations

In general terms, anticyclonic situations are linked to a deficit of precipitation over most regions of the IP. The air subsidence associated with this configuration is one of the main responsible of the lack of precipitation. However, some CTs of the A2 category (CT8/12-wi,CT9-sp,CT10-au) (see Tab 3.1), show weak positive precipitation anomalies in a reduced area in the East of the Cantabrian coast (North of the IP). These positive anomalies are driven by the rising of relatively warm air from the Atlantic Ocean (NW advection) caused by the existence of cold air trapped in this region (favored by orographical conditions) (Sánchez-Rodríguez, 1993).

A larger variability in temperature WTs than in precipitation is observed under the anticyclonic situations. In addition, differences appear even among the WTs related to CTs belonging to a same synoptic category. Differences among categories are mainly due to the position of the centre of the anticyclone and to

Table 3.1: Five general classes of atmospheric situations proposed in García-Valero et al. (2012): Cyclonic (C), Anticyclonic (A), Zonal (Z), Hybrid-Mixed (M) and Summer patterns (S). Subclasses for each class are also shown.

Description	CTs
A1. Anticyclone over the IP at all levels	CT1-wi,CT3-sp
A2. Anticyclone of meridian axis at the eastern Azores	CT8/12-wi,CT9-sp,CT10-au
A3. Anticyclone at the SW UK with anticyclonic circulation aloft over the IP	CT9-wi,CT4-sp,CT9-au
A4. Anticyclone at the NW IP of tilted axis (SW-NE) with northern circulation aloft	CT4-wi,CT6-sp
A5. Anticyclone over the Azores of tilted axis (SW-NE) with NW circulation aloft over the IP	CT6/7-su,CT4-au
A6. Anticyclone of zonal axis over central Europe with anticyclonic circulation aloft over the IP	CT5-wi,CT3-au
C1. Extratropical low at the NW IP	CT6-wi,CT7-sp,CT8-au
C2. Extratropical low towards the S IP	CT11-wi,CT8-sp,CT12-su,CT7-au
C3. Extratropical low at the E IP	CT10-wi,CT10-sp,CT12-au
C4. High-amplitude trough over the IP	CT11-sp
Z1. Extratropical low close to the UK with zonal circulation aloft over the IP	CT3/7-wi,CT5-sp,CT11-su,CT5/11-au
M1. Anticyclone of zonal axis over central Europe with cyclonic circulation aloft over the IP	CT2-wi,CT6-au
M2. Anticyclone at the SW UK with cyclonic circulation aloft over the IP	CT12-sp
M3. Anticyclone of tilted axis (SW-NE) over the Azores with SW circulation aloft over the IP	CT5-su
S1. Stagnant situation over the IP and anticyclonic ridge aloft	CT1-sp,CT1-au
S2. Stagnant situation with SW circulation aloft	CT2-sp,CT4/9-su,CT2-au
S3. Thermal low at the SW IP	CT1-su
S4. Thermal low at the central IP	CT2-su
S5. Thermal low at the SE IP	CT3-su
S6. Thermal low at the central-S IP and trough aloft	CT8/10-su

the atmospheric circulation at higher levels. Both factors inform in relation to the existence of advections, colder/warmer and drier/wetter, over the IP. In general, situations with weak advection (A1) lead to a rise of maximum temperatures giving large and positive T_x anomalies, whereas for T_m anomalies are weaker, being negative in the inner regions of the IP and positive in mountain areas and the coast (CT1-wi/A1 subclass). When advection is important, different WTs patterns are observed. First, if the air flux is from W/NW (A2 situation), T_x and T_m anomalies are positive in the whole of the IP in winter, but they are negative in spring and autumn. This seasonal dependence is mainly due to the difference between the temperatures existing over the IP and the North Atlantic Ocean. In winter the IP is colder than the ocean therefore advection from the Atlantic region is warm in this season. By contrast, advection is colder in the other seasons because the IP is warmer than Ocean. However, with independence of the season, all T_x WTs show a same regional pattern very characteristic of this kind of situation (A2). It exhibits a positive anomaly in the southeastern of the country. This anomaly appears due to the drying and adiabatic compression of the air over this region. If advection is from N/NE (A3/A4), large and negative T_x and T_m anomalies are appreciated in the whole of the IP independently of the season. When advection is from East (A6), a bipolar temperature WT pattern appears. Anomalies are large and negative over the eastern half, probably due to the abundance of clouds over this region (Font-Tullot, 2000), but anomalies are positive towards the Northwest of the country (again by the drying and compression of the air occurred over this area). Finally, A5 category is a mixing of advective situation from the middle of the Atlantic Ocean towards the North, Centre and East of the IP, but advection is weaker at the Southwest. In this case, summer T_x and T_m WTs exhibit negative/positive anomalies in the areas where air advection is stronger/weaker.

3.3.2 Extratropical Lows near IP

The categories belonging to the extratropical lows situation are related to positive anomaly patterns of precipitation. These situations are linked to a great dynamical and static atmospheric instability. The main differences among the WTs linked to the different categories, are observed depending on the position of the main low pressure centers (at surface level) and troughs (at higher levels). With low pressures systems over the Northwest of the IP (C1), positive precipitation anomalies dominates in a wide extension of the West and Center of the IP. Under this situation, precipitation is due to the different fronts crossing the IP from West to East, driven by the strong southwestern flux at all atmospheric levels. The negative anomalies observed in the Southeast and in the Cantabrian coast (in the North), are a consequence of the Föhn effect provoked by orographical configuration. Another extratropical low category is when low pressures are located over the South/Southwest of the IP. This configuration leads to the existence of a strong flux from the Mediterranean Sea towards the IP. In addition, a divergent flux (separation of the isohipses) at higher levels with light southwestern circulation is also present. Both factors contribute to the large and positive anomalies of precipitation at the East and South of the IP with none or negative anomalies towards the Northwest. The main events of heavy precipitation over the Mediterranean region are observed under this atmospheric pattern during autumn (Sánchez-Rodríguez, 1993; Font-Tullot, 2000). In this season large an Complex Convective Systems can develop since the large humidity during this season of the year (Doswell III et al, 1998; Romero et al, 1998). When cyclogenesis is produced over the West of the Mediterranean Sea (C3), low pressure systems provokes North/Northeast circulation accompanied by the passing of different frontal systems over the eastern half of the IP (Sánchez-Rodríguez, 1993). In the northern and eastern areas precipitation anomalies are positive, whereas they are negative towards the western regions. Despite the C4 category (wide Trough over the IP) does not agree with the low-extratropical definition, it has been included here because the important positive precipitation anomalies associated, especially at the East and North of the IP. C4 is more frequent in Spring (García-Valero et al., 2012), and it is accompanied by a very cold irruption of air at higher levels provoking a large static instability.

Similar to the Anticyclonic situations, precipitation WTs are very similar under a given subclass, independently of the season of the year, but some differences appear in the WTs of temperature. When C1 situations occurs in winter (warm advection from the Atlantic Ocean), positive light/large anomalies are observed in the overall of the IP for T_x/T_m temperatures (CT6-wi), but in spring and autumn anomalies are negative (cold advection), being much higher for T_x. In the C2 situation (advection from the Mediterranean Sea) negative anomalies for T_x are distributed along a vast extension of the territory in autumn and winter, and over a more reduced area of the South during spring and summer. Regarding the T_m anomalies, these are more significant in spring (positive) and autumn (negative). Less seasonal differences are appreciated under the C3 subclass. Large and

negative T_x anomalies ,very generalized over the territory, are observed for T_x (cold advection from the North) but for T_m are weaker. This difference between T_x and T_m anomalies, which is translated by a decrease in the diurnal cycle amplitude, could be related to the existence of strong winds and cloudiness. Similar WTs to the C3 situations are appreciated for the C4 category.

3.3.3 Zonal and hybrid-mixed situations

Zonal situation (Z1) is defined as an intense zonal flux at lower and higher levels (García-Valero et al., 2012). This pattern is similar to those related to the C1 category, but in this case wind comes from the West. In this case, precipitation anomalies are positive in the Northwest while they are negative in the East and Southeast. Temperature WTs show patterns very similar to those related to the C1 category, positive anomalies in winter (warm advection) and negative in the other seasons.
Regarding the hybrid mixed situations, M1 and M2 are associated with WTs of precipitation showing positive anomalies over the Southeast of the IP. In both cases, it is appreciated the existence of advection from the Mediterranean Sea to the IP, as well as the existence of a trough over the eastern half. Both factors contribute to the unstabilization of the atmosphere in the East of the IP. Temperature anomalies are negative, being larger for T_m, especially in winter. The M3 situation does not exhibit any significant anomaly of precipitation. Temperature anomalies are similar to those related to the Z1 situation, negative in the North and positive in the South.

3.3.4 Stagnant situations

The configurations S1, S3, S4 y S5 show very weak or inexistent pressure gradients over the IP, then winds are weaker in most regions (Lorente-Plazas et al, 2015). In addition, the prevalence of ridges (at high levels) maintains the sky clair facilitating the insolation. Both circumstances guide in all the IP (García-Valero et al, 2015) positive T_x anomalies. The S2 category is related to the existence of a trough over the West of the IP. This leads to positive precipitation anomalies in the northern (CT9-su) and negative temperature anomalies (both for T_x and T_m) over three quarter parts of the IP, except in the Northeast quadrant where the Föhn effect is present. S6 class is the natural transition to the S2 (García-Valero et al., 2012) class. Under this situation a trough is located just over the Centre of the IP, guiding the largest and positive anomalies of precipitation in the Centre, South and East.

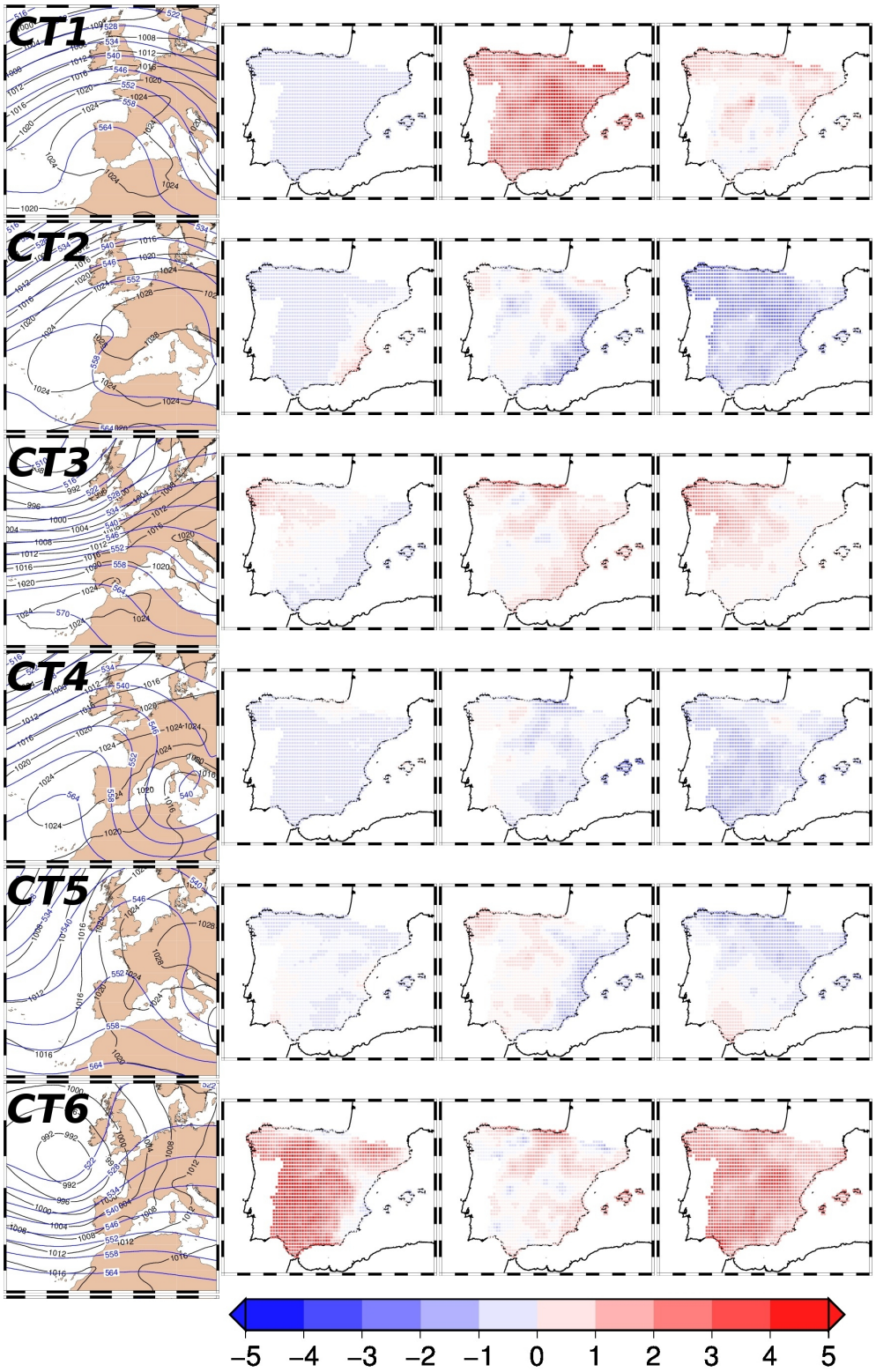

Figure 3.1: Winter. CTs and associated WTs. CTs 1 to 6 (first column) of the García-Valero et al. (2012) atmospheric classification and their related precipitation (second column), T_x (third column) and T_m WTs. Averaged anomalies are represented for temperature (°C) but anomalies divided by standard deviation are represented for precipitation.

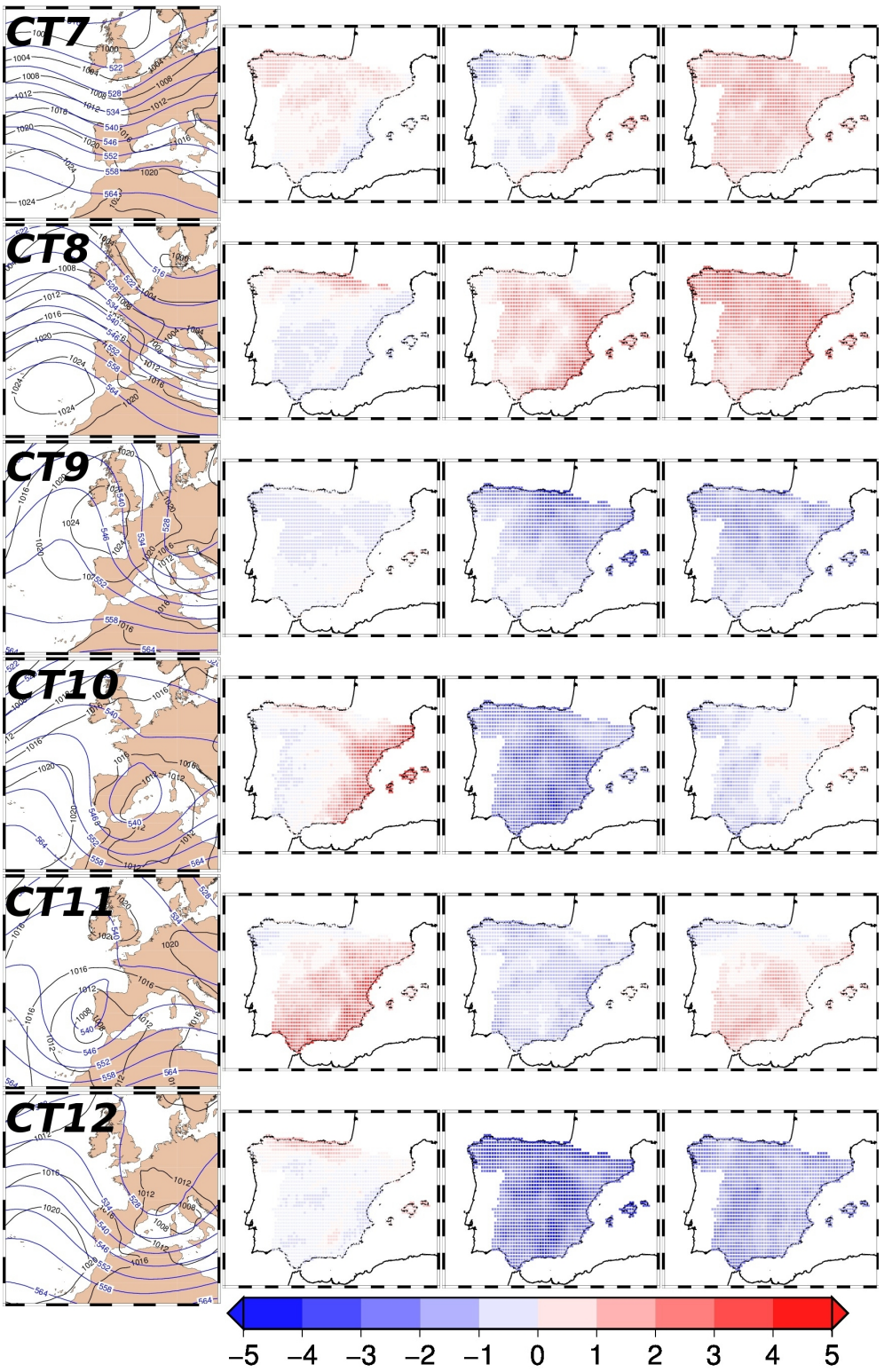

Figure 3.2: Winter. Same as Fig. 3.1 but from CT7 to CT12.

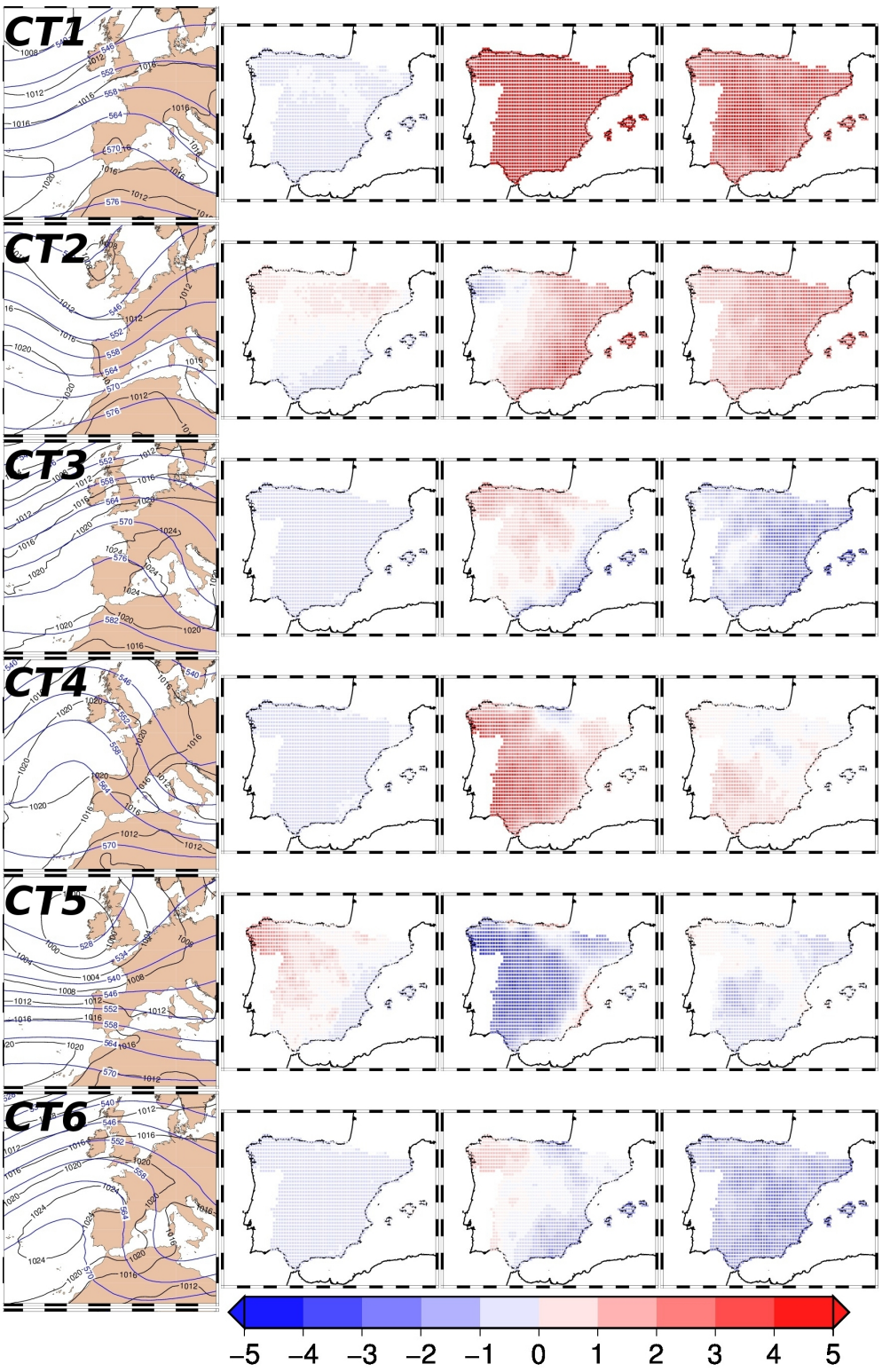

Figure 3.3: As Fig. 3.1 but for spring.

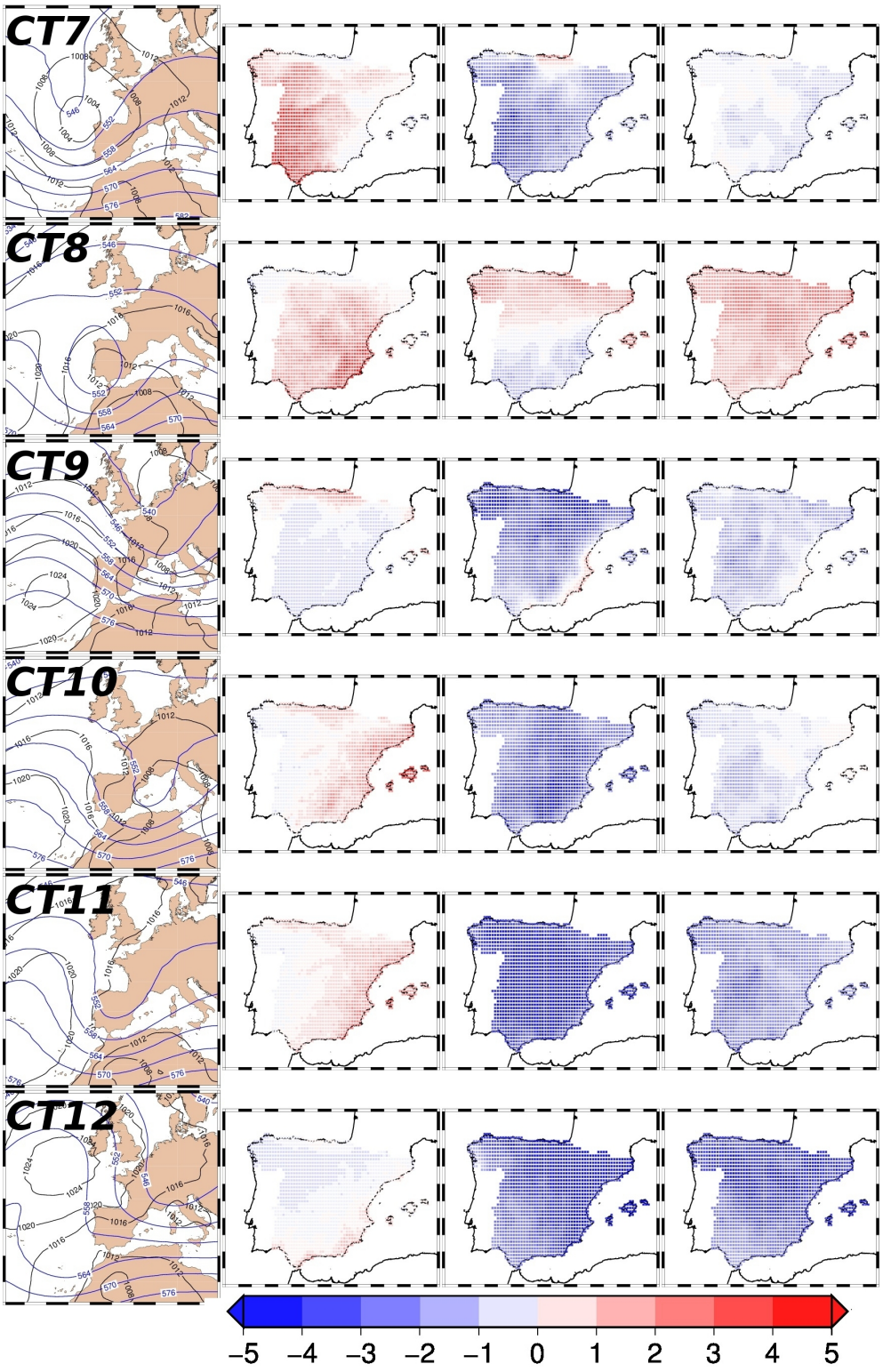

Figure 3.4: As Fig. 3.2 but for spring.

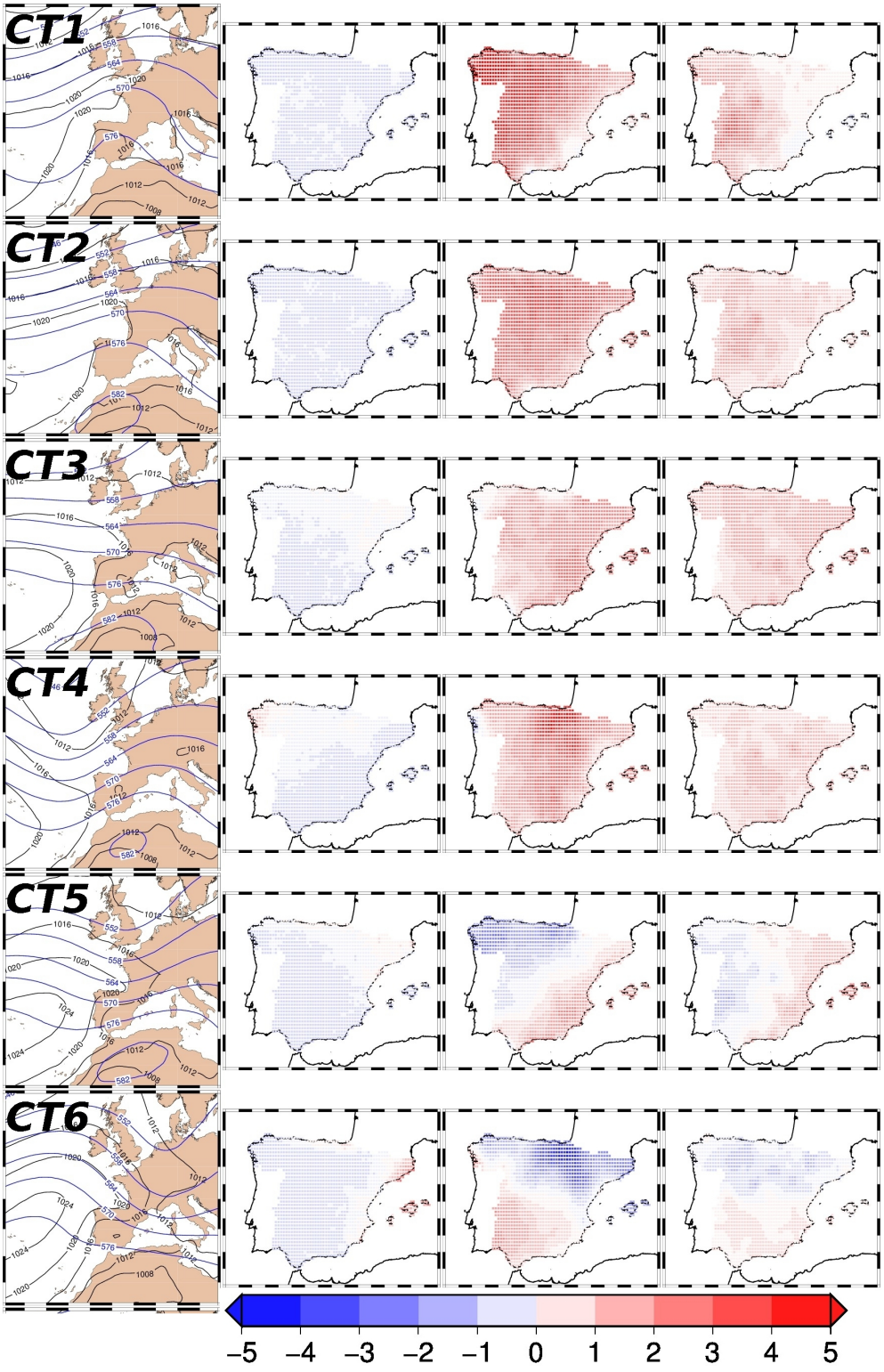

Figure 3.5: As Fig. 3.1 but for summer.

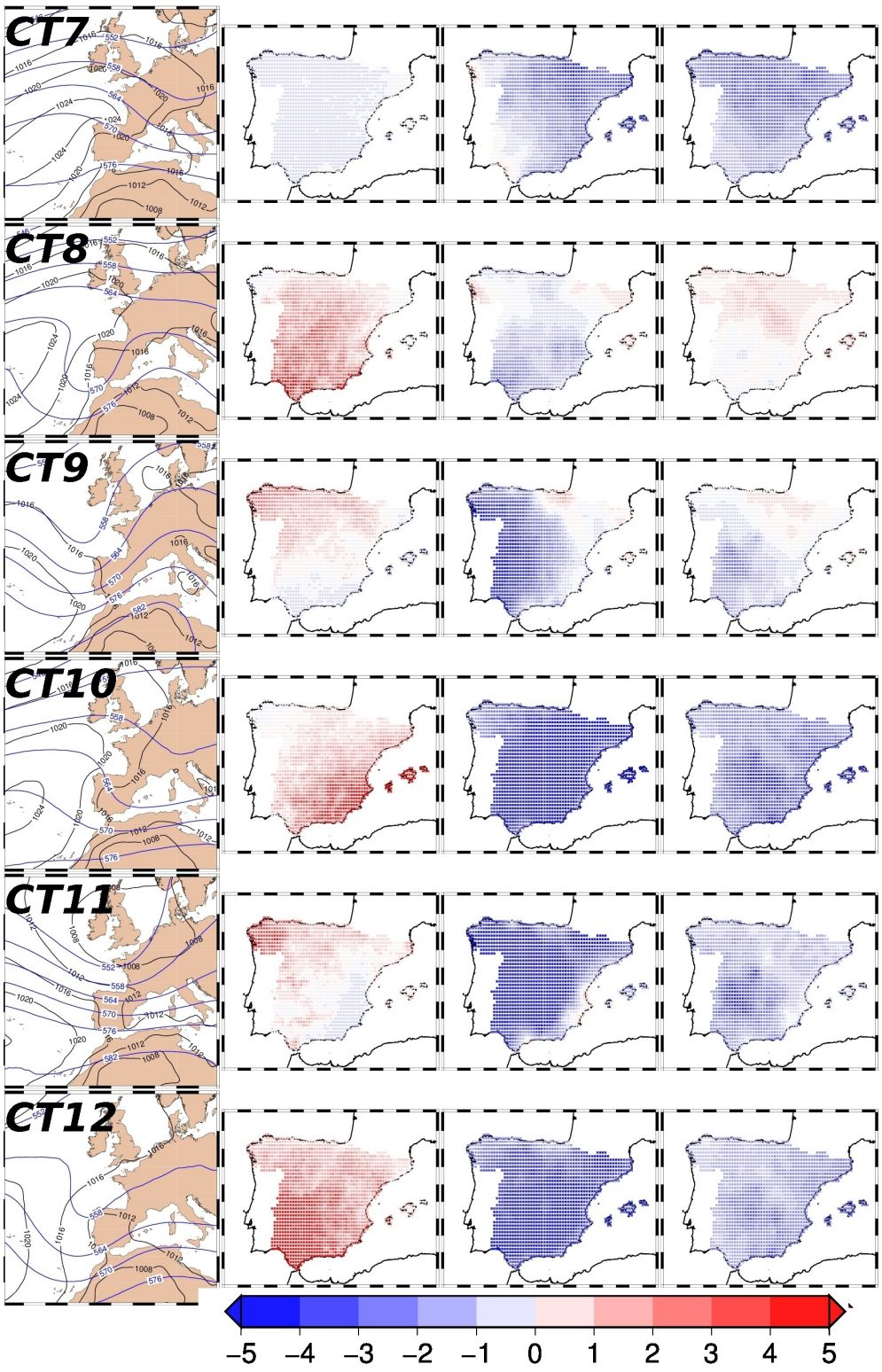

Figure 3.6: As Fig. 3.2 but for summer.

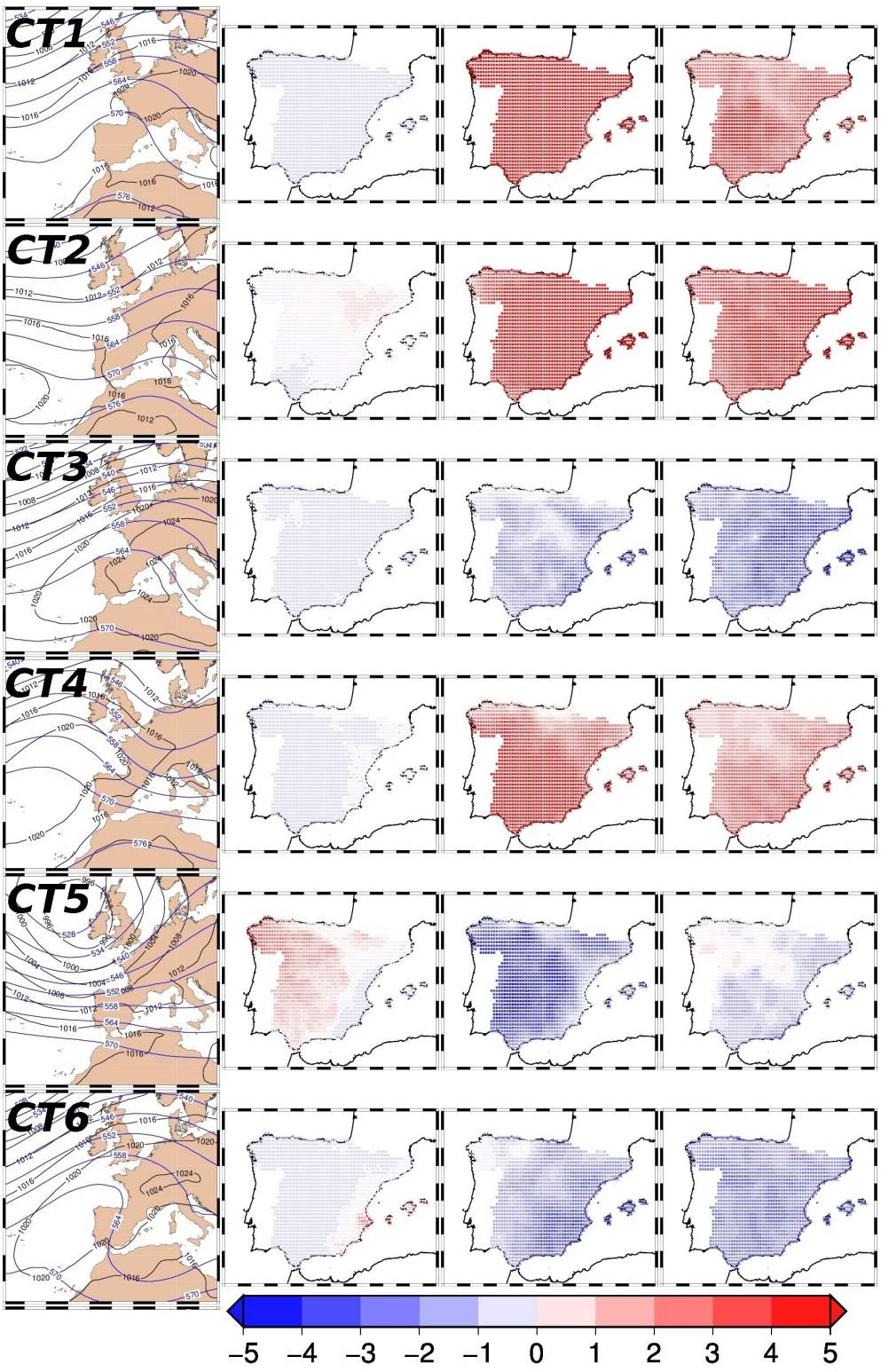

Figure 3.7: As Fig. 3.1 but for autumn.

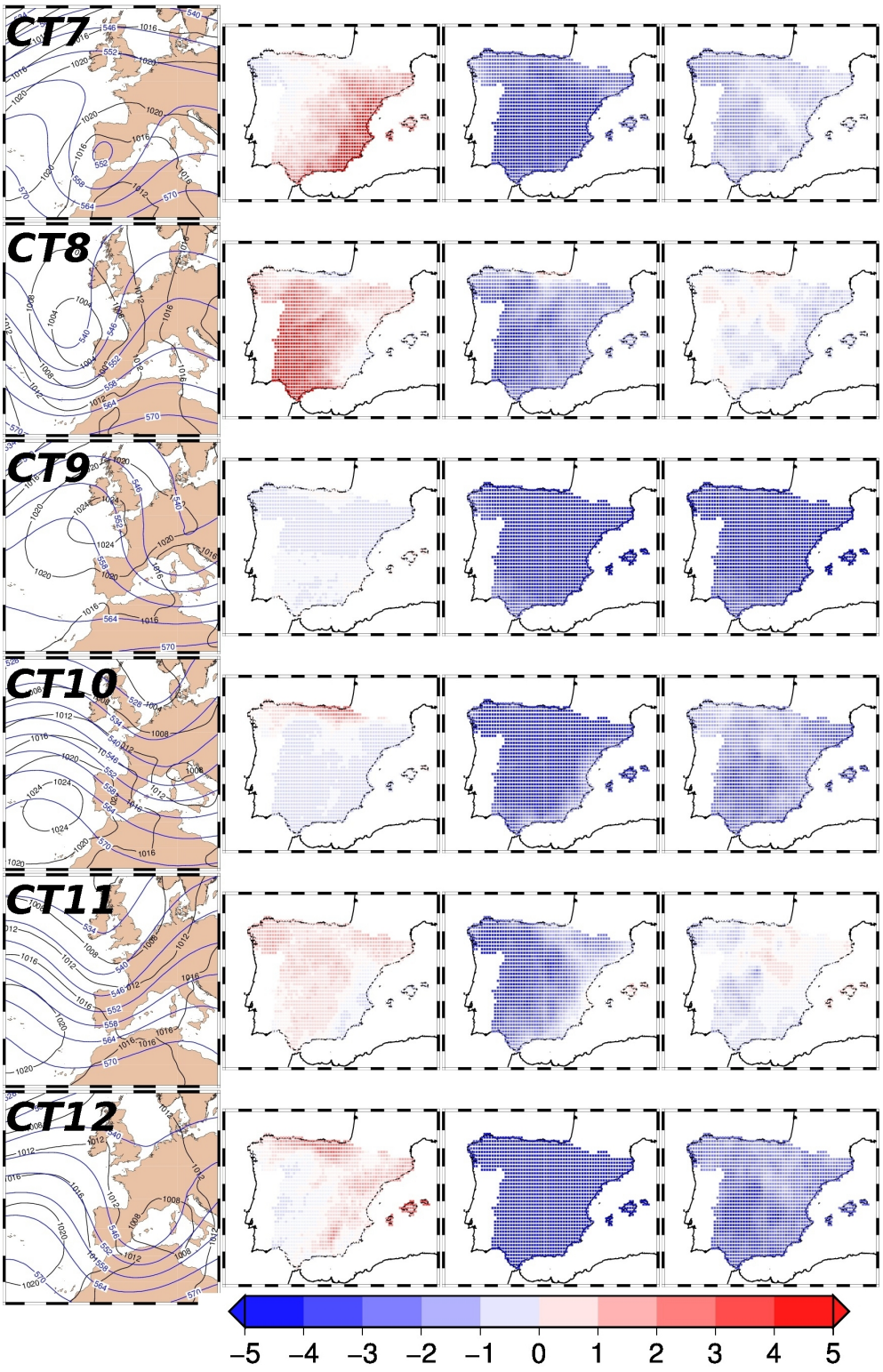

Figure 3.8: As Fig. 3.2 but for autumn.

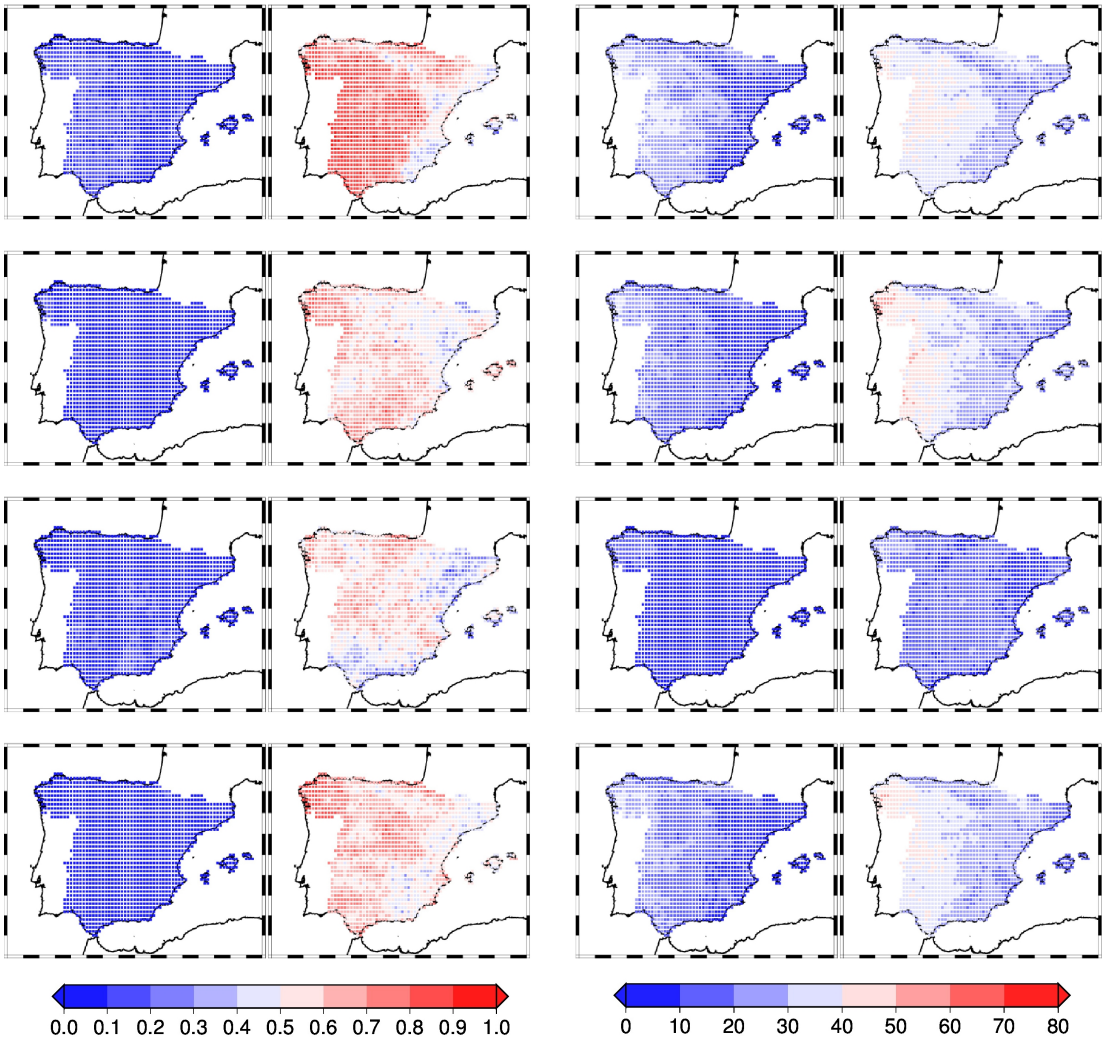

Figure 3.9: Seasonal correlation and explained variance patterns for precipitation. Correlation are obtained between the series reproduced by WTs and observational series derived from Spain02. Left panel shows correlation patterns while variance patterns are represented on the right panel. Each corresponds to each season (from top to bottom: winter, spring, summer and autumn). Patterns are obtained for two time scales represented on each pair of graphics, daily (left) and seasonal (right).

3.4 Influence of the CTs on the observed variability

In this section it is intended to investigate the correspondence between the anomaly series reproduced by the CTs and those derived directly from Spain02. To perform this, some comparisons between both kind of series are carried out following the process explained in the Subsec 3.2.3. This analysis can help to understand better the role of the CTs on the observed variability changes.

3.4.1 Correlation and variance reproduced by WTs

Seasonal spatial patterns of the correlation between the reproduced series and the observational ones, and of the percentage of the total explained variance (EV) by the CTs, obtained for the series of precipitation, T_x and T_m, are represented in the Figures 3.9, 3.10 and 3.11, respectively. As would be expected, daily variability is worse reproduced than seasonal variability, mainly due to the limitations of the methodolgy because it clusters a huge number of daily situations into a reduced number of typical ones. This makes that the dispersion of each CT was very important. An example of this is the large spread existing on each WT of winter which can be seen represented in the Figure 3.12 (figures for the rest of are not shown because they exhibit similar results than winter). Despite this, good results are obtained for T_x and T_m during the equinoctial seasons, especially in autumn, when correlations between 0.5 and 0.6, and EV about 60%, are observed in a large extension of the territory. In general terms, reproduced variability is higher for T_x than for T_m, result which could be due to the existence of a higher number of factors controlling the T_m variability than those affecting to T_x.
Regarding precipitation, daily variability is worse reproduced than for temperature, result which is coherent taking into account the higher variability of precipitation than temperature. However, some relatively good result is observed in the EV in some western areas during winter and autumn (about 40%), coinciding these with those regions whose regime of precipitation is largely controlled by the prevailing circulation from the Atlantic Ocean (Font-Tullot, 2000).

Regarding the results obtained at seasonal scale, a large similarity between the reproduced series and the observational ones is found for all variables. As occurred above, temperature variability is much better reproduced than precipitation one, obtaining also better results for T_x than for T_m. In the case of T_x, correlations reach up to 0.8-0.9 in the four seasons, being these correlations extended over large areas of the territory, especially in spring and summer. The EV is also important, observing generalized values above 70% during spring, summer and autumn. The worse results for T_x are found in winter, especially in the western regions. Regarding T_m, the influence of the orography is observed in the correlation results. Hence, correlations lower than 0.4 are observed in some mountain areas in the northern (Pyrenees, Cantabrian chain and Iberic system) and southern (Betic system (at SE), Grazalema and Ronda (near Gibraltar Strait)), whereas higher correlations (between 0.6-0.7) are observed in many regions of the center. Correlation results are somewhat worse in winter than in the rest of season. In the case of EV, good results are found in spring and autumn (EV about 50-70%), somewhat worse in summer (40-60%) and the worst are obtained in the eastern regions during winter (below 40%). Unlike correlation, EV maps do not exhibit orographical influence, being these spatially more homogeneous. Regarding precipitation, better results are derived from correlation than variance. In general, variance only exceeds 50% in some western regions during winter, spring and autumn, obtaining the worst results in summer. In relation to the corre-

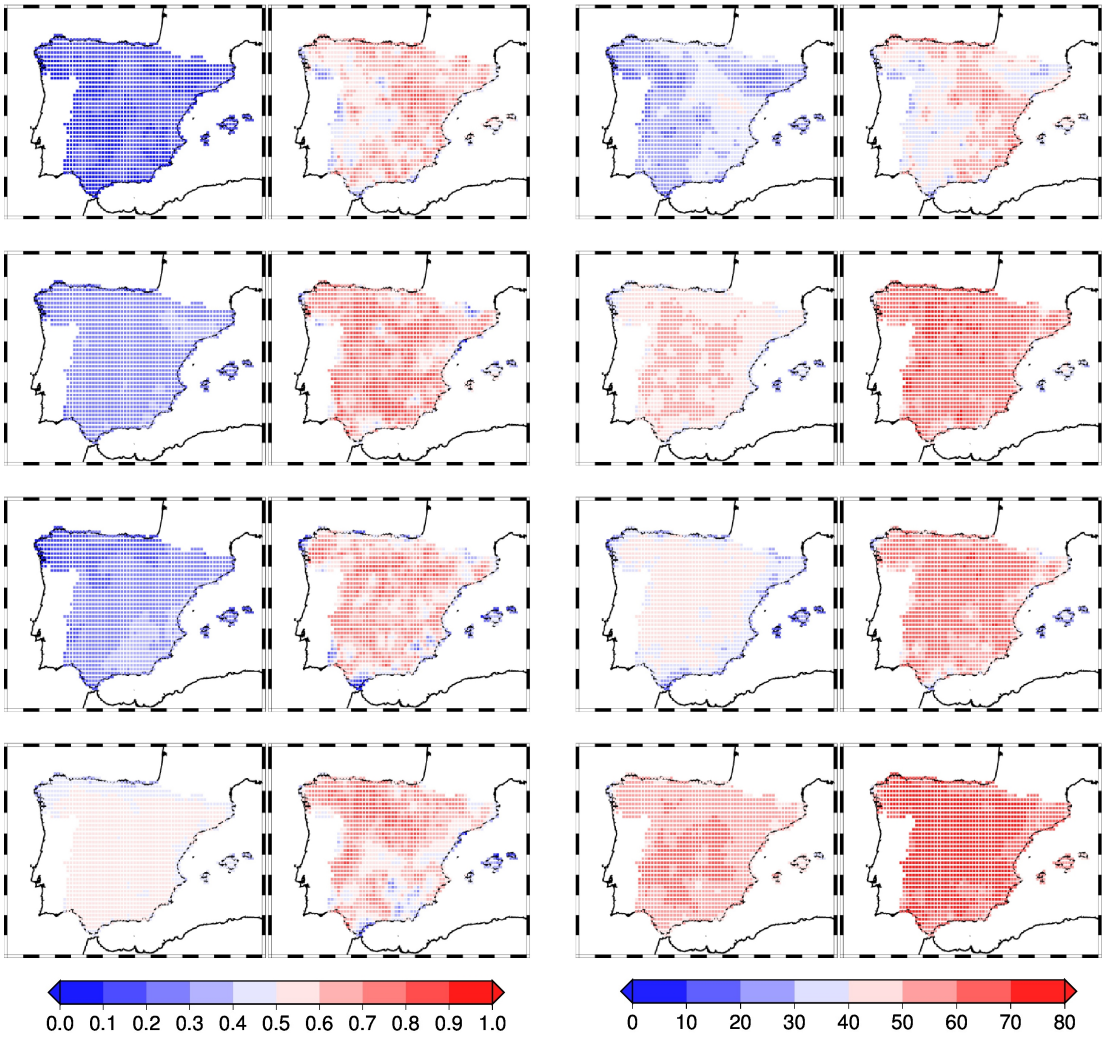

Figure 3.10: As Figure 3.9 but for tmax.

lation, the central and western regions, as well as the Pyrenees, present values above 0.8 in winter, decreasing up to 0.6 in spring and autumn. In summer the worst results are obtained. In summary, a clear difference between the eastern and western halves of the peninsular Spain is observed, both in correlation and EV. This evidences the great difference in the regime of precipitation existing between the atlantic and the mediterranean regions (Font-Tullot, 2000), driven in the formers by large-scale precipitation systems and in the laters by convective precipitation (Font-Tullot, 2000).

3.4.2 Analysis of trends

The existence of long-term seasonal trends from the reproduced and observational series is analyzed in this subsection for the period 1958-2008. As it was mentioned in the introduction (Sec 3.1), important trends in precipitation and temperature

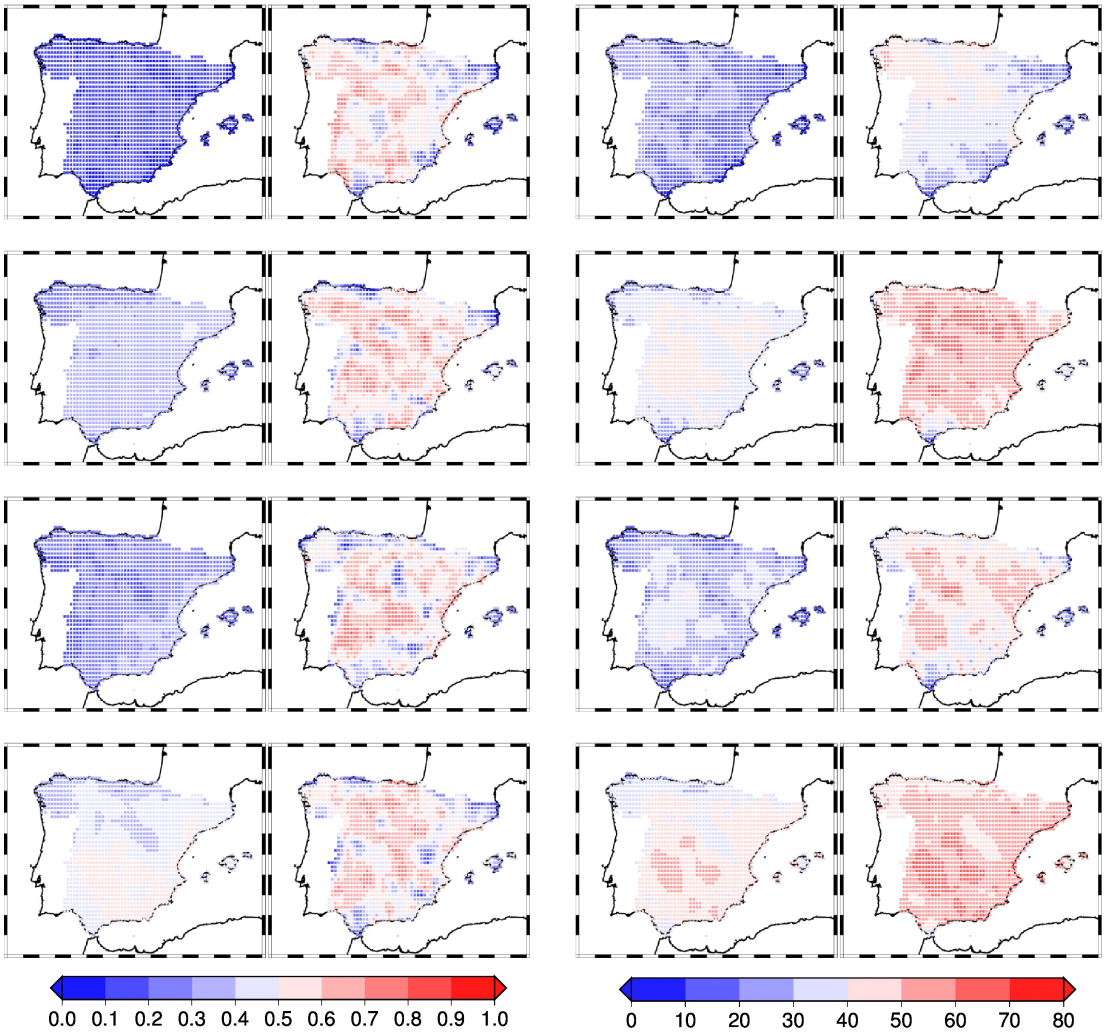

Figure 3.11: As Figure 3.9 but for tmin.

have been reported for the IP along the second half of the past century. The correspondence between the reproduced trends from WTs and those derived from the Spain02 series would help to understand the role of the atmospheric dynamics on the observed changes. Therefore, a high correspondence would mean that changes in the atmospheric circulation are in part responsible on the reported trends.

Only significant trends derived from the seasonal series reproduced by the WTs for precipitation and temperature are found in winter. Figure 3.13 shows these results, representing on the maps only those trends with statistical significance (at 95%; light pink color denotes non-significant trend). Trends for precipitation agree with the results derived from the Spain02 series, but they are different for T_m. Precipitation trends are negative, especially at some regions of the Northwest and Southwest of Spain, coinciding this result with that informed in Corte-Real et al (1998); MJ. et al (1998); Serrano et al (1999); Paredes et al (2006); López-Bustins et al (2008), among others. In relation to T_m, trends are positive in the

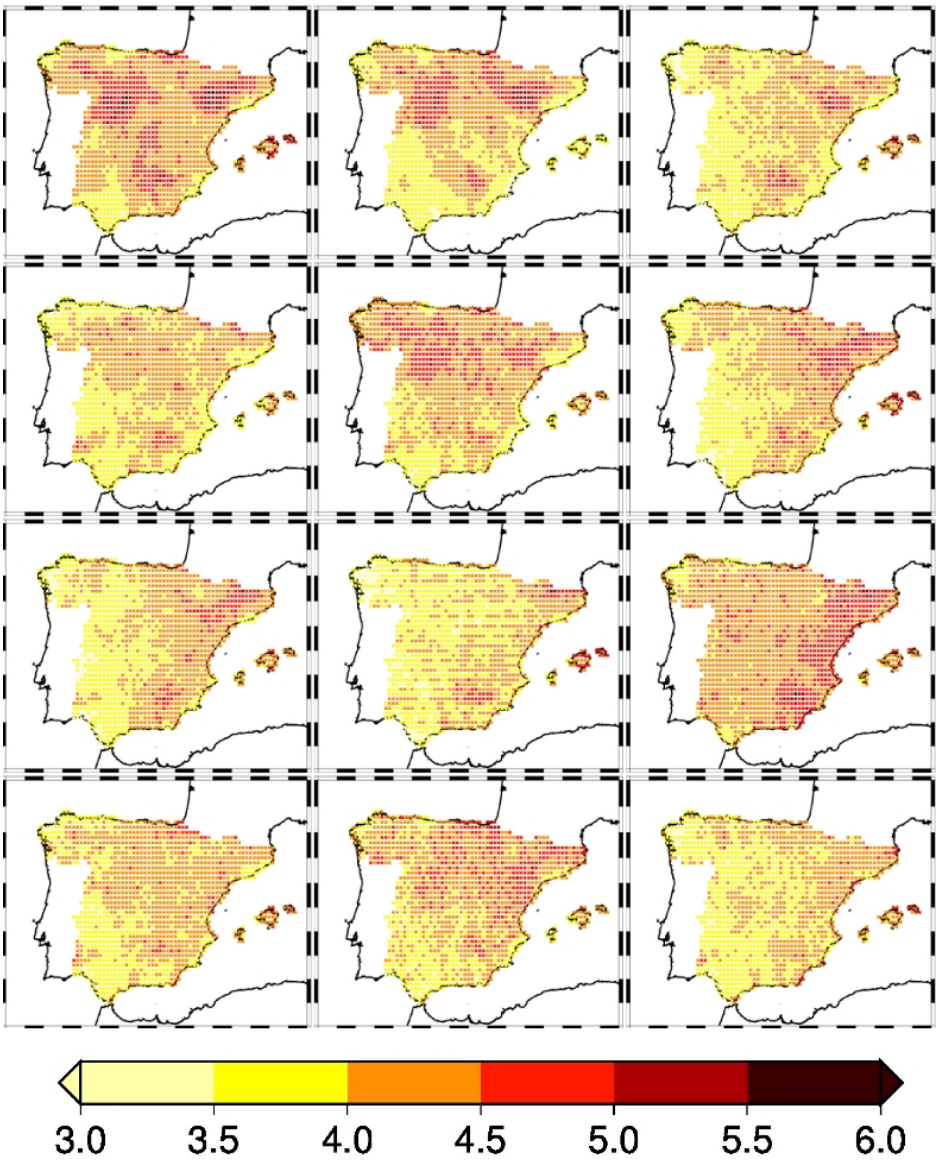

Figure 3.12: Standard deviation inside the WTs for T_x in winter.

Spain02 series at some regions of the northern, central and southern, whereas trends derived from the WT series are weak negative in some areas of the eastern and southern.

For the rest of seasons (Figures not shown here), significant positive trends for temperature are found by using the Spain02 series, but any trend is obtained from the WT series. Brunet et al (2007) presents a complete analysis of trends in T_x and T_m over the IP from 1850 to 2005. In this work, averaged trends for the whole of the IP are obtained for two periods, 1950-1972 and 1973-2005, more or less included in our period of study, obtaining non-significant negative trends for the first period, and significant positive for the second one. These results sug-

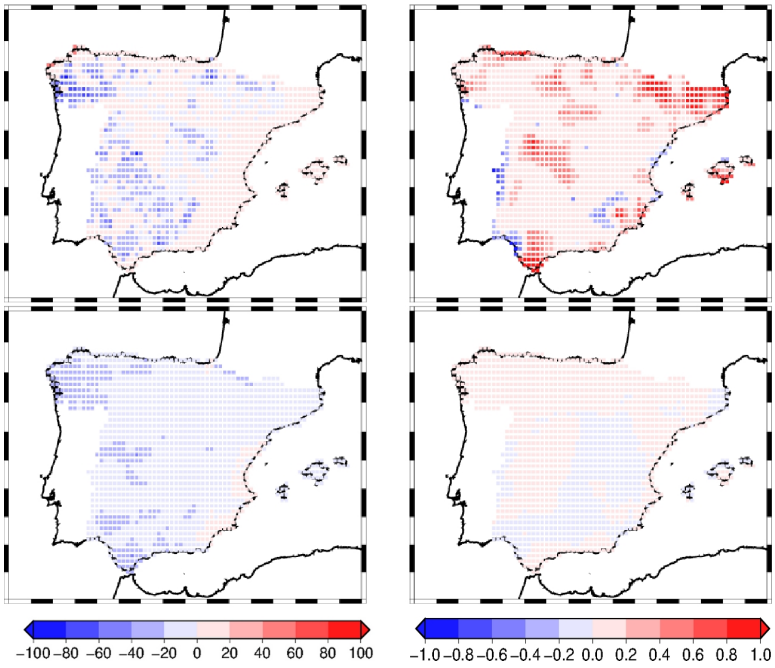

Figure 3.13: Significant decadal trends of seasonal precipitation (left) and minimum temperature (right) in winter. Trends from observations (top) and reproduced series by WTs (bottom).

gest that the net trend could be non-significant for the all period agreeing these with the trends derived from the reproduced WT series. These differences with the Spain02 trends could indicate the existence of some problems in the Spain02 series that should be considered for trend calculations. Actually, for the construction of Spain02, by means of interpolation techniques, the number of available stations grows from 1950 until the early 1970s, when it remains approximately constant, although it decreases in the last years (Herrera et al., 2010; Herrera et al, 2015). This fact, makes than Spain02 series since 1970 can be considered as more homogenous and appropriate for the analysis of trends (Fernandez-Montes and Rodrigo, 2015). Taking all these reasons in consideration, trends have also been calculated for the period 1973-2005 (the same used in Brunet et al (2007)).

The reproduced trends for T_x and T_m are coherent with those observed in Spain02 for the period 1973-2005, especially in summer and spring, and for both T_x and T_m variables. Figures 3.14 and 3.15 show, for both seasons, positive generalized trends around all the territory in both kind of series, Spain02 and the WTs. Therefore, the global signal is a positive trend as that reported in Brunet et al (2007). In addition, for both temperatures (T_x and T_m) the obtained trends are somewhat larger in spring than summer, coinciding with that informed in Brunet et al (2007). However, positive trends for T_m in autumn noticed by Brunet et al (2007) and derived from Spain02, are not reproduced by changes in the frequency of the WTs. Another differentiating element is the largest trends exhibit

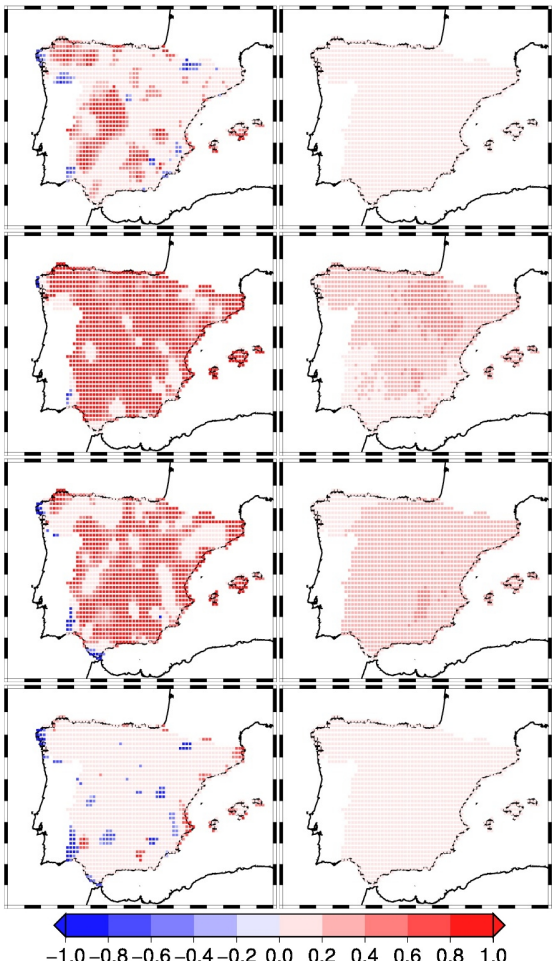

Figure 3.14: Decadal trends of seasonal T_x (ºC/decade) for the period 1973-2005. Trends from observations (left) and from the reproduced series by WTs (right) are shown. Each row is corresponding to each season of the year (from top to bottom: winter, spring, summer and autumn).

in Spain02 and informed in Brunet et al (2007) than those obtained throughout the WT series. This result could indicate that other factors distinct to the changes in the atmospheric circulation could be behind of the observed trends, as for example might be the global warming (IPCC, 2014).

Finally, precipitation trends have also been analyzed for the period 1973-2005 (Figure 3.16). Results show important changes in relation to the longest period (1958-2008). Hence, during winter, if trends from the Spain02 are analyzed, only a reduced area in the northwestern has significant negative trends, but any trend is derived from the reproduced series. Despite this, the reproduced and Spain02 series agree with the trends obtained in the rest of seasons. Thus, in autumn, when the largest trends in precipitation are obtained, positive trends are found in the northwestern quadrant, negative at eastern of the Cantabrian coast during spring, and weak negative during summer in the central and southern.

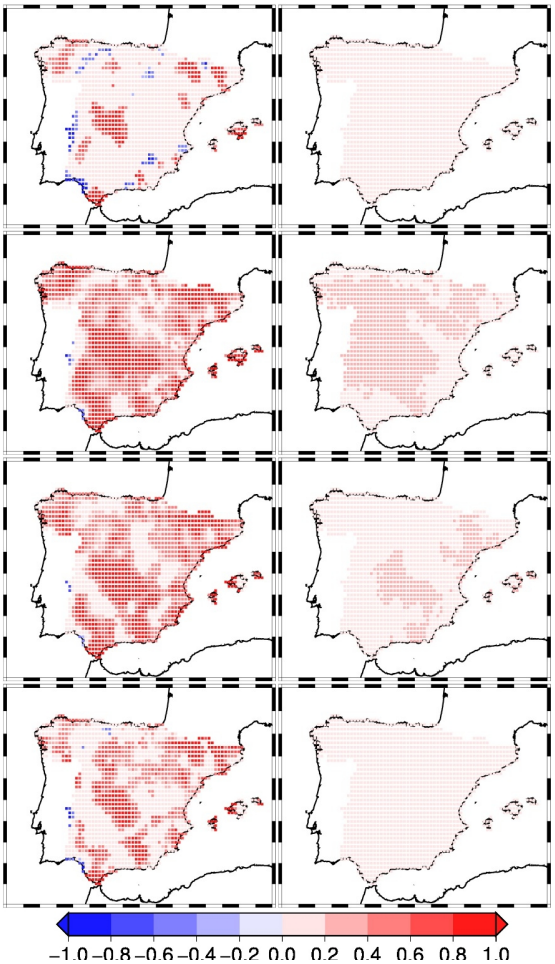

Figure 3.15: As Figure 3.14 but for T_m.

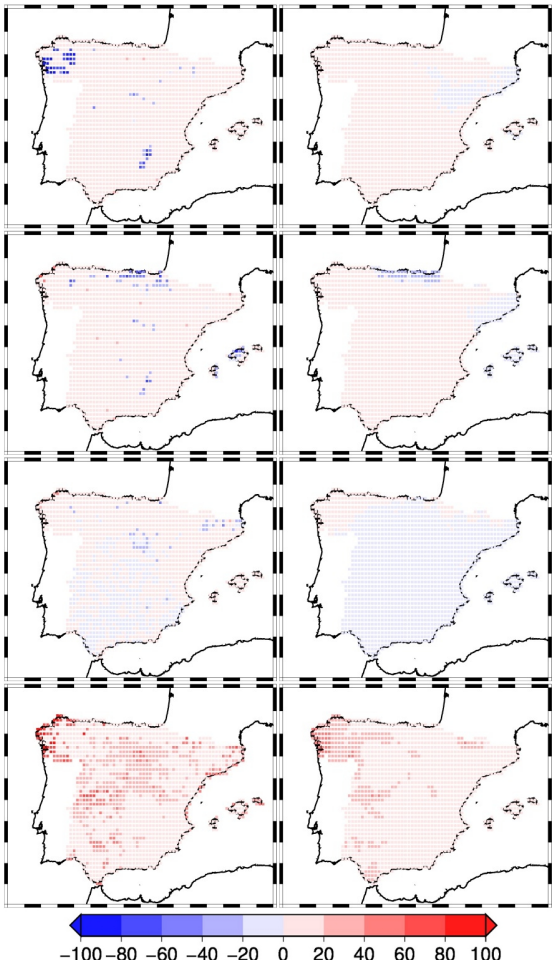

Figure 3.16: As Figure 3.14 but for precipitation. Trends are in mm/decade.

3.5 Conclusions

Main conclusions of this work are summerized as follows:

- In general, the variability of the WTs describe well the seasonal variability of the three considered variables. However, depending on the variable some differences are observed. Hence, the best explained variable is T_x, follows by T_m and precipitation. In addition, there are also a seasonal dependence of the results. In the case of T_x, spring, summer and autumn are the seasons when variability is better explained. For the case of T_m, is during spring and autumn when the best results are achieved, whereas is in winter for precipitation, followed by spring and autumn. Therefore, the worst results, especially due to a bad description of the variance, are obtained in winter(summer) for temperature(precipitation).

- The variability described by the WTs in winter presents significant differences between the eastern and western areas. Hence, whereas temperature variability is well described by the atmospheric circulation at eastern regions, it is bad represented at the western ones. However, a different result is obtained for precipitation, whose variability is better described at western but is poorly reproduced at eastern. This large difference between both areas can be associated with the different precipitation regime of both regions during winter, when a more regular regime is observed at western than eastern areas (Font-Tullot, 2000). Differences in temperature can be due in part by the larger abundance of clouds in the western half of the peninsula in this season, affecting more to the temperature variability of this area.

- Seasonal trends observed in precipitation can be explained by trends detected in the frequency of some CTs and therefore of their associated WTs. For the period 1958-2008 only significant precipitation trends in winter are found in some areas of the central and western of the IP. The trends are mainly due to changes in two CTs. The first one, associated with the decreasing in the occurrence of extratropical lows at NW of the IP (García-Valero et al., 2012) connected to positive precipitation anomalies in the central and western areas. A similar result was reported by other previous works (Corte-Real et al, 1998; Trigo et al, 2000; Fernández-Montes et al, 2012b), relating this change with a polarward of the stormtracks (Paredes et al, 2006). The another CT is related to the increasing of the occuurence of high pressures at the central of Europe (CT2) (García-Valero et al., 2012). A similar change in this CT was reported by Esteban et al (2006); López-Bustins et al (2008) who attributed it to an increase of the positive phases of the AO and NAO teleconnection patterns observed along the second half of the past century.
  For the period 1973-2005 more trends in precipitation are observed in all

seasons. In general, changes in CTs explain relatively well such trends, especially in autumn, spring and summer, when positive trends in some areas of the West and Northwest of Spain, negative trends in the Cantabrian coast, and negative trends in the central and southern regions, respectively, are observed. In this case the negative trend observed in a reduced area in the northwestern of Spain during winter can not be explained by changes in CTs.

- Seasonal temperature trends derived from the WT series along the period 1973-2005 agree with those obtained from the Spain02 series and with the global signal of the peninsular Spanish territory informed in Brunet et al (2007). In the case of T_x, changes are detected only during spring and summer, observing the largest trends in spring at many regions of the central and northern . The largest trends observed in spring in the Spain02 series are also reproduced by the WTs, coinciding this result with that informed by Brunet et al (2007). Regarding T_m, WT trends agree with those derived from the Spain02 series in spring and summer, but not during autumn, when positive trends in the Spain02 series are obtained and no trends are found in the reproduced WT series. Therefore, the autumn T_m trends could be related to other factors distinct to changes in dynamics.

- Temperature trends calculated for the longest period (1958-2008), show great differences beween those derived from Spain02 and WT series. However, results from WT series not show any trend, being this a coherent result which that reported in Brunet et al (2007). In addition, trends detected in Spain02 for temperature could be affected by the existence of less homogeneous series before 1973 (Fernandez-Montes and Rodrigo, 2015), mainly due to the lower number of available stations for developing the Spain02 temperature dataset (Herrera et al., 2010; Herrera et al, 2015). Both results suggest that the application of WTs could be an useful tool for the detection of possible inhomogeneities in the observational series.

The WTs obtained here for the three considered variables have a large physical coherence with their associated CTs. Therefore, they are the basis for understanding the large spatio-temporal of the mean variability caused by the atmospheric dynamics over the studied area. Anyway, they are not an appropriated tool for understanding the daily variability since a large heterogeneity of the atmospheric circulations exits in the different CTs. Therefore, there will be a large variance in the population of anomalies related to a given CT. As consequence, to take an averaged anomaly value for defining the WTs is a great simplification of the existing variability, and much more at daily scales. Therefore, the WTs obtained here can only be used for the description of the averaged variability being the method invalid for the analysis of extreme variability of great interest for society. In conclusion, to better understand changes in the frequency occurrence of extreme events under the optical of the CTs, new classifications obtained for the description of such events should be developed.

Bibliography

Barnston AG, Livezey RE (1987) Classification, seasonality and persistence of low-frequency atmospheric circulation patterns. Monthly weather review 115(6):1083–1126

Beck C, Philipp A (2010) Evaluation and comparison of circulation type classifications for the european domain. Phisics and Chemistry of the Earht 35:374–387

Bermejo M, Ancell R (2009) Observed changes in extreme temperatures over spain during 1957-2002, using weather types. Revista de Climatología 9:45–61

Brunet M, Jones P, Sigró J, Saladié O, Aguilar E, Moberg A, Della-Marta P, Lister D, Walther A, López D (2007) Temporal and spatial temperature variability and change over spain during 1850-2005. Journal of Geophysical Research 112(D12)

Corte-Real J, Qian B, Xu H (1998) Regional climate change in portugal: precipitation variability associated with large-scale atmospheric circulation. International Journal of Climatology 18(6):619–635

Doswell III CA, Ramis C, Romero R, Alonso S (1998) A diagnostic study of three heavy precipitation episodes in the western mediterranean region. Weather and Forecasting 13(1):102–124

El Kenawy A, López-Moreno JI, Vicente-Serrano SM (2012) Trend and variability of surface air temperature in northeastern spain (1920–2006): linkage to atmospheric circulation. Atmospheric Research 106:159–180

Esteban P, Martin-Vide J, Mases M (2006) Daily atmospheric circulation catalogue for western europe using multivariate techniques. International Journal of Climatology 26(11):1501–1515

Fernandez-Montes S, Rodrigo F (2015) Trends in surface air temperatures, precipitation and combined indices in the southeastern iberian peninsula (1970-2007). CLIMATE RESEARCH 63(1):43–60

Fernández-Montes S, Rodrigo F, Seubert S, Sousa P (2012a) Spring and summer extreme temperatures in iberia during last century in relation to circulation types. Atmospheric Research

Fernández-Montes S, Seubert S, Rodrigo F, Hertig E (2012b) Wintertime circulation types over the iberian peninsula: long-term variability and relationships with weather extremes. Clim Res 53:205–227

Font-Tullot I (2000) Climatología de España y Portugal. University of Salamanca (Spain)

Gallego M, Trigo R, Vaquero J, Brunet M, García J, Sigró J, Valente M (2011) Trends in frequency indices of daily precipitation over the iberian peninsula during the last century. Journal of Geophysical Research: Atmospheres (1984–2012) 116(D2)

García-Valero JA, Montávez JP, Gómez-Navarro JJ, Jiménez-Guerrero P (2015) Attributing trends in extremely hot days to changes in atmospheric dynamics. Natural Hazards and Earth System Science 15(9):2143–2159, doi:10.5194/nhess-15-2143-2015, URL `http://www.nat-hazards-earth-syst-sci.net/15/2143/2015/`

García-Valero J, Montavez J, Jerez S, Gómez-Navarro J, Lorente-Plazas R, Jiménez-Guerrero P (2012) A seasonal study of the atmospheric dynamics over the iberian peninsula based on circulation types. Theoretical and Applied Climatology 110:291–310, doi:10.1007/s00704-012-0623-0, URL `http://dx.doi.org/10.1007/s00704-012-0623-0`

González-Hidalgo JC, Brunetti M, de Luis M (2011) A new tool for monthly precipitation analysis in spain: Mopredas database (monthly precipitation trends december 1945–november 2005). International Journal of Climatology 31(5):715–731

Goodess C, Palutikof J (1998) Development of daily rainfall scenarios for southeast spain using a circulation-type approach to downscaling. International Journal of Climatology 18(10):1051–1083

Herrera S, Gutiérrez J, Ancell R, Pons M, Fías M, Fernández J (2010) Development and analysis of a 50-year high-resolution daily gridded precipitation dataset over spain (spain02). International Journal of Climatology

Herrera S, Fernández J, Gutiérrez J (2015) Update of the spain02 gridded observational dataset for euro-cordex evaluation: assessing the effect of the interpolation methodology. International Journal of Climatology

Hertig E, Seubert S, Jacobeit J (2010) Temperature extremes in the mediterranean area: trends in the past and assessments for the future. Natural Hazards and Earth System Science 10(10):2039–2050

Hidalgo-Muñoz J, Argüeso D, Gámiz-Fortis S, Esteban-Parra M, Castro-Díez Y (2011) Trends of extreme precipitation and associated synoptic patterns over the southern iberian peninsula. Journal of Hydrology 409(1):497–511

IPCC (2014) Climate Change 2013: The physical science basis: Working group I contribution to the fifth assessment report of the Intergovernmental Panel on Climate Change. Cambridge University Press

Jacobeit J, Rathmann J, Philipp A, Jones PD (2009) Central european precipitation and temperature extremes in relation to large-scale atmospheric circulation types. Meteorologische Zeitschrift 18(4):397–410

Jiménez P, González-Rouco J, Montávez J, García-Bustamante E, Navarro J (2008) Climatology of wind patterns in the northeast of the iberian peninsula. International Journal of Climatology 29:501–525

Jones P, Lister D (2009) The influence of the circulation on surface temperature and precipitation patterns over europe. Climate of the Past Discussions 5(1)

Jones P, Hulme M, Briffa K (1993) A comparison of lamb circulation types with an objective classification scheme. International Journal of Climatology 13(6):655–663

López-Bustins J, Martín-Vide J, Sánchez-Lorenzo A (2008) Iberia winter rainfall trends based upon changes in teleconnection and circulation patterns. Global and planetary change 63:171–176

Lorente-Plazas R, Montávez J, Jimenez P, Jerez S, Gómez-Navarro J, García-Valero J, Jimenez-Guerrero P (2015) Characterization of surface winds over the iberian peninsula. International Journal of Climatology 35(6):1007–1026

Lorenz E (1956) Technical report, Statistical Forecast Project Report 1. Dep.of Meteorology.MIT 49, vol 1, Massachusetts Institute of Technology, chap Empirical orthogonal functions and statistical weather prediction, p 52

de Luis M, Brunetti M, Gonzalez-Hidalgo JC, Longares LA, Martin-Vide J (2010) Changes in seasonal precipitation in the iberian peninsula during 1946–2005. Global and Planetary Change 74(1):27–33

Luna M, Guijarro J, López J (2012) A monthly precipitation database for spain (1851–2008): reconstruction, homogeneity and trends. Adv Sci Res 8:1–4

MJ EP, Rodrigo F, Castro-Diez Y (1998) Spatial and temporal patterns of precipitation in spain for the period 1880-1992. International Journal of Climatology 18:1557–1574

Paredes D, Trigo R, R GH (2006) Understanding precipitation changes in iberia in early spring: weather typing and storm-tracking approaches. Journal of Hydrometerology 7:101–113

Petisco E (2003) Metodología para una caracterización de la circulación atmosférica en el entorno de la península ibérica y baleares.nt nº 9. Tech. rep., INM

Philipp A, Della-Marta P, JJacobett, Fereday D, Jones P, Moberg A, Wanner H (2006) Long-term variability of day north atlantic-european pressure patterns since 1850 classified by simulated annealing clustering. Journal of Climate 20:4065–4095

Rasilla D (2003) Aplicación de un método de clasificación sinóptica a la península ibérica. Investigaciones Geográficas 30:27–44

Romero R, Ramis C, Alonso S, Doswell III CA, Stensrud DJ (1998) Mesoscale model simulations of three heavy precipitation events in the western mediterranean region. Monthly weather review 126(7):1859–1881

Romero R, Sumner G, Ramis C, Genovés A (1999) A classification of the atmospheric circulation patterns producing significant daily rainfall in the spanish mediterranean area. International Journal of Climatology 19:765–785

Sánchez-Rodríguez J (1993) Situaciones atmosféricas en España. Ministerio de Obras Públicas, transportes y Medio Ambiente

Sen PK (1968) Estimates of the regression coefficient based on kendall's tau. Journal of the American Statistical Association 63(324):1379–1389

Serrano A, Mateos V, Garcia J (1999) Trend analysis of monthly precipitation over the iberian peninsula for the period 1921–1995. Physics and Chemistry of the Earth, Part B: Hydrology, Oceans and Atmosphere 24(1):85–90

Storch V, Zwiers W (1999) Statistical analysis in climate research. Cambridge University Press

Trigo RM, DaCAMARA CC, et al (2000) Circulation weather types and their influence on the precipitation regime in portugal. International Journal of Climatology 20(13):1559–1581

Wilby R, Wigley T (1997) Downscaling general circulation model output: a review of methods and limitations. Progress in Physical Geography 21(4):530

Yiou P, Nogaj M (2004) Extreme climatic events and weather regimes over the north atlantic: When and where? Geophysical Research Letters 31:1–4

Zhang Y, Wallace JM, Battisti DS (1997) Enso-like interdecadal variability: 1900-93. Journal of Climate 10(5):1004–1020, URL `<GotoISI>://A1997XB77300010`

Chapter 4

Attributing trends in extremely hot days to changes in atmospheric dynamics

4.1 Introduction

The climate suffers changes at different time scales driven by several external and internal factors. Human-induced changes in greenhouse gases, land use, etc., have been especially prominent in the last centuries, modifying the energy balance and therefore inducing climate changes (Stocker et al., 2013). The attribution of recent climate change to each factor is an attempt to ascertain the causes for recent changes observed in the Earth's climate and quantify their relative relevance. However, although the main factors perturbing the climate at a global scale have been extensively characterized (Huybers and Curry, 2006; Swingedouw et al., 2011), fewer exercises focusing on regional scales are available (Stott, 2003).

Beyond the average state, the footprint of climate change is manifested through shifts in extreme weather. In recent years there has been an increasing interest in quantifying the role of human and other external influences on climate in specific weather events (Stott, 2003; Zwiers et al., 2011). Therefore, trying to attribute extreme events to climate change at regional scales presents particular challenges for science.

In the last decades, Europe has experienced a prominent increase in the occurrence of extremely warm episodes, especially during summertime (Frich et al., 2002; Klein Tank and Können, 2003; Alexander et al., 2006). The impacts of such events on human health are important, observing high rates of mortality when such extremes occur. Some examples are the summers of 2003 (Trigo et al., 2005) and 2010 (Dole et al., 2011), when persistent episodes of high maximum temperatures in western and eastern Europe took place. Several studies show that days exceeding the 95th percentile of the daily maximum temperature (T_x) series, usually called extremely hot days (EHDs; García-Herrera et al., 2001), cause also an increase in mortality, especially among the elderly and people with cardiovascular diseases (Díaz-Jiménez et al, 2005). Many works have tried to investigate the causes of these trends, concluding that these are largely influenced by anthro-

pogenic activity (Stott, 2003; Zwiers et al., 2011), with summers like that of 2003 expected to become more frequent under several climate change scenarios (Beniston, 2004). However, extreme events are also driven by unpredictable internal variability. Indeed, some authors (Dole et al., 2011) argued that the summer of 2010 was the result of the internal variability of the climate system, rather than a clear response to global warming.

Many works have analysed the influence of the large-scale dynamics on the variability of extreme temperature indices using several methodologies. For example, Della-Marta et al. (2007) and Carril et al. (2008) related the influence of the atmosphere dynamics and sea surface temperature (SST) to heat waves using methods based on empirical orthogonal functions (EOFs) or canonical correlation analysis (CCA). Other studies use circulation types (CTs; Yiou and Nogaj, 2004; Yiou et al., 2008; Van den Besselaar et al., 2010; Fernández-Montes et al, 2012). These are guided by the results obtained by Corti et al. (1999), who pointed out that recent climate changes can be interpreted in terms of changes in the frequency of occurrence of atmospheric circulation regimes. Some patterns related to anticyclonic and blocking situations favour the development of warm extreme events over Europe (Yiou et al., 2008; Carril et al., 2008; Pfahl, 2014). Therefore, trends in the appearance of these situations could be the cause of the observed trends. Many studies using CTs have provided information in relation to the increase observed in the frequency of such patterns since the second half of the past century (Huth, 2001; Kyselỳ and Huth, 2006; Philipp et al., 2006; Cony et al., 2010; Bermejo and Ancell, 2009; Fernández-Montes et al, 2012; García-Valero et al., 2012). On the other hand, based on the robustness of the evidence from multiple models, the last IPCC report (Stocker et al., 2013) concludes that it is likely that human influence has altered sea level pressure (SLP) patterns globally since 1951. In that way, climate change induces changes in circulation that can further modify the occurrence of extreme events.

However, not all studies find strong links between trends in the occurrence of extreme episodes and trends in the frequency of CTs. Jones and Lister (2009), Bermejo and Ancell (2009) and Fernández-Montes et al (2012), among others, found that trends in extreme temperatures are mainly due to the increase of temperature within the CTs, rather than the increase of the frequency of occurrence of the CTs. This could suggest that trends in extremes can be in addition linked to other forcings, such as global warming, teleconnection phenomena (El Kenawy et al., 2012; Della-Marta et al., 2007), dryness of soil, increase of the SST, etc. Discrepancies in relating both kind of trends (in frequency of the CTs and EHDs) might be due to the way that CT classifications are built. An example of this can be found in Fernández-Montes et al (2012), where a study on the relationship of trends in extreme T_x indices and changes in the frequency of CTs is presented. In this work an established CT classification previously obtained by the authors was used. This classification, as well as the majority of classifications proposed in the literature, is obtained using a huge number of days corresponding to a long period of time (general CT classifications, hereafter). The problem of these

classifications for their application to the analysis of extremes is the low statistical load that these specific atmospheric situations, drivers of extreme occurrence, have against the rest of atmospheric situations. This means that these particular situations would be assigned to generalist clusters, since the assignation is controlled by statistical rules that look for a global optimum. Therefore, relating the frequencies of such generalist CTs to extremes might not be appropriate. On the other hand, the use of single composites instead of CTs could solve the above problem, but it has some drawbacks. One is the restriction of the explanation of all extreme occurrences to a unique atmospheric pattern, when there could be several quite different synoptic situations driving to same kind of extreme. Another drawback is the impossibility of its application in attribution exercises since the efficiency would be 100 %, while the experience says that quite similar atmospheric conditions do not necessarily lead to the same effects at the surface, since other forcings could act. Therefore, the use of CT classifications built specifically for the analysis of extremes is the most reasonable methodology for associating large-scale atmospheric conditions to extreme events.

Another aspect to consider is how trends in the frequency of extremes are obtained. Most studies trying to relate local changes (using local series) to changes in dynamics could be problematic for attribution exercises since other forcings, different to dynamics, would have an important control on the variability of these particular events. Regional series composed of a number of local series contain the information of bigger areas (usually of homogeneous orography), filtering out the local noise. Therefore, these are more appropriate for this kind of studies. In principle, series representing a larger area are more homogeneous, and large-scale dynamics has a larger control on its variability. Statistical downscaling is based precisely on this fact, where estimations of local variability are based on predictors, normally large-scale atmospheric fields (representing the dynamics) and the training of statistical models to consider the effects of other forcings which act at more local scales (Wilby and Wigley, 1997). In addition, the larger homogeneity of regional series than local ones is manifested on its extended use in processes of homogenization of climate series. Most methods of homogenization use reference series, formed by the combination of local series to test the relative homogeneity of the local ones (Peterson and Easterling, 1994). In addition, the analysis of frequency of regional series is largely extended on hydrology and water resource applications (Hosking and Wallis, 2005). Therefore, regional series should be used in attribution works in order to reinforce the signal imposed by the dynamics on regional variability. However, it should be checked whether the regional series represent the behaviour of their constituent local ones. Using suitable regionalization procedures should assure this compliance.

This study focuses on mainland Spain and the Balearic Islands for several reasons. First, this region has experienced a significant increase in T_x during summer in the last decades (Brunet et al, 2007; Rodríguez-Puebla et al, 2010; Hertig et al., 2010; El Kenawy et al., 2011). Furthermore, trends would have continuity during all of this century considering the results of the AR4 (Stocker

et al., 2013), which also provides information about the great sensitivity of the region to future changes, especially in the projections of T_x in summer. Second, the complex orography of the study area causes a large spatial variability of climate impacts that the same atmospheric synoptic situation has (Font-Tullot, 2000), making of great interest the studies based on looking for regional differences. In addition, the availability of a high-resolution gridded data set developed over the region in the last years (Herrera et al., 2010; Gómez-Navarro et al., 2012) for the analysis of variability facilitates carrying out studies like this.

In this work a novel way of attributing observed trends in the frequency of EHD occurrence to trends in the frequency of CTs is presented. Unlike previous works, here it is proposed a CT classification built based on the definition of extreme (without using general classifications). For the construction of these classifications, regional information contained in the adopted definition of extreme is used, reinforcing on this way the relationships between EHD variability and dynamics. Furthermore, different CT classifications are obtained in order to test the impact that different combinations of atmospheric fields (used for defining the CTs) have on the final results, this being another important difference with respect to other previous works. In addition, the results of the T_x regionalization in summer contribute to give new insights supplementing the results of previous works performed over the Iberian Peninsula (IP). This contribution is organized as follows: Sect. 6.2 describes the data sets employed. In Sect. 4.3 the regionalization procedure necessary for adopting the definition of extreme and the analysis of the obtained regions are presented. Section 4.4 shows the method followed for characterizing the CTs based on the regional extreme definition as well as a comparative study of the six obtained CT classifications using different combinations of variables. The way of obtaining the links (efficiencies) between the CTs and EHD occurrences, the exercise of attribution and its results, and an analysis of the stability of such links are explained in Sect. 4.5. Main conclusions and discussions are in Sect. 6.5.

4.2 Data

4.2.1 Surface temperature data

Several high-resolution climate databases for the IP (Herrera et al., 2010) or including it (Caesar et al., 2006; Haylock et al., 2008) have been developed during the last years. These databases have been built by interpolation techniques applied to, in principle, a dense observation network. Although generally reliable, these databases present some known inconsistencies (Gómez-Navarro et al., 2012) due to differences in the raw observational series, the interpolation method, or the different quality controls applied to the data.

Daily T_x series of the Spain02 (Herrera et al., 2010) gridded data set are used for this work. This data set was chosen mainly due to the larger number of stations used compared to other similar products available. The large spatial res-

olution over mainland Spain and the Balearic Islands ($0.2° \times 0.2°$), together with the length of the period (1951–2008), ensures a sufficient spatial and temporal coverage over the study area. Since the work focus on extremely hot days, only dates between 16 June and 15 September are considered.

4.2.2 Large-scale atmospheric data

The data for characterizing the structure of the atmosphere consist of daily fields at 12:00 UTC of SLP, temperature at 850 hPa (T850) and geopotential height at 500 hPa level (Z500) extracted from the ERA40 reanalysis (1958–2002; Uppala et al., 2005) and ECMWF analysis (2003–2008). The maximum common resolution (1.125°) is used for the period 1958–2008. The variables considered are commonly used for the diagnostic of meteorological situations potentially leading to extreme heat events. In this context, SLP offers information about fluxes at low levels and, hence, about the area of provenance of the air mass reaching a given region. T850 provides information about the temperature at low atmospheric levels, tightly related to surface temperature (Brands et al, 2011). Finally, Z500 provides a global vision of the mean atmospheric state. Furthermore, it provides some insight into the overall trough and ridge patterns over the study area, indicating large-scale advection and subsidence in the atmosphere (Sheridan et al., 2012).

4.3 Regional series and EHD

This section describes the method of regionalization followed to identify the regions whose constituent local series have similar temporal variability. As was discussed in the introductory section, regional series respond better to changes imposed by dynamics filtering out the signals controlled by other forcings affecting the variability of local series. The definition of EHDs from a regional point of view, the analysis of the variability of the regional series, and the analysis of the coherency of the regions as well as the differences among them are also exposed in this section.

4.3.1 Clustering procedure for regionalization

The procedure applied is similar to that employed by Jiménez et al. (2008) and Lorente-Plazas et al. (2014). First, a Principal Component Analysis (Storch and Zwiers, 1999) in S-mode is applied to the correlation matrix calculated using daily anomalies of T_x (obtained with respect the seasonal cycle). Only the three first EOFs following the scree plot test (Cattell, 1966) were retained, explaining more than 80 % of total variance. Second a two-step clustering method is applied to the loadings of each grid point in the retained EOFs. The Ward algorithm (Ward, 1963) is employed for obtaining the number of groups and centroids that are used as seeds for a definitive K-means clustering (Hartigan and Wong,

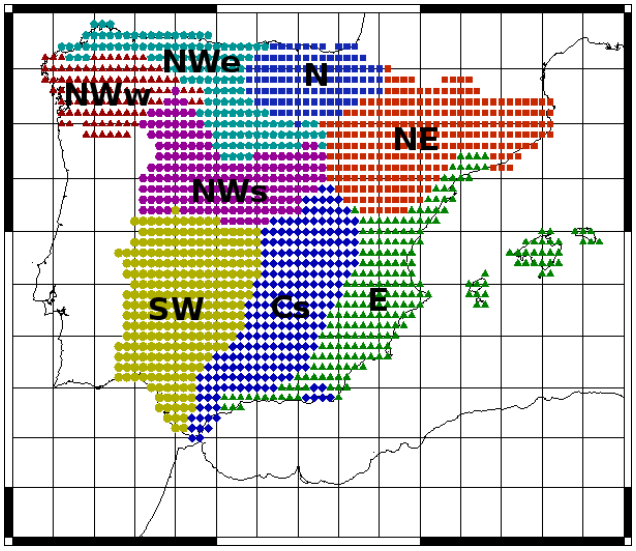

Figure 4.1: The eight obtained regions as a result of the regionalization process applied to the summer maximum daily temperatures (16 June to 15 September) of the Spain02 database (Herrera et al., 2010) for the period 1951–2008.

1979). A more detailed explanation of the regionalization method can be found in Lorente-Plazas et al. (2014).

4.3.2 Regions

The aim of this study is not to perform an exhaustive analysis of the regions, but rather to use the regional series as a tool for achieving the attribution goal, so only some aspects related to the time variability of these series are presented below. Figure 4.1 shows the eight obtained regions. Their names have been established according to their geographical locations: SW, NE, E, Cs (southern central), NWs (south of northwest), NWe (east of northwest), NWw (west of northwest) and N. Regional series have been constructed by averaging the time series of the grid points belonging to the same region. Table 4.1 (first four columns) shows some statistics of the regional series: mean, trend, standard deviation and 95th percentile. A meridional gradient of mean and percentile values is observed, with the warmest regions being located in the southern half of the country (SW and Cs).

The temporal variability of the regional series is presented in Fig. 4.2. Solid black lines represent the T_x mean seasonal series. For all regions two different periods are observed, confirming the results obtained in previous works that analysed the evolution of summer T_x series over the IP (Brunet et al, 2007) and in further Mediterranean regions (Burić et al., 2014). The first lies between 1951 and 1977, when temperatures dropped significantly, with 1977 being the coldest year for most regions. The second period (1978–2007) is characterized by a significant rise of T_x. The 1990s were an especially warm decade, with the hottest

Table 4.1: Statistics summarizing the eight regional series. The second and third columns show the mean and trend (°C decade^{-1}) of the daily maximum temperature series. The standard deviation of the de-trended series is shown in the fourth column. The fifth column exhibits the 95th percentile. Finally, the sixth column shows the EHD trends (days/decade). Bold values (asterisks) indicate significant values at 95 % (90 %) confidence level (estimated with the Mann–Kendall test). Values are obtained for the period 1951–2008, but for EHD trends the 1958–2008 period is considered. Confidence intervals (95 % of significance) for Sen's trends are indicated in parentheses for T_x and EHD trends.

Region	$\bar{T}_{\max}$	$\bar{T}_{\max}$ trend	SD	95th p	EHD trend
SW	32.5	0.13* (−0.03/0.29)	0.98	37.8	**1.00** (0.32/1.67)
NE	27.5	**0.40** (0.23/0.58)	1.07	33.1	**1.19** (0.34/2.1)
E	29.7	0.13* (−0.01/0.27)	0.92	33.5	0.63* (0.00/1.33)
Cs	31.2	**0.28** (0.1/0.44)	1.08	36.1	**1.66** (1.00/2.42)
NWs	28.4	**0.32** (0.16/0.50)	1.04	34.3	**1.54** (0.85/2.22)
NWe	24.7	0.12* (−0.03/0.26)	0.91	30.0	0.45* (0.00/1.15)
NWw	24.5	**0.27** (0.08/0.46)	1.09	30.6	**0.63** (0.00/1.38)
N	24.4	**0.32** (0.14/0.49)	1.08	31.2	**1.05** (0.47/1.67)

year occurring for most regions. In particular, 1994 was the hottest for eastern (NE, E and Cs), 1991 for western (SW and NWs) and 1990 for northern regions. During the last decade, a decrease of the standard deviation is observed in the central, southern and eastern regions, and an increase in the northern ones (N, NWe and NWw).

4.3.3 Extremely hot day definition

The definition of extreme is adopted using the 95th percentile of the regional series (fifth column of Table 4.1). These percentiles are calculated using the entire period of the Spain02 data set (1951–2008; Sect. 6.2). Thus, a day is defined as an EHD when any of the regional T_x series exceeds its 95th percentile. In this way, an ensemble of 863 EHDs were identified in the period 1951–2008.

Figure 4.2 shows the seasonal frequency (bars) and running mean series (11 years) of the regional EHD occurrences (grey line). A noticeable increase is observed in the frequency of EHDs since the 1990s. This finding is in agreement with other studies that found significant increases in climate extreme indices related to T_x over the IP (Brunet et al, 2007; Fernández-Montes et al, 2012) and Europe (Klein Tank and Können, 2003). Comparing for all regions the evolution of seasonal T_x (black curves) and seasonal frequency of EHDs (bars) of Fig. 4.2, it is observed that the warmest year does not necessarily coincide with the year of the highest EHD occurrences. In general, the year with most extreme occurrences was 2003, especially in the northern regions (N, NWe, NWs and NE), coinciding with the extraordinary heat wave that affected many countries

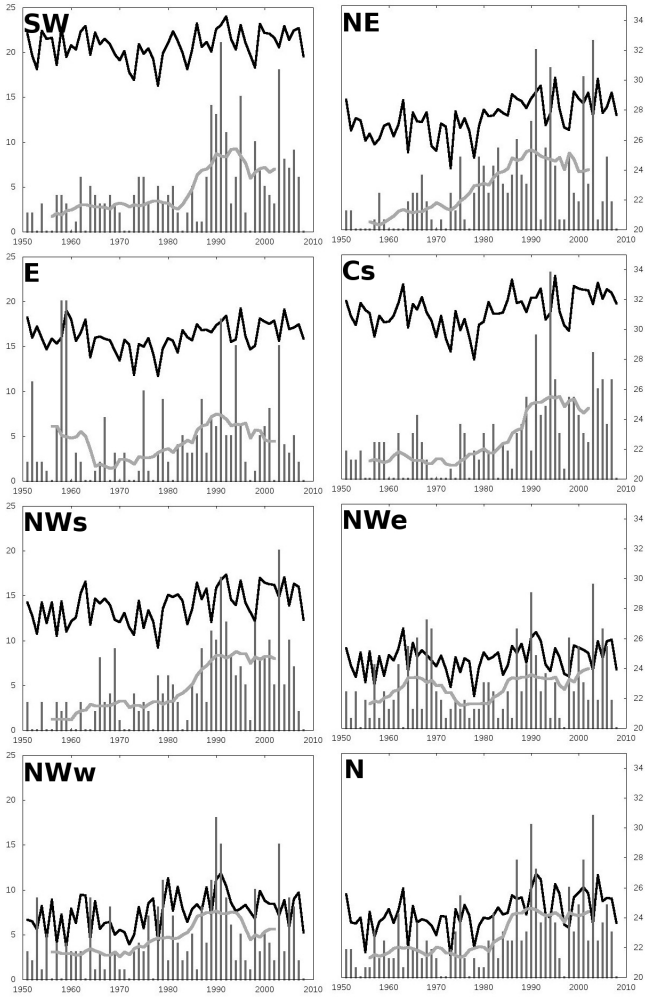

Figure 4.2: Temporal evolution of the eight regional series (see Fig. 4.1). The seasonal mean series of maximum temperature are represented by the black bold curve (right y axis). The yearly number of regional EHDs and its running mean series (of 11 years) are depicted by vertical bars and the grey curve, respectively (left y axis).

of western Europe (Beniston, 2004; Trigo et al., 2005). The persistence of EHDs (number of consecutive EHDs) during this year was also extraordinary in most of our regions, reaching up to 10 days in NE, N, NWe and NWs, and up to 16 days in the SW region. In Cs and NWw the maximum number of EHD occurrences took place in the early 1990s, whereas in the E region it curiously occurred in two consecutive years (1958 and 1959).

A trend analysis of the seasonal EHD series has been performed in order to use them for the attribution exercise. Trends and their statistical significance have been obtained by using Sen's algorithm (Sen, 1968) and the Mann–Kendall test, respectively. In addition, to be able to connect these trends to the trends in the frequency of CTs, EHD trends have been calculated for the period 1958–2008 instead of 1951–2008. The election of this period is in accordance with the non-

Table 4.2: Daily co-occurrence of EHDs between pairs of regions. Non-diagonal elements indicate the probabilities of having a simultaneous EHD between all possible pairs of regions. Diagonal (bold values) indicates the probabilities of having an EHD exclusively over a given region.

Region	SW	NE	E	Cs	NWs	NWe	NWw	N
SW	**0.11**							
NE	0.37	**0.16**						
E	0.25	0.44	**0.40**					
Cs	0.57	0.47	0.40	**0.08**				
NWs	0.62	0.47	0.25	0.59	**0.05**			
NWe	0.38	0.38	0.16	0.31	0.54	**0.07**		
NWw	0.44	0.26	0.15	0.27	0.44	0.56	**0.26**	
N	0.3	0.46	0.22	0.32	0.44	0.60	0.35	**0.19**

availability of atmospheric data used for obtaining the CTs in the period 1951–1957 (see Sect. 6.2). The sixth column of Table 4.1 shows the trends obtained for each region as well as the confidence intervals (95 % of confidence) of these trends. All regions have positive and significant trends (95 % of significance in all regions but 90 % in NWe and E). Largest trends are observed in the inner regions (Cs, NWs and NE), showing a pattern very influenced by the distance to sea, similar to that reported in Bermejo and Ancell (2009) and in Gómez-Navarro et al. (2010), which analysed spatial warming patterns over the IP.

Another important aspect of the obtained regions is its internal coherency and differences among them. Coherency of the regions can be estimated attending to the degree of representation of the region with respect to its constituent series. Thus, a regional EHD should be a signal of many EHD local occurrences at the same time in many of their grids. In this sense, the mean percentage of grid points belonging to the same region that experiences local EHD occurrences when a regional EHD is observed has been obtained for each region. Results show that around 60 % of grid points for most regions have a local EHD when a regional EHD occurs, confirming that regional series, obtained by averaging all the constituent series, are a good thermometer of the global behaviour of the region. NWs and E regions are the most and least homogeneous, with percentages of 65 and 52 %, respectively. In addition, if the 90th local percentile is considered, more than 80 % of grid points overcome this percentile when in the region an EHD occurs. Differences among the regions can be obtained by calculating the probability of simultaneous EHD occurrence among them. Table 4.2 shows a symmetric matrix with these probabilities. The symmetry of the matrix is in accordance with the number of EHDs in the different regions being the same because of the use of the 95th percentile of each region (all regions have the same number of EHDs during the comparison period, 1951–2008). Diagonal values of the matrix show the probability of occurrence only in this region (without EHD occurrences in the remaining regions). Results indicate that the E region

is the most distinctive (40 % of non-simultaneous occurrences), whereas NWs shares many episodes with many of the regions (5 % of occurrences only in this region). The lowest probability of simultaneous occurrence is between E and NWs regions (15 %), and the largest between NWs and Cs (62 %). In general, there are important regional differences, which points to the conclusion that a given large atmospheric pattern could have a different effect over the various regions.

4.4 Characterization of EHD circulation types

As discussed above, links between EHD occurrences and CTs could not be well established when general CT classifications are used. We propose the obtainment of specific CT classifications based on the variable to study, in this case EHD occurrence. Before obtaining the final CT classification, main synoptic situations leading to EHD occurrences at the different regions are characterized. In addition, since the results could depend on the atmospheric fields used for characterizing these situations, six different combinations are examined. This will permit testing the sensibility of the final results to the chosen fields.

4.4.1 Clustering procedure for CT characterization

To characterize the atmospheric patterns drivers of EHD occurrences, a similar procedure to those used for general CT classifications is followed. The main difference is that only days characterized as EHDs are used for the clustering. The two-step method applied in García-Valero et al. (2012) is used here. In the first step, a principal component analysis in T mode (PC-ModeT) clustering is performed (Kyselỳ and Huth, 2006). This clustering allows obtaining the necessary seeds for the second clustering step, defining the number of clusters (a priori unknown). Second, a K-means algorithm is applied over the retained PCs, using for initializing the clustering the seeds obtained in the previous step. The geographical window for clustering is identical to that employed in García-Valero et al. (2012), which covers completely the IP and Balearic Islands (35–45° N and 10° W–6° E). Performing the clustering using larger windows might lead to inclusion of more noise in the classifications, obtaining probably some clusters representing further dynamical structures with little influence on the regional climate variability of the IP. Despite the windows employed covering a small area, the results of clustering are representative of bigger areas (García-Bustamante et al., 2012), so a larger window is used for representation of the centroids (composites of the clusters), allowing for better visualization of the synoptical structures.

Six CT classifications have been obtained. Three of them consider the atmospheric fields individually (SLP, T850, Z500). The other three consist of the combination of all possible pairs of fields (SLP–T850, SLP–Z500 and Z500–T850). The number of clusters of each CT classification depends on the retained PCs used for the PC-ModeT clustering, this being double the retained PCs (García-Valero et al., 2012). For classifications with only one atmospheric field, six clusters are

Table 4.3: Dispersion of the EIs (see main text for the definition of the index). The numbers denote the range–standard deviation of the EIs obtained for each region and CT classification. The last column shows the CTs with EIs (in brackets) above 1 for the best classification of each region (bold numbers).

Region	SLP	Z500	T850	SLP–Z500	SLP–T850	Z500–T850	CTs
SW	1.4–0.54	1.4–0.56	1.9–0.80	1.4–0.53	**2.0-0.72**	1.6–0.58	CT1(1.1),CT2(1.0),CT3(2.0)
NE	0.8–0.29	1.7–0.65	1.7–0.71	3.1–1.01	2.1–0.72	**3.3−1.13**	CT2(3.4),CT7(1.5)
E	4.6–1.76	3.2–1.22	3.7–1.43	**10.2−3.48**	8.3–2.82	8.4–2.84	CT4(1.0),CT8(10.2)
Cs	0.5–0.18	1.2–0.46	2.2–0.80	2.0–0.65	2.6–0.86	**3.4−1.13**	CT2(3.4),CT3(1.1)
NWs	0.8–0.33	1.3–0.46	**1.7−0.74**	1.5–0.53	1.7–0.58	1.5–0.59	CT1(1.0),CT2(1.7) (SLP–T850)
NWe	2.0–0.76	1.0–0.42	1.7–0.66	2.3–0.74	**3.0−0.97**	1.4–0.48	CT2(3.0),CT5(1.0)
NWw	0.9–0.38	1.2–0.48	1.6–0.61	1.3–0.53	1.9–0.64	**2.1−0.71**	CT1(1.0),CT6(2.1)
N	1.3–0.65	1.1–0.41	1.7–0.66	2.0–0.66	**4.0−1.33**	1.36–0.59	CT2(4.0),CT6(1.2)

Table 4.4: Efficiencies before and after the allocation process (in percentage) for the CTs of the best classification (last column) for each region.

Region	CT1	CT2	CT3	CT4	CT5	CT6	CT7	CT8	Classification
SW	53.3–17.6	51.3–44.4	66.7–18.5	31.9–24.8	3.2–0.5	0.0–0.0	20.5–4.9	0.0–0.0	
NWs	46.7–15.4	63.5–54.9	39.8–11.1	38.3–29.8	3.2–0.5	6.6–1.4	38.6–9.2	0.0–0.0	SLP–T850
NWe	25.2–8.3	74.8–64.7	10.2–2.8	21.3–16.5	48.4–7.0	14.3–3.0	41.0–9.8	0.0–0.0	
N	17.0–5.6	80.0–69.2	1.9–0.5	26.6–20.7	25.8–3.7	55.0–11.6	41.0–9.8	0.0–0.0	
NE	26.5–6.7	77.1–72.2	12.0–4.0	45.0–34.0	25.3–8.7	3.1–0.6	59.7–21.5	8.5–0.4	
Cs	3.7–0.9	77.1–72.2	51.3–17.2	42.2–31.9	41.4–14.2	1.0–0.2	6.5–2.3	4.3–0.2	Z500–T850
NWw	50.0–12.6	25.4–23.8	39.3–13.2	27.5–20.8	1.0–0.4	67.7–12.0	3.2–1.2	0.0–0.0	
E	17.9–5.1	19.8–8.8	27.3–12.3	50.0–37.0	2.2–0.3	39.5–6.0	6.3–4.7	91.0–6.7	SLP–Z500

obtained, whereas eight clusters are obtained if two fields are considered. Therefore, three or four PCs are retained if fields are considered individually or in pairs, respectively. In all cases the explained variance by these PCs is over 90 %.

4.4.2 Evaluation of the CT classifications for EHD description

The way of selecting those days defined as EHDs (any EHD occurrence over almost one region) makes an ensemble of situations affecting the various regions in a different way. For a given region, some of the CTs will have great influence on its EHD occurrences, but some others do not have (or little) influence, affecting other regions more. On the other hand, using clustering techniques for classifications, as well as to force the clustering of a great number of events to a reduced number of clusters (6 or 8), causes the existence of noise in the classifications. A question arising is if there is any classification, among the six obtained here, that characterizes better the EHD occurrence for each of the regions. In order to address this question, an index, effectiveness index (EI), is defined. This index is calculated as the ratio between the number of EHD occurrences and non-occurrences in the region under a given CT. Therefore, for a given CT classification and region, there is a set of EIs. The best classification is chosen from that whose standard deviation and range of the EIs are the largest, since it separates better the most- from the least-influential CTs. In addition, those CTs with

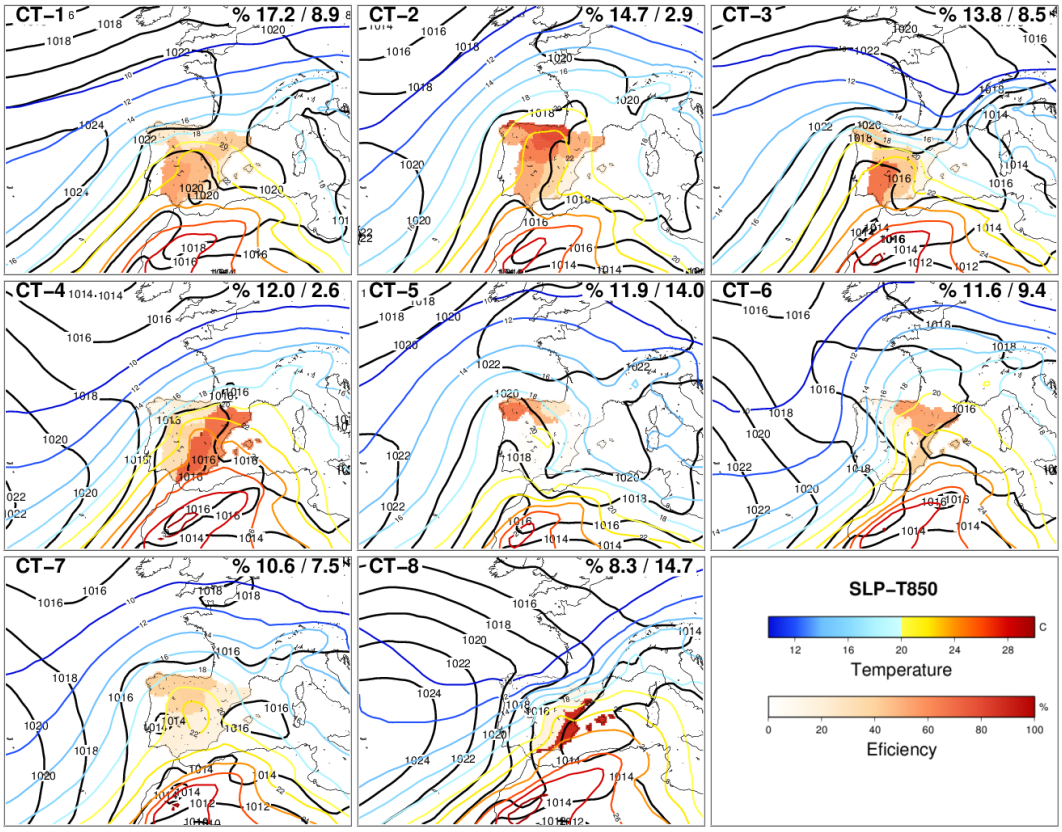

Figure 4.3: Centroids of the CTs for the SLP–T850 classification. SLP and T850 are represented by contours, black lines for SLP and colour lines for T850. Shading denotes the regional EHD efficiencies associated with each CT. The top left corner shows the number of the represented CT. Right corner indicates the frequency (in percentages) of each CT, before and after applying the allocating method (Sect. 4.5.1).

EI > 1 for a given region are defined as "extreme CTs", because the probability of extreme occurrence is larger than the non occurrence.

Table 4.3 shows the range and standard deviation (range–SD) obtained for all the regions and CT classifications. Last column shows for each region its best (highlighted in black) CT classification with its extreme CTs. Results indicate that two synoptic variables characterize better the EHDs for most regions; therefore, hereinafter the remaining analysis will focus only on the CT classifications formed by two atmospheric fields. Z500–T850 is the best one for NE, NWw and Cs (inner-eastern regions and northwestern). SLP–Z500 characterizes better the E region. SLP–T850 is the best for SW, NWe and N (western and northern regions). T850 classification is the best for the NWs region. However, in this area SLP–T850 performs quite similar. Hence, and for the shake of clarity in the analysis, SLP–T850 has been considered as the best classification in this case.

Figures 4.3–4.5 show the centroids (composites) of the CTs (contours) belonging to the CT classifications formed by two atmospheric fields as well as their

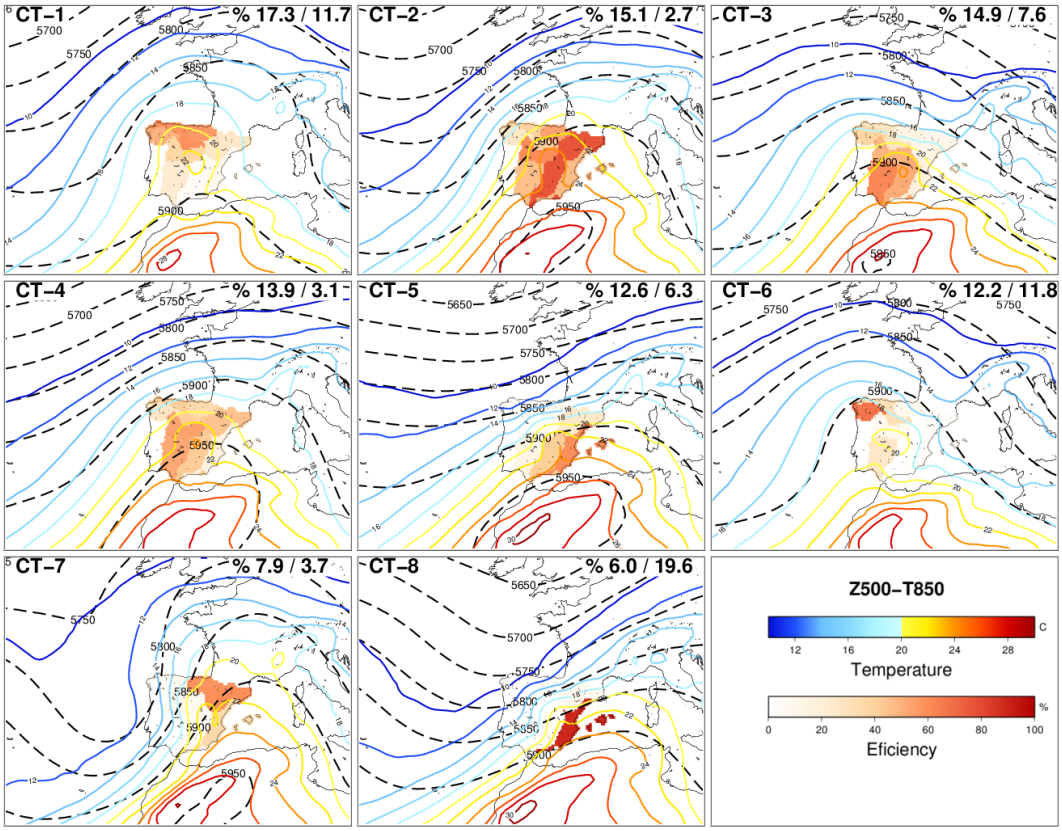

Figure 4.4: Same as Fig. 4.3 but for the Z500–T850 classification. Z500 and T850 are represented by geopotential high contour levels (shaded black lines) and isothermals (colour lines).

efficiencies (shaded) over the different regions. Efficiency is defined as the conditional probability of having an EHD in a region under a given CT. Another interesting parameter is the contribution of a given CT to the occurrence of the EHDs in a given region. The contribution is assessed by calculating the ratio between the number of observed EHDs under a CT and the total EHDs observed in the region. Tables 4.4 and 4.5 depict the efficiencies and contributions values.

The efficiency patterns are quite similar for the three CT classifications. However, for each region the efficiency is higher for the classification that gives larger spreads in the EI (Table 4.3). Some examples follow. The efficiency pattern related to CT8 is equivalent in all classifications and shows high efficiency over the E region. The efficiency is higher for the SLP–Z500 classification, which has the largest EI for E region. Similar results are found for CT5 of SLP–T850, CT6 of Z500–T850 (best) and CT5 of SLP–Z500 in the NWw region, and for CT3 of SLP–T850 (best), CT3 of Z500–T850 and CT1 of SLP–Z500 over the SW region. These results suggest that some CTs belonging to different classifications are equivalent; i.e. they give similar efficiency patterns. In fact, this can be corroborated by calculating the common days of the mentioned CTs (not shown). This highlights the need for studies on the sensitivity of the CT classification to

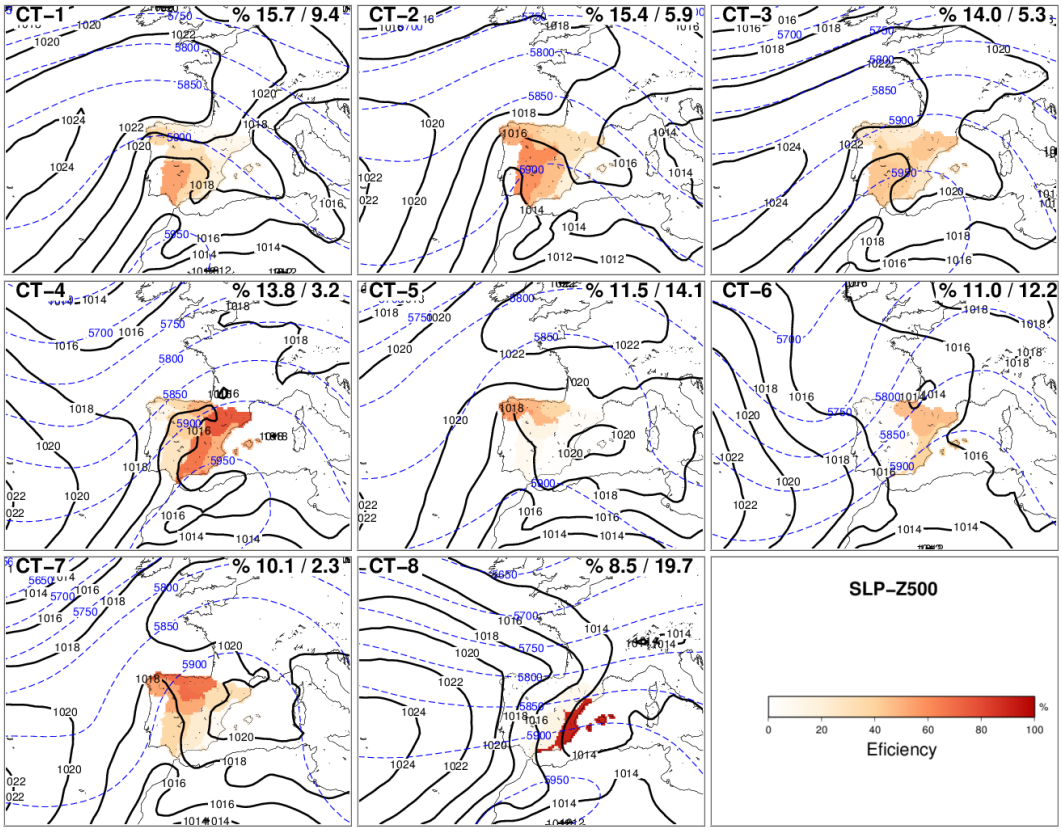

Figure 4.5: Same as Fig. 4.3 but for the SLP–Z500 classification. SLP and Z500 are represented by isobars (black lines) and contour levels (blue shaded lines).

the atmospheric variables employed.

The comparison of the atmospheric situations, among the different classifications, associated with similar efficiency patterns, enables some conclusions to be drawn about the main drivers related to the EHD occurrences. Regarding the T850 variable, the regional efficiency shows the highest values in regions where temperatures are near and above 20 °C. This feature is very common in many CTs of the different classifications such as the CTs 2, 3, 4, 6 and 8 of SLP–T850 and the CTs 1, 2, 3, 4, 5, 7 and 8 of the Z500–T850 classification. The wind provenance, inferred considering the SLP field, is also an important factor contributing the occurrence of EHDs in some regions, because of the warm advection over specific regions. Many CTs are related to situations of wind blowing from inner towards coastal areas, causing the highest efficiencies in the latter. The inner IP regions are highland plateau areas where high temperatures are observed (see Table 4.1). When wind blows from this area towards the sea through valleys, air is adiabatically compressed, causing an important warming in lowland regions. Some examples of these situations can be identified in the classifications by analysing the efficiencies and contributions of some CTs. Five regions are mainly affected by this: NWw, especially when wind blows from the east because of the presence of high pressures over western Europe (CT5 of SLP–T850 and SLP–Z500); SW in

Table 4.5: Contributions (in percentage) of the CTs belonging to the best classification (last column) for each region.

Region	CT1	CT2	CT3	CT4	CT5	CT6	CT7	CT8	Classification
SW	28.5	23.3	28.5	11.9	1.2	0.0	6.7	0.0	
NWs	24.6	28.5	16.8	14.1	1.2	2.3	12.5	0.0	SLP–T850
NWe	14.0	35.4	4.5	8.2	18.5	5.3	14.0	0.0	
N	9.2	36.8	0.8	10.0	9.6	20.0	13.6	0.0	
NE	13.9	35.1	5.4	18.9	9.7	1.2	14.3	1.5	
Cs	2.0	36.4	24.0	18.4	16.4	0.4	1.6	0.8	Z500–T850
NWw	28.1	12.4	19.0	12.4	0.4	26.9	0.8	0.0	
E	9.5	10.3	12.9	23.3	0.9	14.7	2.2	26.3	SLP–Z500

northeastern wind conditions (CTs 1 and 3 of SLP–T850 and CT1 of SLP–Z500) as a result of the presence of high pressure over the Mediterranean and relative low pressures over the southwest of the IP; the E region under strong western zonal wind (CT8 of SLP–T850 and SLP–Z500), induced by the location of high and low pressures over the Atlantic and Mediterranean, respectively; and the NE and N regions in southwestern wind situations (CT6 of SLP–T850 and SLP–Z500). Conversely, CTs with weak SLP gradients (stagnant situations linked to thermal lows) are specially important in the EHD occurrences at Cs and NE (CT4 of SLP–T850 and SLP–Z500), and N, NWe and NWs (CT2 of SLP–T850) regions. Such situations were also pointed out by Pfahl (2014) like those more relevant guiding hot extremes in summer over the IP. Regarding the Z500 field, EHDs are associated with large amplitude ridges over the IP. Regions with the highest efficiencies are located to the west of the ridge axis, where there are high stability and warm advection. The efficiency and contribution are only important in the E region when zonal wind at 500 hPa is strong (CTs 5 and 8 of Z500–T850 and CT8 of SLP–Z500). This pattern usually takes place when hot episodes over the IP are ending up. The analysis of the CT transitions (not shown) for consecutive EHD episodes reinforces this result. The hottest areas travel from western to eastern regions, following the ridge movement.

4.5 Linking EHD trends to CTs

Significant and positive EHD regional trends were found for all regions (Sect. 4.3.3). An interesting question is whether there is any relation between these trends and changes in the frequency of occurrence of the CTs. Therefore, the existence of trends in the frequency of CTs should be assessed. The main problem is that frequencies of CTs only can be obtained during extreme episodes. There are atmospheric situations, similar to that described in the centroids, that were not included in the previous clustering step because EHDs did not occur in any region. As was discussed above (Sect. 6.1), the same atmospheric patterns could lead to some different weather situations. To take this into consideration, the

Table 4.6: Thresholds of the different CTs used for distance/correlation in the allocation process.

Classification	CT1	CT2	CT3	CT4	CT5	CT6	CT7	CT8
SLP–T850	0.06/−0.26	0.06/0.57	0.06/0.40	0.06/0.67	0.05/0.18	0.08/0.36	0.06/0.61	0.07/0.39
Z500–T850	0.07/0.18	0.05/0.14	0.05/−0.09	0.05/0.02	0.05/−0.06	0.05/0.27	0.06/0.36	0.07/0.31
SLP–Z500	0.06/0.10	0.07/0.59	0.06/−0.12	0.06/0.72	0.06/0.17	0.08/0.47	0.05/0.47	0.08/0.04

Table 4.7: Number of days classified within each CT. Each box shows the number of days classified before and after the allocation process. CT9 denotes the unclassified days.

Classification	CT1	CT2	CT3	CT4	CT5	CT6	CT7	CT8	CT9
SLP–T850	135–410	115–133	108–389	94–121	93–644	91–433	83–347	65–677	0–1446
Z500–T850	136–539	118–126	117–349	109–144	99–289	96–541	62–172	47–902	0–1538
SLP–Z500	123–432	121–273	110–243	108–146	90–647	86–563	79–106	67–908	0–1282

rest of the days initially not considered for characterization have to be assigned to one of the obtained clusters. For this reason, links (efficiencies) between CTs and EHD occurrences have to be recalculated. The method of assignation of such days is presented below.

4.5.1 Allocation method

Each CT is the result of a set of similar atmospheric conditions being its associated centroid the mean value (composite) of this ensemble or population. However, there is some dispersion inside each group. To allocate an atmospheric situation (not considered as an EHD) into the CTs means finding the population where such situation fits better. For this task the election of some metrics is fundamental. Two metrics have been used for assignation: the Spearman correlation and the Euclidean distance. The former measures the spatial similarity of two fields (Hofer et al., 2012; Vautard and Yiou, 2009), whereas the latter evaluates the differences in the intensity of patterns (Fettweis et al., 2011). Both metrics are relevant and complementary (Nogaj et al., 2007; Fettweis et al., 2011). The population of a given CT is characterized by the distribution of the distances to and correlations with the centroid using only the days considered in the characterization (Sect. 4.4). To obtain the population of each CT, the atmospheric data are first standarized by grid point; then correlations and distances to the centroid are obtained. Mean and standard deviation for standardization are obtained using all days (extremes and non-extremes) of the study period. A criterion to allocate a situation into a given CT is that the distance to (correlation with) the centroid be lower (higher) than some given thresholds. Hence, the election of these thresholds is a problem to solve. On the one hand, thresholds could be fixed to certain percentiles of the populations, but this could be problematic because this would have strong subjectivity. On the other hand, thresholds could be the maximum (minimum) values of distance (correlation) obtained from days clustered for the characterization of the CT leaders to EHD occurrences (Sect. 4.4). We have

chosen the latter option because this is free of subjectivity. Table 4.6 shows the thresholds considered for all CTs and classifications. Some thresholds of certain CTs are too broad, allowing the assignation of more days into them. These CTs are those with higher noise inside them, and probably they are formed by a larger heterogeneity of situations. By contrast, there are CTs more homogeneous with thresholds more restrictive. In general the most homogeneous CTs agree with atmospheric patterns having high efficiency in most regions simultaneously.

Finally, a given day is allocated to the CT on which distance and correlation are lower and higher, respectively, than the thresholds defined for it. Days that can not be assigned to any CT are then allocated to a new group (unclassified group, CT9; Seubert et al., 2014). This way of assignation might derive from the allocation of a situation to more than one of the established centroids. In these cases, it is allocated to the nearest cluster considering only the Euclidean distance. The use of this criterion is in accordance with the lower spread of the Euclidean distance populations than that observed for correlation.

4.5.2 Analysis of the allocation

Table 4.7 shows the number of days belonging to the different CTs before and after the allocation process. Approximately 70 % of the days for all classifications are assigned, whereas the rest are allocated to the unclassified cluster (CT9), with Z500–T850 (SLP–Z500) being the one with most (fewest) unclassified days (33 % vs. 28 %). There is a large variability in the increase of the days belonging to the different CTs. CT1, CT6 and CT8 have the largest increase (10 times) in all classifications, whereas others like CTs 2 and 4 of SLP–T850 and CTs 2 and 4 of Z500–T850 present small changes (less than 20 % of the initial clustered days). The assessment of the quality of the clusters before and after the allocation is of major relevance. In order to ensure the reliance of the assignation method, the explained cluster variance (ECV) of each classification (Table. 4.8) is analysed. Results show few differences among the classifications. Z500–T850 classification has the best quality, observing even an increase in the quality of clusters after the allocation. The quality of the other classifications worsens slightly after the allocation, with the SLP–T850 classification being slightly better than the SLP–Z500 one. On the other hand, when comparing the quality for the three classifications after the allocation (ECV $>$ 46 % in all cases; see Table. 4.8) with some others obtained using general CT classifications, even better results are observed in our classifications. Hence, in Philipp et al. (2006) an ECV lower than 40 % was obtained in summer, and in García-Valero et al. (2012) of 47.2 %. These results support the suitability of the method followed for allocation.

It is instructive to explore the consequences after applying the allocation procedure on the properties of the groups or CTs. One consequence of the larger number of classified days is the decrease in the efficiency of the CTs (see Table 4.4). Obviously, the lower the increase of the number of days, the smaller the decrease of the efficiency. This effect stands out in CTs 2 and 4 for the SLP–T850

Table 4.8: Explained variance by the clusters (in %) for the three CT classifications before and after the allocation process.

	Z500–T850	SLP–T850	SLP–Z500
Before	49.97	49.65	49.48
After	50.06	47.02	46.59

Table 4.9: Trends in the frequency of CTs for the different CT classifications. One (two) asterisk indicates trends at 90 % (95 %) of the confidence level (Mann–Kendall test).

Classification	CT1	CT2	CT3	CT4	CT5	CT6	CT7	CT8	CT9
SLP–T850	0.00	0.26*	0.00	0.00	−0.43	0.51*	0.00	0.00	−1.3
Z500–T850	0.28	0.45**	0.00	0.00	0.00	−0.53	0.80**	0.00	−0.80
SLP–Z500	0.00	0.57*	0.00	0.00	0.00	0.57*	0.00	−0.30	−0.50

and Z500–T850 classifications, which have the highest efficiencies in most regions. Changes in the efficiency after the allocation also affect the EI used for deciding the best CT classification for each region (Sect. 4.4.2). Following the same criterion as above, results remain unaltered for most regions, except for E and NWw regions, which are now better characterized by the SLP–T850 classification.

The shape of the populations of distances and correlations of each CT can be also affected. The net effect of the allocation process is to include new days located further from the centroid. Nevertheless, a small number of clusters hardly change the populations after the assignation (CTs 2 and 4 of SLP–T850, CTs 2 and 4 of Z500–T850 and CTs 4 and 7 of SLP–Z500), which are coincident with the ones with higher efficiency. Figure 4.6 shows two examples of the correlation histograms before and after the allocation process (top) as well as the empirical cumulative distribution function (bottom). The left and right panels show an example of great and small changes in population, respectively.

Once the allocation is performed, an analysis of trends in the frequency of CTs is carried out. Table 4.9 shows the trends obtained for each CT of the different classifications. Trends and their statistical significance are obtained following the same methods (Sen's algorithm and Mann–Kendall test for trend and its statistical significance, respectively) as used for estimating the regional EHD trends. Results indicate that only two CTs of each classification have trends with statistical significance (one more but without significance). Considering this and their associated efficiencies (Table 4.4), it could be said that trends in CTs would be linked to the increase of EHD occurrences in northern regions (mainly N and NE). It is interesting also to observe that the CT9 (formed by the unclassified days) has a negative trend for the three classifications, meaning that in time a larger number of days are assigned to the centroids linked to EHD occurrences.

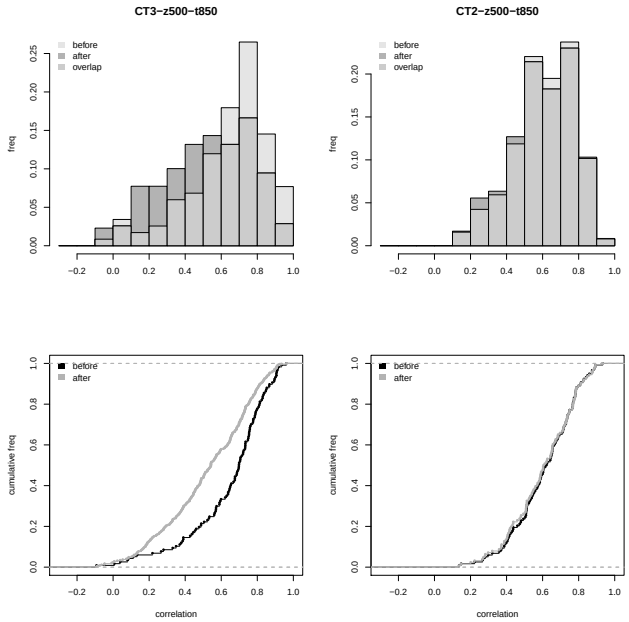

Figure 4.6: Histograms and empirical cumulative distribution functions of the correlations for CT3 of Z500–T850 (left) and CT2 of Z500–T850 (right). Each panel shows the populations before and after the allocation process.

4.5.3 Attribution of EHD trends

Temperature changes can be linked to several factors, one of them being the changes in atmospheric circulation. Trends in the EHDs could be considered also as an indicator of temperature changes. In this subsection, a model to attribute regional EHD trends to trends in the frequency of CTs is presented.

The regional EHD trend in a given region, T^{r}, can be written as the sum of two terms:

$$T^{\mathrm{r}} = T^{\mathrm{r}}_{\mathrm{c}} + T^{\mathrm{r}}_{\mathrm{o}}, \tag{4.1}$$

where $T^{\mathrm{r}}_{\mathrm{c}}$ is the trend attributable to changes in atmospheric circulation and $T^{\mathrm{r}}_{\mathrm{o}}$ the trend related to other factors. Now, $T^{\mathrm{r}}_{\mathrm{c}}$ can be described as a linear function of the changes in the frequency of the CTs. We propose the simple model

$$T^{\mathrm{r}}_{\mathrm{c}} = \sum_{i=1}^{n} T_i \epsilon^r_i, \tag{4.2}$$

where the subscript i denotes the CT number, from 1 to n (the number of CTs); T_i is the frequency trend of the CT_i (Table. 4.9); and ϵ^r_i denotes the efficiency of the CT_i over the region r (Table. 4.4), calculated after the allocation process.

Using this simple model $T^{\mathrm{r}}_{\mathrm{c}}$ can be calculated for all regions using the different CT classifications. The results are summarized in Table 4.10. The last column depicts the observed regional EHD trend. With independency of the CT classification, the reproduced trends are in all cases smaller than those observed for

Table 4.10: Regional EHD trends (days/decade). The first three columns show the trends obtained from the attribution exercise considering the different classifications. Last column shows the observed trends derived from regional series.

Region	$T^{\mathrm{r}}_{\mathrm{SLP–T850}}$	$T^{\mathrm{r}}_{\mathrm{Z500–T850}}$	$T^{\mathrm{r}}_{\mathrm{SLP–Z500}}$	T^{r}
SW	0.11	0.18	0.15	1.00
NWs	0.15	0.29	0.15	1.50
NWe	0.15	0.21	0.11	0.45
N	0.22	0.42	0.12	1.10
NE	0.17	0.51	0.12	1.20
Cs	0.09	0.35	0.12	1.60
NWw	0.08	0.09	0.13	0.63
E	0.08	0.30	0.06	0.60

a given region, but they are strongly dependent on the CT classification, except for SW and NWw regions where few differences are appreciated among classifications. In general terms, the Z500–T850 classification (that of the best quality; see Sect. 4.5.2) obtains the highest reproduced trends except for NWw. Using this classification a fraction between 40 and 50 % of the observed trends is attributed to changes in the frequency of CTs in the E, NE, NWe and N regions, about 20 % in the western and southern regions (SW, Cs and NWs), and only 14 % in NWw.

4.5.4 Within-type variations in the efficiency

In the exercise of attribution, links between CTs and EHD occurrences, established by the efficiency, have been taken as long-term mean values of the efficiency throughout the entire study period (1958–2008), because our main goal is to attribute long-term regional EHD trends. On the other hand, if our purpose were to describe the variability at higher frequencies, an analysis of the stability of links (obtaining the links using higher frequencies) should be carried out. The instability of links is frequently known in the literature as within-type variations (WT). Some of the limitations of the use of CTs for downscaling purposes is precisely the existence of WT, meaning that other factors could be controlling the links. For example, the scarcity of precipitation in spring would lead to drier soils, and during summer land–atmosphere processes would be more intense (Seneviratne et al., 2010; Jerez et al, 2012), enhancing air temperature and efficiency. Another example is the persistence of atmospheric situation drivers of high T_x; this also would cause an enhancement of land–atmosphere processes. Persistence might be originated by the existence of SST anomalies caused by teleconnection phenomena (Della-Marta et al., 2007). In order to evaluate the possibility of using the CTs obtained here for downscaling of annual EHD in the different regions, an analysis of the stability in the efficiency for the different regions has been carried out. To do so, annual efficiency series have been obtained, and, in a way similar to other works (Jacobeit et al., 2009; Fernández-Montes et al, 2012), running mean

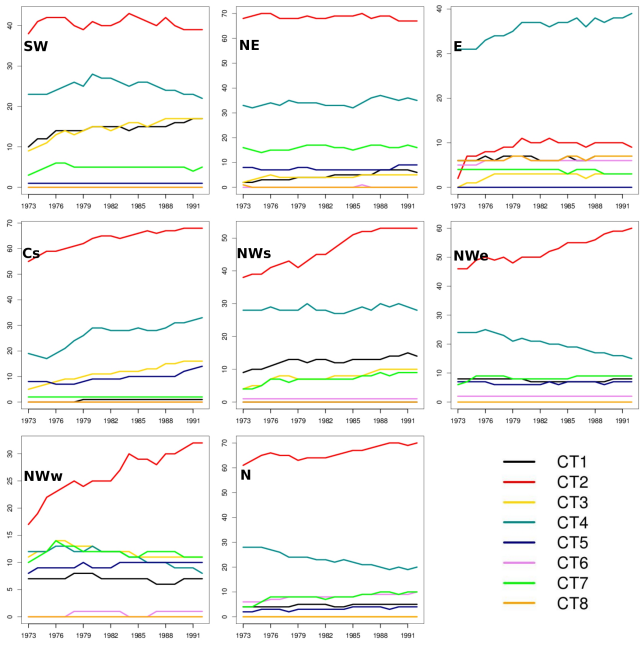

Figure 4.7: Within-type variations. The lines represent the moving average (31 years) of the efficiencies for the CTs composing the best CT classification (colour) for each region (panel) after the allocation process.

series of 31 years are derived for the analysis of the stability.

Figure 4.7 shows the obtained running mean series for every region and for the CTs composing the best CT classification for each region (that with the highest dispersion of the EI after the allocation process; see Sect. 4.5.2). In general terms, those CTs with the highest efficiencies in each region increase its efficiency by 10 % throughout the study period (1958–2008). This is the case of CT2 in the regions Cs, NWs, NWe, NWw and N, and CT4 in the E region. Anyway, there are some other important WT variations in CTs affecting the inner regions more, pointing to a rise of the efficiency. Some examples follow: CT-3/4 for Cs, CT-1/2 for SW and CT-1/3/7 for NWs. Another interesting result is the increase of the efficiency of CT4 in the northern regions (NWw, NWe and N), while it decreases in the E region, confirming once again the remarkable regional differences existing over the studied area. Among all the regions, the least affected by WT is the NE region, where only CT1, with low efficiency over the region, increases its efficiency. This last result is curious because this region was noted by Bermejo and Ancell (2009) as one of the Spanish regions where larger WT in T_x were observed during the second half of the past century, observing warming in T_x inside many of the CTs obtained by these authors. Differences between our results and those found in Bermejo and Ancell (2009) could be in the variable analysed, in our case extreme events and in their case T_x mean. Hence, the increase of T_x mean may not mean an increase in the efficiency of EHD occurrence.

Some reasons for the increase in the efficiency found in the CTs can be linked to the increase of the persistence of CTs. To evaluate this possible influence, the

correlation between the de-trended seasonal frequency series and mean seasonal persistence series of the CTs with the most important WT have been calculated. Results show positive and significant correlations, between 0.6 and 0.7, which support the influence of the persistence on the efficiency rise. In addition, the decline of soil moisture observed over the IP since the 1970s (Sousa et al., 2011) could be another factor contributing to higher efficiencies.

4.6 Conclusions and discussions

This work sets as its intention the attribution of regional trends in EHD occurrences observed at eight Spanish regions (during the period 1958–2008) to changes in the frequency of atmospheric situations linked to the occurrence of such events. The study is centred in summer, when EHDs have a larger relevance. The method followed is based on the procurance of CT classifications using regional information contained in the same definition of extreme. This differs from others studies based on general CT classifications. Therefore, a regionalization of daily T_x series is carried out, deriving from this exercise the regional series used for adopting the definition of extreme. In addition, the internal coherency of the regions and differences among them are also analysed. Later, a characterization of the atmospheric situations, drivers of EHD occurrences in the different regions, has been obtained, centring these classifications only on those days defined as EHDs. In this way, six CT classifications each using a different combination of atmospheric fields have been obtained, and an analysis for finding the most suitable classification for each region has been performed. Links between CTs and EHD occurrences have been defined by means of the efficiency that a given CT leads to a regional EHD in each region. To establish such links, the CT classifications obtained in the characterization step have been extended to the rest of days (non-EHDs). To do so, a method of allocation of these days to the centroids obtained in the characterization is presented. Finally, the method of attribution is presented as well as an analysis of the stability of the links between large-scale dynamics and EHD occurrence. The main conclusions are summarized below.

- Eight regions with different daily T_x variability are identified. Regions have high internal coherency and important differences among them. Positive and significant regional EHD trends are found across most regions. Generally, such trends are larger in central and northern regions, and lower in the SE and NWe regions.

- To find CT classifications describing the extreme occurrences, it is convenient to base them on the variables to analyse, as well as on a characterization of the associated atmospheric patterns using exclusively those days defined as extremes. The method proposed here produces CT classifications of similar quality to those obtained in general CT classifications which use other clustering techniques. However, this method ensures a more precise

allocation of the extreme days to the correct clusters than general CT classifications.

- The choice of the most suitable combination of atmospheric variables to define the CTs becomes of major relevance. This study finds that classifications using combinations of two atmospheric variables generally perform better than those using only one. In the case of the studied area, SLP–T850 characterizes better the EHD occurrences for most regions. However, other combinations, such as Z500–T850, have better results in the Cs and NE regions. In addition, Z500–T850 is the CT classification with the best quality, whereas SLP–Z500 has the worst quality in terms of the explained variance by the clusters.

- In the different obtained classifications, only a small number of CTs have significant trends of its seasonal frequency, a result which is in line with other studies using general CT classifications (Fernández-Montes et al, 2012; Bermejo and Ancell, 2009). Such trends depend on the atmospheric variables used for the classification, with the largest trends occurring in the classification of the best quality (Z500–T850). CT2 of the Z500–T850 and SLP–T850 classifications have the largest trends. This atmospheric pattern is associated with high occurrence of EHDs in most regions simultaneously, specially in the central and northern regions.

- Part of the EHD trends observed in some regions can be attributed to changes in the CT frequencies. However, the trends reproduced by the attribution method are in all cases lower than the observational ones, indicating that part of the trend has to be attributed to other factors. The attributed trends have a great dependence on the region, as well as on the CT classification. Thus, the best-quality classification, Z500–T850, is able to attribute the larger part of the observed regional EHD trends for most regions except for NWs. Considering this classification, a fraction between 30 and 50 % of the observed trends is attributed in the E, NE, NWe and N regions, about 20 % in the western and southern regions (SW, Cs and NWs), and hardly 14 % in the NWw.

- Some of the most-influential CTs in terms of leading to EHD occurrences in the different regions present WT variations in relation to their efficiency, except for NE. Approximately the most efficient CTs have increased their efficiencies by 10 % during the study period. These changes may be associated, among other things, with the increase of the persistence of such CTs through time.

The attribution exercise reveals that the observed regional EHD trends can be only partially attributed to changes in the atmospheric dynamics and that they have an important regional component. This suggest that there are other factors involved in the EHD trends – such as global warming, soil–atmosphere

feedbacks or changes of surface properties – that contribute to increasing positive changes in EHD frequency. A fact that reinforces this asseveration is that the trends in central regions are less affected by changes in atmospheric dynamics. This could be related to a depletion of soil moisture that enhances the positive land–atmospheric feedback, as previously stated by other authors (Jerez et al, 2012). This also supports the WT variations mentioned above.

The links obtained here between regional EHD and CTs, and the allocation method followed, can be used for estimating the role of the atmospheric dynamics in the long-term regional changes of EHD occurrence over the different regions under different climate change scenarios. This is a natural extension of this work. In addition, the methodology applied here could be extended to other extreme events such as floods, droughts, heat waves, etc. The robustness of the regional series as well as the identification of the best large-scale atmospheric variables characterizing such events could be of crucial importance when trying to relate regional extreme behaviour to atmospheric dynamics.

Bibliography

Alexander, L., Zhang, X., Peterson, T., Caesar, J., Gleason, B., Klein Tank, A., Haylock, M., Collins, D., Trewin, B., Rahimzadeh, F., Tagipour, A., Rupa, K., Revadekar, J., Griffiths, G., Vincent, L., Stephenson, D., Burn, J., Aguilar, E., Brunet, M., Taylor, M., New, M., Zhai, P., Rusticucci, M., and Vazquez-Aguirre, J.: Global observed changes in daily climate extremes of temperature and precipitation, J. Geophys. Res.-Atmos., 111, D05109, doi:10.1029/2005JD006290, 2006.

Beniston, M.: The 2003 heat wave in Europe: A shape of things to come?. An analysis based on Swiss climatological data and model simulations, Geophys. Res. Lett., 31, L02202, doi:10.1029/2003GL018857, 2004.

Bermejo, M. and Ancell, R.: Observed changes in extreme temperatures over Spain during 1957–2002, using Weather Types, Revista de Climatología, 9, 45–61, 2009.

Brands, S., Taboada, J., Cofiño, A., Sauter, T., and Schneider, C.: Statistical downscaling of daily temperatures in the NW Iberian Peninsula from global climate models: validation and future scenarios, Clim. Res., 48, 163–176, 2011.

Brunet, M., Jones, P., Sigró, J., Saladié, O., Aguilar, E., Moberg, A., Della-Marta, P., Lister, D., Walther, A., and López, D.: Temporal and spatial temperature variability and change over Spain during 1850–2005, J. Geophys. Res., 112, D12117, doi:10.1029/2006JD008249, 2007.

Burić, D., Luković, J., Ducić, V., Dragojlović, J., and Doderović, M.: Recent trends in daily temperature extremes over southern Montenegro (1951–2010), Nat. Hazards Earth Syst. Sci., 14, 67–72, doi:10.5194/nhess-14-67-2014, 2014.

Caesar, J., Alexander, L., and Vose, R.: Large-scale changes in observed daily maximum and minimum temperatures: Creation and analysis of a new gridded data set, J. Geophys. Res.-Atmos. (1984–2012), 111, D05101, doi:10.1029/2005JD006280, 2006.

Carril, A. F., Gualdi, S., Cherchi, A., and Navarra, A.: Heatwaves in Europe: areas of homogeneous variability and links with the regional to large-scale atmospheric and SSTs anomalies, Clim. Dynam., 30, 77–98, 2008.

Cattell, R. B.: The scree test for the number of factors, Multivar. Behav. Res., 1, 245–276, 1966.

Cony, M., Martín, L., Hernández, E., and Del Teso, T.: Synoptic patterns that contribute to extremely hot days in Europe, Atmósfera, 23, 295–306, 2010.

Corti, S., Molteni, F., and Palmer, T.: Signature of recent climate change in frequencies of natural atmospheric circulation regimes, Nature, 398, 799–802, 1999.

Della-Marta, P., Luterbacher, J., Von Weissenfluh, H., Xoplaki, E., Brunet, M., and Wanner, H.: Summer heat waves over western Europe 1880–2003, their relationship to large-scale forcings and predictability, Clim. Dynam., 29, 251–275, 2007.

Díaz-Jiménez, J., Linares-Gil, C., and García-Herrera, R.: Impacto de las temperaturas extremas en la salud pública:Futuras actuaciones, Revista Española de Salud Pública, 79, 145–157, 2005.

Dole, R., Hoerling, M., Perlwitz, J., Eischeid, J., Pegion, P., Zhang, T., Quan, X.-W., Xu, T., and Murray, D.: Was there a basis for anticipating the 2010 Russian heat wave?, Geophys. Res. Lett., 38, L06702, doi:10.1029/2010GL046582, 2011.

El Kenawy, A., López-Moreno, J. I., and Vicente-Serrano, S. M.: Recent trends in daily temperature extremes over northeastern Spain (1960–2006), Nat. Hazards Earth Syst. Sci., 11, 2583–2603, doi:10.5194/nhess-11-2583-2011, 2011.

El Kenawy, A., López-Moreno, J. I., and Vicente-Serrano, S. M.: Trend and variability of surface air temperature in northeastern Spain (1920–2006): linkage to atmospheric circulation, Atmos. Res., 106, 159–180, 2012.

Fernández-Montes, S., Rodrigo, F. S., Seubert, S., and Sousa, P. M.: Spring and summer extreme temperatures in Iberia during last century in relation to circulation types, Atmos. Res., 127, 154–177, 2013.

Fettweis, X., Mabille, G., Erpicum, M., Nicolay, S., and den Broeke, M.: The 1958–2009 Greenland ice sheet surface melt and the mid-tropospheric atmospheric circulation, Clim. Dynam., 36, 139–159, 2011.

Font-Tullot, I.: Climatología de España y Portugal, University of Salamanca (Spain), 422 pp., 2000.

Frich, P., Alexander, L., Della-Marta, P., Gleason, B., Haylock, M., Klein-Tank, A., and Peterson, T.: Observed coherent changes in climatic extremes during the second half of the twentieth century, Clim. Res., 19, 193–212, 2002.

García-Bustamante, E., González-Rouco, J., Navarro, J., Xoplaki, E., Jiménez, P., and Montávez, J.: North Atlantic atmospheric circulation and surface wind in the Northeast of the Iberian Peninsula: uncertainty and long term downscaled variability, Clim. Dynam., 38, 141–160, 2012.

García-Herrera, R., L. Prieto, Díaz, J., Hernández, E., and del Teso, T.: Synoptic conditions leading to extremely high temperatures in Madrid, Ann. Geophys., 20, 237–245, 2001.

Garcîa-Valero, J., Montavez, J., Jerez, S., Gómez-Navarro, J., Lorente-Plazas, R., and Jiménez-Guerrero, P.: A seasonal study of the atmospheric dynamics over the Iberian Peninsula based on circulation types, Theor. Appl. Climatol., 110, 291–310, doi:10.1007/s00704-012-0623-0, 2012.

Gómez-Navarro, J., Montávez, J., Jimenez-Guerrero, P., Jerez, S., Garcia-Valero, J., and González-Rouco, J.: Warming patterns in regional climate change projections over the Iberian Peninsula, Meteorol. Z., 19, 275–285, 2010.

Gómez-Navarro, J., Montávez, J., Jerez, S., Jiménez-Guerrero, P., and Zorita, E.: What is the role of the observational dataset in the evaluation and scoring of climate models?, Geophys. Res. Lett., 39, L24701, doi:10.1029/2012GL054206, 2012.

Hartigan, J. A. and Wong, M. A.: Algorithm AS 136: A k-means clustering algorithm, J. R. Stat. Soc. C-Appl., 28, 100–108, 1979.

Haylock, M., Hofstra, N., Klein Tank, A., Klok, E., Jones, P., and New, M.: A European daily high-resolution gridded data set of surface temperature and precipitation for 1950–2006, J. Geophys. Res.-Atmos., 113, D20119, doi:10.1029/2008JD010201, 2008.

Herrera, S., Gutiérrez, J., Ancell, R., Pons, M., Fías, M., and Fernández, J.: Development and analysis of a 50-year high-resolution daily gridded precipitation dataset over Spain (Spain02), Int. J. Climatol., 32, 74–85, doi:10.1002/joc.2256, 2010.

Hertig, E., Seubert, S., and Jacobeit, J.: Temperature extremes in the Mediterranean area: trends in the past and assessments for the future, Nat. Hazards Earth Syst. Sci., 10, 2039–2050, doi:10.5194/nhess-10-2039-2010, 2010.

Hofer, D., Raible, C., Merz, N., Dehnert, A., and Kuhlemann, J.: Simulated winter circulation types in the North Atlantic and European region for preindustrial and glacial conditions, Geophys. Res. Lett., 39, L15805, doi:10.1029/2012GL052296, 2012.

Hosking, J. and Wallis, J.: Regional frequency analysis: an approach based on L-moments, Cambridge University Press, 224 pp., 2005.

Huth, R.: Disaggregating climatic trends by classification of circulation patterns, Int. J. Climatol., 21, 135–153, 2001.

Huybers, P. and Curry, W.: Links between annual, Milankovitch and continuum temperature variability, Nature, 441, 329–332, 2006.

Jacobeit, J., Rathmann, J., Philipp, A., and Jones, P. D.: Central European precipitation and temperature extremes in relation to large-scale atmospheric circulation types, Meteorol. Z., 18, 397–410, 2009.

Jerez, S., Montavez, J., Gómez-Navarro, J., Lorente-Plazas, R., García-Valero, J., and Jiménez-Guerrero, P.: A multiphysic ensemble of regional climate change projections over the Iberian Peninsula, Clim. Dynam., 41, 1749–1768, doi:10.1007/s00382-012-1551-5, 2012.

Jiménez, P., García-Bustamante, E., González-Rouco, J., Valero, F., Montávez, J., and Navarro, J.: Surface wind regionalization in complex terrain, J. Appl. Meteorol. Climatol., 47, 308–325, 2008.

Jones, P. D. and Lister, D. H.: The influence of the circulation on surface temperature and precipitation patterns over Europe, Clim. Past, 5, 259–267, doi:10.5194/cp-5-259-2009, 2009.

Klein Tank, A. and Können, G.: Trends in indices of daily temperature and precipitation extremes in Europe, 1946–99, J. Climate, 16, 3665–3680, 2003.

Kysely, J. and Huth, R.: Changes in atmospheric circulation over Europe detected by objective and subjective methods, Theor. Appl. Climatol., 85, 19–36, 2006.

Lorente-Plazas, R., Montávez, J., Jimenez, P., Jerez, S., Gómez-Navarro, J., García-Valero, J., and Jimenez-Guerrero, P.: Characterization of surface winds over the Iberian Peninsula, Int. J. Climatol., 35, 1007–1026, doi:10.1002/joc.4189, 2014.

Nogaj, M., Parey, S., and Dacunha-Castelle, D.: Non-stationary extreme models and a climatic application, Nonlinear Processes in Geophysics, 14, 305–316, 2007.

Peterson, T. C. and Easterling, D. R.: Creation of homogeneous composite climatological reference series, Int. J. Climatol., 14, 671–680, doi:10.1002/joc.3370140606, 1994.

Pfahl, S.: Characterising the relationship between weather extremes in Europe and synoptic circulation features, Nat. Hazards Earth Syst. Sci., 14, 1461–1475, doi:10.5194/nhess-14-1461-2014, 2014.

Philipp, A., Della-Marta, P., J.Jacobett, Fereday, D., Jones, P., Moberg, A., and Wanner, H.: Long-term variability of day North Atlantic-European pressure

patterns since 1850 classified by simulated annealing clustering, J. Climate, 20, 4065–4095, 2006.

Rodríguez-Puebla, C., Encinas, A. H., García-Casado, L. A., and Nieto, S.: Trends in warm days and cold nights over the Iberian Peninsula: relationships to large-scale variables, Climatic Change, 100, 667–684, 2010.

Sen, P. K.: Estimates of the regression coefficient based on Kendall's tau, J. Am. Stat. Assoc., 63, 1379–1389, 1968.

Seneviratne, S. I., Corti, T., Davin, E. L., Hirschi, M., Jaeger, E. B., Lehner, I., Orlowsky, B., and Teuling, A. J.: Investigating soil moisture–climate interactions in a changing climate: A review, Earth-Sci. Rev., 99, 125–161, 2010.

Seubert, S., Fernández-Montes, S., Philipp, A., Hertig, E., Jacobeit, J., Vogt, G., Paxian, A., and Paeth, H.: Mediterranean climate extremes in synoptic downscaling assessments, Theor. Appl. Climatol., 117, 257–275, 2014.

Sheridan, S., Lee, C., Allen, M., and Kalkstein, L.: Future heat vulnerability in California, Part I: projecting future weather types and heat events, Climatic Change, 115, 1–19, doi:10.1007/s10584-012-0436-2, 2012.

Sousa, P. M., Trigo, R. M., Aizpurua, P., Nieto, R., Gimeno, L., and Garcia-Herrera, R.: Trends and extremes of drought indices throughout the 20th century in the Mediterranean, Nat. Hazards Earth Syst. Sci., 11, 33–51, doi:10.5194/nhess-11-33-2011, 2011.

Stocker, T., Dahe, Q., and Plattner, G.: Working Group I Contribution to the IPCC Fifth Assessment Report Climate Change 2013, The Physical Science Basis, 1535 pp., 2013.

Storch, V. and Zwiers, W.: Statistical analysis in climate research, chap. Empirical ortogonal functions,135–192, Cambridge University Press, 1999.

Stott, P. A.: Attribution of regional-scale temperature changes to anthropogenic and natural causes, Geophys. Res. Lett., 30, 1724, doi:10.1029/2003GL017324, 2003.

Swingedouw, D., Terray, L., Cassou, C., Voldoire, A., Salas-Mélia, D., and Servonnat, J.: Natural forcing of climate during the last millennium: fingerprint of solar variability, Clim. Dynam., 36, 1349–1364, 2011.

Trigo, R., García-Herrera, R., Díaz, J., Trigo, I., and Valente, M.: How exceptional was the early August 2003 heatwave in France?, Geophys. Res. Lett., 32, L10701, doi:10.1029/2005GL022410, 2005.

Uppala, S., Kallberg, P., Simmons, A., Andrae, U., da Costa Beechtold, V., Fiorino, M., Gibson, J., Haseler, J., Hernandez, A., Kelly, G., Li, X., Onogi,

K., Saarinen, S., Sokka, N., Allan, R., Andersson, E., Arpe, K., Balmaseda, M., Beljaars, A., van de Berg, L., Bidlot, J., Bormann, N., Caires, S., Chevallier, F., Dethof, A., Dragosavac, M., Fisher, M., Fuentes, M., Hagemann, S., Holm, E., Hoskins, B., Isaksen, L., Janssen, P., Jenne, R., McNally, A., Mahfouf, J., Mocrette, J., Rayner, N., Saunders, R., Simon, P., Sterl, A., Trenberth, K., Untch, A., Vasiljevic, D., Viterbo, P., and Woollen, J.: The era-40 re-analysis, Royal Meteorological Society, 131, 2961–3012, 2005.

Van den Besselaar, E., Tank, A. K., and Van der Schrier, G.: Influence of circulation types on temperature extremes in Europe, Theor. Appl. Climatol., 99, 431–439, 2010.

Vautard, R. and Yiou, P.: Control of recent European surface climate change by atmospheric flow, Geophys. Res. Lett., 36, L22702, doi:10.1029/2009GL040480, 2009.

Ward, J.: Hierarchical grouping to optimize an objetive function, J. Am. Stat. Assoc., 58, 236–244, 1963.

Wilby, R. and Wigley, T.: Downscaling general circulation model output: a review of methods and limitations, Prog. Phys. Geogr., 21, 530, doi:10.1177/030913339702100403, 1997.

Yiou, P. and Nogaj, M.: Extreme climatic events and weather regimes over the North Atlantic: When and where?, Geophys. Res. Lett., 31, 1–4, 2004.

Yiou, P., Goubanova, K., and Nogaj, M.: Weather regime dependence of extre value statistics for summer temperature and precipitation, Nonlinear Proc. Geoph., 15, 365–378, 2008.

Zwiers, F. W., Zhang, X., and Feng, Y.: Anthropogenic influence on long return period daily temperature extremes at regional scales, J. Climate, 24, 881–892, 2011.

Chapter 5

EHD Future projections

5.1 Introduction

The global warming observed since the past century is accompanied by an increase in the number of extreme events in most areas. In continental areas of North America, Europe and Australia (Field et al, 2012) a significant increase of the frequency of warm days events have been reported in the last decades. In Europe, the largest trends are detected since middle 70's of past century (Klein Tank and Können, 2003), being remarkable those observed in maximum temperature (T_x) and related to extreme occurrences over the Iberian Peninsula (IP) and the South of France (Brunet et al, 2007; Rodríguez-Puebla et al, 2010; Ramos et al, 2011; Fernández-Montes et al, 2012). In addition, the enhanced variability of summer temperature has contributed to more frequent, persistent and intense heatwaves (Schär et al, 2004; Barriopedro et al, 2011), as well as to positive trends of hot summer extremes (Seneviratne et al, 2014).At global scale, climate change projections show that changes will continue along this century (Stocker et al, 2013). In the IP, the highest temperature trends are projected for the summer season (Stocker et al, 2013). Therefore, the study of the frequency evolution of extreme temperatures in the future acquires a great relevance due to the larger impacts on human health, ecosystems, agriculture and infrastructures.

The observed trends in the occurrence of warm days have been clearly attributed to the anthropogenic emissions of greenhouse gases at global and continental scales (Stocker et al, 2013). However, attribution at smaller scales has not yet been strongly stablished, primarily due to the low signal-to-noise ratio and the difficulties of attributing effects to a wide range of possible driving processes (Field et al, 2012). To understand the processes leading to an enhancement of extreme temperatures at regional scales is a challenge because of the prominent impact on human health, specially among people with cardiovascular diseases (Díaz-Jiménez et al, 2005)

The appearance of extreme temperatures is related to the occurrence of some specific Circulation Types (CTs) (Rasilla et al, 2010; Fernández-Montes et al, 2012; García-Valero et al, 2015). CTs control the characteristics of air masses over

a given region, as well as the incident air fluxes over it. The combination of dry air conditions, clear sky and stagnant situations favors the development of warm events. In addition, interaction of air flux with orography can provoke intense warming in the region by adiabatic air compression occurred when wind blows from high to low altitude regions. Therefore, the changes in the atmospheric circulation can partially explain regional trends, as well as the differences among different areas (García-Valero et al, 2015). Other factors such as changes in land use (Christidis et al, 2013) and aerosols can have relevance at more local scales. In addition, positive land-atmosphere feedbacks play an important role in the occurrence of extreme temperature at regional scales. On the one hand, prevailing dry conditions of soil enhances the exchanges of sensitive heat from land to atmosphere increasing the air temperature; on the other hand, persistence of high air temperatures lead to the increase of evapotranspiration provoking the dryness of soil.

In García-Valero et al (2015) an attribution exercise of the regional extremely hot days (EHDs) trends observed at eight Spanish regions to the changes in the frequency of specific CTs drivers of EHDs during summer was performed. EHDs were defined as those days when T_x exceeds the 95th percentile of the regional series derived from the period 1951-2008. To perform this, a methodology to obtain the CTs was proposed. This consisted first of the identification of an ensemble of atmospheric patterns obtained only for those days when an extreme event occurred at any of the regions. Second, the final CT classification was obtained assigning the rest of days -non-extreme days- to the clusters obtained in the first step. Therefore, an assignation method was proposed. The authors found that between 30-50% of the observed trends were able to be attributed to changes in the frequency of CTs for most regions. This percentage was lower for those regions with the largest observed EHD trends, mainly located in the inner of the IP.

The objective of this work is to obtain climate change projections of EHD occurrences at the same regions defined in García-Valero et al (2015). For that a method based on the possible changes in the frequency of the CTs of the García-Valero et al (2015) under future climate change scenarios is used. In this way, climate change projections of the frequency of such CTs is analyzed by using atmospheric data of three climate Earth System Models. Changes under two representative concentration pathways (RCP4.5/8.5) are investigated. This contribution is organized as follows: Sec 5.2 describes the data and methodology for obtaining the EHD projections. Sec 5.3 shows the skill of ESMs on reproducing the frequency of CTs and an analysis of the future changes projected for the frequency of the CTs as well as for the EHD occurrence in the different regions. Conclusions and discussions are summarized in Sec 5.4.

5.2 Data and Methodology

Table 5.1: Earth System Models used in this study

Model	lon/lat resolution	member	References
CCSM4	1.250º x 0.950º	r6i1p1	Gent et al (2011)
MPIM-ES-MR	1.875º x 1.875º	r1i1p1	Stevens et al (2013)
EC-Earth	1.125º x 1.125º	r7i1p1	Hazeleger et al (2010)

5.2.1 Atmospheric data

Historical simulations (1958-2005) and climate change projections (2006-2100) from three Earth System Models (ESMs) have been used for this work. Projections are obtained under two representative concentration pathways (scenarios hereafter), RCP8.5 and RCP4.5 (Taylor et al, 2012). Table 5.1 shows the main characteristics of the models employed. Data are subtracted from the Earth System Grid Federation (ESGF) gateway Program for Climate Model Diagnosis and Intercomparison `http://pcmdi9.llnl.gov`.

The CTs used in this work are those obtained in García-Valero et al (2015). The large scale atmospheric variables used were Sea Level Pressure (SLP), Temperature at 850 hPa level (T850) and Geopotential Height at 500 hPa level (Z500). SLP is usually a prefered parameter to characterize circulation anomalies over the IP (Fernández-Montes et al, 2012; Perez et al, 2014), being as well considered as less influenced by global warming shift (Zorita and Von Storch, 1999). However, anomalies in the mid-upper troposphere described by Z500 are usually important drivers of temperature anomalies in the IP (García-Herrera et al, 2005; El Kenawy et al, 2013), and T850 is also a parameter with significant influence on surface temperatures (Brands et al, 2011). Three different CTs classifications composed by two atmospheric variables are used: SLP-T850, SLP-Z500, T850-Z500.

In addition, reanalysis from ERA40 (1958-2002) and operational analysis from ECMWF (2003-2005) of the same atmospheric fields are used for evaluating the skill of the models in reproducing the frequencies of the CTs in the historical period. To analyze EHD in the IP, daily maximum temperature (T_x) from the Spain02 dataset (Herrera, 2011) is used. This database, derived from the interpolation of a high density net of stations, has a large spatial resolution (0.2ºx0.2º) over the peninsular Spain and the Balearic Islands.

5.2.2 Methodology

Method for EHD projections

The main task of this work is to obtain climate change projections of the EHD in the eight regions identified in García-Valero et al (2015). To perform this, many of the results and methods presented in García-Valero et al (2015) are considered.

The method used for projecting consists of several steps. First, the centroids

from the three CT classifications defined in García-Valero et al (2015) formed by two atmospheric fields (SLP-T850, SLP-Z500 and Z500-T850) are employed for allocating the future projections derived from the different models and scenarios (Subsec. 6.2). For the allocation, the same procedure explained in García-Valero et al (2015) is used here. It is based on the Euclidean distance and spatial correlation metrics as well as on an esemble of thresholds defined for each metric and for the different centroids. More details can be found in García-Valero et al (2015). However, this method has the limitation that it can be applied only to atmospheric fields disposed into the same grid where centroids were obtained. In this case, centroids were calculated in the grid used in the ERA40 dataset (1.125º), therefore previous to the allocation the outputs of the different ESM simulations (see Table 5.1) are remapped into the ERA40 grid using a bilinear interpolation. Furthermore, thresholds of both metrics were calculated from standardized reanalysis data (García-Valero et al, 2015), so the data of models are standardized at each gridpoint. For the standardization of models mean and standard deviation derived from the historical period (1950-2005) were considered. Second, once the groups of days belonging to the CTs for the three classifications are obtained in future scenarios, the number of EHDs for a given region EHD_i is calculated by:

$$EHD_i = \sum_j e_j^i N_j \tag{5.1}$$

where e_j^i is the efficiency of the CT_j over the region i calculated in García-Valero et al (2015) (efficiency is defined as the probability of having an EHD occurrence in the region under the CT) and N_j the number of days grouped in the CT_j for a given period of time (one year). j runs from 1 to the number of CTs (8 for all classifications) and i from 1 to the number of regions (8).

Uncertainty evolution

Taking into account the method explained above, for each region an ensemble of 18 EHD projections combining ESMs, CT classifications and RCP scenarios is obtained. This ensemble of EHD projections are linked to three sources of uncertainty: models, classifications and scenarios. Here, it is presented a method for analysing the time evolution of each uncertainty source along the period 1950-2100.

To separate the uncertainty related to each source, an ANOVA analysis applied over the EHD annual series is employed. For that, if a given source is considered, for example the climate models, three different ensembles can be obtained, formed by six EHD projections (2 scenarios x 3 CT classifications using a same model) each one. Then, mean values of each ensemble are obtained for each year of the series, and the range obtained from these values is considered as a measure of the uncertainty associated to this source. Similar considerations

can be adopted for the other sources of uncertainty. In this way, for each year, the different uncertainties related to each source is normalized by the sum of the different uncertainties, obtaining in this manner the relative importance of each source to the total uncertainty of the year.

Once the relative importance of the uncertainties is calculated for each year, the range (in days) corresponding to each source can be obtained using this result and the total range obtained from the global ensemble formed by the 18 EHD projections. In order to analyze long-term variations of the uncertainty, running mean series of 31 years can be applied over the annual series before aplying the normalization. Hence, once the running series are obtained they are normalized in the same way explained above.

Validation of method

A leave-one-out cross validation has been carried out for analyzing the skill of the statistical method used for EHD projections. This validation consists of comparing the seasonal frequency of EHD obtained by this method with the frequency observed in the different regions during the period 1958-2008. The validation is centered on evaluating the sensitivity of the results on the efficiency values. To perform this, the seasonal frequency of CTs obtained by García-Valero et al (2015) are used, whereas the efficiencies of García-Valero et al (2015) have been recalculated by averaging the efficiencies values for all the observational years (1958-2005) except the validation one. Annual temporal correlation between the seasonal reproduced and observational EHD series have been evaluated for this exercise.

The highest correlations are between 0.60 and 0.70 (Table 5.2) for most regions. The highest values are obtained when considering the SLP-T850 classification, but for NE and Cs where Z500-T850 is employed. However, the method subestimates the EHD frequency during the most extreme years. Figure 5.1 shows an example of this for the North region (N). Left-panel represents the seasonal series of the reconstructed EHDs considering the three CT classifications (color lines), as well as the observed EHD series (black line) for the period 1958-2005. It is observed that the frequency of EHDs is strongly underestimated during the years of high occurrence and slightly overestimated the years with scarce number of EHDs. This can be more clearly stated by analyzing the QQ-plot of the right panel of Figure 5.1. The larger the number in EHDs the larger the underestimation. The reason for these differences could be the influence of other factors controlling the occurrence of extreme daily temperature in a concrete year, such as: moisture of soil, land-atmosphere feedback processes, sea surface temperature, etc.

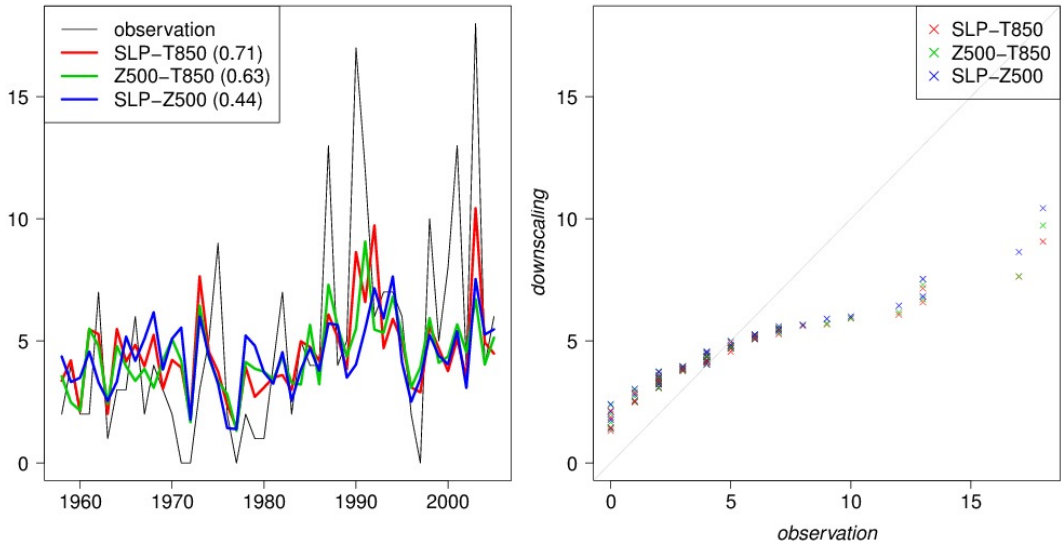

Figure 5.1: Leave-one-out cross validation for the North Region. Left panel depicts the modeled (in colors) and observed (black) summer frequencies. Right Panel shows the QQ-plot (modeled vs observational series).

Table 5.2: Leave-one-out cross validation. Regional correlations for the three CT classifications between EHD estimated series and observational ones.

Region	SLP-T850	SLP-Z500	Z500-T850
SW	0.69	0.55	0.58
NE	0.61	0.54	0.67
E	0.61	0.42	0.60
Cs	0.63	0.57	0.66
NWs	0.65	0.61	0.64
NWe	0.61	0.46	0.56
NWw	0.63	0.55	0.51
N	0.71	0.44	0.63

5.3 Results

5.3.1 Skill of ESMs

This section analyzes the skill of ESMs on reproducing the seasonal frequencies of the CTs, as well as the EHD occurrences in the different regions during the historical period (1958-2005). To perform this, the existence of biases in the frequency of CTs and regional EHD occurrences reproduced by the ESMs using the different CT classifications is analyzed. Biases in the frequency of CTs are calculated respect to the frequency of CTs derived from reanalysis during the historical period, while EHD biases have been obtained against the occurrences derived from the Spain02 dataset.

Figure 5.2 represents the mean seasonal bias (modeled-observed) in the frequency of CTs (left graphics) as well as in the regional EHD frequencies (right) for SLP-T850, SLP-Z500 and Z500-T850 classifications (rows). Biases in the frequency of CTs are lower than one day in all cases, showing a well performing of the three ESMs on reproducing the historical CT's frequencies. In general, the models give similar biases although these for EC-EARTH are slightly higher (for example CT1 of SLP-T850 and CT2 of SLP-Z500). Comparing the biases between the CT classifications these are a bit lower in Z500-T850 and some larger in SLP-T850.

Obviously, the low bias found in the frequency of CTs are translated into low bias in EHD frequency. Graphics on the right-panel of Figure 5.2 corroborate this, observing in general a slightly overestimation of EHD by the three models in all regions. Anyway, in all cases, the biases are lower than 10% of the observational frequency (around 5 days). In general, MPIM-MR gives the lowest bias, whereas EC-EARTH causes the largest ones.

5.3.2 Changes in CTs

Once projected the CT classifications to the future, the first step is to analyze possible changes in the frequency of CTs. These changes have been calculated respect to the frequency of the reanalyis CTs during the historical period.

Figures 5.3 and 5.4 show the running mean (31 years) of future changes in CTs frequency obtained by using the three CT classifications (columns) and the three ESMs (rows) under the RCP8.5 and RCP4.5 scenarios, respectively. It is observed similar characteristics in the evolution of the changes in the three classifications and under the different scenarios, although changes are more marked under RCP8.5. Most CTs increase strongly their frequency to the end of the century whereas some others decrease. Under a given CT classification the differences among the models are small. This would indicate some consistence of future projections among the different ESMs. However, larger differences appear among

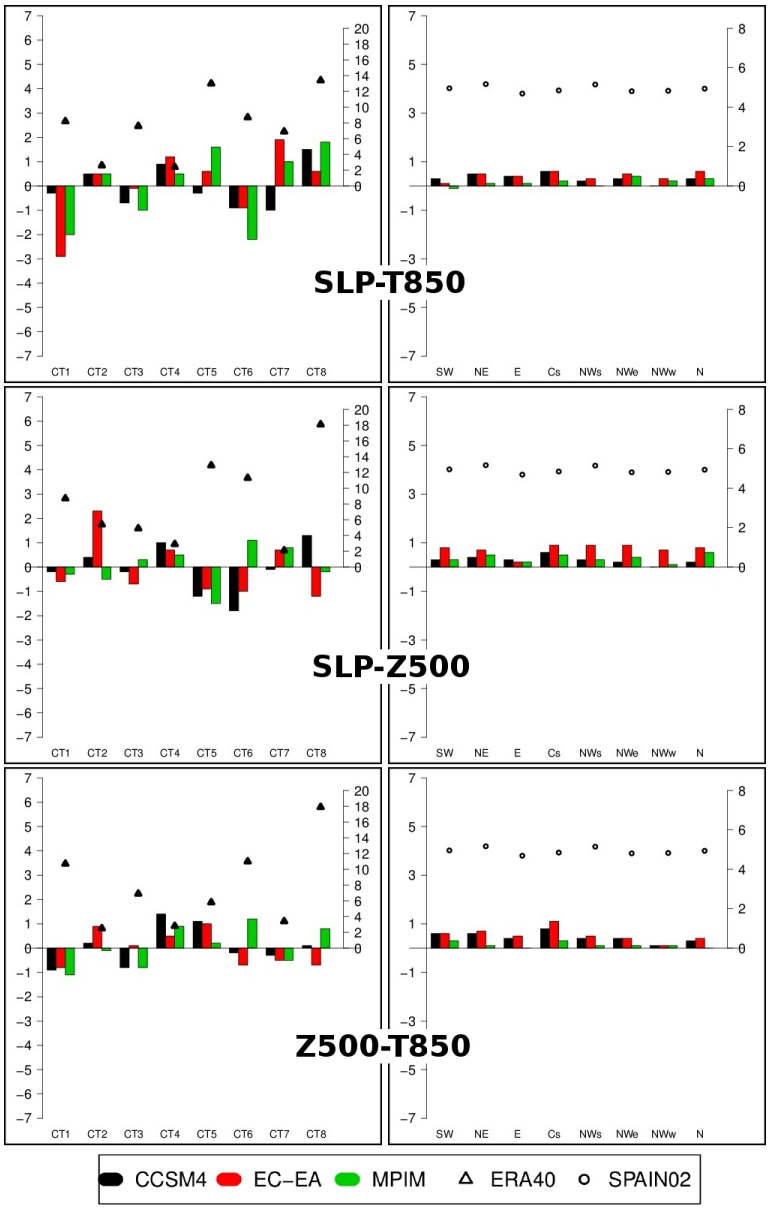

Figure 5.2: Mean seasonal bias for the period 1958-2005. Rows show the biases obtained for the different CT classifications. Columns indicate the different kind of biases: CT's frequency (left) and EHDs (right). Biases in the frequency of CTs are calculated respect to the frequency of CTs derived from reanalysis data for the historical period, while EHD biases are obtained against the EHD occurrences derived from the Spain02 dataset. Absolute CT's frequencies of reanalysis and EHDs for Spain02 are shown by triangles and circles (right y-axis of the different graphics).

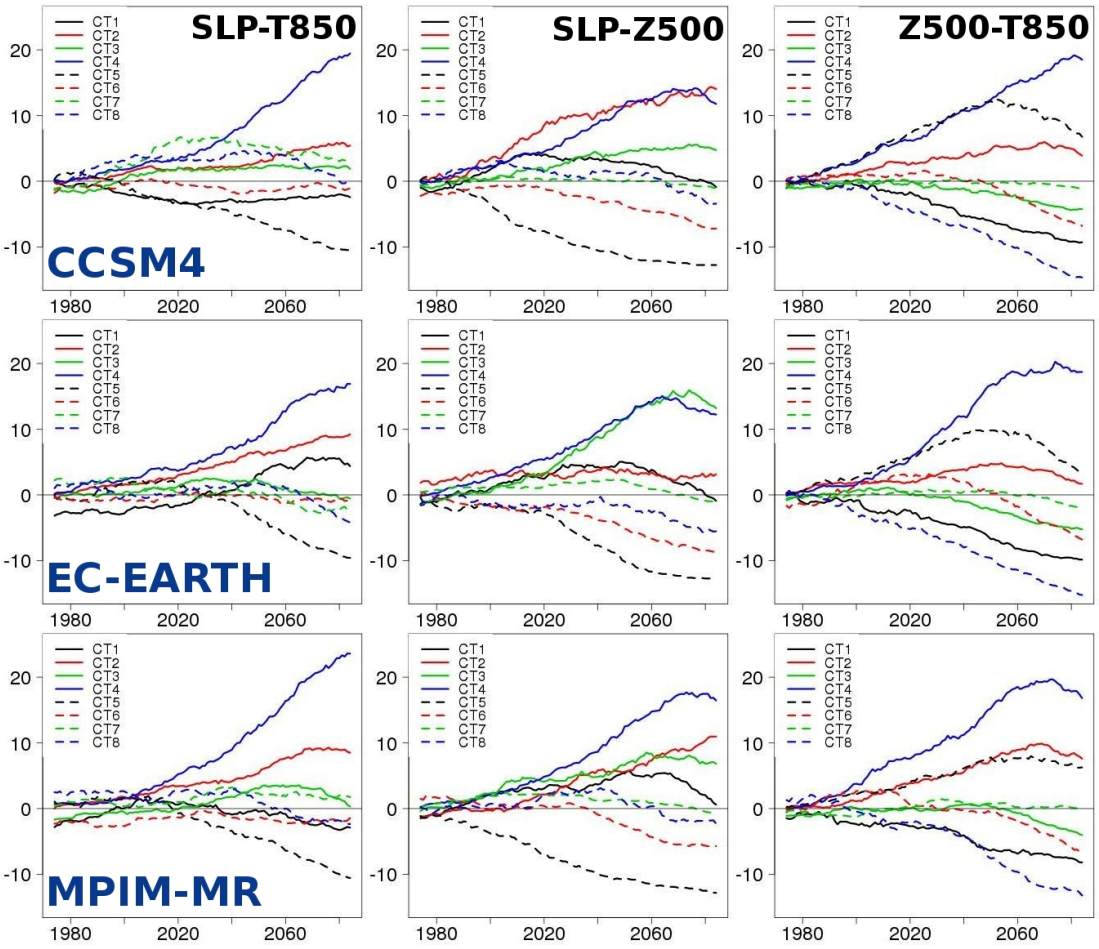

Figure 5.3: Changes in the frequency of CTs relative to the historical (1958-2005) reanalysis frequency. Running mean series (31 years) of the changes in the frequency of the CTs obtained by the three CT classifications (columns), three ESMs (rows) under the RCP8.5 scenario.

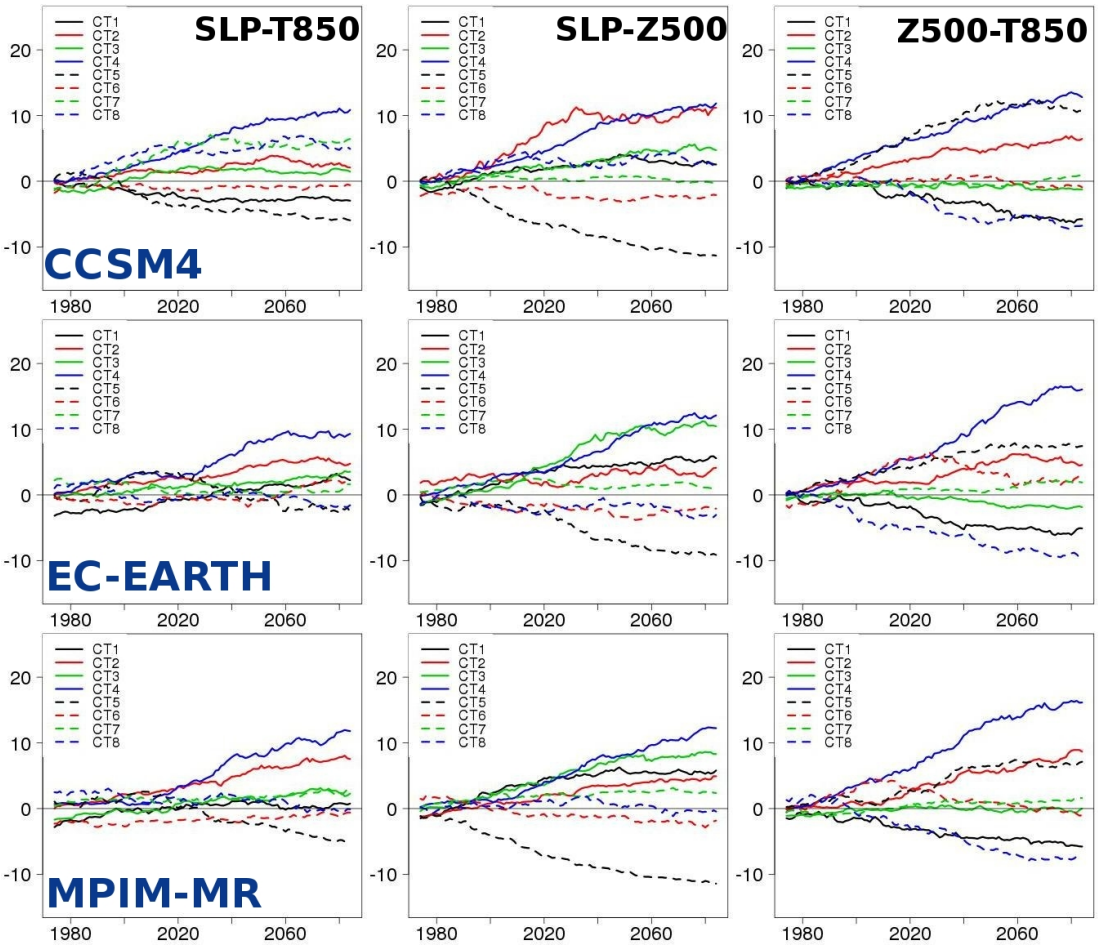

Figure 5.4: Same as Figure 5.3 but for the RCP4.5 scenario.

the different CT classifications considering a given model. In general terms, under the SLP-T850 classification changes are less pronounced than in the other classifications, whereas the largest ones are obtained for Z500-T850.

Among the CTs which more increase their frequencies they are two strongly related to EHD occurrences in most regions simultaneously (García-Valero et al, 2015). This result is observed in all classifications and models. The former CT (CT4 of SLP-T850 and SLP-Z500 and CT2 of Z500-T850 classifications) is an atmospheric pattern related to the highest EHD efficiencies in the Cs and NE regions, some lower efficiency in the rest but inefficient in NWw. This CT has the highest increase in all models and classifications. It is related to an intense ridge at 500 hPa of great amplitude extending from the eastern of the IP towards the western/central Europe. The axis of the ridge is located over the mediterranean area of the IP and it is slightly tilted in the direction NNE-SSW. This inclination favors warm-advection at higher atmospheric levels. In addition, it is associated with an stagnant situation at surface with relative low pressures towards the central of the IP. Furthermore, an intense thermal ridge is over the IP reaching temperatures near 24 ºC at 850 hPa level over the central of the IP. The latter CT increasing its frequency is the one with large efficiency in the SW and NWs regions (CT2 of SLP-T850 and SLP-Z500 and CT4 of Z500-T850 classifications). This pattern is very similar to the one explained above but it appears some displaced towards the West. Hence, the axis of the ridge at 500 hPa is over the central of the IP, making that warm-advection towards western regions are larger. Anyway, this situation seems to be the precursor of the another situation. In fact, most of the hot episodes over the IP begin in the western regions and later are translated towards the eastern ones (García-Valero et al, 2015). An interesting aspect is that both CTs were identified in García-Valero et al (2015) as the most homogeneous clusters. This means that the thresholds of correlation and distance used for assigning the future days to these CTs are more restrictive than those used for another CTs, and therefore the higher allocation of future days to these CTs means a clear projection on future dynamics over these CTs of great relevance in EHD occurrences.

However, there are some CTs like CT5 of the SLP-T850 and SLP-Z500 classifications (CT6 in Z500-T850), and the CTs 1, 3 and 8 of the Z500-T850 classification whose frequencies decrease drastically. CT5 is associated with an anticyclone located over the English Channel provoking eastern circulation over the IP, and with the largest EHD efficiency over the NWw region but lacking efficiency in the rest of regions. Regarding the Z500-T850 classification, CTs 1 and 3 are ridge configurations with low geopotential values at 500 hPa over the IP and higher efficiencies over the northern and southwestern regions, whereas CT8 reflects a strong temperature gradient in the NW-SE direction.

Another important result is the decreasing (or stabilization) in the frequency

of some CTs after a period of important increasing. By contrast, the opposite situation (first decreasing and later increasing) does not occur in any CT. This evolution can be seen clearly in some CTs of the SLP-Z500 and Z500-T850 classifications under the RCP8.5 escenario (Figure 5.3). This result could be linked to two factors. On the one hand it would be due to large changes in dynamics would provoke that new CTs appear under forcing scenarios, and so they can not be assigned to the CTs defined in the historical period. On the other hand, it would be possibe that the intense warming expected under RCP scenarios of great emissions, like RCP8.5, leads to important changes in the mean values of Z500 and T850, increasing them despite the shape of patterns would keep unaltered. This would provoke that the more intense fields could not be allocated to the CTs because its distance to the centroids could be larger than the thresholds stablished with lower mean values. A fact wich could corroborates this latter supposition is that changes in the evolution of the CT frequency are observed first for those CTs related to lower temperature and geopotential, like is CT5 in the Z500-T850 classification, whereas the change is observed after for those CTs associated with higher values of temperature and geopotential (CT4 of Z500-T850). In addition, this idea is in agreement with the increase of the frequency observed in the cluster formed by those days not classified at any CT. This increase is produced at the same time than starts the decreasing of the frequency of CTs. Figure 5.5 shows an example of the evolution of frequencies of the CTs 4 and 5 of the the Z500-T850 classifications, as well as of the unclassified-cluster, obtained by the MPIM-MR model runned under RCP8.5 conditions.

EHDs projected changes

Figures 5.6 5.7 and 5.8 show for each region the ensemble of projections in EHD frequency (running mean of 5 years) obtained for the SLP-T850, SLP-Z500 and Z500-T850 classifications, respectively. The ensemble mean is also shown on each picture (black curve).

For all regions a noticeable increase of the EHD frequency is projected along the century in the three classifications. For a given region the ensemble mean produces similar results in the three CT classifications. In all regions and classifications the ensemble mean follows a linear progression during a great part of the period but it keep stationary and even decreases to the end. This effect is more clear in the SLP-Z500 and Z500-T850 classifications than in SLP-T850. This result is in agreement with the changes in the frequency of CTs mentioned above. During a long part of the time (before 2080), EHD projections under RCP8.5 scenario are higher than those obtained following the RCP4.5 scenario, but towards the end, the frequency of EHD based on RCP8.5 decreases while projections obtained by RCP4.5 continue increasing. This different evolution makes that towards the end of the period the uncertainty of the EHD projections linked to the RCP scenarios decrease.

Table 5.3 summarizes the results derived from the ensemble. In averaged terms, it is obtained that the frequency of EHD occurrences will be duplicated to the

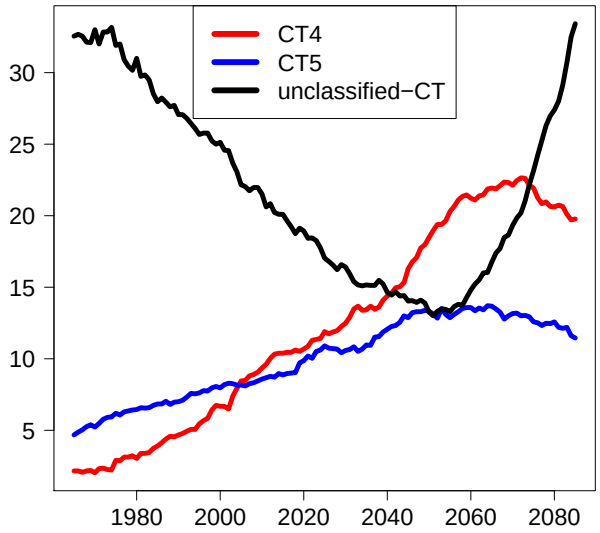

Figure 5.5: Running mean series (31 years) of seasonal EHD frequencies corresponding to CTs 4 and 5 of the Z500-T850 classification obtained by MPIM-MR model under RCP8.5 scenario. The evolution of the frequency assigned to the unclassified cluster for this simulation is also shown.

end of this century for most regions and will triple for NE and Cs regions. The larger increase in the inner regions go in line with the regional trends found in the historical period (García-Valero et al, 2015), and is consistent with the warming patterns of T_x projected in summer for the IP pointed out by (Gómez-Navarro et al., 2010; Seubert et al, 2014).

An analysis of the uncertainty evolution in the different regions along the period 1950-2100 is represented on Figures 5.9 and 5.10. Left graphics of figures show the relative importance of the three uncertainty sources, whereas on the right ones, the evolution of the total uncertainty, defined as the total range

Table 5.3: Mean and Uncertainty in the seasonal number of EHDs projected for the period 2071-2100. Values are derived from the ensemble of EHD projections combining the all models, CT classifications and scenarios. Uncertainty values are the intervals corresponding to the range of the ensemble (in days) centered in the mean values.

Region	SW	NE	E	Cs	NWs	NWe	NWw	N
Mean	12.5	15.4	11.0	15.2	13.6	10.9	8.3	11.8
Uncertainty	±2.5	±4.3	±4.3	±4.4	±2.8	±3.3	±2.3	±4.0

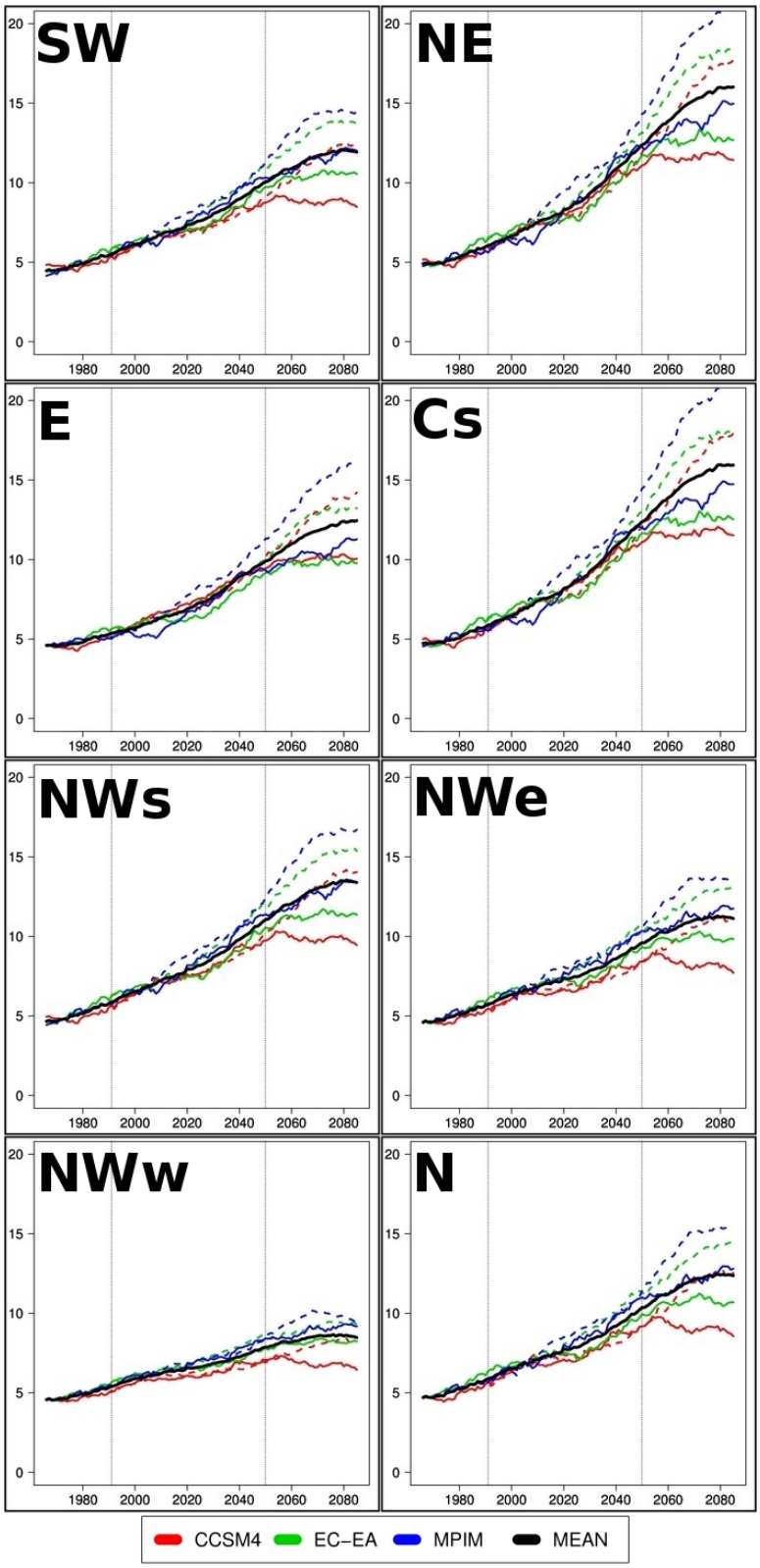

Figure 5.6: Regional EHD projections under the SLP-T850 classification. Dashed/solid lines represent the RCP8.5/RCP4.5 run mean series (31year)

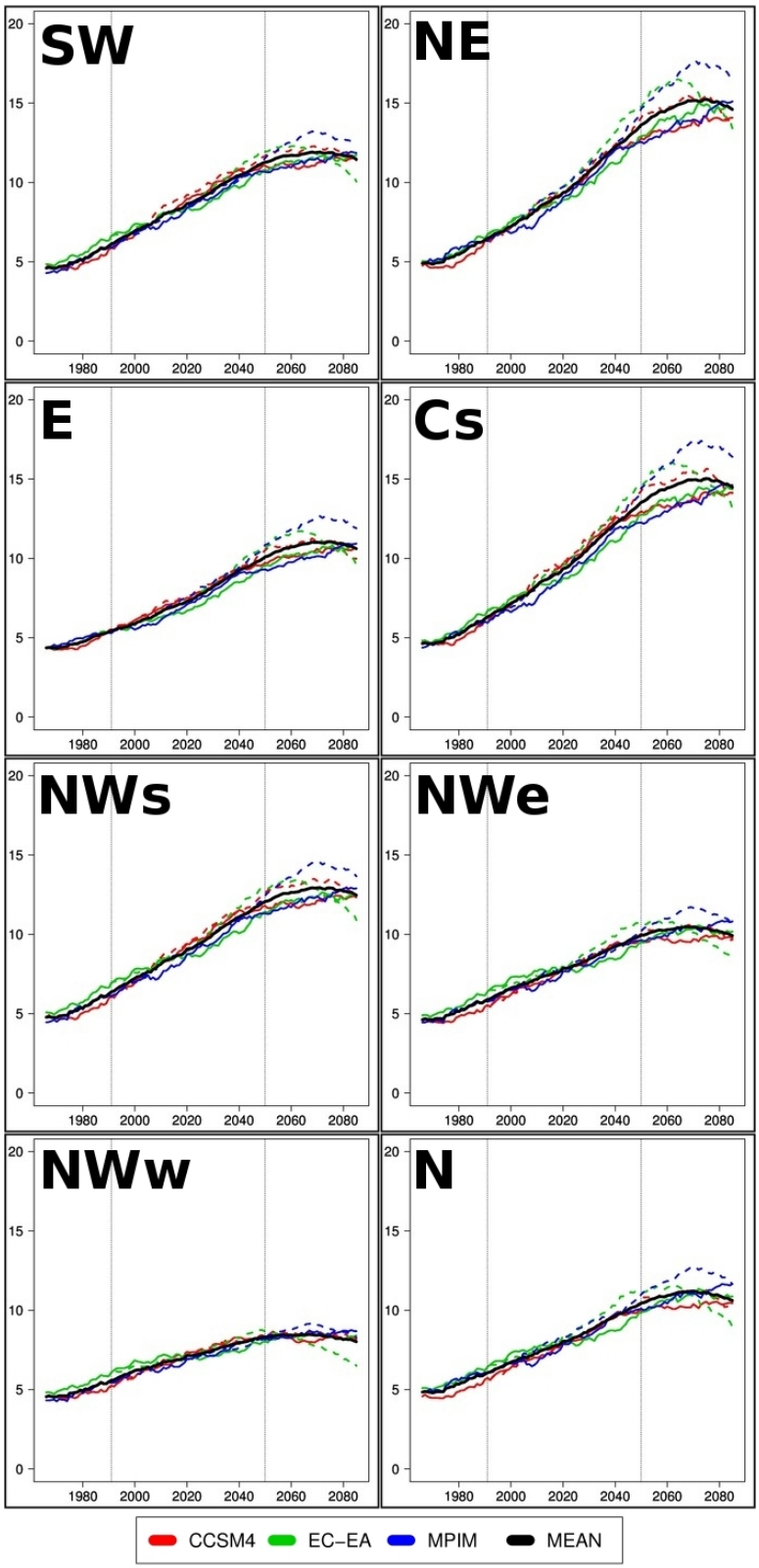

Figure 5.7: Same as Figure 5.6 but for SLP-Z500 classification.

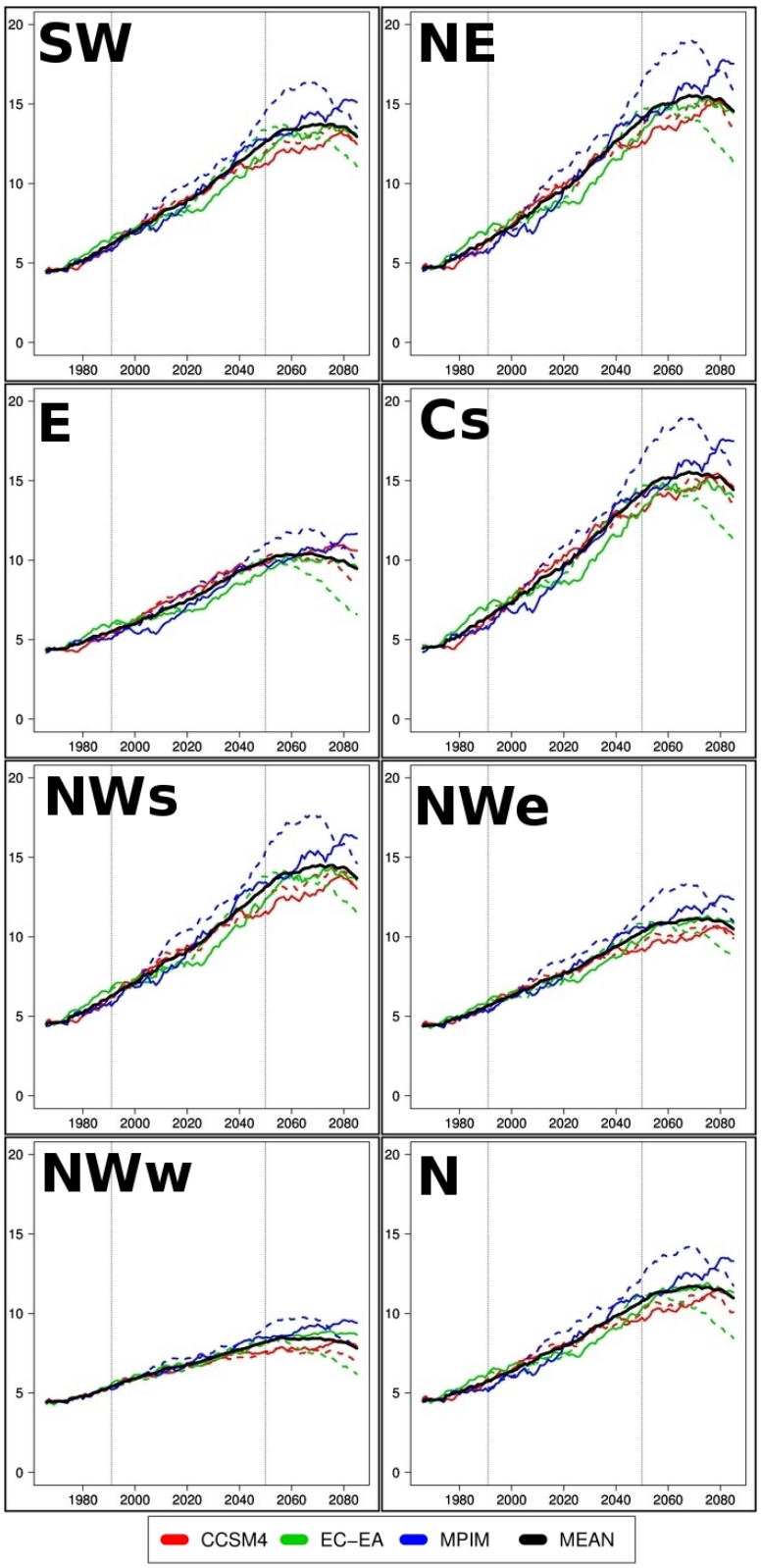

Figure 5.8: Same as Figure 5.6 but for Z500-T850 classification.

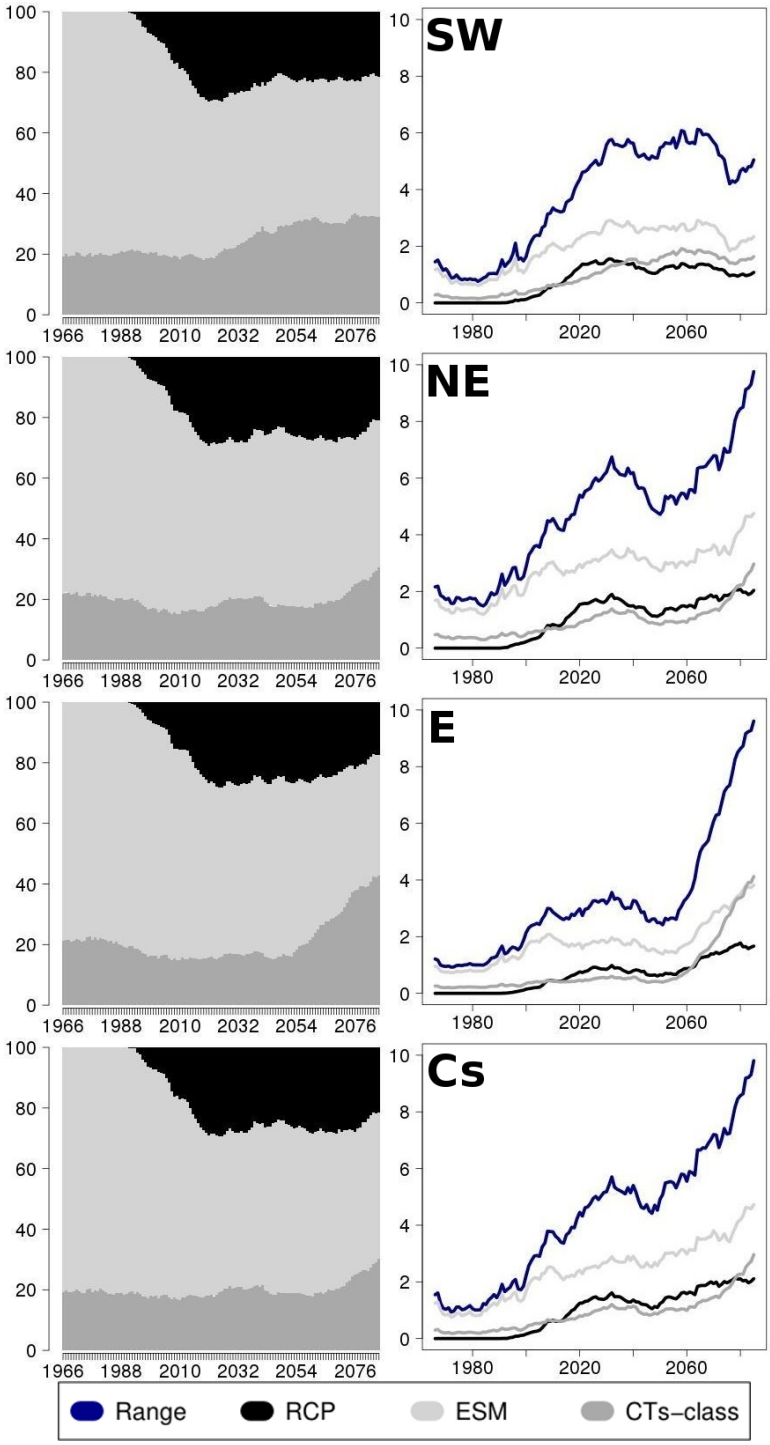

Figure 5.9: Uncertainty analysis for SW, NE, E and Cs regions. Left graphics show the relative importance (in percentage) of each uncertainty source (RCP, ESM and CT-class) on the EHD projections along the time. Right graphics show the absolute contribution of each uncertainty source as well as the total uncertainty. Analysis is performed by using running mean (31 years) of EHD projections series for the period 1950-2100.

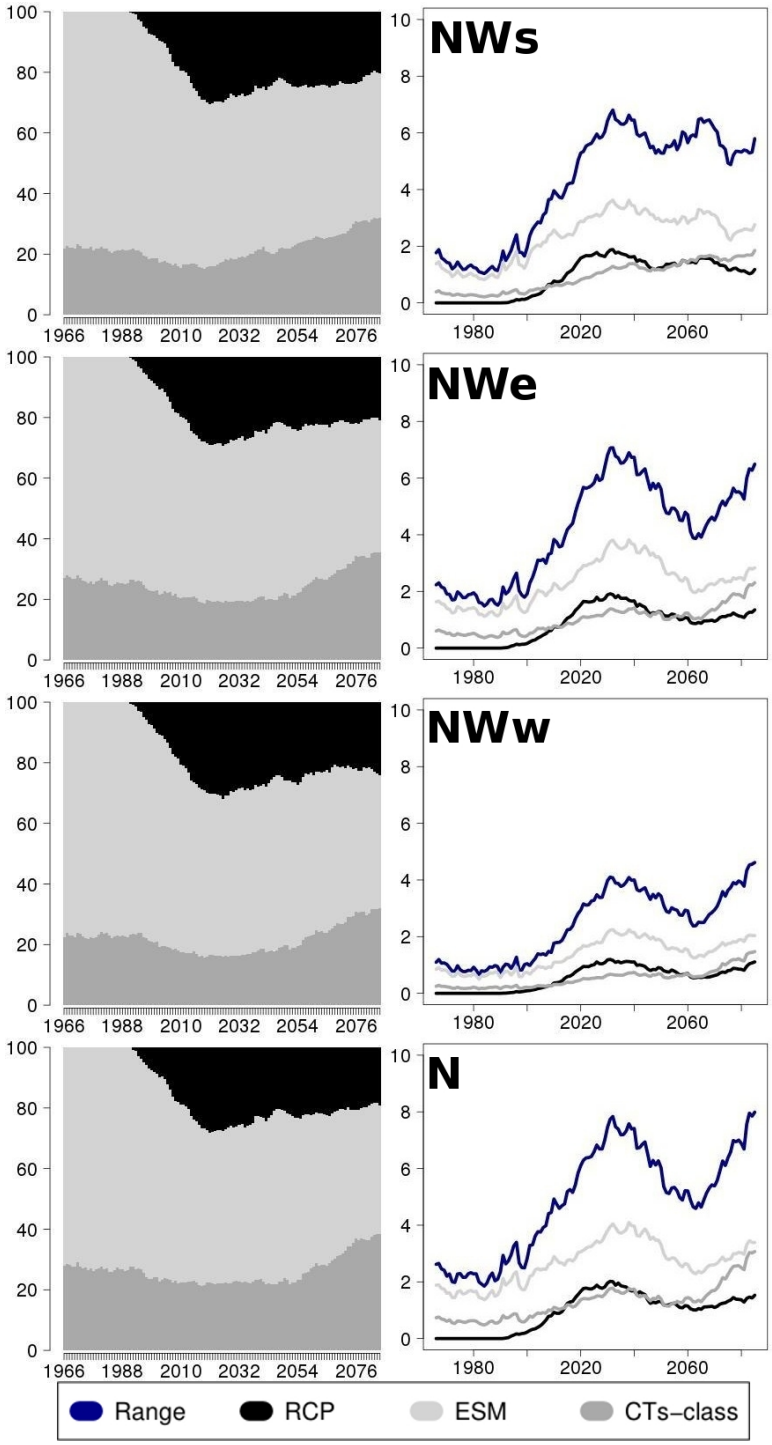

Figure 5.10: As Figure 5.9 but for regions NWs, NWe, NWw and N.

of the ensemble projections, as well as the individual uncertainty introduced by each source is represented. For most regions, the relative importance of the three sources present a similar evolution. In general, models control the highest part of the uncertainty along the global period. Hence, during the historical period around 80% of the uncertainty is due to this source and about 50% during the middle and until the end of the current century. For most regions, the relative importance of the uncertainty associated with CT classifications keep mainly stationary from the beginning to near 2050 when experiment an increase in all regions, becoming from 20% to 30-40% at the end of the period. The increase of the classifications uncertainty to the end of the period is especially prominent in the E region, where the importance of this source is of the same order that the one linked to models. Regarding the uncertainty related to RCP, this reaches its maximum relative importance between 2020-2040, when it is about 30% of the total uncertainty. This value decreases gradually towards the end until 20-25% depending on the region. The decrease and increase of the scenarios and CT classifications uncertainty, respectively, at the end of the period evidence the problem argued above related to the limitation of the methodology on assigning atmospheric patterns to the centroids considered here, when climate conditions change largely (as occurs under RCP8.5 scenario).

Despite the relative importance of the three uncertainty sources changes similarly in the different regions, the uncertainty, defined as the range in days between the maximum and minimum EHD values projected, of each source is dependent of the considered region (Lef panel of Figures 5.9 and 5.10). In all regions an important increase of the total uncertainty is observed from the historical period to 2020, observing a relative maximum between 2020-2040 due mainly to the important increase of the uncertainty related to RCP scenarios. Since this maximum, the evolution differs from some regions to anothers. In the most northern regions, NWw, NWe and N, the uncertainty decreases until 2060 linked to similar evolution of the scenarios and models uncertainty, but from 2060 to the end the uncertainty increases as consequence of the increase classifications uncertainty. However, in the SW and NWs, the evolution from 2040 to the end practically keep constant. Finally for the southern and eastern regions, Cs, E and NE, an small decrease of the uncertainty is obtained from 2040 to 2050 but a prominent increase is produced during the all second half of the century. This increase is especially associated with the uncertainty linked to classifications and models, suggesting that EHD projections for these regions are the most sensitive to the atmospheric fields chosen for defining the CTs. Anyway, centering the uncertainty ranges in the mean values from the ensemble EHD projections, the uncertainty corresponding to the last 31 years period (2071-2100) does not overcome the 30% of these values for the different regions, with the exception of E and N regions where the uncertainty is about 39% and 34%, respectively (Table 5.3)

5.4 Conclusions and discussions

A methodology based on CTs have been used for obtaining future EHD projections at eight Spanish regions. For projections the outputs of three Earth System Models (MPIM-MR, EC-EARTH and CCSM4) run under two RCP scenarios (RCPs 4.5 and 8.5) available for the period 1950-2100 have been employed. Main conclusions and discussions are summarized as follows:

- The method used for EHD projections reproduces reasonably well the seasonal EHD variability in the different regions. This result is derived from a validation test of the method performed for the historical period. In addition, the methodology underestimates the EHD seasonal frequency for those years when the highest EHD occurrences.

- ESMs reproduce well the frequencies of the different CTs during the historical period independently of the considered CT classifications. For most CTs , the bias are lower than one day although they are a bit higher in the SLP-T850 classification. In general, small differences appear among the models observing a more similar behavior between CCSM4 and MPIM-MR. .

- Mean EHD seasonal occurrences are slightly overestimated by the models in all regions during the historical period. In most cases, the bias are lower than 0.5 days, being something lower using the SLP-T850 classification. For most regions the lowest bias are obtained by using the MPIM-MR model and the highest by means of EC-EARTH.

- Under forcing scenarios, the frequency of some CTs changes largely. Some of them increase significantly their frequency but in some others decrease. Two CTs with large efficiency in most regions simultaneously, increase the frequency independently of the considered CT classifications and ESMs. They represent intense ridges of great amplitude at 500 hPa level whose axis is located over the central and eastern of the IP being associated also with thermal ridges at 850 hPa level and stagnant situation at surface over the IP. Among the CTs whose frequency decrease, one of them is related to an anticyclonic situation located over the North of France and driver of EHD occurrences over the NWw region. In addition, two other situations related to low amplitude ridges at higher levels decrease their frequency under forcing scenarios.

- The method used for projections could have important limitations using RCP scenarios of great emissions as RCP8.5. The use of atmospheric variables largely linked to temperature, as T850 and Z500, causes that CTs of the future were more intense (with higher values of Z500 and T850) and they can not be assigned to the CTs despite they could have a similar atmospheric pattern. Therefore, when temperature changes significantly, EHD occurrences could decrease because to this limitation. However, among the

three considered CT classifications, this effect is less significant for SLP-T850.

- Regional EHD projections show a prominent increase of the occurrence of such extreme events in the different regions. Hence, considering the mean of the ensemble, during the period 2071-2100 the seasonal EHD occurrence will be duplicated or even will triple in relation to the one observed during the historical period (1950-2005). The highest increase is expected in NE, Cs and NWs, coinciding these regions with the areas where the highest positive trends in maximum temperature projected for summer were found by other authors (Gómez-Navarro et al., 2010; Belleflamme et al, 2014). By contrast, the lower increase is projected for the most northwestern region (NWw).

- The uncertainty in the projections for the last 31 years period (2071-2100) does not reach the 30% of the mean projected value for most regions. The highest values are obtained in the E (39%) and N (34%) regions, whereas the lowest are found in SW (20%) and NWs(21%).

- The evolution of the uncertainty in the EHD projections for all regions is controlled in a great extent (more than 50%) by the uncertainty linked to ESMs. However, to the middle of the 21st century RCP scenarios is the second source introducing uncertainty (30%). To the end of the century the CTs classifications are the second source provoking uncertainty, causing even at some regions, E, NE and Cs, the same uncertainty than models (around 40% for these regions).

In García-Valero et al (2015) was pointed out that the largest trends in EHD occurrences from 1958 to 2007 were observed in the inner regions, while the lowest ones in the NWw. Also Rodríguez-Puebla et al (2010) found larger trends in (annual) warm days towards the NE and SW IP during the last half century. Therefore, EHD projections obtained here are consistent with the observed EHD trends in the past. Projections obtained here are leaded exclusively by changes projected in the frequency of CTs, and so, they should be taken carefully. In García-Valero et al (2015) was pointed out that between 30-50% of the observed EHD trend in most regions could be attributed to changes in the frequency of CTs, decreasing this percentage in the inner regions. Dryness of soil is another factor responsible of the trends, enhancing the positive land-atmospheric feedback (Jerez et al, 2012) which increases the air temperature (Whan et al, 2015) and therefore, the probability of EHD occurrence. Along this century, climate change projections over the IP points out to an important decrease in precipitation in summer and spring (Stocker et al, 2013), accentuating the dryness of soil. Largest dryness is expected at inner regions (Jerez et al, 2012), hence -as it has been observed in the past- EHD occurrences for the inner regions could be even larger to the ones obtained here. In addition, the methodology explained here has some limitations underestimating the EHD frequency once the climate has changed largely

after a prominent increase of the mean temperature. Therefore, a revision of the methodology in order to reduce this drawback should be considered for future works.

Bibliography

Barriopedro D, Fischer EM, Luterbacher J, Trigo RM, García-Herrera R (2011) The hot summer of 2010: redrawing the temperature record map of europe. Science 332(6026):220–224

Belleflamme A, Fettweis X, Erpicum M (2014) Do global warming-induced circulation pattern changes affect temperature and precipitation over europe during summer? International Journal of Climatology

Brands S, Taboada J, Cofiño A, Sauter T, Schneider C (2011) Statistical downscaling of daily temperatures in the nw iberian peninsula from global climate models: validation and future scenarios. Climate Research 48(2-3):163–176

Brands S, Herrera S, Fernández J, Gutiérrez J (2013) How well do cmip5 earth system models simulate present climate conditions in europe and africa? Climate Dynamics pp 1–15

Brunet M, Jones P, Sigró J, Saladié O, Aguilar E, Moberg A, Della-Marta P, Lister D, Walther A, López D (2007) Temporal and spatial temperature variability and change over spain during 1850-2005. Journal of Geophysical Research 112(D12)

Christidis N, Stott P, Hegerl G, Betts R (2013) The role of land use change in the recent warming of daily extreme temperatures. Geophysical Research Letters 40:589–594, doi:10.1002/grl.50159

Díaz-Jiménez J, Linares-Gil C, García-Herrera R (2005) Impacto de las temperaturas extremas en la salud pública:futuras actuaciones. Revista Española de Salud Pública 79:145–157

El Kenawy A, López-Moreno JI, Brunsell NA, Vicente-Serrano SM (2013) Anomalously severe cold nights and warm days in northeastern spain: their spatial variability, driving forces and future projections. Global and Planetary Change 101:12–32

Fernández-Montes S, Rodrigo F, Seubert S, Sousa P (2012) Spring and summer extreme temperatures in iberia during last century in relation to circulation types. Atmospheric Research

Field CB, Barros V, Stocker TF, Qin D, Dokken D, Ebi K, Mastrandrea M, Mach K, Plattner G, Allen S, et al (2012) Managing the risks of extreme events and disasters to advance climate change adaptation. Cambridge University Press Cambridge

García-Herrera R, Díaz J, Trigo R, Hernández E (2005) Extreme summer temperatures in iberia: health impacts and associated synoptic conditions. In: Annales Geophysicae, vol 23, pp 239–251

García-Valero JA, Montávez JP, Gómez-Navarro JJ, Jiménez-Guerrero P (2015) Attributing trends in extremely hot days to changes in atmospheric dynamics. Natural Hazards and Earth System Sciences Discussions 3(5):3323–3367, doi:10.5194/nhessd-3-3323-2015, URL `http://www.nat-hazards-earth-syst-sci-discuss.net/3/3323/2015/`

Gent PR, Danabasoglu G, Donner LJ, Holland MM, Hunke EC, Jayne SR, Lawrence DM, Neale RB, Rasch PJ, Vertenstein M, et al (2011) The community climate system model version 4. Journal of Climate 24(19)

Gómez-Navarro J, Montávez J, Jimenez-Guerrero P, Jerez S, JA: GV, González-Rouco J (2010) Warming patterns in regional climate change projections over the iberian peninsula. Meteorologische Zeitschrift 19(3):275–285

Hazeleger W, Severijns C, Semmler T, ŞŞtefăănescu S, Yang S, Wang X, Wyser K, Dutra E, Baldasano JM, Bintanja R, et al (2010) Ec-earth: A seamless earth-system prediction approach in action. Bulletin of the American Meteorological Society 91(10)

Herrera S (2011) Desarrollo, validación y aplicaciones de spain02: Una rejilla de alta resolución de observaciones interpoladas para precipitación y temperatura en españa. PhD thesis, Ph. D. dissertation, Universidad de Cantabria, 129 pp.[Available online at www. meteo. unican. es/tesis/herrera.]

Jerez S, Montavez J, Gómez-Navarro J, Lorente-Plazas R, García-Valero J, Jiménez-Guerrero P (2012) A multiphysic ensemble of regional climate change projections over the iberian peninsula. Climate Dynamics 41:1749–1768, doi:10.1007/s00382-012-1551-5

Klein Tank A, Können G (2003) Trends in indices of daily temperature and precipitation extremes in europe, 1946-99. Journal of Climate 16(22):3665–3680

Perez J, Menendez M, Mendez FJ, Losada IJ (2014) Evaluating the performance of cmip3 and cmip5 global climate models over the north-east atlantic region. Climate Dynamics 43(9-10):2663–2680

Ramos AM, Trigo RM, Santo FE (2011) Evolution of extreme temperatures over portugal: recent changes and future scenarios. Climate Research 48(2):177

Rasilla DF, García-Codron JC, Carracedo V, Diego C (2010) Circulation patterns, wildfire risk and wildfire occurrence at continental spain. Physics and Chemistry of the Earth, Parts A/B/C 35(9):553–560

Rodríguez-Puebla C, Encinas AH, García-Casado LA, Nieto S (2010) Trends in warm days and cold nights over the iberian peninsula: relationships to large-scale variables. Climatic change 100(3-4):667–684

Schär C, Vidale PL, Lüthi D, Frei C, Häberli C, Liniger MA, Appenzeller C (2004) The role of increasing temperature variability in european summer heatwaves. Nature 427(6972):332–336

Seneviratne SI, Donat MG, Mueller B, Alexander LV (2014) No pause in the increase of hot temperature extremes. Nature Climate Change 4(3):161–163

Seubert S, Fernández-Montes S, Philipp A, Hertig E, Jacobeit J, Vogt G, Paxian A, Paeth H (2014) Mediterranean climate extremes in synoptic downscaling assessments. Theoretical and applied climatology 117(1-2):257–275

Stevens B, Giorgetta M, Esch M, Mauritsen T, Crueger T, Rast S, Salzmann M, Schmidt H, Bader J, Block K, et al (2013) Atmospheric component of the mpi-m earth system model: ECHAM6. Journal of Advances in Modeling Earth Systems 5(2):146–172

Stocker TF, Dahe Q, Plattner GK (2013) Climate change 2013: The physical science basis. Working Group I Contribution to the Fifth Assessment Report of the Intergovernmental Panel on Climate Change Summary for Policymakers (IPCC, 2013)

Taylor KE, Stouffer RJ, Meehl GA (2012) An overview of cmip5 and the experiment design. Bulletin of the American Meteorological Society 93(4)

Whan K, Zscheischler J, Orth R, Shongwe M, Rahimi M, Asare EO, Seneviratne SI (2015) Impact of soil moisture on extreme maximum temperatures in europe. Weather and Climate Extremes

Zorita E, Von Storch H (1999) The analog method as a simple statistical downscaling technique: comparison with more complicated methods. Journal of climate 12(8):2474–2489

Chapter 6

Influence of the external forcing on Circulation Types in the Atlantic European region during the second half past millennium

6.1 Introduction

In the detection and attribution of climate change, it is fundamental to understand the role of the natural variability at several time scales, as well as to be capable of quantifying the effects of external forcings on climate evolution (Hegerl et al., 2011). However, this analysis requires the knowledge of the coevolution of climate and its forcings during long time periods (Huybers and Curry, 2006). Unfortunately, the instrumental observational period only extends to the last 150 years and for some places, being inadequate to perform this task.

There are mainly two methodologies which try to give a response to this problem: climate reconstructions and climate models. The formers can be based on indirect information from natural sources (Beltrami, 2002; Büntgen et al., 2011), as well as on historical documentation from human activities (Rodrigo et al., 2012). These reconstructions constitute an important source of evidence which allows to examine the climate evolution in the past. On the other hand, the use of climate models permits to build a plausible evolution of climate in a physically consistent way where some forcings, taken as starting hypothesis, are employed (Zorita et al., 2005; Ammann et al., 2007; Gómez-Navarro et al., 2011). Thereby, climate simulations can be used for understanding the climate interactions and testing hypothesis about the different forcings which have been able to play an important role in the changes occurred in the past and that may occur in the future.

There exist many techniques for analyzing the real climate evolution and the climate simulations, that are of great utility for validating many aspects of models

against observations. At synoptical scale, one of the tools frequently used consist of establishing a classification of the main Circulation Types (CTs). These are some stereotyped atmospheric situations that could be considered as the attractors of the chaotic system that constitute the atmospheric dynamics (Lorenz, 1956). In the last years many clustering techniques have been developed to establish objective CT classifications (Beck and Philipp, 2010). However, there is still some margin for the researcher's subjectivity, as the election of the clustering algorithm, the variables for defining the CTs, the choosing of the size and resolution of window and the number of clusters to group (García-Valero et al., 2012). Once stablished a CT classification, the analysis of CTs allows to simplify in a handy number of situations the huge number of meteorological states defining the atmospheric dynamics. In a paleoclimate context, this analysis facilitates to better understand the influence of the external forcings on changes in circulation during the past centuries, favoring the higher or lower occurrence of some CTs. This could have let its footprint in the climate evolution at synoptical and regional scales.

This study is centered in the Euroatlantic window where there are available climate reconstructions (Jones et al., 2003; Rodrigo et al., 2012) and simulations (Zorita et al., 2005; Gómez-Navarro et al., 2011, 2012) for the last millennium. All studies show an important climate variability linked, in a great extent, to changes in the external forcings. Hence, it is observed colder periods during the litte Ice Age (Mann et al., 2009) associated with low solar activity as the Maunder Minimum occurred around 1700, or to a higher volcanic activity as the Dalton Minimum about 1800. In addition, the great increase of the anthropogenic forcing since the second half of the ninetieth century leads to the significant warming recorded in the last century (IPCC, 2014). Some works have found response signals of the atmospheric dynamics to these changes in forcings but some others did not found a direct or linear response, probably due to the low signal-to-noise ratio imposed by the natural internal variability (Gómez-Navarro and Zorita, 2013). However, there is a larger agreement in the changes induced in the dynamics by large volcanic eruptions. The most clear response to volcanoes is the prevalence of the positive phase of the North Atlantic Oscillation (NAO) mode of variability during the following winters (Fischer et al., 2007; Mann et al., 2009; Zanchettin et al., 2013). In addition, regional changes observed in the global warming pattern under climate change projections, suggest the idea that changes in circulation regimes could be one of the causes of such changes (Zorita et al., 2005).
There are few studies using CTs for the analysis of the influence of the external forcings. In Huth et al. (2008) the response of the Hess-Brezowsky synoptic types to the solar activity was analyzed in the period 1949-2003, finding an increase(decrease) of westerlies(easterlies) over the central Europe in winter during high(low) solar activity. Inside the European and North Atlantic daily to MULtidecadal climATE variability project (EMULATE), the influence of the anthro-

pogenic forcing on the frequency of the CTs was investigated by using climate simulations forced with and without anthropogenic GHGs. Results from this exercise noticed significant changes in the frequency of CTs when GHGs were considered, observing a larger response in the CTs of summer than in the rest of seasons. On the other hand, the influence of volcanoes has not yet been analyzed under the CTs perspective.

This work explores for the first time the response to the external forcings of a set of CTs obtained for the period 1500-1990. To perform this, four paleosimulations forced by the same set of external forcings (total solar irradiance, volcanic eruptions and anthropogenic GHGs) are used, allowing the analysis in the response of the CTs to each forcing as well as to the ensemble of forcings. This work is organized as follows: Sec 6.2 describes the paleosimulations employed and the methods used for obtaining the CT classifications and to test the influence of the different forcings on the CTs. Main results are presented in Sec 6.3. Conclusions and discussions are in Sec 6.5.

6.2 Data and Methods

6.2.1 Paleosimulations

Circulation Types are obtained by using daily Sea Level Pressure (SLP) data for the period 1500-1990. Data are derived from 4 paleoclimate simulations. Two of the simulations were obtained by means of the global circulation model (GCM) ECHO-G (Legutke and Voss, 1999). Both simulations were run by using the same set of external forcings (see Figure 6.1): greenhouse gases (GHGs) concentrations, total solar irradiance (TSI) and an estimation of the global mean radiative forcing of stratospheric volcanic aerosols. However, they were started from different initial conditions, one from warming conditions (ERIK1 experiment) and the other for colder conditions (ERIK2). A complete descriptions of these simulations can be found in Zorita et al. (2005).
The other two paleosimulations considered were performed with the regional climate model (RCM) MM5 (Dudhia, 1993; Grell et al., 1994; Gómez-Navarro et al., 2010). Each of these simulations used as boundary conditions the above simulations obtained with ECHO-G. A detailed description of the regional simulations can be read in Gómez-Navarro et al. (2010); Gómez-Navarro et al. (2011). Hereafter, the four paleosimulations will be referred as ECHOG-ERIK1, ECHOG-ERIK2, MM5-ERIK1 and MM5-ERIK2. Taking into account that one of the main tasks of this work is to obtain the CTs of the different paleosimulations, as well as to compare them among the four simulations, a remapping of the RCM simulations to the coarser grid of the GCM ($\sim$ 3.75^o x 3.75^o) by using bilinear interpolation is applied. In this way, the possible influence of the window resolution on the results García-Valero et al. (2012) is avoided. The window used for the analysis covers an Euroatlantic region of ranges [35^o-54^o] for latitude and

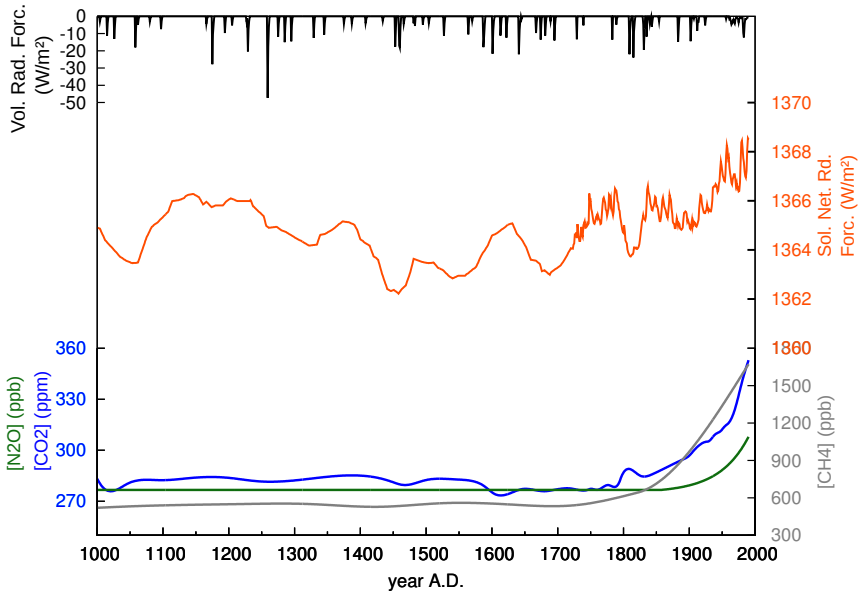

Figure 6.1: External forcings considered for the paleosimulations (Zorita et al., 2005; Gómez-Navarro et al., 2010).

[-19º-23º] for longitude, including this area 72 grid-points.

Despite SLP data could be affected by temperature, and considering that important changes in temperature occurred over the study period, the CTs classifications could be affected by this dependence. In order to reduce this dependence the SLP data have been normalized at each grid-point of the window considered dividing the local SLP value by the averaged value over the geographical window used for the method of classification.

6.2.2 Clustering procedure

A similar approach to that explained in García-Valero et al. (2012) for clustering atmospheric situations into a discrete number of clusters or Circulation Types (CTs) is used here. This consist of a two-step clustering procedure. In the first step, a PC-ModeT clustering is performed (Kyselỳ and Huth, 2006). This clustering allows to obtain the necessary seeds for the second step, defining the number of clusters (a priori unknown). Second, a K-means algorithm is applied over the retained PCs, using for initializing the clustering the seeds obtained in the previous step. For each simulation, two CT classifications are obtained, one for winter (DJF) and the other for summer (JJA). The number of clusters considered in the different classifications depends on the number of the retained PCs used in the PC-ModeT clustering, being this the double of the retained PCs (García-Valero et al., 2012). To define the retained PCs, the method using the log(eigenvalue) vs. number of PCs (Wilks, 2006) is employed.

In this case, seven(five) PCs leading to 14(10) clusters were retained for winter(summer) in the four simulations. The total variance explained by the retained PCs in the global(regional) simulations is 94.5%(86.4%) for winter, and 93.7%(82.8%) for summer.

6.2.3 Methods for analyzing external forcings influence

Evolution of climate is governed by a combination of internal variability and external forcings. This work is centered in the analysis of the influence of the external forcings (TSI, volcanoes and GHGs) on the frequency appearance of the CTs. To perform this, a similar approach to that proposed by Gómez-Navarro et al. (2012) is used. It consists of analyzing the temporal correlation between the series of frequencies of the same CT obtained in two different simulations performed with the same model forced by the same external forcings, but started with different initial conditions. Hence, for a given CT, if significant positive correlation exist, it would mean that the evolution of the CT is driven by external forcings rather than internal variability. Therefore, for implementing this methodology, is necessary to obtain those CTs which are similar among the different simulations, in relation to its spatial structure (representing the same atmospheric circulation). To perform this, the spatial correlation between all possible pairs of CTs between the different simulations is carried out. Once defined the similar CTs, those with a high value of correlation and whose centroids are subjectively similar, the time correlation among them is obtained. In order to reduce the higher variability presents in the annual frequency series, correlation is obtained for different moving average series of 31 (high frequency), 61 (medium frequency) and 91 (low frequency) years, therefore different responses are analyzed. Previous to the calculation of correlation, series are detrended to avoid the influence of long-term trends on the results. The statistical significance of correlations is analyzed by means of the t-test.

Another tasks of this work is to research, by separately, the influence of TSI changes, GHGs and big volcanoes on the frequency of the CTs. The three forcings have a different nature. The two formers (TSI and GHGs) present gradual changes, affecting more to the long-term evolution of climate, whereas the latter (volcanoes) represent a pulse acting at higher frequencies. Therefore, the proposed methods for analyzing the effects of each forcing on the CTs are different.

In the case of TSI and GHGs, the same procedure to that mentioned above is followed. Correlation between the moving average series of the frequency of CTs and TSI or GHGs concentrations are obtained. In this case it is considered that these forcings affects to the variability of a given CT when correlation is significant at the same extend, negative or positive, either in the two global or regional simulations.

The analysis of the influence of the volcanic activity (VA) is based on a superposed epoch analysis (Jones et al., 2003; Fischer et al., 2007). This method consist of comparing the common signals of changes obtained during great volcanic events against others obtained when these events do not occur. Therefore, when a common signal is obtained for an important number of volcanic events, there is a larger reliance of the influence of volcanoes. In this work 19 volcanic events, included in the external forcings used in the simulations, are considered. All of them have in common a reduction of more than 10 W/m^2 in the TSI. The signal considered to detect the fingerprint of volcanoes over the frequency of CTs consists of obtaining the relative changes in the frequency of CTs after big volcanoes respect to the prevailing five years before the eruption. To analyze possible delays in the signal, lag-time from 0 (for the same year of the eruption) to 4 years after the eruptions have been obtained. Hence, for a given CT, the population of changes composed by the volcanic events is compared to the populations of changes obtained for the rest of years when non-volcanic events occurred. These are taken without considering the 5 years after and before of the considered volcanic events. The test two-sided Mann-Withney is then used to analyze the significance of the differences among the two kind of populations using as null-hypothesis that which consider that the mean of both populations is the same. Finally, as considered for TSI, only those CTs with significant differences between post and pre-eruptions periods, observed either in the two global or regional simulations are considered as sensitive to this forcing.

6.3 Results

A total of 14(10) CTs are obtained in the four paleosimulations for winter(summer). This is a coherent result considering that two simulations are obtained with the same global model, and the other two are driven by such global simulations.
Figures 6.2 and 6.3 show the centroids of the CTs corresponding to the CTs of ECHOG-ERIK1 (the CTs of the other simulations are not shown by reasons of space). On the right of each CT, the precipitation (above) and temperature (bellow) weather types (WTs) associated with the CT are represented. Temperature WTs are daily anomalies, whereas for precipitation standardized anomalies are represented. All the WTs have a high physical coherence with their associated CTs, reinforcing the validity of the clustering results. Some examples follows: CTs 3 and 7 are related to southern and northern circulation over western Europe, respectively, causing the former positive temperature anomalies and the latter negative ones over this area; CTs 2 and 8 of winter describe the prevalence of ridges and troughs over western-central Europe, provoking negative precipitation anomalies and positive ones, respectively.

To simplify the comparison analysis about the similarity of the CTs of the dif-

Table 6.1: Similar CTs of the different simulations in winter. The spatial correlation between the given CT and its corresponding CT in the ECHOG-ERIK1 simulation is shown in brackets. Third and sixth columns depict the time correlation (in black those which are statistically significant) between the seasonal frequency series of the similar CTs of the two simulations, either global or regional. Correlations are obtained by using moving average series of 31-61-91 years.

DESCRIPTION	ECHOG-ERIK1	cor (31 / 61 / 91)	ECHOG-ERIK2	MM5-ERIK1	cor (31 / 61 / 91)	MM5-ERIK2
Anticyclon at southern and zonal circulation at northern Europe	CT1	–	CT1 (0.95)	CT1 (0.85)	–	–
Anticyclon over France	CT2	–	CT4 (0.96)	CT7 (0.95)	–	CT4 (0.98)
Southern circulation	CT3	–	CT6 (0.96)	CT6 (0.97)	–	CT6 (0.98)
Zonal circulation	CT4	–	CT3 (0.86)	CT2 (0.93)	–	CT9 (0.61)
Ridge at western Europe	CT5	–	CT2 (0.97)	CT3 (0.95)	–	CT3 (0.89)
Low pressures at northern UK and eastern of the Mediterranean Sea	CT6	–	CT5 (0.91)	CT4 (0.87)	–	CT7 (0.83)
Northwestern circulation over western Europe	CT7	–	CT8 (0.98)	–	–	CT2 (0.93)
Ridge/Trough over western/central Europe	CT8	–	CT12 (0.71)	CT11 (0.55)	–	CT11 (0.71)
Low pressures at western of the Mediterranean Sea	CT9	–	CT11 (0.99)	CT9 (0.89)	– / **0.10** / **0.14**	CT8 (0.69)
Ridge of large amplitude over central-western Europe	CT10	–	–	–	–	–
Low pressures at western of the IP	CT11	–	CT14 (0.90)	CT13 (0.87)	–	CT14 (0.87)
Low pressures at eastern of the Mediterranean Sea	CT12	–	CT10 (0.98)	CT10 (0.86)	–	CT12 (0.92)
Low pressures at western Europe	CT13	–	CT13 (0.97)	CT14 (0.81)	–	CT13 (0.94)
Low pressures at western of France	CT14	**0.12** / **0.12** / **0.10**	CT9 (0.72)	CT8 (0.72)	– / **0.14** / **0.11**	CT10 (0.70)
	–	–	CT7	–	–	CT5
	–	–	–	CT5	–	–
	–	–	–	CT12	–	–
	–	–	–	–	–	CT1

Table 6.2: As table 6.1 but for summer. In asteriks the synoptical description of the CT2 of both regional simulations.

DESCRIPTION	ECHOG-ERIK1	cor (31 / 61 / 91)	ECHOG-ERIK2	MM5-ERIK1	cor (31 / 61 / 91)	MM5-ERIK2
Zonal circulation at northern and stagnant situation at southern	CT1	–	–	–	–	–
Ridge of large amplitude at western Europe	CT2	–	CT7 (0.68)	CT4 (0.86)	**0.11** / **0.16** / –	CT3 (0.86)
Zonal circulation	CT3	–	CT1 (0.87)	CT3 (0.92)	– /**0.13** / –	CT1 (0.98)
Anticyclon at eastern Europe	CT4	–	CT2 (0.99)	CT1 (0.96)	–	CT5 (0.84)
Low/High pressures at Northeastern/southwestern Europe	CT5	–	CT3 (0.56)	CT6 (0.89)	–	CT4 (0.91)
Deep Low at western Europe	CT6	**0.10** / – / –	CT6 (0.86)	CT10 (0.64)	–	CT9 (0.84)
Low pressures over central Mediterranean Sea	CT7	**0.10** / **0.10** / –	CT9 (0.89)	–	–	–
Ridge of large amplitude at central/eastern Europe	CT8	– / **0.13** / –	CT10 (0.68)	–	–	–
Deep Low at eastern Europe and anticyclon over the IP	CT9	–	CT8 (0.86)	CT9 (0.76)	–	CT10 (0.81)
High Pressures at northwestern Europe and north Atlantic Ocean	CT10	**0.10** / – / –	CT4 (0.76)	CT8 (0.91)	–	CT8 (0.99)
	–	–	CT5	–	–	–
	–	–	–	CT5	–	–
	–	–	–	CT7	–	–
*Stagnant situation in Europe and relative low pressures in the IP	–	–	–	CT2	–	CT2
	–	–	–	–	–	CT6
	–	–	–	–	–	CT7

ferent simulations, the CT classification derived from the ECHOG-ERIK1 simulation is taken as reference. Tables 6.1 and 6.2 show the results of this comparison. Each row depicts the CTs whose spatial pattern is very similar among the different simulations. The similarity of each CT is indicated by means of its spatial correlation (in brackets) with its corresponding CT in the reference simulation. In addition, a synoptical description of the different CTs can be seen in the first column of both Tables.

In general, there exists a biunique correspondence between the majority of the CTs of the global and regional simulations in winter, observing a lower correspondence in summer (lower spatial correlations). In winter, CT10 of ECHOG-ERIK1 and CT7 of ECHOG-ERIK2 does not have correspondence. Same result is observed for the CTs 5 and 12 of MM5-ERIK1 and CTs 1 and 5 of MM5-ERIK2. Regarding summer, only one CT of each global simulation is unpaired, CT1 of ECHOG-ERIK1 and CT5 of ECHOG-ERIK2, whereas two CTs of each regional simulation does not have correspondence. However, the CT2 of both regional

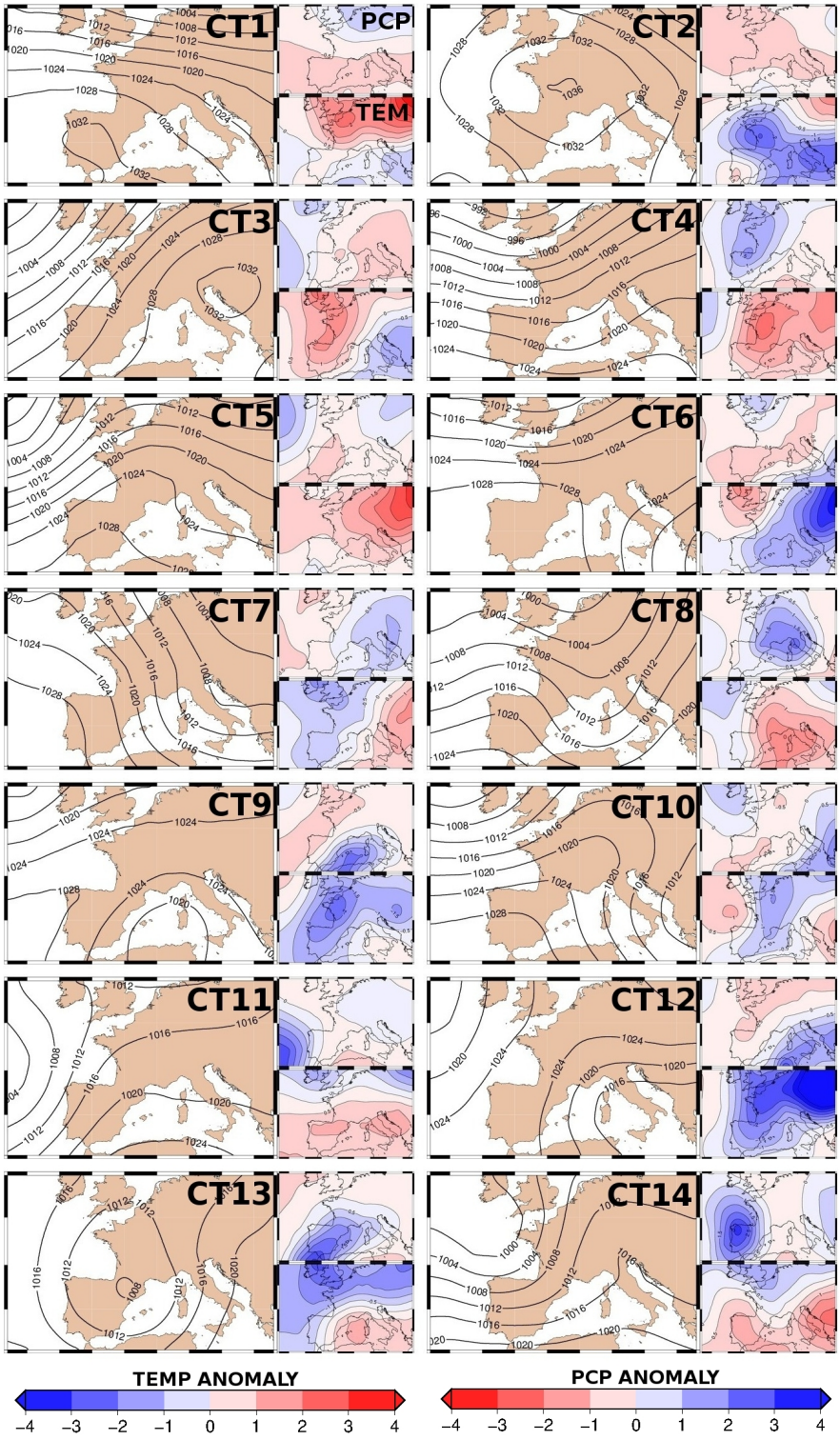

Figure 6.2: CTs (SLP field) and their associated WTs (anomalies) of temperature (ºC/day) and precipitation (mm/day).

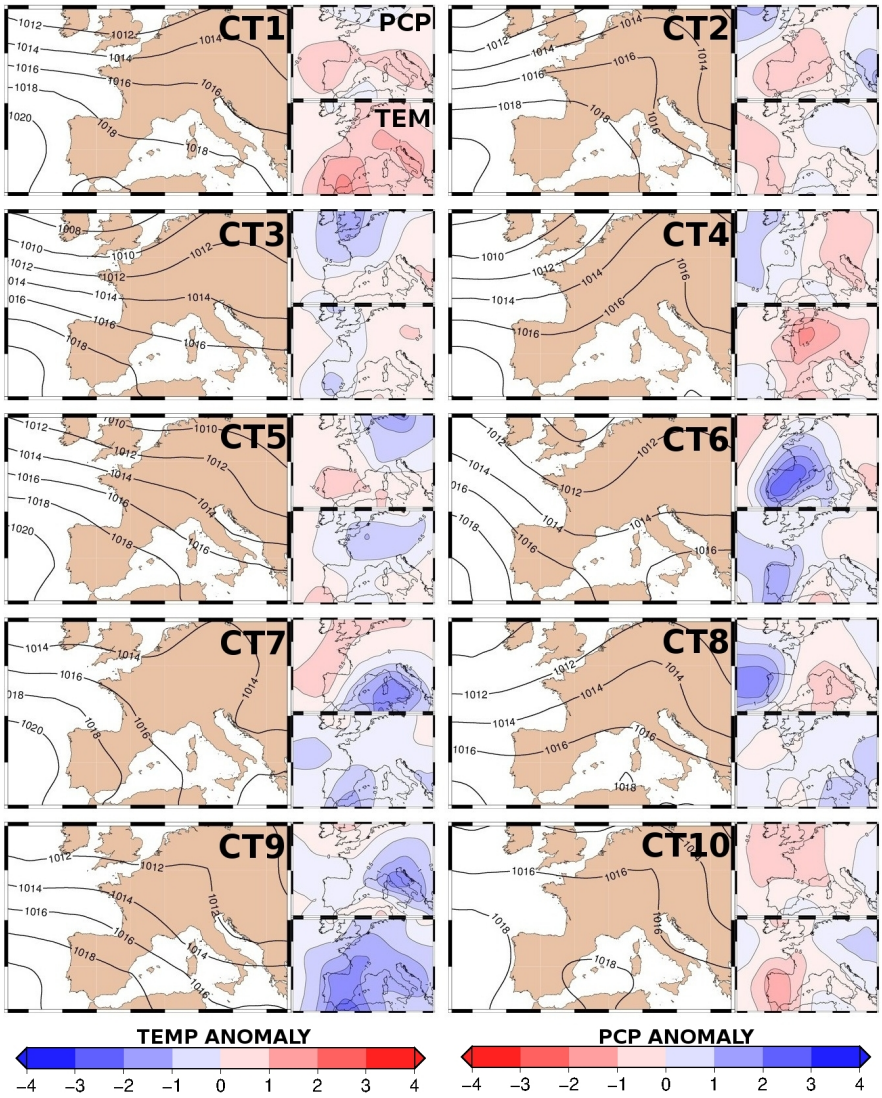

Figure 6.3: Same as Figure 6.2 but for summer.

simulations are similar but they are unpaired in relation to the CTs of the global simulations.

6.4 External forcings influence on the CTs time variability

Table 6.1 and 6.2 show the time correlations (third and sixth columns) between the pairs of the similar CTs of the global and regional paleosimulations, considering the period 1500-1990. Only significant positive correlations are shown (higher than 95% of confidence level). Two CTs in winter, CT14 and CT9, and six CTs in summer, CTs 2,3,6,7,8 and 10, are sensitive to the external forcings. In general, significant correlations are obtained in either global or regional simulations, but not differences among simulations are found for CT14 which exhibits a large sensitivity both in regional and global simulations. In addition, external forcings controls the time variability of the CTs at different time scales. Hence, in summer, the majority of the affected CTs respond to the forcings at higher/medium frequencies (31/61 years), whereas in winter the forcings control more the CTs variability at medium/lower frequencies (61/91 years).

A question arises from this, it is wether the sensitivity of the CTs at these long-time scales is mainly due to ITS changes, or to anthropogenic GHGs emissions, or to a combination of both forcings. Furthermore, it is interesting the analysis of changes at shorter time scales (in the order of some few years) that the volcanoes could print in the variability of the CTs. These analysis are presented in the next subsections.

6.4.1 ITS changes and GHGs influence

Only the CT9 of winter presents some significant positive correlation with ITS changes, although this is only observed in the two regional simulations (CT9 of MM5-ERIK1 and CT8 of MM5-ERIK2). Despite the statistical significance of correlation, the value of correlation is low, of 0.12 and 0.15 for the moving average series of 31 and 61 years, respectively in both simulations. This CT is related to low pressure systems over the west of the Mediterranean Sea and with southwestern circulation over the northern of Europe (Figure 6.2). Westerly circulation in the northern agrees with the results found by Waple et al. (2002); Huth et al. (2008); Mann et al. (2009); Swingedouw et al. (2011), among others, who pointed out to an enhancement of the positive phase of the NAO during periods of high irradiance. At southern of Europe, the higher frequency of low pressure systems over the west of te Mediterranean Sea leads to positive(negative) anomalies of precipitation(temperature). This last result does not have precedent in other related works, and it is contrary to the natural increase of temperature under higher ITS context.
Anyway, this result could be hampering the influence of ITS because this include

the twentieth century when anthropogenic GHGs forcing have more relevance (see Figure 6.1). Therefore, correlations have been calculated also for the preindustrial period 1650-1850 when ITS shows larger variability (Waple et al., 2002) and the anthropogenic influence is almost inexistent. Hence, using this period no differences are appreciated confirming the non-existence of relationship between the solar activity and the CTs variability.

The lack of influence of ITS on the CTs variability could indicate that the anthropogenic GHGs emissions are the main external forcing responsible of the significant correlations obtained in Tables 6.1 and 6.2. To investigate this, the calculation of the correlation among pairs of similar CTs for a period of time when GHGs emissions become prevalent over ITS variations, as is the 1850-1990 period (industrial period), could elucidate some insights at this respect.
In winter, the results obtained for the industrial period confirms the significant correlations found during the longer period for CTs 14 and 9 (ECHOG-ERIK1), although in this case CT9 also reflects significant sensitivity in the global simulations. In addition, the CT12 has a large response to the forcings during this period, obtaining for this situation the largest correlations (0.32) only observed in the regional simulations. This pattern is associated with a ridge configuration over the central-western Europe, driver of negative anomalies of precipiation and temperarute in this region. Regarding summer, only three of the six sensitive CTs found in the longer period have significant correlation in the shorter one. These are the CTs 2, 6 and 10. As it was obtained for the longer period, CT2 shows only relation to external forcings in the regional simulations, whereas the sensitivity of the other CTs is only obtained in the global simulations.

However, these results do not demonstrate the exclusive influence of GHGs on the CTs variability, therefore correlations between CTs and concentration of CO_2 series have been also calculated in a similar way that they were obtained in relation to the ITS forcing. In addition, these correlations have been calculated for the complete period (1500-1990) and for the industrial period (1850-1990). Thus, the non-significant correlations derived from this exercise using the methodology explained in Subsection 6.2.3, evidence that changes in CTs can not be attributed to the anthropogenic CO_2 emissions.

6.4.2 Volcanoes influence

Table 6.3 shows the CTs found (referred to ECHOG-ERIK1) affected by big volcanoes. Three CTs in winter (CTs 2, 6 and 14) and only one in summer (CT6). On the one hand, the most robust result is that obtained for CT2 in winter. This CT presents the same significant response in the four simulations. On the other hand, for the rest of CTs significant response is observed either in the global or regional simulations. Hence, in the case of CT6 (both in winter and summer) similar results are obtained in three of the four simulations, whereas only in the

Table 6.3: Sensitive CTs to big volcanoes (ITS is reduced more than 10 W/m2). The number of the CTs are referred to the ECHOG-ERIK1 simulation. The lag-year when the change is most significant after the eruption is also shown (fourth column), as well as the sign and the mean percentage of the relative change derived from all the volcanic events during the indicated lag-year. The interval in the third column represent the minimum and maximum mean relative changes derived from the mean relative changes obtained in the different simulations that the CT has a significant response. In addition, the number of the volcanic events whose relative change exceeds the mean percentage derived from the total of the volcanic events in a given simulation,and the relative change for this number of events (in brackets) are presented in the columns 5-8.

Season	CTs	relative change (%)	lag-year	ECHOG-ERIK1	ECHOG-ERIK2	MM5-ERIK1	MM5-ERIK2
Winter	CT2	-[17–29]	0	10 (-85)	10 (-24)	11 (-41)	10 (-46)
	CT6	+[15–33]	2	11 (81)	–	8 (103)	7 (97)
	CT14	-[16–34]	2	13 (-66)	13 (-47)	–	–
Summer	CT6	-[16–26]	2	11 (-45)	12 (-37)	10 (-61)	–

global simulations a clear response of CT14 in winter is found.

CT2 of winter, linked to high pressure systems over western Europe, decreases its frequency after volcanoes. CT14, also reduces its frequency significantly. This pattern resembles to the negative phase of the NAO whose print on the anomaly patterns of precipitation and temperature is clear (Figure 6.2). Conversely, the CT6 pattern, compatible to the positive phase of the NAO, increases its frequency. Another significant result is the same lag-year obtained for the both atmospheric complementary patterns (CT6 and CT14). Thus, the net effect of all these changes is to increase the western circulation over northern Europe and to diminish zonal circulation over the southwest of Europe favoring on this region the prevalence of higher pressures. Both effects lead to positive temperature and precipitation anomalies in the north of Europe and negative ones in the southern European regions. These results agree with those provided by Jones et al. (2003); Shindell et al. (2004); Fischer et al. (2007); Zanchettin et al. (2013) who found the enhancement of the positive phase of the NAO after big eruptions.

Regarding summer, the only one CT found affected by volcanoes reduces significantly its frequency. It is linked to troughs of large amplitude over western Europe causing in this region, the highest positive precipitation anomalies and negative temperature anomalies. This result is clearly in disagreement with those obtained from reconstructions which informed that the general cooling is one of the most clear fingerprints in the following summers to big eruptions (Zanchettin et al., 2013).

6.5 Conclusions and discussions

This works analyzes the response of the atmospheric dynamics to different external climate forcings such as: changes in ITS, volcanic activity and anthropogenic GHGs. Changes in dynamics are analyzed through the changes in the frequency of appearance of a set of CTs obtained from the SLP field of four paleosimulations corresponding to the period 1500-1990. Responses to external forcings are analyzed for winter and summer. The methodology used for the analysis of the influence of the solar activity and anthropogenic forcings is mainly based on the analysis of correlations between the frequency series of CTs and series of forcings, whereas for volcanoes, changes in the frequency after big eruptions are analyzed using a superposed epoch analysis based on big 19 volcanic eruptions. In both cases, the method tries to look for common signals obtained for a given CT present in the different simulations.

The results prove a lack of significant response to the solar and anthropogenic forcings when the influence of this forcing is analyzed separately. However, some results manifest the existence of a significant weak signal of response to the ensemble of external forcings. This is obtained for two winter CTs (CTs 9 and 14, see Table 6.1) and six summer CTs (CTs 2, 3, 6, 7, 8 and 10, see Table 6.2). Despite this result, the weak responses found avoid to discard the internal variability as the main factor of the CTs variability.

These results have a large dependence of the method followed which could have important limitations. On the one hand, the small number of the considered CTs could provoke a large variability of atmospheric situations inside each cluster or CT, contributing this to increase the noise against the signal. On the other hand, the use of the correlation for finding the links between forcings and CTs limits this study to the analysis of linear responses, which could not corresponding with possible non-linear links as was pointed in Huth et al. (2006); Barriopedro et al. (2014). Therefore, it should be explored new methodologies which consider to work with more specific CTs derived from exercises of characterization of some climate variables like extremes (García-Valero et al., 2012), or to work with a higher number of CTs facilitating the increase in the quality of the clusters (Bermejo and Ancell, 2009), or to calculate different CT classifications for different periods with large differences in the external forcings analyzing the possible changes of the CTs not only in the frequency (Knight et al., 2007) rather also in the changes in the shape of the CTs (Huth et al., 2008).

Circulation types are an usefulness tool to test the changes in the atmospheric circulation after big volcanic eruptions. Hence, the results obtained for winter agree with previous works mainly based in reconstructions. These show an increasing(decreasing) in the occurrence of the positive(negative) phase of the NAO, explaining the delayed warming observed in the northern of Europe dur-

ing winters after great eruptions. However, during summer, the only CT with significant changes, related to positive precipitation and negative temperatures in the western of Europe, decreases its frequency after volcanoes. This would be in disagreement with the characteristic cooling observed in the reconstructions. Maybe, the response to the cooling does not have a dynamical interpretation rather to a radiative explanation, because is during this season when there are a larger impact of the aerosols due to the higher irradiance than in winter (IPCC, 2014). A fact which could corroborate this, is the general cooling observed in the overall Europe in the following summers after the eruption, especially at the higher latitudes (Fischer et al., 2007) where the increasing of the albedo could be higher due to the larger tilt of the irradiance over these latitudes.

Bibliography

Ammann, C. M., Joos, F., Schimel, D. S., Otto-Bliesner, B. L., and Tomas, R. A.: Solar influence on climate during the past millennium: Results from transient simulations with the NCAR Climate System Model, Proceedings of the National Academy of Sciences of the United States of America, 104, 3713–3718, doi:10.1073/pnas.0605064103, 2007.

Barriopedro, D., Gallego, D., Alvarez-Castro, M. C., García-Herrera, R., Wheeler, D., Peña-Ortiz, C., and Barbosa, S. M.: Witnessing North Atlantic westerlies variability from ships' logbooks (1685–2008), Climate dynamics, 43, 939–955, 2014.

Beck, C. and Philipp, A.: Evaluation and comparison of circulation type classifications for the European domain, Phisics and Chemistry of the Earht, 35, 374–387, 2010.

Beltrami, H.: Earth's long-term memory, Science, 297, 206–207, 2002.

Bermejo, M. and Ancell, R.: Observed changes in extreme temperatures over Spain during 1957-2002, using Weather Types, Revista de Climatología, 9, 45–61, 2009.

Büntgen, U., Tegel, W., Nicolussi, K., McCormick, M., Frank, D., Trouet, V., Kaplan, J. O., Herzig, F., Heussner, K. U., Wanner, H., Luterbacher, J., and Esper, J.: 2500 Years of European Climate Variability and Human Susceptibility, Science, 331, 578–582, doi:10.1126/science.1197175, 2011.

Dudhia, J.: A nonhydrostatic version of the Penn State-NCAR mesoscale model: Validation tests and simulation of an Atlantic cyclone and cold front, Monthly Weather Review, 121, 1493–1513, 1993.

Fischer, E., Luterbacher, J., Zorita, E., Tett, S., Casty, C., and Wanner, H.: European climate response to tropical volcanic eruptions over the last half millennium, Geophysical Research Letters, 34, 2007.

García-Valero, J., Montavez, J., Jerez, S., Gómez-Navarro, J., Lorente-Plazas, R., and Jiménez-Guerrero, P.: A seasonal study of the atmospheric dynamics over the Iberian Peninsula based on circulation types, Theoretical and Applied Climatology, 110, 291–310, doi:10.1007/s00704-012-0623-0, URL `http://dx.doi.org/10.1007/s00704-012-0623-0`, 2012.

Gómez-Navarro, J., Montávez, J., Jimenez-Guerrero, P., Jerez, S., JA:, G.-V., and González-Rouco, J.: Warming patterns in regional climate change projections over the Iberian Peninsula, Meteorologische Zeitschrift, 19, 275–285, 2010.

Gómez-Navarro, J. J., Montávez, J. P., Jerez, S., Jiménez-Guerrero, P., Lorente-Plazas, R., González-Rouco, J. F., and Zorita, E.: A regional climate simulation over the Iberian Peninsula for the last millennium, Climate of the Past, 7, 451–472, doi:10.5194/cp-7-451-2011, 2011.

Gómez-Navarro, J. J., Montávez, J. P., Jiménez-Guerrero, P., Jerez, S., Lorente-Plazas, R., González-Rouco, J. F., and Zorita, E.: Internal and external variability in regional simulations of the Iberian Peninsula climate over the last millennium, Climatic of the Past, 8, 25–36, doi:10.5194/cp-8-25-2012, 2012.

Grell, G. A., Dudhia, J., and Stauffer, D. R.: A description of the fifth-generation Penn State/NCAR mesoscale model (MM5), Tech. rep., National Center for Atmospheric Research, 1994.

Gómez-Navarro, J. J. and Zorita, E.: Atmospheric annular modes in simulation over the past millennium: No long-term response to external forcing, Geophysical Research Letters, pp. 1–5, doi:10.1002/grl.50628, URL `http://onlinelibrary.wiley.com/doi/10.1002/grl.50628/abstract`, 2013.

Hegerl, G., Luterbacher, J., González-Rouco, J. F., Tett, S. F. B., Crowley, T. J., and Xoplaki, E.: Influence of human and natural forcing on European seasonal temperatures, Nature Geoscience, 4, 1–5, doi:10.1038/ngeo1057, 2011.

Huth, R., Pokorná, L., Bochníček, J., and Hejda, P.: Solar cycle effects on modes of low-frequency circulation variability, Journal of Geophysical Research: Atmospheres (1984–2012), 111, 2006.

Huth, R., Kyselỳ, J., Bochníček, J., and Hejda, P.: Solar activity affects the occurrence of synoptic types over Europe, in: Annales Geophysicae, vol. 26, pp. 1999–2004, Copernicus GmbH, 2008.

Huybers, P. and Curry, W.: Links between annual, Milankovitch and continuum temperature variability, Nature, 441, 329–332, doi:10.1038/nature04745, 2006.

IPCC: Climate Change 2013: The physical science basis: Working group I contribution to the fifth assessment report of the Intergovernmental Panel on Climate Change, Cambridge University Press, 2014.

Jones, P., Moberg, A., Osborn, T., and Briffa, K.: Surface climate responses to explosive volcanic eruptions seen in long European temperature records and mid-to-high latitude tree-ring density around the Northern Hemisphere, Geophysical monograph, 139, 239–254, 2003.

Knight, J., Scaife, A., Fereday, D., Folland, C., and Xoplaki, E.: EMULATE Deliverable D13: Assessment of the relative influence of external forcing factors (natural and human) and internal variability and their seasonal differences, Tech. rep., Hadley Center, 2007.

Kyselỳ, J. and Huth, R.: Changes in atmospheric circulation over Europe detected by objective and subjective methods, Theoretical and Applied Climatology, 85, 19–36, doi:10.1007/s00704-005-0164-x, 2006.

Legutke, S. and Voss, R.: The Hamburg atmosphere-ocean coupled circulation model ECHO-G, Tech. rep., DKRZ, 1999.

Lorenz, E.: Technical report, Statistical Forecast Project Report 1. Dep.of Meteorology.MIT 49, vol. 1, chap. Empirical orthogonal functions and statistical weather prediction, p. 52, Massachusetts Institute of Technology, 1956.

Mann, M. E., Zhang, Z., Rutherford, S., Bradley, R. S., Hughes, M. K., Shindell, D., Ammann, C., Faluvegi, G., and Ni, F.: Global signatures and dynamical origins of the Little Ice Age and Medieval Climate Anomaly, Science, 326, 1256–1260, 2009.

Rodrigo, F. S., Gómez-Navarro, J. J., and Montávez, J. P.: Climate variability in Andalusia (southern Spain) during the period 1701-1850 AD from documentary sources: evaluation and comparison with climate model simulations, Climate of the Past, 8, 117–133, 2012.

Shindell, D. T., Schmidt, G. A., Mann, M. E., and Faluvegi, G.: Dynamic winter climate response to large tropical volcanic eruptions since 1600, Journal of Geophysical Research: Atmospheres (1984–2012), 109, 2004.

Swingedouw, D., Terray, L., Cassou, C., Voldoire, A., Salas-Mélia, D., and Servonnat, J.: Natural forcing of climate during the last millennium: fingerprint of solar variability, Climate Dynamics, 36, 1349–1364, 2011.

Waple, A., Mann, M., and Bradley, R.: Long-term patterns of solar irradiance forcing in model experiments and proxy based surface temperature reconstructions, Climate Dynamics, 18, 563–578, 2002.

Wilks, D.: Statistical methods in the atmosphere sciencies, Academic, San Diego, 2006.

Zanchettin, D., Timmreck, C., Bothe, O., Lorenz, S. J., Hegerl, G., Graf, H.-F., Luterbacher, J., and Jungclaus, J. H.: Delayed winter warming: A robust

decadal response to strong tropical volcanic eruptions?, Geophysical Research Letters, 40, 204–209, doi:10.1029/2012GL054403, 2013.

Zorita, E., González-Rouco, J. F., von Storch, H., Montávez, J. P., and Valero, F.: Natural and anthropogenic modes of surface temperature variations in the last thousand years, Geophysical Research Letters, 32, 755–762, 2005.

Chapter 7

Conclusiones Generales

El objetivo principal de la tesis ha consistido en la búsqueda de relaciones entre la Circulación Atmosférica, caracterizada por una serie de Tipos de Circulación (TCs), y la variabilidad climática. Para ello se han analizado diferentes períodos temporales. El primero de ellos corresponde a un período histórico reciente, 1958-2008, en el que se ha analizado la variabilidad climática de las variables: precipitación (pcp), temperatura máxima (T_x), temperatura mínima (T_m) y ocurrencia de días extremadamente cálidos (EHDs) sobre el territorio español peninsular y las Islas Baleares. En el caso de las tres primeras variables, se ha analizado su variabilidad en las diferentes estaciones del año, tanto a escala diaria como estacional, mientras que la variabilidad de los días EHDs se ha analizado sólo en verano. Otro período temporal analizado es el que se corresponde con proyecciones de Cambio Climático, como es el período 2006-2100, obteniéndose proyecciones climáticas de la variable EHD con el fin de detectar tendencias a largo plazo. Por último, se ha analizado el período 1500-1990 dentro de un contexto paleoclimático. Para este último período no se ha analizado ninguna variable climática específica, pero sí la evolución de una serie de TCs con el fin de dar respuesta sobre el grado de influencia de los forzamientos externos sobre la circulación atmosférica.

Este estudio requiere el diseño de diferentes clasificaciones de TCs, para lo cuál ha sido necesario el uso de datos de reanálisis, de observaciones, así como de simulaciones de Cambio Climático y Paleoclimáticas. En total se han obtenido 14 clasificaciones de TCs. 4 de ellas estacionales para el período histórico reciente, de tipo generalista (usada por otras investigaciones). Otras 6 para el mismo período, pero diseñadas para el análisis de eventos extremos (EHDs) en verano, dónde además ha sido necesario el uso de la base de datos reticular Spain02. Se han obtenido otras 6 clasificaciones más para el período futuro, obtenidas con 3 modelos del Sistema Tierra (CCSM4, MPIM-ES-M y EC-EARTH), sólo para verano, y que consisten en una proyección de 3 de las clasificaciones obtenidas (aquellas definidas con 2 variables atmosféricas) en el período histórico reciente y desarrolladas para el análisis de extremos. Por último, se han obtenido 8 clasificaciones paleoclimáticas de tipo generalista (4 para invierno y otras 4 para verano),

a partir de las salidas de dos simulaciones obtenidas con el modelo global ECHO-G y otras dos obtenidas con el modelo regional MM5 en su versión climática.

Aparte de estas clasificaciones de TCs, se han obtenido otros resultados que permiten profundizar en el conocimiento de la variabilidad espacial sobre el territorio peninsular español y las Islas Baleares. Entre ellos están los regímenes de tiempo de pcp, T_x y T_m asociados a los TCs del periodo reciente pasado, así como de aquellos otros de pcp y temperatura media correspondientes a las simulaciones paleoclimáticas y una regionalización de las temperaturas máximas estivales.

Uno de los puntos principales de esta tesis se ha centrado en el desarrollo de una clasificación de TCs para el período 1958-2008 y en el análisis de la frecuencia, persistencia y transiciones de los TCs mostrados en el Capítulo 2. Las principales conclusiones de este estudio son:

- El algoritmo de agrupación utilizado para la obtención de las clasificaciones de TCs proporciona grupos estables y de calidad. Éste se basa en parte en el algoritmo K-medias que en general presenta un mejor índice de estabilidad de los grupos, que es notablemente mejor que el obtenido para el algoritmo SANDRA durante el invierno sobre una ventana geográfica centrada sobre la Península Ibérica (PI).

- Se han obtenido 12 TCs para cada estación del año observándose diferencias muy notables entre los TCs de invierno y verano. Entre las estaciones de transición las diferencias son menores, observándose en ellos una mezcla de situaciones de invierno y verano. El conjunto de las situaciones descritas en los TCs se puede resumir de manera subjetiva en 5 categorías principales de situaciones: Anticiclónica, Ciclónicas, Zonales, Híbridas y de Verano.

- Del análisis de tendencias en la frecuencia de los TCs se deriva que hay pocas tendencias significativas, aunque sí hay una tendencia general al aumento de la frecuencia de las situaciones anticiclónicas frente a las ciclónicas en invierno y primavera. Entre las tendencias más significativas se encuentran 4 tipos de situaciones en invierno. Dos de ellas relacionadas con bajas extratropicales al NW de la PI y sobre el Mediterráneo Occidental que presentan tendencia negativa, mientras que las otras dos, una parecida al patrón de la fase positiva de la NAO, y otra relacionada con altas presiones sobre el interior del continente europeo presentan una tendencia positiva. En cuanto a la primavera, al igual que sucedía en invierno, la situación de baja al Noroeste de la PI presenta una tendencia negativa. En verano, sólo la situación de baja térmica sobre el SE de la península presenta una tendencia positiva. Por último, ninguno de los TCs de otoño presenta tendencia significativa.

- En general, los TCs de primavera y otoño pueden presentar persistencias más altas que los de invierno y primavera. En otoño e invierno, las situaciones más persistentes están relacionadas con altas presiones que cubren

una amplia extensión del Oeste de Europa, mientras que en verano y primavera están asociadas a situaciones de pantano barométrico. Por el contrario, las situaciones menos persistentes en invierno y otoño están asociadas a la existencia de circulación zonal del Oeste, en primavera a situaciones anticiclónicas, y en verano con situaciones que marcan un flujo del Suroeste sobre la PI en niveles altos.

- Algunos TCs presentan tendencias en su persistencia. Las más destacables son la tendencia negativa en invierno de la situación de la baja al Noroeste de la PI y de una situación en primavera relacionada con una configuración de dorsal sobre el Océano Atlántico Norte.

- Las transiciones de mayor probabilidad entre los TCs nos muestran la existencia de ciclos, que comienzan y acaban en el mismo TC. Los ciclos más largos se producen en invierno con transiciones entre situaciones anticiclónicas, relacionándose este resultado con la alta frecuencia de este tipo de situaciones durante el invierno. El resto de ciclos representan la inestabilización y posterior estabilización de la atmósfera sobre la PI, con transiciones entre situaciones zonales a situaciones de paso de vaguada y el posterior paso de dorsales de pequeña amplitud.

- Aparte de los ciclos, las transiciones revelan la existencia de secuencias interesantes como el paso de las bajas extratropicales por la PI desde su posición inicial al Noroeste de la PI hacia dos posiciones alternativas, una hacia el sur de la Península (hacia el golfo de Cádiz) y otra hacia el Mediterráneo. Ésta transición revela que la probabilidad de transición hacia ambas ubicaciones es similar en invierno, pero su probabilidad de transición en primavera y otoño es prácticamente el doble hacia su posición al sur de la PI que hacia el Mediterráneo.

En el Capítulo 3 de la tesis, la clasificación de TCs se emplea para analizar la influencia de la dinámica atmosférica en la variabilidad climática observada en la región de estudio. Para ello, se obtienen los Tipos de Tiempo (TTs) asociados a los distintos TCs. Estos TTs además de constituir una herramienta muy útil para entender la variabilidad espacial sobre nuestra región de estudio, también se pueden usar para reconstruir series de anomalías climáticas. Esto permite analizar qué parte de la varianza y variabilidad temporal observada en la variable climática está controlada por la circulación atmosférica. Las principales conclusiones de este capítulo son:

- Una parte muy importante de la variabilidad temporal a escala estacional de la pcp, T_x y T_m puede interpretarse en términos de la variabilidad atmosférica. La dinámica presenta un mayor control sobre las temperaturas que sobre la precipitación. Dependiendo de la variable, se observa una dependencia estacional. Ésta explica mejor la variabilidad de T_x en primavera, verano y otoño, de T_m en primavera y otoño, y de la precipitación en invierno.

- En invierno se observa un importante contraste entre las fachadas Oeste y Este peninsular. Al Oeste, la dinámica ejerce un mayor control sobre la precipitación, mientras que al Este el control es mayor sobre T_x.

- Parte de las tendencias negativas en precipitación en amplias zonas de la mitad Oeste de la PI, obtenidas en el período 1958-2008, pueden entenderse por las tendencias en los TCs. También, aquellas observadas en el período 1973-2005 en primavera (tendencias negativas en zonas de la vertiente cantábrica), verano (tendencias negativas en el centro y sur península) y otoño (tendencias positivas en zonas del Centro/Oeste y Noroeste de la PI).

- Los TTs reproducen razonablemente bien parte de las tendencias positivas observadas para T_x y T_m en primavera y verano en el período 1973-2005. No obstante, no reproducen las tendencias positivas de T_m en otoño observadas en ese mismo período, las cuáles deben esta relacionadas con otros factores distintos a la dinámica atmosférica.

- Excepto para T_x y T_m en otoño, los TCs no explican bien la variabilidad a escala diaria. Esto puede ser por el método utilizado para la reconstrucción de las series de anomalías. Este sólo sólo tiene en cuenta el valor medio de la anomalía asociada a cada TC, a pesar del enorme ruido presente en estas clasificaciones.

En el Capítulo 4 se presenta una nueva metodología para analizar qué parte de las tendencias observadas en la ocurrencia de días extremadamente cálidos (EHDs) en un conjunto de regiones españolas, puede atribuirse a cambios en la dinámica. Para ello, se ha desarrollado una nueva clasificación de TCs que parte de una previa caracterización de las situaciones sinópticas presentes en los días de ocurrencia de eventos extremos. Por otro lado, con el fin de analizar el impacto que tiene la elección de las variables atmosféricas que definen los TCs sobre los resultados de atribución, se ha obtenido un conjunto de clasificaciones distintas considerando las variables SLP, T850 y Z500 de forma individual y emparejadas. Los principales resultados obtenidos son:

- La regionalización de T_x en verano nos muestra ocho regiones con una variabilidad temporal distinta. En todas ellas hay una tendencia significativa y positiva en la frecuencia de ocurrencia de EHDs en el período 1958-2008, siendo la tendencia mayor en las regiones del interior peninsular.

- El método utilizado en la obtención de clasificaciones de TCs útiles para el análisis de la ocurrencia de estos eventos extremos proporciona grupos de calidad. Éste asegura una agrupación más correcta de las situaciones atmosféricas asociadas a los días extremos, la cuál no puede garantizarse en las clasificación de tipo generalista (aquellas donde se agrupan todos los días), dónde el pequeño peso estadístico de estas situaciones puede conducir a que queden equirepartidas entre los diferentes grupos que componen la clasificación.

- Las clasificaciones obtenidas combinando dos variables caracterizan en general mejor la ocurrencia de EHDs en todas las regiones. La clasificación SLP-T850 caracteriza mejor estos eventos en la mayoría de regiones, excepto en Cs y NE donde la combinación Z500-T850 presenta mejores resultados.

- La probabilidad de ocurrencia de EHD en las diferentes regiones bajo los distintos TCs, definida como eficiencia, presenta una tendencia positiva en muchas regiones en parte relacionada con un aumento de la persistencia de los distintos TCs. En general estos cambios son mayores en las regiones del interior.

- La mayoría de los TCs no presentan tendencias significativas en su frecuencia a lo largo del período de estudio. Tan sólo unos pocos TCs tienen tendencia significativa, los cuáles a su vez presentan una eficiencia importante en muchas regiones de forma simultánea. Esta eficiencia es mayor en las regiones del centro y del norte.

- En todas las clasificaciones definidas con dos variables se obtiene que un porcentaje inferior al 50% de la tendencia en la frecuencia de EHDs observada en las distintas regiones, puede atribuirse a cambios en la circulación. Esta atribución presenta una fuerte dependencia de la clasificación utilizada. Z500-T850 es la que puede atribuir un mayor porcentaje de la tendencia en las diferentes regiones.

Una vez definida la clasificación de TCs para el análisis de eventos extremos, en el Capítulo 5 se plantea su proyección hacia el futuro con el fin de obtener un conjunto de proyecciones de cambio climático de la frecuencia de EHD en las diferentes regiones identificadas. Para ello, se ha hecho uso de las salidas de diferentes simulaciones climáticas obtenidas con tres Modelos climáticos del Sistema Tierra (ESMs por sus siglas en inglés): MPIM-ES-M, EC-EARTH y CCSM4. Las proyecciones de EHD se han obtenido usando las simulaciones de los ESMs efectuadas para dos escenarios distintos, RCP4.5/8.5 en el período 2006-2100. La validación del método de proyección, la evaluación de los distintos modelos en relación a cómo reproducen las frecuencias de los TCs en un período histórico-reciente (1958-2005), el análisis de los cambios proyectados en la frecuencia de los TCs, así como de las proyecciones EHD obtenidas en las diferentes regiones y de su incertidumbre, son los principales aspectos tratados en este capítulo. Las principales conclusiones son:

- Los resultados sobre la validación del método de proyección indican que el modelo reproduce bien la variabilidad estacional de EHD en las diferentes regiones aunque no es capaz de reproducir correctamente la frecuencia en los años con mayores ocurrencias. De este modo, el método es válido para reproducir los cambios a largo plazo.

- En el período histórico los modelos reproducen bien la frecuencia de los TCs de las distintas clasificaciones obteniéndose sesgos muy pequeños, inferior

a un día en la mayoría de ellos, en comparación con la frecuencia de los TCs obtenidas con reanálisis. Los pequeños sesgos en la frecuencia de los TCs, conducen a pequeños desviaciones en la frecuencia de días extremos en las diferentes regiones, produciéndose una ligera sobreestimación de ésta en todas las regiones que apenas supera los 0.5 días.

- Las frecuencias de algunos TCs cambian muy significativamente bajo los diferentes escenarios de futuro. Algunos de ellos aumentan su frecuencia, mientras en otros disminuye. Aquellos que más aumentan se corresponden con dos TCs (TCs 2 y 4 en las distintas clasificaciones) cuya eficiencia es muy alta en muchas de las regiones en relación al resto de TCs, y en particular algo mayor en las regiones del centro peninsular. Ambas situaciones se corresponden con una configuración de dorsal de gran amplitud sobre la PI, localizada sobre el Este y Centro peninsular y asociadas a configuraciones de pantano barométrico en superficie y dorsal térmica en 850 hPa. Por otro lado, TC5 es el que más disminuye y está relacionado con una situación anticiclónica centrada al Norte de Francia y con una eficiencia alta en el desarrollo de eventos cálidos en la región NWw.

- Las proyecciones EHD obtenidas para las diferentes regiones muestran un aumento notable y gradual a lo largo de todo el siglo de la frecuencia de EHD en todas las regiones. En términos generales, y para el último período de 30 años del siglo (2071-2100) la frecuencia proyectada en muchas regiones es el doble e incluso el triple, en regiones del centro peninsular (CS, NWs y NE), que la observada en el período histórico. Siendo su incertidumbre no superior al 30% de la frecuencia media proyectada en la mayoría de regiones, aunque en algunas de ellas, sobre todo en la región E la incertidumbre es algo mayor entorno al 40%.

- El análisis de la evolución temporal de la incertidumbre en las proyecciones muestra que a lo largo de todo el período (1950-2100) la incertidumbre está controlada en más del 50% por la incertidumbre asociada a los modelos climáticos, y por más del 80% en el período histórico. No obstante, la incertidumbre asociada a los escenarios controla el 30% del total de la incertidumbre a partir del 2020, disminuyendo ligeramente hasta el 20-25% al final del período, cuando la incertidumbre relativa a las clasificaciones de TCs aumenta considerablemente, especialmente en las regiones del Centro y Este peninsular.

- Algunos de los resultados obtenidos en relación con las proyecciones obtenidas mediante las distintas clasificaciones, así como del análisis de los cambios de las frecuencia de algunos TCs bajo los distintos escenarios, evidencian una limitación de la metodología seguida relativa a la dependencia de algunas variables empleadas en la definición de los TCs a la temperatura, y por tanto al calentamiento global. Esta limitación hace que las proyec-

ciones EHD como consecuencia de cambios en la circulación queden en parte subestimadas.

En el Capítulo 6 se presenta un estudio sobre la influencia de diferentes forzamientos externos en la circulación atmosférica. Los forzamientos externos considerados son: los cambios en la irradiancia total solar, las concentraciones de Gases de Efecto Invernadero (GEI) y la actividad volcánica. Se analizaron 2 simulaciones paleoclimáticas, cada una de ellas con diferentes condiciones iniciales, efectuadas con el modelo global ECHO-G. Ambas simulaciones se emplearon como condiciones de frontera de otras dos simulaciones llevadas a cabo con el modelo regional MM5. A partir de los datos de estas 4 simulaciones se han obtenido un total de 8 clasificaciones de TCs, 4 para invierno y otras tantas para verano. El estudio constituye la primera vez que se lleva a cabo este análisis desde el punto de vista de los TCs, especialmente si tenemos en cuenta el análisis de la influencia volcánica y el largo período temporal utilizado, 1500-1990. Los principales resultados son:

- La variabilidad temporal de algunos TCs responde a cambios en el conjunto de los forzamientos pero la señal de respuesta es débil. Se observa además un mayor número de TCs sensibles a los forzamientos en verano que en invierno. Este resultado concuerda con otras investigaciones en las que se encontró una mayor sensibilidad en verano de la variabilidad climática sobre la PI a los forzamientos externos.

- Cuando se aplica la metodología propuesta para analizar la influencia por separado de los forzamientos solar y de GEI, se obtiene que ninguno de los TCs es sensible a ellos, excepto TC 9 de invierno (bajas presiones al Oeste del Mar Mediterráneo) cuya correlación con el forzamiento solar es positiva aunque también muy débil.

- La respuesta de algunos TCs al forzamiento volcánico en invierno se relaciona con un aumento de situaciones que favorecen el flujo del componente Oeste sobre el norte de Europa (TCs 2, 6 y 14). Este resultado reafirma lo encontrado en otros trabajos, en los que se apreció un aumento de la fase positiva del patrón de teleconexión dominante en Atlántico Norte (NAO). Por contra, el cambio observado en verano (disminución de la situación TC6) no concuerda con los resultados de otros trabajos en los que se destaca el enfriamiento generalizado en toda Europa en los años posteriores a una gran erupción. Este enfriamiento podría tener como principal responsable al factor radiativo, resultado del aumento del albedo global, y no a cambios en la circulación atmosférica.